AAiT
ADDIS ABABA INSTITUTE OF TECHNOLOGY
አዲስ አበባ ቴክኖሎጂ ኢንስቲትዩት
ADDIS ABABA UNIVERSITY
አዲስ አበባ ዩኒቨርሲቲ

SCHOOL OF GRADUATE STUDIES
SCHOOL OF CIVIL AND ENVIRONMENTAL ENGINEERING
MASTERS OF SCIENCE IN CIVIL ENGINEERING

THESIS

ON

GEOTECHNICAL EVALUATION AND REMEDIATION STRATEGIES FOR SEEPAGE, PIPPING AND LIQUEFACTION HAZARDS AT YANDA DAM.

BY

MESFIN KERE DESSIE

ADVISOR: TEZERA FIREW(Ph.D)

CO-ADVISOR: YARED MULAT

NOVEMBER, 2023G.C
ADDIS ABABA,ETHIOPIA

ADDIS ABABA UNIVERSITY

ADDIS ABABA UNIVERSITY INSTITUTE OF TECHNOLOGY

SCHOOL OF GRADUATE STUDIES

SCHOOL OF CIVIL AND ENVIRONMENTAL ENGINEERING

(SPECIALIZATION: DAM ENGINEERING)

Geotechnical Evaluation and Remediation Strategies for Seepage, Pipping, and Liquefaction Hazards at Yanda Dam.

By

Mesfin Kere Dessie

"*A thesis submitted to the School of Civil and Environmental Engineering in partial fulfillment of the Degree of Masters of Science in Civil Engineering (Specialized in Dam Engineering)*"

November, 2023G.C
Addis Ababa,
Ethiopia

APPROVAL SHEET

ADDIS ABABA UNIVERSITY

ADDIS ABABA UNIVERSITY INSTITUTE OF TECHNOLOGY

SCHOOL OF GRADUATE STUDIES

SCHOOL OF CIVIL AND ENVIRONMENTAL ENGINEERING

(SPECIALIZATION: DAM ENGINEERING)

This is certify that the thesis prepared by Mesfin Kere Dessie, entitled: **"Geotechnical Evaluation and Remediation Strategies for Seepage, Piping, and Liquefaction Hazards at Yanda Dam"** and submitted in fulfillment of the requirements for the Degree of Master of Science complies with the regulations of the Addis Ababa University and meets the accepted standards with respect to the originality and quality.

By:

MESFIN KERE

APPROVED BY OF EXAMINERS BOARD:			
	NAME	SIGNATURE	DATE
ADVISOR	Dr. Tezera Feren		27/11/2023
INTERNAL EXAMINER	Dr Asie Kemal		27/11/2023
EXTERNAL EXAMINER	Dr. Daneal PhD/Assoc Dam) PhD		27/11/2023
CHAIR MAN	Abrham Gebre (Dr.) School of Civil & Environmental Engineering		

Director of Postgraduate Program
Addis Ababa University
Addis Ababa Institute of Technology

DECLARATION

I, Mesfin Kere, hereby certify that the information contained in this paper was acquired and provided in compliance with laws and ethical standards. I have conducted my research with honesty, integrity, and transparency, striving to adhere to the highest standards of academic and professional ethics.

I further declare that, under these rules of conduct, I have accurately referenced and cited any data, ideas, and results that are not original to this work. I have meticulously acknowledged the contributions of other researchers and authors by providing appropriate citations throughout this thesis. I have taken care to avoid any form of plagiarism, ensuring that all sources are properly attributed.

By my signature below, I confirm that the work included in this thesis is entirely original to me. I have diligently conducted my research, crafted my arguments, and presented my findings based on my own efforts and intellect. Any assistance received from colleagues, advisors, or other individuals has been acknowledged and duly credited.

I further confirm that all information sources used in the preparation of this thesis have been correctly cited, referring to the original works and authors in a consistent and accurate manner. I have utilized a recognized citation style and followed its guidelines to ensure the proper documentation of my sources.

I understand the importance of academic integrity and take full responsibility for the accuracy and integrity of this research work. In the event that any discrepancies or issues are discovered, I am committed to addressing them promptly and transparently.

By signing below, I affirm that this certification is true and accurate to the best of my knowledge.

Signature: 

Date: 27/11/2023

ACKNOWLEDGEMENT

My first and foremost thanks are dedicated to the Almighty God, who always helps me overcome life challenges with success and happiness.

I am also grateful to my beloved family for their love and encouragement. I am indebted to my research advisor, Tezera Firew (Ph.D.), for his sincere understanding and compassionate support. I also want to express my heartfelt appreciation to Yared Mulat, who is a senior engineer and my co-advisor, and it is my pleasure to extend my thanks to Assie Kemal (Ph.D.).

I am grateful to my friends Yeshmebet Yitbarek and Yonas Abraham, who provided excellent support during my studies.

Of course, I also thank the firm 'Ethiopian Construction Design and Supervision Work Corporation' for providing me with the majority of the information I needed for my study.

Finally, I would like to express my special gratitude to my friends from the class of Dam Engineering (2014E.C.), Alemayehu M., Amdemariam S., Esubalew M., Hafsoa G., and Tegegn F., for having friendly and best academic relations throughout the past two crucial years.

Contents

APPROVAL SHEET ..... **Error! Bookmark not defined.**
ACKNOWLEDGEMENT iv
LIST OF TABLE viii
LIST OF GRAPH ix
LIST OF CHART ix
LIST OF PHOTO ix
ABSTRACT x
ABBREVIATIONS and SYMBOLS xi
1. INTRODUCTION ..... - 1 -
1.1. Background of the Study Project ..... **- 1 -**
1.2. Problem Statement ..... **- 3 -**
1.3. Research Questions ..... **- 3 -**
1.4. Objective of the study ..... **- 4 -**
1.4.1. General objective ..... - 4 -
1.4.2. The specific objectives are: ..... - 4 -
1.5. Scope of the study ..... **- 4 -**
1.6. Limitations of the study ..... **- 5 -**
2. LITERATURE REVIEW ..... - 6 -
2.1. Embankment dam ..... **- 6 -**
2.1.1. Geotechnical Investigation of the Dam Foundation ..... - 6 -
2.1.2. Dam's Foundation and Its Challenges ..... - 7 -
2.1.3. Earthquake ..... - 8 -
2.1.4. Mechanism of Seepage in the Dam Foundation ..... - 13 -
2.1.5. The Three Theories for Piping ..... - 16 -
2.1.6. Control Methods of Foundation Piping ..... - 19 -
2.1.7. Case Studies Based on Seepage Analysis ..... - 24 -
2.1.8. Liquefaction Under Dam Foundation ..... - 25 -
2.1.9. Case Studies of Liquefaction with Alluvial Foundation ..... - 37 -
2.1.10. Liquefaction Ground Improvement Remediation ..... - 38 -
2.2. Scientific Modeling ..... **- 41 -**
2.2.1. Numerical Modeling ..... - 42 -
2.2.2. Finite Element Method (FEM) and Challenge with Anisotropic Materials ..... - 43 -
2.2.3. Finite Element Nodes ..... - 43 -
2.2.4. Numerical Analysis for Determination of Piping and Liquefaction ..... - 44 -
2.2.5. Seismic Analysis Method ..... - 45 -
2.2.6. Relation of Stress and Strain ..... - 52 -
3. METHODOLOGY ..... - 54 -
3.1. General Description ..... **- 54 -**
3.1.1. Methodology's Work Flow ..... - 54 -
3.2. Data Collection, Preparation and Analysis ..... **- 56 -**
3.2.1. Primary Data Collection ..... - 56 -
3.2.2. Secondary Data Collection ..... - 58 -
3.2.3. Tests in Geotechnical Investigation ..... - 66 -
3.2.4. Yanda Dam Site Geotechnical Layer Characterization ..... - 67 -
3.2.5. Geological Profile ..... - 71 -
4. DATA ANALYSIS, RESULTS AND DISCUSSION ..... - 72 -
4.1. Previous Yanda Dam Design Geometry ..... **- 72 -**

4.2. The River Course's Physiography ..... - 72 -

4.3. The Dam Site Topography ..... - 74 -

4.4. Adjusted Yanda Dam's cross-section profile ..... - 75 -

4.5. Numerical Modeling and Analysis ..... - 76 -

4.5.1. SEEP/W Analysis ..... - 76 -

4.5.2. Parameters used for seepage analysis ..... - 77 -

4.6. Determine the Seepage Protection Options ..... - 79 -

4.6.1. Seepage Control Options at chainage 0+110.3 ..... - 81 -

4.6.2. Seepage Control Options at Chainage 0+327.5 ..... - 85 -

4.6.3. Seepage Control Options at Chainage 0+630 ..... - 90 -

4.7. The Recommended Cross-Section Profile for the Excessive Seepage Controlled Mechanism ..... - 95 -

4.7.1. Comparing the Cost ..... - 96 -

4.7.2. Estimation of Hydraulic Gradient and Factor of Safety ..... - 98 -

4.7.3. Why Upstream Clay Blanket is not recommended for this study? ..... - 101 -

4.8. Yanda Dam's Liquefaction Analysis ..... - 102 -

4.8.1. Evaluation of Liquefaction ..... - 102 -

4.8.2. Methods of Evaluation ..... - 103 -

4.8.3. Susceptibility of liquefaction for Yanda Based on Grain Size ..... - 105 -

4.8.4. Proving liquefiable Fine-Grained and Clayey for Yanda ..... - 105 -

4.8.5. Earthquake in the Project Area and its Susceptibility ..... - 106 -

4.8.6. Proving Susceptibility of Liquefaction using LiqiT Software ..... - 109 -

4.8.7. Proving Prone to Liquefaction using LiqiT at 0+110.3 PGA 0.197g ..... - 109 -

4.8.8. Proving Prone to Liquefaction using LiqiT at 0+110.3 PGA 0.497g ..... - 110 -

4.8.9. Proving Prone to Liquefaction using LiqiT at 0+327.5 PGA 0.197g ..... - 111 -

4.8.10. Proving Prone to Liquefaction using LiqiT at 0+327.5 PGA 0.497g ..... - 112 -

4.8.11. Proving Prone to Liquefaction using LiqiT at 0+630 PGA 0.197g ..... - 112 -

4.8.12. Proving Prone to Liquefaction using LiqiT at 0+630 PGA 0.497g ..... - 113 -

4.8.13. Summary of the above LiqIT Analysis ..... - 114 -

4.9. Evaluating the Liquefaction Using Quake/W ..... - 114 -

4.9.1. Final Prepared Drawing for this Research of Dynamic Analysis ..... - 114 -

4.9.2. The Procedure of Quake/W Analysis ..... - 115 -

4.9.3. This Research's Quake/W Output and Visualized Results ..... - 128 -

4.9.4. Effects of the Dam's Loaded Stress ..... - 139 -

4.9.5. Yanda Dam's Ground Response Analysis Result ..... - 148 -

4.9.6. Settlement Result and Allowance of Yanda Dam ..... - 150 -

4.9.7. Slope Stability ..... - 152 -

5. CONCLUSION AND RECOMMENDATION ..... - 154 -

5.1. Conclusion and ..... - 154 -

5.2. Recommendations ..... - 156 -

5.3. Limitations to doing Yanda Dam analysis ..... - 157 -

5.4. Validations of the Results ..... - 157 -

REFERENCES ..... - 158 -

Appendix 1. Photographs Taken as primary data ..... - 161 -

Appendix 2. Yanda Dam site location view from Google Earth ..... - 162 -

Appendix 3. U/S Dam Geometry Adjustment ..... - 163 -

Appendix 4. Photos of Long Armed Excavator for Slurry Cutoff ..... - 166 -

Appendix 5. Laboratory Test Result at Dam Foundation Soil Material ..... - 167 -

LIST OF FIGURES

Figure 1 Location map of the Yanda Dam Project ..... - 1 -
Figure 2 Location of Yanda Dam Project from Google Earth ..... - 2 -
Figure 3 Dam site photo (taken by the author, Jan 28, 2023) ..... - 2 -
Figure 4 How an earthquake occurs ..... - 9 -
Figure 5 Earthquake Frequency and Destructive Power ..... - 9 -
Figure 6 Seepage in hydraulic structure ..... - 13 -
Figure 7 Process of Failure due to piping backward erosion ..... - 16 -
Figure 8 Khosla's Flow Net ..... - 17 -
Figure 9 Options of expansion of flow path ..... - 19 -
Figure 10 Remedial impervious u/s blanket ..... - 21 -
Figure 11 Backhoe (Long armed Excavator) for soil bentonite cutoff work ..... - 22 -
Figure 12 Mechanism of soil Liquefaction ..... - 27 -
Figure 13 Photo DDC field applications. ..... - 40 -
Figure 14 Geological map of Yanda dam site, reservoir area, and surroundings ..... - 61 -
Figure 15 Location of VES points and Geo Electric Section ..... - 64 -
Figure 16 Geo-electric Section obtained along ..... - 65 -
Figure 17 Geological profile and Profile with borehole Pattern ..... - 71 -
Figure 18 Previous Typical cross-section of Yanda dam at 0+327.5 ..... - 72 -
Figure 19 Satellite images to show the river meandering in Years(2013-2022) ..... - 73 -
Figure 20 Current Google Earth satellite imaging of the dam site in 2022 ..... - 74 -
Figure 21 Actual Yanda Dam longitudinal section using surveying data ..... - 74 -
Figure 22 Comparison of the topo created using surveying data and satellite photographs ..... - 75 -
Figure 23 Adjusted Cross sections of Yanda dam for next modeling work ..... - 76 -
Figure 24 Adjusted design Drawings for importing into Geo-Studio work ..... - 77 -
Figure 25 Boundary condition of Seep/W Yanda dam ..... - 79 -
Figure 26 Final Drawing with Selected Remedial Measure and Cross Sections ..... - 94 -
Figure 27 Longitudinal Section of researched remedial cutoff and slurry drawing ..... - 95 -
Figure 28 Cross Section of Yanda Dam ..... - 115 -
Figure 29 Providing FE mesh, water pressure boundary, water table, and history points ..... - 117 -
Figure 30 Vertical and Horizontal Boundary conditions for the dynamic analysis. ..... - 121 -
Figure 31 Crest and Base History Point for the dynamic analysis ..... - 121 -
Figure 32 CSR Contours that Prone to Liquefaction at 0+110.3 ..... - 127 -
Figure 33 CSR Contours that Prone to Liquefaction at 0+630 ..... - 127 -
Figure 34 CSR Contours that Prone to Liquefaction at 0+327.5 ..... - 128 -
Figure 35 Dynamic analyzed model of CSR Output display with contour using PGA 0.197g ..... - 129 -
Figure 36 Dynamic analyzed model of CSR Output display with contour using PGA 0.497g ..... - 130 -
Figure 37 Yanda Dam & Foundation Cross Section at 0+327.5 ..... - 141 -
Figure 38 Total Stress, Water Pressure, and Effective Stress Distribution at 0+327.5 ..... - 141 -
Figure 39 Yanda Dam & Foundation Cross Section at 0+110.3 ..... - 143 -
Figure 40 Total Stress, Water Pressure, and Effective Stress Distribution at 0+110.3 ..... - 143 -
Figure 41 Yanda Dam & Foundation Cross Section at 0+630 ..... - 145 -
Figure 42 Total Stress, Water Pressure, and Effective Stress Distribution at 0+630 ..... - 145 -
Figure 43 Quak/W output result of Vertical Settlement with Counters ..... - 150 -
Figure 44 Quak/W output result of Settlement with Counters for 0+327.5 ..... - 151 -
Figure 45 Quake/W output result of Settlement with Counters Display for 0+630 ..... - 151 -
Figure 46 U/S Slope Stability -The critical Safety factor value is 2.417. So the slope stability is safe ..... - 152 -
Figure 47 D/S Slope Stability - The critical Safety factor value is 1.807. So the slope stability is safe. ..... - 152 -
Figure 48 U/S Slope Stability - The critical FoS value is 2.15. So the slope stability is safe. ..... - 152 -
Figure 49 D/S Slope Stability - The critical Safety factor value is 1.67. So the slope stability is safe. ..... - 152 -
Figure 50 U/S Slope Stability - The critical FoS value is 1.895. So the slope stability is safe. ..... - 153 -
Figure 51 D/S Slope Stability - The critical FoS value is 1.551. So the slope stability is safe ..... - 153 -

LIST OF TABLE

Table 1 Rate of Seismic Hazard ..... - 11 -
Table 2 Soil versus Cement-Bentonite Slurry Cutoffs. ..... - 23 -
Table 3 Magnitude Scaling Factor Values Defined by Various Investigators ..... - 34 -
Table 4 Ground Improvements Mechanism and Methods ..... - 39 -
Table 5 This research methodology's Activities ..... - 55 -
Table 6 Tests executed in Geotechnical investigation ..... - 66 -
Table 7 Geotechnical core drilling investigation activities and quantities. ..... - 66 -
Table 8 Zoned Dam bodies cross-section description ..... - 72 -
Table 9 Parameters used for seepage analysis ..... - 78 -
Table 10 Permeability of various embankment materials ..... - 78 -
Table 11 Pore-Pressure Ratio (ECDSWC's Yanda Dam design Report(2022) ..... - 79 -
Table 12 Summarized the remedial options of 0+110.3 ..... - 84 -
Table 13 Summarized the remedial options of 0+327.5 ..... - 89 -
Table 14 Summarized the remedial options of 0+630 ..... - 93 -
Table 15 Summary of Added Dimensions of Remedial Cross-Section ..... - 93 -
Table 16 U/S blanket's cost for comparison with complete and slurry cutoff ..... - 96 -
Table 17 Complete and slurry cutoff cost comparison with U/S blanket ..... - 97 -
Table 18 Comparing Annual Water Flow Under the Foundation ..... - 98 -
Table 19 Specific Gravity from ECDSWC's Report ..... - 99 -
Table 20 Porosity from Standard reference ..... - 99 -
Table 21 Calculation of Factor of Safety at chainage of 0+327.5 ..... - 99 -
Table 22 Calculation of Factor of Safety at chainage of 0+110.3 ..... - 100 -
Table 23 Calculation of Factor of Safety at chainage of 0+630 ..... - 100 -
Table 24 Suitability of Soils for Construction of Earth Dams(IS 8826-1978.) ..... - 101 -
Table 25 Each Layer's data for Liquefaction evaluation(ECDSWC's Report) ..... - 106 -
Table 26 Summary of the earthquake near SNNPR from the above figure ..... - 107 -
Table 27 PGA values evaluated and reported by Prof.Ataly Ayele/AAU(2020). ..... - 108 -
Table 28 PGA value listed (ECDSWC's Yanda Dam design report, 2022.) ..... - 108 -
Table 29 Input data & Result of FoS for proving prone to liquefaction at 0+110.3 & PGA 0.197g ..... - 110 -
Table 30 Input data & Result of FoS for proving prone to liquefaction at 0+110.3 & PGA 0.497g ..... - 111 -
Table 31 Input data & Result of FoS for proving prone to liquefaction at 0+327.5 & PGA 0.197g ..... - 111 -
Table 32 Input data & Result of FoS for proving prone to liquefaction at 0+327.5 & PGA 0.497g ..... - 112 -
Table 33 Input data & Result of FoS for proving prone to liquefaction at 0+630 & PGA 0.197g ..... - 113 -
Table 34 Input data & Result of FoS for proving prone to liquefaction at 0+630 & PGA 0.497g ..... - 114 -
Table 35 Summarized the Poisson's ratio of different materials (K.R. Arora, 2004) ..... - 122 -
Table 36 Yanda Dam Summarized needed parameters as input data ..... - 122 -
Table 37 Calculation of factor of safety from output result of CSR at 0+110.3 & PGA 0.197g ..... - 131 -
*Table 38 Calculation of factor of safety from output result of CSR at 0+110.3 & PGA 0.497g ` * ..... - 132 -
Table 39 Calculation of factor of safety from output result of CSR at 0+327.5 & PGA 0.197g ..... - 133 -
Table 40 Calculation of factor of safety from output result of CSR at 0+327.5 & PGA 0.497g ..... - 134 -
Table 41 Calculation of factor of safety from output result of CSR at 0+630 & PGA 0.197g ..... - 135 -
Table 42 Calculation of factor of safety from output result of CSR at 0+630 & PGA 0.497g ..... - 136 -
Table 43 Comparison of alternative ground improvement options with cost and duration ..... - 138 -
Table 44 Yanda Dam Soil characteristic ..... - 139 -
Table 45 Determination and comparison of effective stress and shear strength at 0+327.5 ..... - 142 -
Table 46 Determination and comparison of effective stress and shear strength at 0+110.3 ..... - 144 -
Table 47 Determination and comparison of effective stress and shear strength at 0+630 ..... - 146 -
Table 48 Comparison of selected remedy option with Other Options ..... - 155 -

LIST OF GRAPH

Graph 1 Gradation Curve for Liquefaction Evaluation ..... - 31 -
Graph 2 Magnitude Scaling Factor Vs Earthquake Moment Magnitude ..... - 35 -
Graph 3 Modulus and damping Ratio curves (Seed and Idriss, 1970) ..... - 49 -
Graph 4 Cyclic Load (Vikram Anand) ..... - 50 -
Graph 5 Vs versus SPT N-value ..... - 51 -
Graph 6 Graphs of Stress-Strain Relationships ..... - 52 -
Graph 7 Grain size distribution curve ..... - 105 -
Graph 8 Chosen El Centro Earthquake data recorded ..... - 118 -
Graph 9 Showing Modified Elcentro Record for this study's dynamic analysis ..... - 119 -
Graph 10 Modified Elcentro Record for dynamic analysis 25.02sec duration. ..... - 120 -
Graph 11 Calculated MSF using a graph for converting $CRR_{7.5}$ *to* $CRR_{6.3}$ ..... - 125 -
Graph 12 Comparison of MES and Shear Strength with Excel Graph ..... - 147 -
Graph 13 Summarized MES with Excel Graph for 0+110.3 ..... - 147 -
Graph 14 Summarized MES with Excel Graph for 0+630 ..... - 148 -
Graph 15 Comparison of Ground Response at the Crest with Base for 0+110.3, 0+327.5, and 0+630 ..... - 149 -
Graph 16 Relative Vertical and Horizontal Settlement at 0+110.3 ..... - 150 -
Graph 17 Relative Vertical and Horizontal Settlement at 0+327.5 ..... - 151 -
Graph 18 Relative Vertical and Horizontal Settlement at 0+630 ..... - 151 -

LIST OF CHART

Chart 1 Failure path diagram due to foundation-suffusion (Foster, 1999) ..... - 15 -
Chart 2 Failure path diagram due to foundation-backward erosion (Foster, 1999) ..... - 15 -
Chart 3 Flow of Modeling ..... - 42 -
Chart 4 Procedures of analysis in this research of Seep/W and Quake/W ..... - 116 -
Chart 5 Flow of activities in Calculation of FoS ..... - 123 -

LIST OF PHOTO

Photo 1 Upstream side view of the dam (Panorama photo from left to right Abutment) ..... - 57 -
Photo 2 Deposited material by meandering the Yanda River ..... - 57 -
Photo 3 Small village in the area ..... - 57 -
Photo 4 Right abutment of the dam ..... - 58 -
Photo 5 Top layer transported and deposited sediment material ..... - 58 -

ABSTRACT

The Yanda Dam project is a proposal for a dam on the Yanda River in the Southern Nations, Nationalities, and Peoples' Region, Ethiopia. Its purpose is to irrigate a 5,500-hectare command area. However, the dam's foundation poses challenges due to its deep alluvium deposit and shallow groundwater conditions. This makes it susceptible to issues such as seepage, piping, and liquefaction potential. To address these concerns, this research paper presents a methodologies (empirical and numerical methods) for studying and simulating the dam's alluvial foundation, as well as suggesting remedial measures for the deep alluvial soil. The alluviums at the Yanda dam site consist of loose sand and silty sand soils. These soils have been classified into two categories: cohesion soils and cohesion-less soils. The cohesion soils include silty clay with a trace of sand, silty clay with a trace of sand and gravel, and clayey silt with a trace of gravel. The cohesion-less soils include fine-grained silty sand and coarse gravel.

Due to the lateral variability in the soil condition of the foundation, three representative cross-sections were selected for the analysis. This approach helps to address the issue of soil heterogeneity in both the vertical and horizontal directions, providing a more accurate understanding of the foundation's behavior. To control excessive seepage and piping in the alluvium foundations, various remedial measures have been considered. These include the use of an upstream blanket, a cutoff wall, and a clay core trench. To determine the effectiveness of these seepage control methods, a comparison was made by conducting seepage analysis using Geo-Studio’s SEEP/W software, and liquefaction assessment of the foundation was also conducted using Quake/W. The method of extending the clay core key trench to create a barrier against seepage and piping. In addition to the clay core key trench, a soil-bentonite slurry trench is also constructed. This slurry trench helps further prevent piping by creating a low-permeability barrier. To perform these remedial measures, equipment such as long (12.8m) and short (5m) armed excavators, roller compactors, and dozers are used. To address liquefaction hazards, the method of removal and replacement is used for upstream issued part and for downstream sections, densification by deep blasting compaction would be recommended. This method involves using controlled explosions to compact the soil and increase its stability, thus minimizing the risk of liquefaction.

Key Words: *Dam, Foundation, Alluvial, Seepage, Piping, Liquefaction.*

ABBREVIATIONS and SYMBOLS

AAU	Addis Ababa University	**MCM**	Million cubic meter
ATH	Acceleration Time History	**MCM**	Million Cubic Meter
ASTM	American Society for Testing and Materials	**MER**	Main Ethiopian Rift
B	Bentonite	**MSF**	Magnitude Scaling Factor
C	Cohesion	**MWL**	Maximum Water Level
CCL	Core Crest Level	**N**	Northing
CDCL	Coffer Dam Crest Level	**NMC**	Natural Moisture Content
CH.	Chainage	**NW-SE**	North West- South East
CRR	Cyclic Resistance ratio	**OBE**	Operating Basis Earthquake
CSR	Cyclic Stress Ratio	**OCR**	Over consolidation ratio, soil
D/s	Downstream	**OGL**	Original Ground Level
DBE	Design base earthquake	**PEER**	Pacific Earthquake Engineering Research
DCL	Dam Crest Level	**PGA**	Peak Ground Acceleration
DDC	Deep Dynamic Compaction	**PI**	Plasticity index, soil
e	Void ratio, soil	**PI**	Plasticity Index
E (Es)	Elastic modulus or modulus of elasticity	**PVC**	Polyvinyl chloride
E	Easting	**PWP**	Pore Water Pressure
EBCS	Ethiopian Building Code Standard	**RWC**	Residual Water Content
EERC	Earthquake Engineering Research Center	**SDS**	Screw Driving Sounding
Eq.	Equation	**SDS**	Screw Driving Sounding test
EQL	Equivalent Linear	**Sec**	Second
FEM:	Finite element method	**SEE**	Safety Evaluation Earthquake (),
FRL	Full Reservoir Level	**SMER**	Southern Main Ethiopian Rift
FS	Factor of Safety	**SPT**	Standard Penetration Test
G	Shear modulus, soil	**SWC**	Saturated Water Content
g	Gravity	**U/s**	Upstream
GFL	General Foundation Level	**UCS**	Unconfined compressive strength (q_{uc})
G_{max}	Very small-strain shear modulus, soil	**UCS**	Un-confined compressive shear strength
Ha	Hectare	**UD**	Undisturbed
ICOLD	International Commission on Large Dams	**USGS**	United States Geological Survey
Ka	Correction factor for initial static stress	**USSD**	United States Society on Dams
Kh	Horizontal seismic coefficient	**UTM:**	Universal transverse Mercator
Km	Killo meter	**YDBH**	Yanda Dam Bore hole
Km^2	Killo meter square	**γ**	Shear strain
KPa	Kilopascal	**ε**	Axial strain
Ks	Correction factor for overburden stress	**ζ**	Damping ratio (denoted by (zeta))
Kv	Vertical seismic coefficient	**ν**	Poisson ratio
LEM	Limit equilibrium method	**σ'**	Effective stress, soil
LL	Liquid Limit	**σ_D**	Deviatory stress, soil
m.a.s.l	Meters Above Sea Level	**μ**	Poisson ratio
MCE	Maximum Credible Earthquake	**Ø**	Angle of internal friction
MCE	Maximum credible earthquake		

AASHTO	American Association of State Highway and Transportation Officials
ECDSWC	Ethiopian Construction Design and Supervision Works Corporation
WES	Waterways Experiment Station (U. S. Army Engineer)
IGSSA	Institute of Geophysics Space Science and Astronomy
NCEER	National Center for Earthquake Engineering Research

1. INTRODUCTION

1.1. Background of the Study Project

Dams are structures made of concrete or earthen materials that can withstand the pressure of water. Dams are civil engineering constructions that are built across a river valley to impound significant amounts of water for various uses, according to Sissakian et al. (2019). In general, a dam is a hydraulic structure, and its main goal is to capture and store flowing water and release it during the dry season for uses such as irrigation, flood control, hydropower generation, drinking water supply, and industrial and recreational uses. However, dams can have negative impacts, such as ecological damage and displacement of communities, so careful planning and management are required for sustainable development.

The Yanda dam is a Zoned Earth-fill (Shell) dam with a clay core and it is found in SNNPR, Konso Zone Konso special Woreda. The project is located 20 km away from Konso Town that far about 630km from Addis Ababa. The site is also located at Easting 340687.99 and Northing 593324.85 UTM in specific Jarso Kebele. The dam site is nearly 3.2km away from the irrigable command area. The Segen basin, where Yanda Valley is located, is a part of the Southern Segment of the Ethiopian Rift Valley which is known as a huge gorge and measures 1km deep, 700km long, and 70 up to 80 km broad. The Segen basin is characterized by multiple phases of volcanic mountain chains. The Yanda Dam construction project is a kind of embankment dam that is planned to be constructed on and by crossing the Yanda River to store the river water to irrigate the anticipated 5500ha of gross command area. According to ICOLD, the Yanda dam is considered as large dam due to its maximum height of 42m and its reservoir holding capacity of 46MCM.

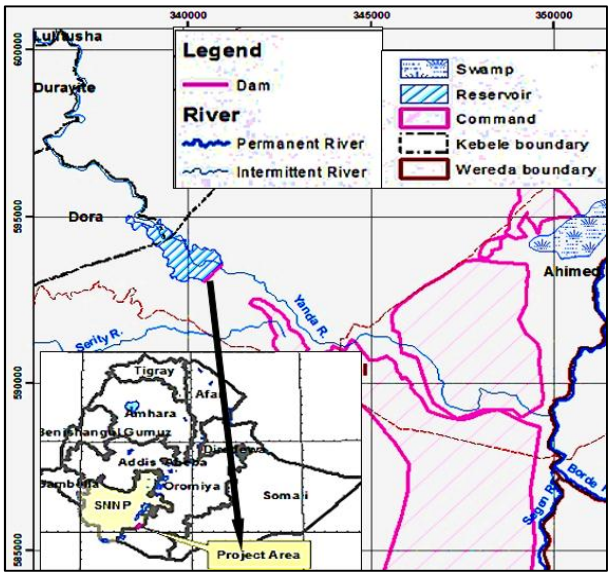

Figure 1 Location map of the Yanda Dam Project

The Yanda Dam Project is part of the Ethiopian Rift System, and its geographic area is the result of geomorphological activities. Those activities are doming, elevating, rifting, volcanism, erosion, sedimentation, and other geologic processes that result in the current geomorphologic features of the site. Locally, the lithological configurations of the Yanda dam and reservoir region are characterized by meandering braided stream channels together with broader flats of flood plains. The land is divided by the meandering Yanda River and its tributaries.

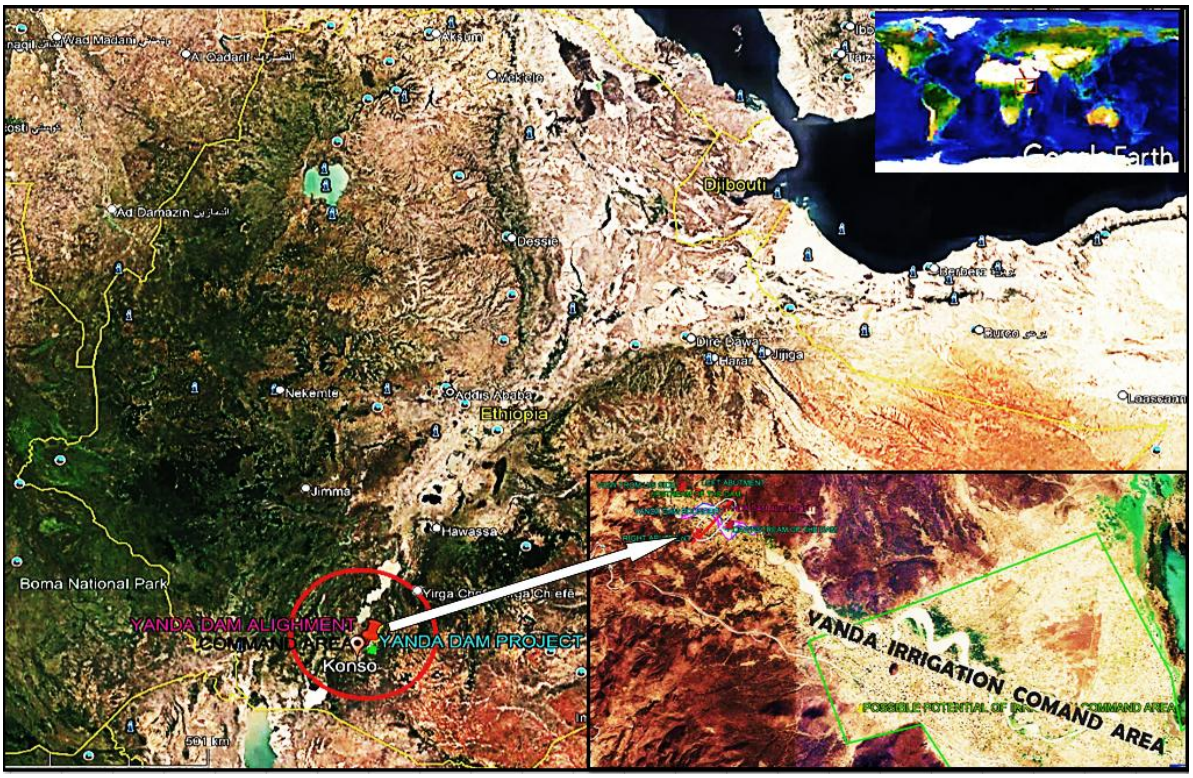

Figure 2 Location of Yanda Dam Project from Google Earth

The dam is 42.0m high above the river bed at the deepest section and 770m crest length at the top dam crest level of 982.00 m.a.s.l.

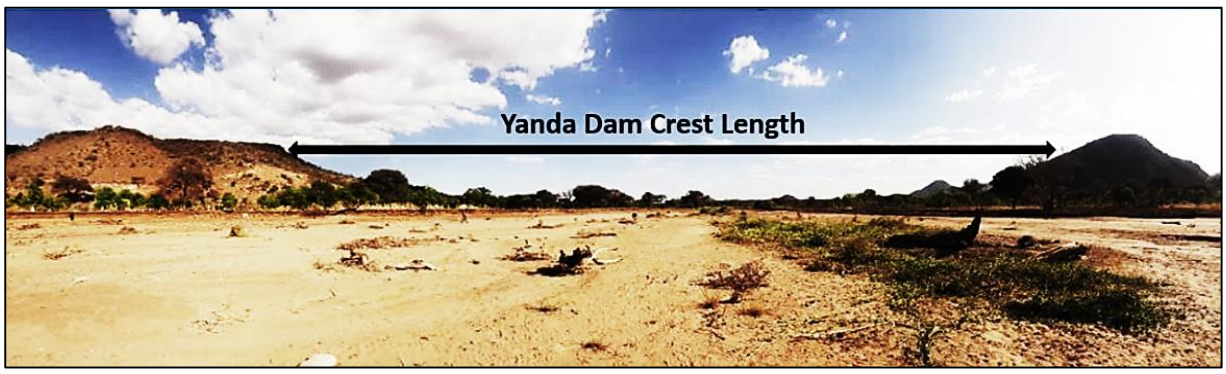

Figure 3 Dam site photo (taken by the author, Jan 28, 2023)

The area around the dam site is in a seismically active region, according to the geotechnical engineering investigation report. Tertiary volcanic, which include basaltic, rhyolite, and trachytic volcanic flow units, quaternary sediments, clastic sediment sequence, and alluvial deposits in the river channel and its flood plains, are outcropped in the vicinity of the Yanda Dam Reservoir. The findings of a field assessment conducted at the Yanda dam site, together with subsequent laboratory studies, indicate that the loose sand and silty sand soils make up the majority of the alluvium foundation beneath the dam seat. Based on the evaluation of liquefaction susceptibility based on grain size distribution, the majority of alluvium foundation soils have been classified as liquefiable because they mostly fall within the range of possibly liquefiable soils.

1.2. Problem Statement

Dams are critical infrastructure components that provide essential services, such as hydroelectric power generation, flood control, and irrigation water supply. However, their construction and maintenance can be costly, and if minor issues are not addressed promptly, dam rehabilitation or reconstruction may be necessary, leading to significant financial and societal impacts (USACE, 2006). Dam failures are often attributed to foundation-related issues, particularly in the presence of alluvial soils that are susceptible to excessive seepage, piping, and liquefaction.

Yanda Dam, situated in Ethiopia, is founded on a thick alluvial layer that poses a potential risk of seepage, piping, and liquefaction, which could compromise the dam's stability and safety if appropriate remedial measures are not implemented. This thesis aims to comprehensively assess the potential impacts of seepage, piping, and liquefaction on Yanda Dam and evaluate the effectiveness of various remedial measures to mitigate these risks. Additionally, a thorough liquefaction assessment of the foundation will be conducted, and a suitable remedial measure will be recommended to ensure the long-term stability and safety of the dam.

1.3. Research Questions

The following issues have been identified as needing attention based on the problem description above;

1. What are the engineering geological features(like soil type, grain size distribution, permeability, and shear strength) of the foundation materials at the Yanda Dam site?
2. What is the potential for excessive seepage through the foundation, the risk of piping, and the likelihood of liquefaction under seismic load at the Yanda dam site?
3. What corrective actions are being taken to fix the deep alluvial deposit foundation associated with the problem of abnormal seepage, piping, and liquefaction to make the dam project safe and stable?

1.4. Objective of the study

1.4.1. General objective

The main goal of this study is to evaluate the Yanda Dam foundation's susceptibility to excessive seepage, piping, and liquefaction and recommend effective remedial measures to mitigate these risks.

1.4.2. The specific objectives are:

The following particular objectives are listed to fulfill the study's general objective:

- To characterize the engineering geological features of the Yonda dam foundation, including the soil type, grain size distribution, density, permeability, and shear strength.
- To evaluate the potential of excessive seepage, piping, and liquefaction through the Yanda Dam foundation, taking into account the hydraulic gradient, soil permeability, foundation geometry, soil density groundwater table, and seismic load, using both empirical and numerical methods.
- To recommend cost-effective and sustainable remedial measures for mitigating the risks of seepage, piping, and liquefaction in the Yanda Dam foundation.

1.5. Scope of the study

The scope of this study has been to assess the foundation of the Yanda Dam construction project, specifically the deep alluvium deposit foundation, and to identify and evaluate cost-effective and sustainable remedial measures for mitigating the risks of seepage, piping, and liquefaction in the foundation.

1.6. Limitations of the study

Since the project is far from Addis Ababa, about 630km, it was difficult to study the case as closely as possible and transportation cost was also high.

The Yanda Dam Project has a report on the final design and the paperwork proving its viability. In-situ and laboratory test output data are also included in the project. The well-known organization ECDSWC carried out the geotechnical investigation and then developed the design. However, some of the data is limited and insufficient for a comprehensive, advanced numerical analysis. Although the materials' strength (c and ø) and some of their elastic (ρ, v, G_{max}) characteristics were known, no data on their compressibility was provided. The permeability of the materials and the hydraulic conductivities at a certain depth of the foundation layer were also unknown. As a result, the author has employed typical values of the materials' permeability that have been accepted by various standards.

The biggest challenge was that the engineering design team used PGA data, and the values of PGA obtained from a geotechnical section were completely different. The justifications for both sections for adopting the various PGA values are that the engineering team claimed that the PGA value obtained from the geotechnical section is significantly higher. As a result, the amount of dam fallout that was planned would not be feasible or economical. The geotechnical section, however, asserts that the PGA value should be utilized exactly as it is for design purposes because the PGA was conducted by AAU and by the specialist, Prof. Ataly.

To make an informed decision, a detailed analysis was conducted to compare and contrast the two PGA values. The objective was to understand and justify the positions of both sections. The dam was modeled using both PGA values of 0.197g (from the engineering design team) and 0.497g (from the geotechnical section) to see the implications of the design. By analyzing the outcomes and evaluating how the dam performed under both PGA values, the decision-makers could better understand the implications of each value. This would help in determining the most suitable PGA value to use for the design of the dam.

In summary, the challenge arose from the discrepancy between the PGA values used by the engineering design team and the geotechnical section. To resolve this, a detailed analysis was conducted to compare the outcomes of using both PGA values in the dam design, aiming to justify the reasoning behind each section's position.

2. LITERATURE REVIEW

This literature review has focused on some studies, books, journals, and reports that have been used to discuss the challenges of foundations with deep alluvium deposits and problems like seepage, piping, and liquefaction. Here also discussed the lessons gotten from those studies and evaluated options for remedial measures.

2.1. Embankment dam

Overall, embankment dams have been the most commonly constructed type of dam throughout history. They are designed to take into account various topographic and foundation conditions, as well as utilize locally accessible geological resources. These dams make up about 85–90% of all dams and have several advantages that contribute to their dominance. (ICOLD, 1995).

Based on Novak et al. (2007) and Zhang, Y., & Zhang, C. (2004), embankment dams are versatile structures that can be constructed in various topographic and geologic conditions using natural materials like earth-fill and rock-fill, which lower construction costs. The mechanized construction process allows for quick and efficient project completion. The unit prices of these materials are also lower, making embankment dams cost-effective. They can withstand significant deformation and settlement, making them stable structures. However, there is a potential for anomalous seepage or piping, which can undermine the dam's integrity and pose risks to human lives. Overall, embankment dams offer a cost-effective and versatile solution for various construction needs.

It is important to note that dams come in different sizes, forms, and types. Regardless of the specific characteristics of an embankment dam, appropriate research and considerations should be conducted before making any decisions regarding its construction. (Sissakian et al., 2019).

2.1.1. Geotechnical Investigation of the Dam Foundation

The detailed engineering geology and geotechnical investigations of dam sites, which include surface discontinuity surveying and borehole data in situ as well as laboratory testing (Nezhad et al., 2012), may be used to determine dam foundation characteristics. Assessment of the ground condition above and below the surface is a part of engineering geological inquiry for engineering projects.

Due to the complexity of dam design and construction and the variety of foundation conditions, a geological study of the dam site is regarded as being of significant importance, especially because several projects have failed as a result of unfavorable geologic conditions (Agerie Genetu, 2007).

The design and construction process carefully considers geotechnical studies to guarantee the safety of a dam's foundation (Umoren et al., 2016). Drilling activities along with appropriate geotechnical on-site and laboratory tests, satellite image analysis, engineering geology mapping, seismicity research, and pertinent geophysical techniques may all be used to analyze the dam foundation (Barzegari, 2017).

2.1.2. Dam's Foundation and Its Challenges

According to Fell, R. (2005), accurately assessing the characteristics of a dam's foundation is crucial for ensuring dam safety. Factors such as the strength, permeability, and compressibility of the foundation contribute to the potential risks and vulnerabilities of the dam. Porous soil foundations are prone to leakage and erosion and require measures like filter drains and cutoffs to prevent seepage. Loose to medium-thick sandy soils and deep alluvium are susceptible to liquefaction and settlement, necessitating effective foundation compaction and filtering. By incorporating the findings of the foundation assessment into the dam's design, engineers can calculate its safety through data analysis, interpretation, and ongoing monitoring. Dam failure often starts with unnoticed abnormalities like seepage and liquefaction, emphasizing the importance of timely evaluation and interpretation of foundation data to ensure dam safety. Careful attention to foundation evaluation and monitoring is vital to mitigating risks and preventing catastrophic failures.

Dam failure is a complex process that often begins with unnoticed abnormalities like seepage and liquefaction. Rapid data analysis and interpretation are crucial for identifying and addressing these issues. A thorough evaluation of the dam foundation is necessary to ensure stability, considering factors like strength and permeability. Continuous monitoring of the dam and its foundation helps detect changes and potential risks, allowing for early interventions. This proactive approach, combined with data analysis and monitoring, is vital for preventing dam failure and ensuring safety (Johansson, 1997).

2.1.2.1. Alluvial Soils

Alluvial soil, or loose sediments, is formed from materials like clay, silt, sand, gravel, cobbles, and boulders eroded by streams. These materials are transported by floodwater or river water and eventually settle at low flow velocity. This process continues annually, increasing deposition thickness and raising river flow levels. Alluvial soil has several layers with unique coefficients of permeability, each with a significant thickness. These deposits are susceptible to differential settling, which can cause catastrophic collapse of constructions atop them. (Fell et al., 2014).

The significant variations in the thickness of the alluvial deposits and the presence of low strength are the two primary problems to consider while constructing a dam on alluvial deposits (Pawson and Rusell, 2014; Hedayati Talouki et al., 2015).

The heterogeneous nature of alluvial soil can make it anisotropic, meaning it has different properties in different directions. This must be considered during construction to ensure the stability and integrity of the project. The alluvium is not formed into a solid rock and can be easily eroded and transported by moving water. This means that erosion control measures must be implemented to prevent the loss of soil and maintain the stability of the construction site. Thesis No. G011/074: Dahal M., 2020.

Overall, construction projects on alluvial soil require careful planning and consideration of the soil's characteristics to mitigate the risks associated with its dynamic nature and potential for erosion.

2.1.3. Earthquake

Understanding the processes leading to earthquakes and their effects on the ground is crucial for earthquake engineering. Rock disintegration at a plate boundary releases strain energy, which causes an earthquake. Plate tectonics stores strain energy, and Earth's lithosphere moves widely due to plate tectonics. Dam reservoir filling can also cause an earthquake, as a strain-growing area has higher pore water pressure, reducing shear strength. The region where strain energy is released at plate boundaries is referred to as a focus or hypocenter. The epicenter is located just above the surface's focal point. The epicenter distance and hypocenter distance are

the distances between the observation location and the epicenter and hypocenter, respectively, according to L. Kramer (1996).

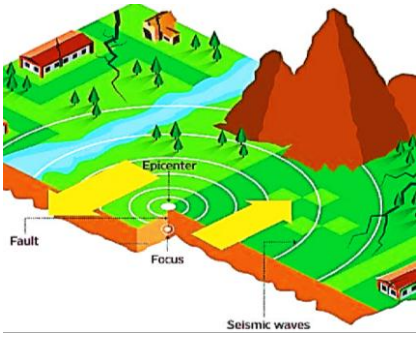

Figure 4 How an earthquake occurs
(https://www.pinterest.co.kr /pin/154740937174469866/)

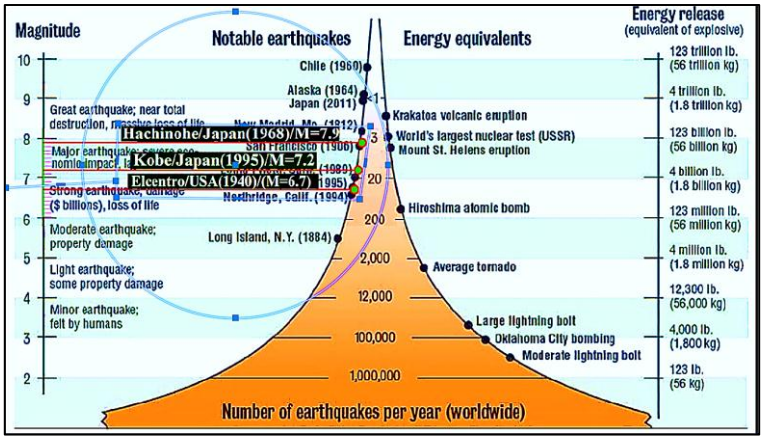

Figure 5 Earthquake Frequency and Destructive Power (Source: U.S. Geological Survey)

Based on the Geotechnical engineering of dams, by Fell R. et al., Earthquakes generate extra strain on embankment dams, which results in unanticipated, cyclical motion in both the horizontal and vertical dimensional axes. On faults running through the dam foundation, these impacts may result in internal erosion, liquefaction, and differential movements.

2.1.3.1. Seismic Design Criteria

Earthquakes have a major detrimental impact on social stability and economic prosperity, particularly in developing countries. An evaluation of the seismic hazard is necessary for prevention, preparedness, and response to reduce seismic risk. Sianko L. et al., 2020. ICOLD Bulletin 72 lists three categories for earthquake acceleration consideration based on Return Period. They are Design-Basis Earthquake (DBE), Operating-Basis Earthquake (OBE), and Safety Evaluation Earthquake (SEE). However, according to Wieland M. (2014) and [ICOLD Bulletin 148], the following design earthquakes are essential for a substantial dam project's seismic design:

2.1.3.1.1. Safety Evaluation Earthquake (SEE)

In the context of dam safety evaluation and seismic design, the Safety Evaluation Earthquake (SEE) is the main ground motion used. It is crucial to consider the highest possible ground motion to ensure that the dam can withstand seismic loads and prevent uncontrolled water

discharge. The SEE is determined based on the level of motion that is consistent with the maximum credible earthquake, which typically has a long return period of around 10,000 years. To determine the SEE ground motion, a seismic hazard analysis can be conducted using either a probabilistic or deterministic approach. The analysis takes into account the worst-case earthquake scenarios and calculates the ground vibrations that the dam body can endure. For large dams, the SEE can be calculated either as the Maximum Credible Earthquake (MCE) or the Maximum Design Earthquake (MDE), depending on the specific requirements and performance standards. MDE, Design Basis Earthquake (DBE), and Operating Basis Earthquake (OBE) ground motion parameters are typically calculated using a probabilistic method, which considers the probabilities of different earthquake scenarios occurring. On the other hand, MCE uses deterministic earthquake scenarios, which are pre-selected based on their potential to generate extreme ground motion.

2.1.3.1.2. Maximum Credible Earthquake (MCE)

The maximum credible earthquake (MCE) is the highest anticipated earthquake causing the highest ground motion at a dam site, determined using deterministic earthquake scenarios. It is the highest reasonably conceivable earthquake likely along a fault or within a geographically specified tectonic region. In cases where no evident earthquakes occur, a probabilistic technique with a long return period, like 10,000 years, is used to predict ground vibrations at dam sites, which may be weaker or more powerful than MCE ground motions assessed using a deterministic method.

2.1.3.1.3. Maximum Design Earthquake (MDE)

This is an important consideration in the design of dams, with return durations ranging from 10,000 years for major dams to shorter periods for smaller or dams with lower damage potential. The mean values of the calculated MDE ground motion parameters are collected after they have been estimated using a PSHA.

2.1.3.1.4. Design Basis Earthquake (DBE)

It has a 475-year return time and is a reference design earthquake for appurtenant structures. PSHA may be used to estimate ground motion parameters and provide the mean values.

2.1.3.1.5. Operating Basis Earthquake (OBE)

It is predicted to happen at some point throughout a dam's lifespan, with a 50% chance of doing so. According to Wieland (2014), the return period is 145 years, and a PSHA was used to determine the ground motion parameters. Only limited damage is authorized at the dam site, which is represented by the OBE. According to ICOLD Bulletin 72, the required minimum return period is 145 years.

2.1.3.2. Peak Ground Acceleration (PGA)

The calculation of ground motion characteristics like peak ground acceleration (PGA) and response spectra is the sole thing that seismic hazard evaluations typically focus on. For seismic hazard assessment, two methods are frequently used: probabilistic seismic hazard analysis (PSHA) and deterministic seismic hazard analysis (DSHA). A measurement of the ground's acceleration during an earthquake is called Peak Ground Acceleration (PGA).

To design, this is the most crucial parameter. Although ground movement can occur in any direction, it is commonly simulated horizontally (in two directions) and vertically because earthquake energy propagates from the hypocenter in waves. Table 1 below shows a relationship between seismic hazard rate and site characteristics. (ICOLD, 1989)

Condition(PGA)	Hazard	Remark
PGA < 0.1g	Low	
0.1g≦ PGA ≦ 0.25g	Medium	
PGA ≧ 0.25g	High	No active fault in 10km radius
PGA ≧ 0.25g	Extreme	With active fault in 10km radius

Table 1 Rate of Seismic Hazard

2.1.3.3. Acceleration Time History Data(ATH)

Time history data is needed to define the earthquake's character. Time history data are essential for earthquake dynamic research, but they are also frequently unavailable as data input. For the Yanda dam site, recorded time history data are not available. As a result, for this research, other recorded time history data have been compared by taking into account the points of ***Tectonic Environment***, ***Earthquake source to site distance***, ***Earthquake Magnitude***, ***and*** hypocentral distance for resemblance with the site which is under analysis, by the U.S. Army Corps of Engineers recommendation. However, the site peak ground acceleration should be scaled back

or modified, Messele (2006). Horizontal acceleration time histories are key input parameters for the dynamic Quake/W analysis. For an analysis of a dam, site-specific acceleration time history is used.

The Thesis of Yeabsra Tesfaye(2020), Getu Debebe(2022), Melaku Sitotaw (2017), Yared Mulat(2016), and ECDSWC's Feasibility Study and Detail Design of Yanda Dam used the following three recorded acceleration time-histories that are recorded elsewhere having their different unique features, this research also has used recorded data with further study of using PEER ground motion database.

The Imperial Valley Earthquake (1940) Elcentro Record in USA. (***M=6.7, H=11km, R=11.5km***)
The Hyogo ken-nanbu Earthquake (1995) Kobe JMA Record. (***M=7.2, H=14.3km, R=19km***)
The Tokachi-oki Earthquake (1968) Hachinohe Record in Japan. (***M=7.9, H=0 km, R=200 km***)

> **Where;** *M is ground motion magnitude, H is focal depth (distance from the epicenter to the focus) and R is the epicentral distance (distance from the point of interest to the epicenter) from a near source, Yeabsra Tesfaye(2020).*

2.1.3.4. Dam's Ground Response Analysis

Moustafa, A. (2012, February 10), in full non-linear dynamic analysis, soil stiffness reduction is automatically taken into account upon the constitutive model of soil and just the initial shear modulus is needed as an input parameter. Therefore, it is important to be sure that in the numerical model, the tendency of shear modulus decrease and damping ratio increase are in agreement with those of laboratory test results during dynamic loading.

If the dam materials keep their elastic behaviors during dynamic loading, then the horizontal acceleration increases along the dam height (from the base to the top). In this case, the higher dams show larger amplifications, especially if the natural periods of their bodies coincide with the periodical nature of earthquake waves.

When the dam body shows non-linearity or the materials go towards plastic behavior during strong shaking, the attenuation of acceleration waves in the dam body becomes more effective. Consequently, the amplitudes of earthquake accelerations decrease when moving from the base towards the top. Regarding a dam subjected to an earthquake with lower energy, the dam body behaves as an elastic material. Therefore, the induced seismic accelerations inside the dam body

become larger from the base of the dam to its top. In this case, small plasticity zones are developed in the dam body

According to the non-linear elastic-plastic analyses, when the height of the dam increases, the strongest dynamic loading induces plasticity in large parts of the dam body. Strong earthquakes are more effective in changing the material behavior from elastic to plastic condition in comparison with weak earthquakes. To this effect, The higher dams are more flexible than the smaller ones. Consequently, the flexibility affects the shear strains which influence the shear modulus reduction and attenuating coefficient. All these effects are on the trend of weakening the accelerations along the height.

2.1.4. Mechanism of Seepage in the Dam Foundation

Seepage is the pressure-induced flow through an earth mass. It is also used to describe the volume of water running through a foundation, soil structure, or soil deposit (Arora K.R., 2004). Seepage force is the force exerted by water on soil particles, causing pressure and dragging in the direction of its motion.

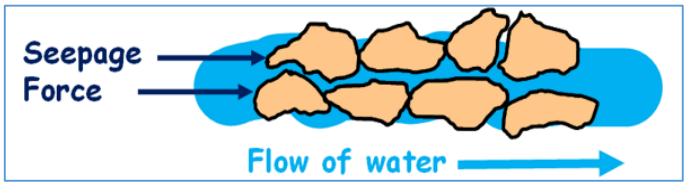

Figure 6 Seepage in hydraulic structure
https://elementoryengineeringlibrary.com

Water flow is influenced by energy gradients, pressure head, and elevation. Seepage, a term for flow issues involving gravity, refers to seepage losses from reservoirs to downstream departure points. In geotechnical engineering, seepage losses are calculated based on flow quantity.

A dam foundation is the primary area where seepage occurs most frequently. Dams cannot be entirely impermeable to their foundation, abutment, or embankment, but when they exceed the designed point, they become severe and abnormal (Gebremedhin Berhane, 2017). Therefore, engineering measures are crucial to take engineering measures to overcome these technical challenges (Chen et al., 2010) during the design process.

2.1.4.1. Mechanism of Piping

Piping is the creation of an open channel that runs from one place to another, Lane (1934). Seepage force applied horizontally or vertically, can cause soil particles to move in its path, potentially forming soil channels known as piping. Effective management and recovery of seepage through foundations are crucial to avoid piping and material removal. Dams on alluvial foundations may blow up, boil, or liquefy if seepage water comes from downstream at an excessively high gradient, causing slope instability and pipe failure.

Dams with high hydraulic gradients and previous foundations may experience piping failure due to soil particles being carried by water, causing the foundation to take the shape of pipes. Piping is a type of seepage failure, where reservoir water exerts a tractive force on soil particles, causing them to be removed at an unprotected seepage exit point. According to a summary by Foster et al. (2000a) of data from ICOLD and other research, 46% of all dam collapses could be attributable to pipes.

Based on the type of erosion that occurs, earth dam piping may be divided into four categories: Concentrated Leak Erosion, Backward Erosion, Suffusion(internal instability), and Soil Contact Erosion (Bonelli 2013; ICOLD 2015; USACE and USBR 2015).

2.1.4.1.1. Concentrated Leak Erosion

According to Fell and Fry (2007), ***Concentrated Leak Erosion*** refers to the erosion of soil in a fracture or a network of connected voids in an earth dam or its foundation. (Chart 1)

2.1.4.1.2. Internal Instability (Suffusion)

Suffusion is the process by which the finer grains of broadly graded or gap-graded soil are carried away, leaving only the bigger grains to keep the soil structure together (Bonelli, 2013). Only the bigger grains contribute to the soil skeleton in an internally unstable soil, whereas the finer grains "float" freely in the voids. (Chart 1)

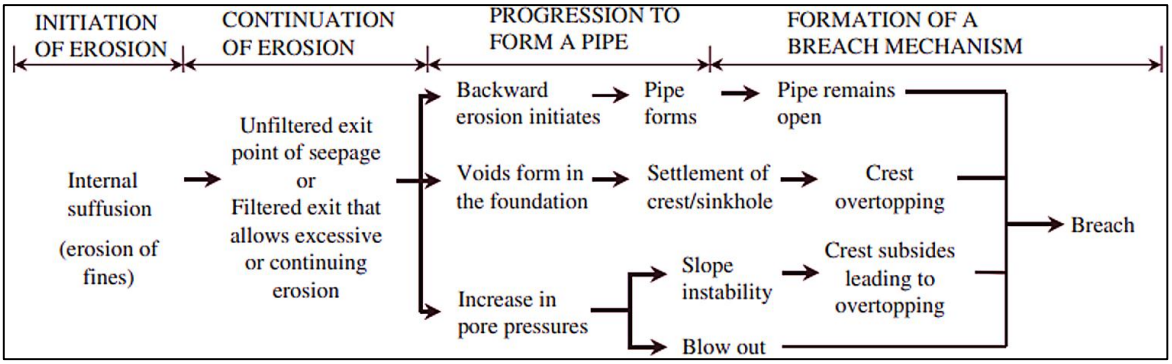

Chart 1 Failure path diagram due to foundation-suffusion (Foster, 1999)

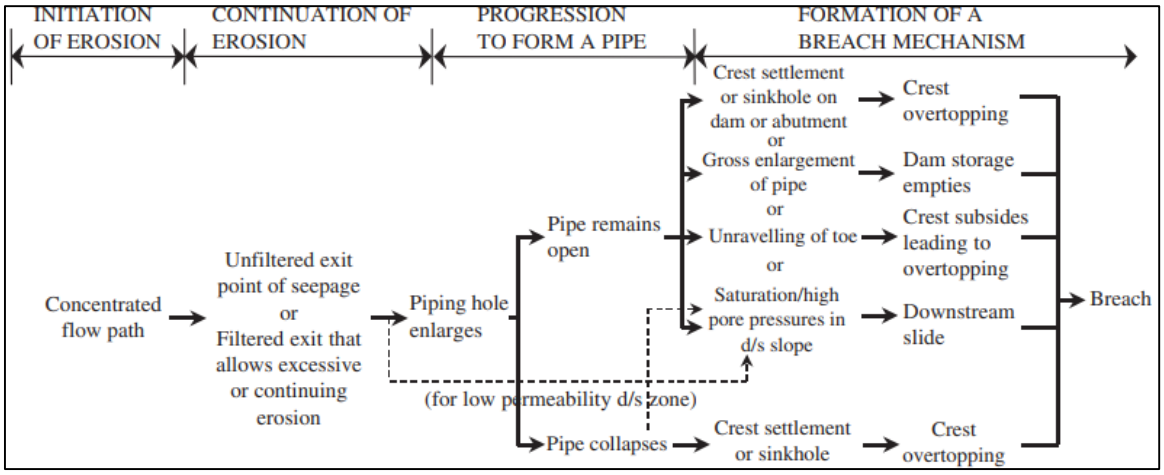

Chart 2 Failure path diagram due to foundation-backward erosion (Foster, 1999)

2.1.4.1.3. Heave Piping Failure

Heave is a condition when a building's foundation grows, pushing it upward and potentially undermining its structural integrity. Strong gradients can reduce effective stresses along the vertical to zero, putting the soil in a fluidized condition or quicksand formation. The heave equation or critical exit gradient from Terzaghi (1943) is given by;

$$i_{cr} = \frac{\gamma_b}{\gamma_w}$$ where γ_b = buoyant unit weight of the soil; and γ_w = unit weight of water.

The Terzaghi rule (1929) is a useful criterion for heaving control, with a safety factor of 3-4.

2.1.4.1.4. Backward-Erosion Piping (BEP)

Terzaghi characterized piping as the gradual backward erosion of particles from concentrated leakage exit points (Terzaghi 1922,1939,1943). BEP will begin when a "heave" or zero effective stress situation arises in sands, as stated by Terzaghi et al. in 1996. Hydraulic systems allow water to percolate through the soil and escape vertically upward at the downstream end.

This process creates a pipe-like opening below the dam, which is moving upstream in the reverse direction, known as backward erosion piping. This phenomenon is provoked as the hydraulic gradient becomes strong, shortening the flow path and further removing particles. Backward erosion pipe failure occurs when the exit gradient is greater than the critical hydraulic gradient.

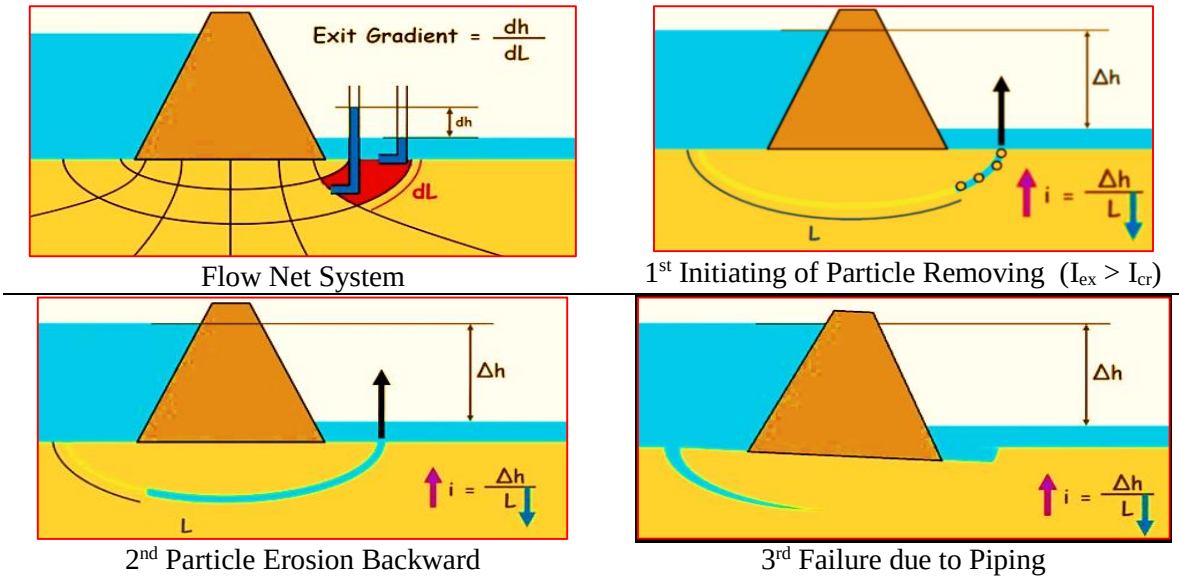

Figure 7 Process of Failure due to piping backward erosion
https://elementoryengineeringlibrary.com

In the situation of critical hydraulic gradient; The force of water and the particle's force are balanced and the soil grain particles become buoyant. The line-of-creep approaches of Bligh (1910), Lane (1935), and Khosla's Theory are all techniques for determining the crucial gradient for a pipe's advancement.

2.1.5. The Three Theories for Piping

2.1.5.1. Bligh's Creep Theory for Seepage Flow

In this theory, Water creeps down the structure's bottom in a contour form. The length of the creep is the distance traveled by water along the contour route. Here assumed that the head loss is proportionate to the length of the creep. The limitation of Bligh was that he failed to distinguish between the length of creep that was horizontally and vertically oriented. Bligh asserted that the safety against pipes would be maintained by giving enough creep length, denoted by **L = C.H**, where C is the soil's Bligh's Coefficient.

2.1.5.2. Lane's Weighted Creep Theory

The empirical "Weighted-Creep" hypothesis was established by Professor E. W. Lane after studying dam designs all across the world on 200 dams. According to this hypothesis, a dam's base and its vertical contact create a line of flow, with vertical contact being more effective than horizontal contact. For horizontal creep, the theory recommended that weightage factor of 1/3, compared to 1.0 for vertical creep. Although the flow pathways were treated differently, Lane's empirical correlation and Bligh's are similar.

The empirical calculation procedure developed by Lane's equation, known as the weighted creep method, is shown below:

$$Ln = cH \text{ and } c = Ln/H$$

Where: *- Ln = minimum safe flow length,*
C = safe weighted creep ratio
H = hydrostatic head across the structure.

It is noted that The hydraulic gradient, H/L, becomes equal to 1/C as a result.

2.1.5.3. Khosla's Theory and Concept of Flow Nets

This theory's central tenet is that seepage water flows through a series of streamlines rather than following the bottom contour as Bligh had originally proposed. For homogeneous soil, the Laplacian equation has been used for this theory in the condition of steady seepage. The streamline and the equipotential line, two sets of curves that meet one other orthogonally, are represented by the following equation. A Flow Net is the name for the resulting flow diagram that displays both curves as shown in Figure 8.

$$\frac{d^2\phi}{dx^2} + \frac{d^2\phi}{dz^2}$$

Where; ø = flow potential = Kh; K = the co-efficient of permeability of soil as defined by Darcy's law, and **h** is the residual head at any point with the soil

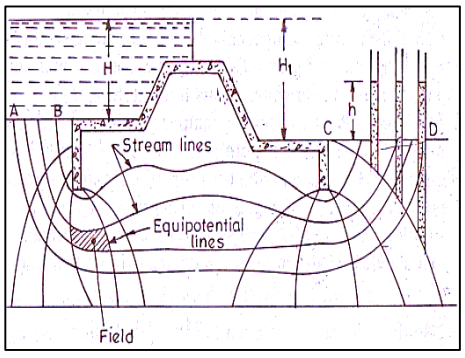

Figure 8 Khosla's Flow Net

Streamlines represent water flows through the sub-soil, with particles entering at specific points upstream of the work following their paths. The first streamline, which is the same as Bligh's path of creep follows the bottom contour, while the remaining streamlines follow smooth curves from the foundation outline to a semi-ellipse. Equipotential lines represent the joining of points with equal residual heads, allowing water to rise in all of them up to the same level.

Khosla's exit gradient is formulated as follows;

$$G_E = \frac{H}{d} \times \frac{1}{\pi\sqrt{\lambda}}$$

Where;
b = floor length,
d = vertical cut-off of depth

$$\lambda = \frac{1+\sqrt{1+\alpha^2}}{2}$$

α = b/d
H = Maximum Seepage Head

2.1.5.4. Exit and Critical Gradient

A tangential force ***f*** is generated by water seeping the subsoil and is always tangential to the streamline. The weight of the soil particle submerged in the fluid causes the streamlines to bend upward, producing a tangential force ***f*** that has a downward force ***w*** and a vertical component ***f1*** as well. The submerged weight needs to be heavier than the upward vertical component of ***f1*** to prevent soil particle dislodgement, guarantee soil stability, and avoid erosion and piping. The water pressure gradient ***dp/dl*** determines the force of the vertical component that points upward. The force ***f1*** equals the weight of the soil particle immersed, suggesting a critical gradient, if the exit gradient is critical.

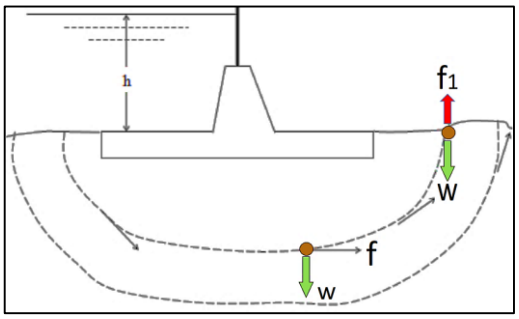

Where;
f_1 is the upward disturbing force on the grain,
w = Submerged Weight,
f = Pressure gradient at a point,
Gs = Specific Gravity,
n = Porosity,
γ_w = unit weight of water
$dp/dl = \gamma_w * dh/dl$, $dh/dl = (G_s - 1)(1-n)$

In the equations below, According to EM 1110-2-190, i_{cr} will be approximately 1 if normal sand Gs, e, and n values are utilized. According to their research, the ranges for the escape gradient's factor of safety ranges from 1.5 to 15, depending on the soil's properties and any potential seepage situations.

$$i_{cr} = (G_s - 1)(1 - n)$$ ……*Equation 1*

$$n = \frac{e}{1 + e}$$ ……*Equation 2*

$$i_{cr} = \frac{G_s - 1}{1 + e}$$ ……*Equation 3*

$$I_e = (h_1 - h_2)/L$$ ….*Equation 4*

$$FS = \frac{i_{cr}}{i_e}$$ Equation 5

Where;
Gs = Specific Gravity
e =Void Ratio
n = Porosity
FS = Factor of Safety
I_e = Exit Gradient
h_1 = U/S hydraulic head
h_2 = D/S hydraulic head
L = Length flow path

2.1.6. Control Methods of Foundation Piping

Based on Arora K.R.,2004, the percolation route (L) affects the hydraulic gradient (i). When the path's length is expanded, the exit gradient will drop to a safe level. Adopting the following (*figure 9 a, b, c*) strategies would lengthen the percolation process. As flow length is increased, the Exit Gradient becomes lower.

As stated in the US Army Corps of Engineers / EM 1110-2-1901, The techniques for preventing under-seepage in dam foundations include Horizontal Drains and Cutoff(Complete and Partial).

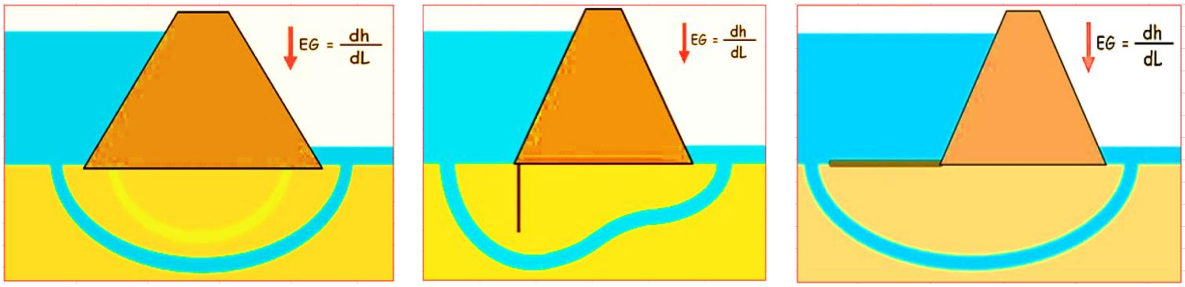

(a) Base width option *(b) Cutoff option* *(c) U/S blanket option*

Figure 9 Options of expansion of flow path *https://elementoryengineeringlibrary.com*

2.1.6.1. Increasing The Dam's Base Width

To preserve pipes, the percolation length is made longer by lengthening the dam's base (*figure 9a*)to the extent that the design requires. Although there is a possibility to expand the flow route, the project costs increase and become uneconomical because of the greater amount of embankment dam fill material. Therefore, it is best to think about other choices.

2.1.6.2. Cutoffs.

There are two types of Cutoff Control methods. The first one is ***Complete Cutoff*** (compacted backfill trench, slurry trench, or concrete wall, see *Figure 9b*) and the other is ***Partial Cutoff*** (U/S impervious blanket, D/S seepage berm, toe trench drain, or relief walls). It may be recommended when the dam foundation is made of a relatively thick deposit of previous alluvium.

According to Sherard (1968), the following factors should be taken into account when choosing the sort of under-seepage control measure:

i. A cost-benefit analysis of the potential loss of water versus the price of the complete cutoff
ii. A complete cutoff is preferable to the foundation which has layers of fine sand or cohesion-less silt, especially if these soils are exposed on the surface of the valley floor when compared with the foundation which is mostly made of gravel or coarse sand. In fine cohesion-less soils, even a small concentrated leak that emerges below the dam might be harmful, however, If a substantial leak occurs in coarse alluvium, backward erosion is probably protected.
iii. When the amount of silt and clay-sized particles suspended in river water increases over time, a reservoir tends to silt-up and seepage capacity tends to decrease gradually.

2.1.6.3. Compacted Backfill Trench

Excavating a trench through previous foundation strata and backfilling it with compacted impermeable material is the most effective way to manage under-seepage.

2.1.6.4. U/S Blanket fill

According to EM 1110-2-2300, Barron 1977 and Thomas 1976, an upstream impervious blanket, tied into the dam's impervious core, can be used to minimize underseepage when a complete cutoff is not required or is too costly. However, it should not be used when the reservoir head exceeds 60.96m as the hydraulic gradient acting across the blanket may result in piping and leakage. The effectiveness of upstream impervious blankets depends on their length, thickness, and vertical permeability, as well as the stratification and permeability of soils on which they are placed. The benefits of the impervious blanket are due to the dissipation of a part of the reservoir head through the blanket. A filter material is typically required between the blanket and foundation.

Design considerations for upstream impervious blankets include the flow through the blanket being vertical, the flow through the previous foundation being horizontal, all flows being laminar and steady state, the dam (or core of a zoned embankment) being impervious, and both the blanket and substratum having a constant thickness and horizontal permeability.

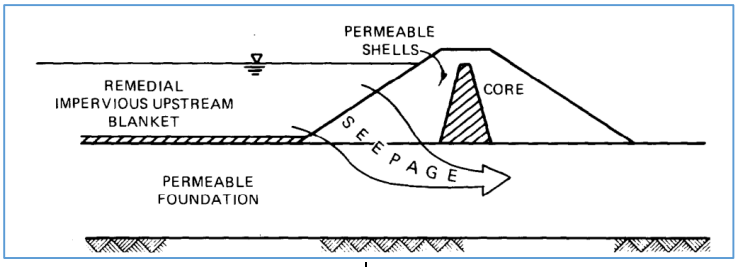

Figure 10 Remedial impervious u/s blanket | (prepared by WES, EM 1110-2-1901, Page 12-5)

2.1.6.5. Slurry Trench Cutoff.

The slurry trench cutoff may be an effective solution for controlling under-seepage when the compacted backfill trench is too expensive and/or unfeasible due to the expense of dewatering and/or the depth of the previous foundation. Slurry trench cutoffs consist of a continuous trench excavated utilizing a backhoe, dragline (clamshell), or a combination thereof. The trench is dug through the previous foundation and the sides are supported by a slurry of water and sodium bentonite clay. The slurry-filled trench is backfilled by replacing the slurry with a backfill material(soil) that contains enough fines (at least 10% silt and clay particles that pass the No. 200 sieve) to make the cutoff somewhat impervious but enough coarse particles to minimize trench settlement, forming a **Soil-Bentonite Cutoff** (American technique).

The slurry trench is constructed 1 m to 3 m wide. The maximum depth depends on the method of excavation. ICOLD (1985) and Xanthakos (1979) indicate that practical maximum depths are: 10m Backhoe (Excavator), 20 m Dragline, and 25 m Dragline and Clamshell for slurry trench, cutoffs. ICOLD (1985) indicates that the backfill will normally consist of bentonite slurry, with 5–15% bentonite (by weight). 0.6 to 0.9 m of concrete may be poured at the **bottom of the trench** in some circumstances to prevent the base from eroding due to seepage flows.

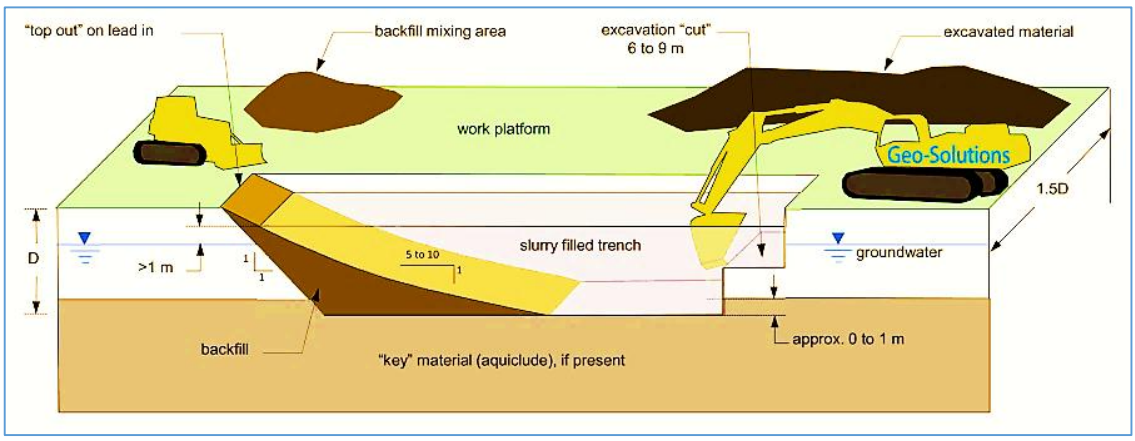

a. *Schematic (cross-section) of slurry trench construction (courtesy of Geo-solutions, Inc.)*

b. *Backhoe (Excavator) https://www.geo-solutions.com/services/slurry-walls/cement-bentonite/*

c. *Photo of long-armed excavator taken in the Kuraz Irrigation Project(See more in Appendix)*

Figure 11 Backhoe (Long armed Excavator) for soil bentonite cutoff work

Alternately, cement may be added to the slurry-filled trench and allowed to harden or set, making a **Cement-Bentonite Cutoff** (also known as a grouted diaphragm wall or the European technique). (US Army Corps of Engineers/EM 1110-2-2300). Trench Cutoffs for Soil-Bentonite and Cement-Bentonite Slurry are compared. A soil-bentonite slurry trench cutoff has no shear strength and can only impose hydrostatic pressure and as was done at West Point Dam in Alabama and Georgia, when the groundwater table is situated some distance below the surface of the ground, it is typically more cost-effective (U.S. Army Engineer District, Savannah 1968).

Based on USSD(2011), materials for embankment dams, comparisons between soil-bentonite and cement-bentonite cutoffs are frequently done since they are widely employed technologies in the US. Hydraulic conductivity, deformability, and strength are the main attributes to be concerned about. A soil-bentonite wall will often have lower strength than a cement-bentonite wall, but it will also be more flexible and less permeable. Cement-bentonite walls may therefore be particularly susceptible to cracking when significant foundation deformations are predicted

underneath an embankment dam. However, due to issues with backfill proportioning, mixing, and placing, soil-bentonite walls are more susceptible to construction errors than cement-bentonite walls. In addition, because of their lesser strength, soil-bentonite walls could be more prone to hydraulic fracturing than cement-bentonite walls under high heads.

Item	Soil Bentonite Slurry Trench Cutoff	Cement-Bentonite Slurry Trench Cutoff
Excavation	-Difficult to work with coarse gravels, with ***Backhoe*** and/or ***Dragline***. - Wider trench required to prevent segregation during backfilling (≥ 91.44 cm) and prevent piping failure of the slurry trench	- Construction sequence is more flexible to meet site Constraints. - Easier to remove coarse gravels with ***Clam Shell Mounted***. - Narrower trench (60.96 – 91.44 cm) may be used.
Slurry	Mixture of Soil, bentonite and water used to support excavation during trenching. Slurry displaced by backfill is desanded and reused.	Mixture of cement, bentonite, and water used to support excavation for panel and later sets to form permanent backfill. No disposal or desanding of slurry required.
Permeability	= 10e-09 m/sec (≥ 1 percent bentonite)	=10e-08 m/sec
Groundwater	Not Susceptible to Chemical Sensitivity	Yes cement may be Susceptible to Chemical Sensitivity
Relative Cost	Generally lower	Generally higher due to cost of cement.

Table 2 Soil versus Cement-Bentonite Slurry Cutoffs.
(US Army Corps of Engineers EM1110-2-1901)

Historically, to create a partial cutoff along the Mississippi River levee, the U.S. Army Engineer District in Memphis first started using the slurry trench construction technique in 1945. In 1952, a soil-bentonite slurry trench cutting was built in Washington beneath the Kennewick Levee near the Columbia River. At Wanapum Dam on the Columbia River in Washington, a soil-bentonite slurry trench cutoff was used for the first time in 1959 to manage under-seepage at a significant earth dam. At some dams, soil-bentonite cutoffs have been employed to reduce under-seepage. In 1969, the Razaza Dam on the Euphrates River in Iraq first employed the cement-bentonite slurry trench cutoff to connect to the abutment zones.

For the management of seepage, soil-bentonite slurry trench cutoff walls are frequently employed, according to Evans & Ruffing's 2017 article, "Design and Construction of an Experimental Soil-Bentonite Cutoff Wall" (researchgate.net). The soil-bentonite (SB) slurry trench cutoff wall is the most popular form of vertical barrier in the US. It gets its name from the final barrier materials' nature (SB) and the construction process (slurry trench).

According to Javanmard et al.'s (2018) investigation on the impact of the cutoff wall's penetration length on the earth dam's core and foundation, for engineering embankment dams, seepage and water movement in the soil are two of the most crucial factors. Using a plastic concrete cutoff wall is one way to prevent seepage in the alluvial foundations of earth dams. As one popular way of connecting the cutoff wall and the core, the cutoff wall continues within

the clayey core for improved seepage control. In many static and dynamic load circumstances, the interaction between the core and foundation with the cutoff wall is particularly significant due to the stiffness difference between the core material and the cutoff wall, as well as due to the geological condition, and physical and mechanical characteristics of rock and foundation. Cut-off wall failure occurs at the junction between the cut-off wall and core. Therefore, it is crucial to investigate their interplay, especially when an earthquake occurs.

Based on Brown and Anderson (1980), D'Appolonia (1980a), and D'Appolonia (1980b), interaction with soil and groundwater can have different kinds of effects on the physical characteristics of the soil-bentonite slurries. Batches of soil-bentonite mixtures will be tested in the lab to understand how the bentonite reacts with the local soil and groundwater and to determine the physical characteristics that result, such as consistency, strength, and permeability, that will be used to ensure the construction of the soil-bentonite cut-off walls. To ensure that design functions are satisfied, additives may be included in the mix design, if necessary.

2.1.7. Case Studies Based on Seepage Analysis

2.1.7.1. Ghordanloo Dam, Iran

The research was done by Hedayati Talouki .H., Lashkaripour, G.R., Ghafoori, M. et al. 2015. Was aimed to assess the seepage problems in the Ghordanloo dam foundation and present a proper method of water-proofing. The maximum thickness of alluvium in the dam axis is up to 60 meters. To prevent seepage, the permeability of alluvium was determined to be between 10-2 to 10-6 cm/s.

Based on the rate of seepage, hydraulic gradient values, and safety considerations, a suitable water-proofing technique was suggested. Seepage and hydraulic gradient are the two considerations when selecting the best possible water-proofing system. The dam body and alluvial foundations were modeled using SEEP/W software, and water seepage potential was determined through numerical analyses. The ideal depth and position for water-proofing the dam foundation were determined using SEEP/W program analysis.

Clay blankets may be in danger of collapse in the event of a rapid drawdown in the reservoir's water level, but this risk is reduced when the blankets are positioned beneath the crest.

Therefore, an appropriate method for preventing seepage and raising the safety factors of dams is to use a clay blanket beneath the upstream crest of dams and to place cutoff walls. The cutoff wall will be built at the upstream toe at its ideal depth, which is 40 meters. As a result, seepage is decreased by 50%, and the safety factor is calculated at 1.53.

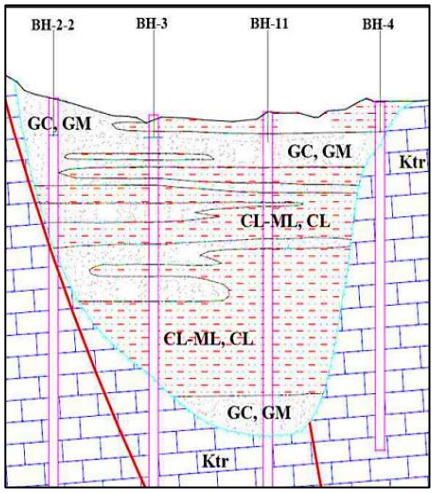

a. Cross-section A-B of the soil deposits

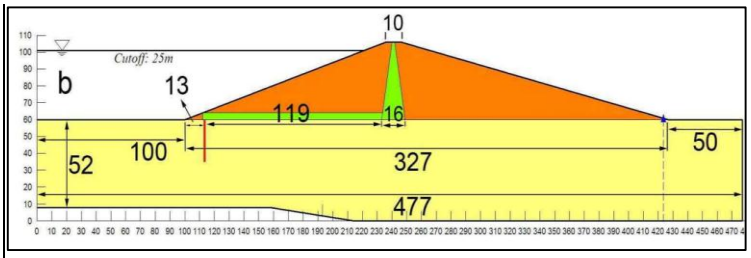

b. *Dam and the foundation model in software*

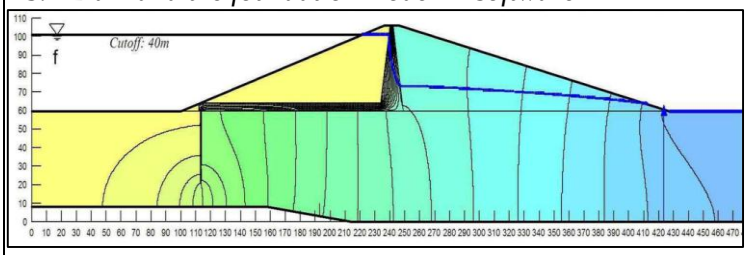

c. Results of seepage analysis

2.1.7.2. Alluvium Foundation of Tarbela Dam Project, Pakistan.

As document World Bank Project Completion Report Of Tarbela Dam,1986, and The research, which was done by Muhammad Tariq S.2003, demonstrated that immediately following its first filling in 1974, Tarbela Dam, the highest volume rock and earth fill dam, experienced significant seepage issues through its 210 m deep alluvium foundation and its dam high was 143m. Due to the significant seepage, the reservoir was empty during an emergency drawdown. Upon emptying the reservoir, many sinkholes in the impermeable blanket upstream that had been causing significant seepages were discovered. During the investigation and searching experience, subsequent inquiries revealed that sinkholes had occurred in the upstream blanket of Arrow Dam in Canada (subsequently renamed the Keenleyside Dam which was completed in 1968). It was concluded that based on the Tarbela experience it was recognized that sinkholes must be anticipated where blankets rest on gravel and sand alluvial foundations and differential settlement can occur.

2.1.8. Liquefaction Under Dam Foundation

Allen Hazen used the word "liquefied" in soil mechanics to describe the collapse of the Californian Calaveras Dam in 1918. According to the stating of *Sarfraz Ali, 2012, Arthur*

Casagrande introduced the concept of liquefaction in 1935 and 1938, involving concepts like *Shear Strength*, *Effective Stress*, and *Pore Water Pressures*. By losing their shear strength temporarily, soil sediments below the water table behave more like a viscous liquid than a solid. This is a phenomenon also known as liquefaction.

In an earthquake, soil can fail due to liquefaction, which can have devastating effects like land sliding, lateral spreading, or significant ground settlement, according to the book Advances in Geotechnical Earthquake Engineering-Soil Liquefaction and Seismic Safety of Dams and Monuments, edited by Abbas Moustafa (2012). Engineers became aware of the soil liquefaction phenomenon during the 1964 Alaska earthquakes and the Niigata earthquakes. When soil loses strength and rigidity due to earthquake shaking or other sudden loads, it is said to liquefy. In past earthquakes all around the world, liquefaction and associated processes have caused enormous amounts of damage (Borchardt, 1991). During the Bhuj earthquake on 26th January 2001 (M=7.7) a lot of damages occurred due to liquefaction.

Liquefaction is a significant earthquake effect, causing water-saturated cohesion-less soil to lose strength and fail during shaking. This occurs due to cyclic shear stresses reducing effective stress, which controls soil strength. In saturated cohesion-less soils, liquefaction occurs due to increased reducing effective stress during rapid ground movement. The strength and shear stiffness of the soil is decreased by the passage of a seismic wave, increasing the pore water pressure brought on by cyclic deformations (Taiebat, Shahir, and Pak, 2007). Similarly, *Getu Debeb,(Thesis 2022 AAU),* in seismically active regions, an embankment dam with a liquefiable soil foundation may experience severe instability as a result of earthquakes.

2.1.8.1. Mechanism of Soil liquefaction

It is important to comprehend the mechanism of soil liquefaction, where it occurs, and why it occurs so frequently during earthquakes, claims Abbas Moustafa (2012). The soil liquefaction mechanism is well seen in *Figure 12*. Particle form, size, and gradation all affect how pore water pressure develops. When a shear wave travels through saturated soil layers during an earthquake, the granular soil structure deforms and the weak area of the soil starts to collapse. As the lower layer is filled with collapsed soil, the pore water pressure in this layer is forced to rise. Increased water pressure will continue to build up if it cannot be discharged, and beyond a certain point, the effective stress on the soil is zero. When this happens, the soil layer loses its shear strength and is unable to guarantee the weight of the soil layer above as a whole. As a

result, the soils in the upper layer are prepared to slide downward and act like a viscous liquid. Soil liquefaction is then claimed to have taken place.

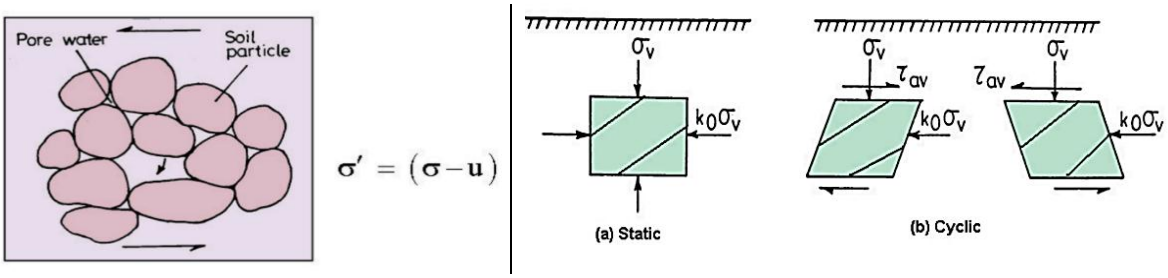

Figure 12 Mechanism of soil Liquefaction

2.1.8.2. Factors Influencing Liquefaction Susceptibility

Soil can be stated whether it has the potential of liquefaction or not depending on various factors. Those factors are;

Earthquake intensity and duration: If the intensity of the earthquake or its magnitude of the required dam site is higher, there is a chance of the phenomenon of liquefaction. In addition to that, if the duration of that earthquake is more, there is also the chance of liquefaction existence.

Soil type: If the soil of the required site is characterized as loose, the site is more susceptible than dense soil.

Particle size distribution: When the particle size distribution is uniformly or poorly graded, the kind of soil will be more prone to liquefaction than the soil well-graded.

Contents of plastic fines: The presence of high plastic fines in the required soil helps to reduce the risk of liquefaction to some extent compared to the absence of fine content.

Groundwater table location: The site where the groundwater table is closer to the ground surface is more susceptible than that where it is deeper from the ground surface.

Hydraulic conductivity (permeability): When a foundation has a high value of permeability, it is not prone to liquefaction. Because, during the seismic load, the water can move out easily before developing the pore water pressure. Since there is sufficient ability for water to escape through the grain structure of that soil without a pore water pressure effect in the soil and the effective stress is not reduced, liquefaction cannot be the problem.

Placement conditions or depositional environment: The soil, which is placed in a natural process like alluvial or colluvium transport on a required site, is considered prone to liquefaction. However, the soil, where it is placed layer by layer with a fixed depth and compacted regularly, is not susceptible to liquefaction.

Aging and cementation: When a foundation soil is found in deep depth from the ground surface, that soil layer is considered aged, and the soil particles are highly bonded due to cementation, the soil is going to be characterized as not liquefiable material.

Overburden pressure: Where the soil is found under the overburden load of a natural mountain, structural dam, or others, the soil layer does not have the chance of liquefaction susceptibility. Under those overburden loads, the effective pressure is higher than in other places. (See this research in the title of stress distribution.)

Historical liquefaction: If a required site or project is located around or in an area that has had an earthquake recorded and has experienced the earthquake two or more times, the site has the chance of being susceptible to liquefaction.

2.1.8.3. Liquefaction Types and Loading

The static and dynamic stresses (repeated loading) that take place during earthquakes speed up the development of periodic liquefaction-related deformations. In cohesion-less soils, rapid loading causes densification, which raises pore pressures and lowers effective stresses. **Flow liquefaction** and **cyclic mobility** are two different forms of liquefaction phenomena (Kramer, 1996).

i. Flow Liquefaction;

It is the most serious occurrence, known as flow failures, and occurs when the static shear stress is greater than the liquefied soil's shear strength. Flow failures refer to the situation in which there is a strain-weakening reaction to undrained loading. Note that strain-softening soils can also experience cyclic softening (cyclic liquefaction or cyclic mobility), depending on the ground geometry. A process known as "**flow liquefaction**" occurs when the static equilibrium of sedimentary soils with residual resistance is disturbed by static or dynamic stresses. If the

initial shear stress state of a soil sample is greater than the steady-state strength, the soil will experience **flow liquefaction**.

ii. Cyclic Mobility;

Cyclic mobility, also known as **temporary liquefaction or** "**cyclic liquefaction,"** occurs when the shear stresses are never zero. It happens when a liquefaction phenomenon in soil deposits with static shear stresses less than soil strength occurs in cyclic loading due to static and dynamic forces during earthquakes. While an earthquake is shaking, failure increases with time. **Temporary liquefaction** refers to the situation when there is a limited reaction to strain weakening in undrained loading; with greater strain, the characteristic is strain hardening. The phenomena occur in both cohesion-less and clay-content soil, and they apply to monotonic (static) as well as cyclic loading. During **cyclic loading**, the situation known as ***"initial liquefaction"*** occurs when effective stress is suddenly zero. If the initial stress state of a soil sample is less than the steady-state strength, the soil is susceptible to **cyclic mobility.** It occurs as the pore pressures accumulate with each loading cycle. Most engineers agree that initial liquefaction occurs when pore pressure equals the effective confining stress.

$$r_u = \frac{u}{\sigma_v'} = \frac{\sigma_v'}{\sigma_v'} = 1.0$$

Where: r_u=Pore Water Ratio
u=Excess Pore Pressure
σ_v'=Effective stress

Liquefaction initiation is potentially expressed in terms of capacity, demand, and factor of safety.

$$FS_{Liq} = \frac{capacity}{demand} = \frac{resistance}{loading} = \frac{\tau_{cyc,L}}{\tau_{cyc}}$$

FS_{Liq}=factor of safety against liquefaction triggering
$\tau_{cyc,L}$= lab cyclic shear stress required to trigger liquefaction
τ_{cyc}= applied lab cyclic shear stress

Then, when the cyclic shear stresses are normalized by the effective vertical stress, the factor of safety is going to be correlated with the division of the Cyclic Resistance Ratio(CRR) and Cyclic Stress Ratio(CSR).

$$FS_{Liq} = \frac{\tau_{cyc,L}/\sigma_v'}{\tau_{cyc}/\sigma_v'} = \frac{CRR}{CSR}$$

Cyclic Stress Ratio (CSR): it is represented as the load that is applied to the soils, and it is computed in one of the two options.

1. **Site-Specific Site Response Analysis:** in this analysis, an equivalent linear or nonlinear site response analysis is performed and directly computes the cyclic shear stress with depth (layers). Usually, the average is taken from a bunch of ground motions.
2. **Simplified Method** (Originally Seed & Indriss, 1971) This method is also called the empirical approach, and the majority of engineering practices have used this approach.

Cyclic Resistance Ratio (CRR); CRR is measured either directly in the lab or using in-situ tests (SPT N values) and adjusted by multiplying with the Magnitude Scaling Factor (MSF), initial shear stress correction factor, and overburden correction factor. However, even though it accounts for any initial shear stresses already in the soil, it is usually neglected by most methods today for flat ground conditions.

2.1.8.4. Evaluation of the Liquefaction Potential

A serious impact of earthquake shaking is liquefaction. Depending on their original formation density and cyclic stress history, cohesion-less soils are capable of developing pore pressures high enough to result in total shear strength loss at no effective stress or severe deformations with limited space for strain. [Seed et al., 1975]

2.1.8.4.1. Liquefaction Evaluation related to Granular material

This criterion considers the uniformity, grading, and particle size of the material for determining liquefaction potential. According to design standards No. 13 of Embankment Dams, non-cohesive (granular) soils, such as clean sands or sand-gravel mixes, silty sands with non-plastic fines, non-plastic silts, etc., are principally responsible for liquefaction. In general, well-graded soils are less prone to liquefaction than poorly-graded soils. The bulk of liquefaction failures in the field, according to Seged and Haile (2010), have been caused by uniformly graded soils. Kramer said that the majority of liquefaction failures in the field had been caused by unevenly graded soils. Hence, the pore water pressure development primarily depends on particle shape, size, and gradation. It may be very hazardous to build a dam on loose, saturated granular soil.

Identification of the soil's grain size distribution is therefore the first stage in assessing the risk of liquefaction. The assessment of liquefaction potential and limits between liquefiable and non-liquefiable soils has been conducted using the particle size distribution based on Graph-a, which was developed by Tsuchida in 1971 and is widely utilized by geotechnical engineers across the world, and Graph-b describes *limitations in the particle size gradation curves as suggested by the USNRC (1985).* In the graph, there is a region of boundary for most liquefiable soil that is narrow, showing more uniformity of particle size.

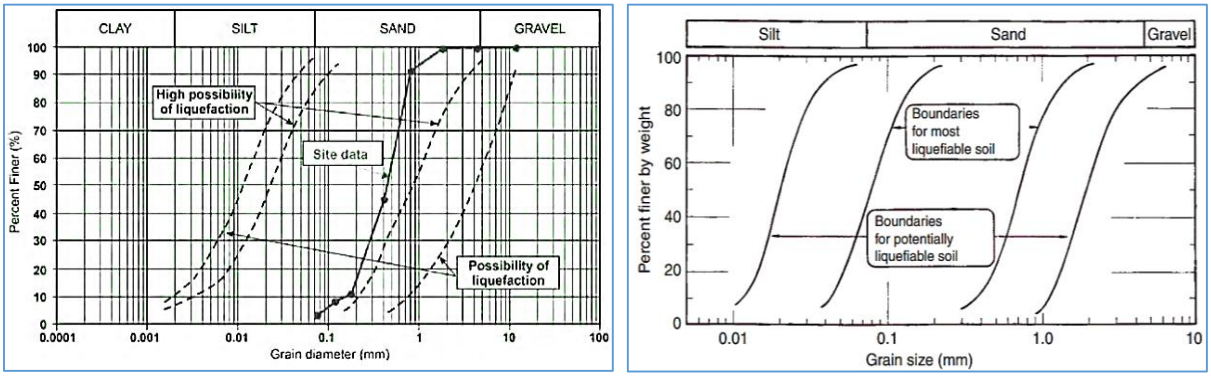

a: Tsuchida curve by Tsuchida 1971 *b: Gradation Curve (USNRC, 1985).*

Graph 1 Gradation Curve for Liquefaction Evaluation

2.1.8.4.2. Liquefaction Evaluation Related to Fine-Grained and Clayey

Clayey soils are frequently more liquefaction-resistant. Ishihara (1993), for instance, found that for PI larger than 10, the liquefaction resistance improves with increasing PI from laboratory cyclic shear testing on Mochi-Koshi gold mine tailings (waste material). In clays, liquefaction has only ever happened close to the ground's surface, where there is little effective pre-consolidation stress and little consolidation of the soil to a low void ratio and low water content. When liquefaction does occur in claylike soils, it is often under greater stress and is more likely to take the form of cyclic mobility than flow liquefaction (Bray and Sancio, 2006).

Granular soils and clay-like soils differ from each other in numerous significant ways. In comparison to clean sand, clays are less prone to particle rearrangement and loss of connections when disturbed by small shear stresses due to their soil skeleton's greater compressibility and ability to recover slightly with reductions in effective stress.

Boulanger and Idriss (2004) reviewed the state of the art on the cyclic resistance of fine-grained soils. Clays with high sensitivity might behave much like liquefied sands. According to Jonathan D. B. et al. (2006), In the article, Assessment of the Liquefaction Susceptibility of

Fine-Grained Soils, the best indicator of a soil's vulnerability to liquefaction is not the quantity of "clay-size" particles present but rather the quantity of clay minerals. Thus, the plasticity index of soil is a better indicator. Hence, Bray and Sancio (2006) substituted the older Chinese criteria (which are widely used for defining potentially liquefiable soil) and provided below the criteria for categorizing the susceptibility of liquefaction based on laboratory tests:

- If the PI is larger than 12, the soil may be deemed non-liquefiable if the water content is less than 85% of the liquid limit (LL).
- Even if the soil has ***significant plasticity*** and the PI is below 12, it may still be regarded as non-liquefiable if the water content is less than 80% of the LL.
- The soil is potentially susceptible to liquefaction if the PI is between 12 and 18 or if the water content is between 80 and 85 percent (Wc/LL) of the LL; however, further analysis is necessary.

2.1.8.5. Liquefaction Determination Using "Simplified Procedure"

Professor H.B. Seed and his colleagues initially developed the method that is now the most widely used, simplest, and most useful for determining whether there is a risk of liquefaction for horizontal ground conditions (Seed and Idriss, 1971; Seed, 1979b; Seed and Idriss, 1982; Seed et al., 1985b; Seed and De Alba, 1986). The approach is semi-empirical and is based on the maximum acceleration caused by the earthquake, $\mathbf{a}_{max}$, the SPT "N" value adjusted for the SPT hammer energy and overburden pressure $(N_1)_{60}$), earthquake magnitude (M_W), and soil fines content (% passing 0.075 mm). It is based on reports of liquefaction during earthquakes in the United States, Japan, and China. The "**Simplified Procedure**" has evolved over the past 25 years to evaluate the seismic liquefaction resistance of soils. It has become the standard of practice in North America and worldwide.

2.1.8.5.1. Liquefaction Evaluations Using SPT

The 1996 workshop, sponsored by NCEER, concluded that the cone penetration test (CPT), standard penetration test (SPT), measurement of shear-wave velocity (V), and Becker penetration test (BPT) are the four field tests that are generally advised for use in evaluating liquefaction resistance. However, SPT N-values are most of the time preferable to liquefaction evaluations because the others due to the Simple and empirical method for evaluating soil resistance against liquefaction is based on the results of SPT, according to Reza Mahinroosta

(2012). Based on the Robert E. Kimmerling (1994) (Final Report), to mitigate the potential for earthquake-induced liquefaction, it was determined, using Seed's criteria, that corrected Standard Penetration Blow-counts, $(N_1)_{60}$, would need to be above about 25 within the upper 15 meters of the deposit and above about 20 below 15 meters.

2.1.8.5.2. Cyclic Stress Ratio (CSR)

A Simplified Procedure to estimate CSR (seismic demand on a soil layer) was developed by Seed and Idriss (1971). Kramer (1996) also used the symbol CSR for the Cyclic Stress Ratio and stated that CSR is the most popular method for the evaluation of the initiation of liquefaction. The Simplified Procedure can be summarized as follows:

$$CSR = \frac{\tau_{av}}{\sigma'_{vo}} = 0.65\left(\frac{a_{max}}{g}\right)\left(\frac{\sigma_{vo}}{\sigma'_{vo}}\right)r_d$$ ……*Equation 2*

Where;			
CSR	= Cyclic Stress Ratio	σ'_{vo} =	Effective vertical overburden stresses
τ_{av}	= Average cyclic shear stress	σ_{vo} =	Total vertical overburden stresses
a_{max}	= Maximum horizontal acceleration at the ground surface	**g** =	Acceleration due to gravity

r_d

Stress reduction factor which is dependent on depth.
The factor r_d can be estimating using the following tri-linear function, which provides a good fit to the average of the suggested range in ra originally proposed by Seed and Idriss (1971):

r_d	= 1.0 - 0.00765 z = 1.174 - 0.0267 z	if z < 9.15 m if z = 9.15 to 23 m	The formulae were recommended by Liao and Whitman (1986). For depths less than 23 m.
r_d	= 0.744 - 0.008 z	if z = 23 to 30 m	The formula has been added here to provide a better match with the average of the range in r_d suggested by Seed and Idriss (1971) at depths between 23 m and 30 m.
r_d	= 0.5	if z > 30 m	The formula has been added as a conservative cutoff at large depth.
	Where :- **z** is the depth in meters		

These formulae are approximate, at best, and represent only average values since r_d shows considerable variation with increasing depth (Seed and Idriss, 1971).

2.1.8.5.3. Cyclic Resistance Based on Field Testing

Estimation of soil resistance to liquefaction is the most important step in many geotechnical studies in earthquake-prone areas of the world. Based on the SPT, Seed (1979) created a technique to calculate the CRR for sand under level ground circumstances. After Seed et al., 1985, the Relationship between cyclic resistance ratio (CRR) and SPT for sands and silty sands has been based on field performance data. Currently, the most popular simple method for estimating CRR makes use of the penetration resistance from the **Standard Penetration Test (SPT)**. $CRR_{7.5}$ is the Cyclic Resistance Ratio for magnitude 7.5 earthquakes; which is approximated by Thomas F. Blake(1996) with the following equation:

$$CRR_{7.5} = \frac{a+cx+ex^2+gx^3}{1+bx+dx^2+fx^3+hx^4}$$

…….Equation 3

Where;

x= $(N_1)_{60}$; a = 4.844E-02, d= 9.578E-03,
e =6.136E-04, b = -1.248E-01, g= -1.673E-05;
f= -3.285E-04, c = - 4.721E-03, h= 3.714E-06.
This equation is valid for $(N_1)_{60}$ less than 30

The Cyclic Resistance Ratio (CRR), for specific projects, can be calculated using the above equation and empirical adjustments like MSF. $CRR_{7.5}$ is the resistance ratio at the moment magnitude of earthquake at the scale level of 7.5 which is taken as the standard referencing point. There are three corrections in the calculation of cyclic resistance ratio such as moment magnitude correction, overburden correction, and sloping ground correction. Therefore, the CRR for any other size earthquake can be estimated using the following equation which had been recommended by Youd et al. (1997).

$CRR_m = (CRR_{7.5})*(MSF)$…… Equation 4	**Where**: *MSF = Magnitude Scaling Factor* *m = Site Specific earthquake magnitude*

2.1.8.5.4. Magnitude Scaling Factors

Seed and Idriss (1982) developed a simplified procedure by analyzing data from sites where liquefaction occurred during earthquakes with magnitudes near 7.5. To adjust the simplified base curve to magnitudes smaller or larger than 7.5, Seed and Idriss (1982) introduced "Magnitude Scaling Factors" to scale the simplified base curve upward or downward on the plot. Both correcting CRR and CSR using magnitude scaling factors yield the same final result.

Mag-nitude, M (1)	Seed and Idriss (1982) (2)	Idriss (3)	Ambraseys (1988) (4)	Arango (1996) (5)	(6)	Andrus and Stokoe (in press) (7)	Youd and Noble (this report) P_L<20% (8)	P_L<32% (9)	P_L<50% (10)
5.5	1.43	2.20	2.86	3.00	2.20	2.8	2.86	3.42	4.44
6.0	1.32	1.76	2.20	2.00	1.65	2.1	1.93	2.35	2.92
6.5	1.19	1.44	1.69	1.60	1.40	1.6	1.34	1.66	1.99
7.0	1.08	1.19	1.30	1.25	1.10	1.25	1.00	1.20	1.39
7.5	1.00	1.00	1.00	1.00	1.00	1.00			1.00
8.0	0.94	0.84	0.67	0.75	0.85	0.8?			0.73?
8.5	0.89	0.72	0.44			0.65 ?			0.56?

Table 3 Magnitude Scaling Factor Values Defined by Various Investigators

I.M. Idriss reevaluated the data that he and the late Professor Seed had used to determine the magnitude scaling factors in their original calculations from 1982. In doing so, Idriss established a new set of magnitude scaling factors according to the findings of this reevaluation.

These factors are listed in Column 3 of *Table 3*, plotted on Graph 2b, and are defined by the following equation:

$$\mathbf{MSF} = \frac{10^{2.24}}{M^{2.56}} \qquad \text{..... Equation 5}$$

But afterward, Idriss (1999) reassessed the data at hand and suggested the following improved relationship for the MSF. Idriss also re-plotted the information on a log-log plot Graph 2a and discovered the updated formula that follows:

$$\mathbf{MSF} = 6.9\exp\left(\frac{-M}{4}\right) - 0.058 \leq 1.8 \qquad \text{..... Equation 6}$$

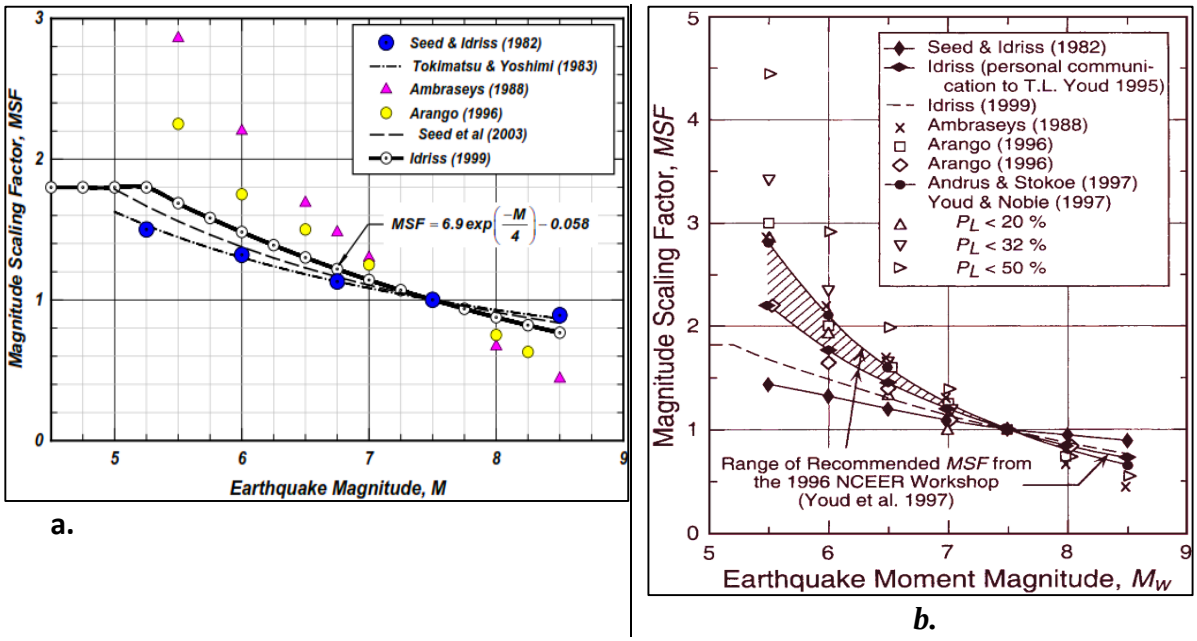

Graph 2 Magnitude Scaling Factor Vs Earthquake Moment Magnitude

- Both MSF curve Focused on the re-assessed Idriss(1999), (for this Research)

2.1.8.5.5. Factor of Safety

The factor of safety against the development of liquefaction at a site is directly proportional to the magnitude scaling factor selected. To illustrate the influence of magnitude scaling factors on calculated hazard in terms of factor of safety, the following equations can be used.

$$\mathbf{FS} = \left(\frac{\mathbf{CRR}_{7.5}}{\mathbf{CSR}}\right) * \mathbf{MSF} \qquad \text{..... Equation 7}$$

2.1.8.6. Liquefaction Evaluation Related to Stress

Load increases pore-water pressure, lowering effective stress on soil particles and affecting shear strength and tension. When the effective stress is zero, the soil has no shear strength and transforms into a liquefied condition. It is claimed that because the soil lacks cohesiveness, negative pore water pressure cannot happen under dynamic loading. ***Negative pore pressure*** arises during shear in extremely over-consolidated clays, and the undrained strength is greater than the drained strength. Compacted (partially saturated) clays behave generally similarly to over-consolidated clay. Stress that keeps the soil particles together is known as ***effective stress,*** which, in a matrix of soil, is the difference between total stress and pore water pressure. According to Terzaghi's principle of effective stress, if the pore water pressure (u) increases, the effective stress will decrease.

$$\sigma_v' = \sigma - u \quad \text{.....Equation 8}$$

Where: σ' = Effective Stress
σ = Total Stress
u = Pore Water Pressure

Particles will strive to reorganize their distribution in an embankment dam during loading to maintain equilibrium. A rise in pore water pressure will occur during this period when a load is transmitted to the pore water. In turn, the stress and internal friction angle components of shear strength are reduced as the effective stress on the soil solid particle is minimized. Liquefaction will happen once it reaches zero.

Soil-effective stress is a crucial parameter that influences its shear strength. A higher effective stress results in stronger soil and ground layers, while a zero effective stress leads to soil looseness and liquefaction. This stress is influenced by total stress, soil water pressure, and the height of the water table. Subsurface confinement affects water pressure, with more confinement causing more pressure under confinement. As the water pressure increases, effective stress decreases. When total stress equals water pressure, soil stiffness and shear strength weaken.

Soil layers can be easily affected by cyclic loads, such as earthquakes or manmade loads, leading to liquefaction. Loose, saturated, and cohesion-less soil is reduced by earthquake shaking or other loading. Increased pore water pressure during un-drained shearing reduces effective stress, reducing shear strength. The strength of cohesion-less soil is a function of

overburden pressure and the angle of internal friction. For cohesion-less soil, when the mean effective stress is zero, the shear strength is zero.

$$\tau = \sigma'_v \tan \emptyset \ldots\ldots\ldots\ldots\ldots \textit{Equation 9}$$

However, for C-soil, which is called cohesive soil, while the effective stress is zero, even if the soil is dominated by water, the shear strength will not be zero for the case of some shear strength for the reason of having the presence of the cohesion component as a constant.

$$\tau = c + \sigma'_v \tan \emptyset \ldots\ldots\ldots\ldots\ldots \textit{Equation 10}$$

However, it does not mean that the cohesive soil does not have liquefaction potential. Cohesive soil is not as liquefied as cohesion-less soil, but Technically, the process commonly called ***clay pumping*** or ***mud pumping*** will happen when the effective stress becomes zero and the pore water pressure becomes higher. Even though there is some shear strength in the soil structure, during the condition of mud pumping phenomenal, any load of built structures cannot be supported by the soil layer. (See YouTube: Example_of_Liquefaction_2 (2018).) However, in general, the process of losing effective stress and weakening the strength of shear in both kinds of soil material is known as ***liquefaction (flow-like fluid)***. On the other hand, the process of losing effective stress and shear strength by the time cyclic loading in the dry sandy soil occurs is called ***shear fluidization***. It is also technically different from that kind of liquefaction of saturated sandy soil. However, shear fluidization, like clay pumping, is generally referred to as liquefaction. In general, whenever soil flows like fluid in any load situation, this is known as liquefaction.

2.1.9. Case Studies of Liquefaction with Alluvial Foundation

Fattah M.Y. et al. 2014., as stated in the Journal of Predicting Liquefaction Potential and Pore Water Pressure under dynamic loading on fully saturated sandy soil using the finite element method and QUAKE/W computer program. The case study analyzes machine foundations in different soil densifications (loose, medium, and dense sand). The study investigates the effect of parameters like dynamic load amplitude and frequency on soil behavior. Results show that liquefaction and deformation develop rapidly with increasing loading amplitude and frequency. Liquefaction zones increase with load frequency and amplitude, with soil overburden pressure affecting resistance at large depths.

The author **Reza Mahinroosta in 2012 stated in the article** Modeling the effect of embankment dam construction on the liquefaction potential of alluvial foundation, One of the most important parameters which affects liquefaction resistance is initial stress. Liquefaction potential in alluvium will change after the construction of heavy structures on them, which is due to changes in earthquake loads, overburden pressures, and soil densification. In his study, a new methodology was explained to calculate changes in compaction of alluvial foundations after dam construction, which influence both shear strength and dynamic shear stresses. With this new method, one can determine the shear strength of alluvium against liquefaction and compare its values with induced dynamic shear stresses to evaluate the factor of safety. The effect of dam construction on the liquefaction potential of alluvium is investigated through dynamic analysis based on an equivalent linear approach. The liquefaction potential of an alluvial foundation without dam construction is compared to that potential after construction by considering the effect of induced stresses on the liquefaction potential in the numerical analysis and relative density of the alluvium strata. Finally, the Results of analyses show that the liquefaction potential of the alluvial foundation decreases significantly after construction in various alluvial strata. Considering the results derived from this study, if the selected site for dam construction is prone to liquefaction, engineers might have an economic project with keeping alluvium beneath the dam instead of totally excavating.

2.1.10. Liquefaction Ground Improvement Remediation

Remedial measures for the stabilization of potentially liquefiable soils are recommended. To select the most efficient and economical remedial technique, a thorough review of geotechnical site investigation, liquefaction hazard susceptibility, soil compatibility, and cost-benefit analysis of techniques is necessary. The first step to evaluating the potential of liquefaction is, therefore, the identification of the grain size distribution of the soil. Methods for improving liquefiable soil foundation conditions include blasting, dynamic compaction, compaction grouting, chemical grouting, jet grouting, etc. *(Ledbetter 1985; Hausmann 1990; Moseley 1993).*

Ground improvement is a field in geotechnical engineering that involves modifying the natural condition of the soil to suit project needs, often leading to savings on building costs and shorter implementation times. Compaction procedures are effective in enhancing soil strength, especially in granular soils. Ground improvement is necessary to boost shear strength, lower permeability, and minimize compressibility. Shear strength is the principal property parameter

in soil, similar to how compression is the main property parameter in concrete. Techniques for ground improvement can be physically or chemically altered to make the soil more favorable for design. It is generally expensive, costing between 3 and 10% of the total project budget. There are various types of ground improvement for various applications, with six modes: densification, drainage, reinforcement, compensation, replacement, and confinement. Soil liquefaction can be improved through various methods. Understanding the ground is the first step in ground improvement, followed by choosing the best-engineered solution, based on Cox and Griffiths (2010. Presented by Mohammed Osman Ali Khan. There are six modes of soil enhancement and some improvement methods:

Mechanism of Improvements	Types of Improvement Methods	Basic Operations
Reinforcement	Stone columns, Jet Grouting, Fiber Reinforcement, Vibro-Concrete Column,	Soil and reinforcing material act as a structure in which reinforcing elements take a majority of the load.
Drainage	Dewatering, Earthquake drain, Stone columns, Vibratory compaction,	Earthquake drain is effective under small seismic loads. Dewatering, to prevent liquefaction in the short-term like construction duration
Replacement	Removal and replacement, Jet Grouting,	In alluvial deposits, it is not economical to excavate out all the designed depths.
Confinement	Deep Soil Mixing	The auger method, which works with most soil types, is mixing cement or grout with soil to build columns of soil-crete that are often organized in a pattern.
Densification	Deep dynamic compaction, Deep blasting compaction, Compaction Grouting, Stone Columns, Vibratory Compaction,	Increasing soil density by removing air voids and pore water. Since the liquefaction concerned and Yanda Dam Foundation made of sedimentation, in this research, the author would decide to focus on the densification of mechanism for improvements.
Compensation (Treatment)	Chemical grouting,	Changing soil properties by adding chemicals or admixtures or other.

Table 4 Ground Improvements Mechanism and Methods

2.1.10.1. Removal and Replacement

To enhance soil, unsatisfactory sediment must be removed and replaced with compacted fill, which is frequently employed to manage loose soil. This approach is frequently utilized to address issues with collapsible soils since it has better engineering qualities. However, earthwork activities become more challenging when the soil is extremely moist, and removal and replacement are only possible above the groundwater table. While this approach is expensive at depths of more than 6.096m, it is the most cost-effective option for shallow problems. In general, earthwork activities are avoided unless they are essential.

2.1.10.2. Deep Dynamic Compaction(DDC)

Densification enhances the ground. Densification requires dropping a substantial quantity of weight from heights between 15 and 40 meters. Cohesion-less soils can be properly densified. In fine-grained soils, nevertheless, it is ineffective. Alternatively, in soils with a fine-grained surface layer, according to the Nicholson PG (2015) study, the method of soil compaction known as dynamic compaction, which is also known as DDC, heavy tamping, dynamic consolidation, etc., is affordable. It is widely used, costs up to 50% less than other deep densification solutions, and is around two-thirds less expensive than stone columns. Effective densification typically occurs at depths of 10 meters or more, with the groundwater table at least 1.8 meters below the working surface, and the effective densification depth can reach 12.5 meters, according to El-Reedy MA, 2017.

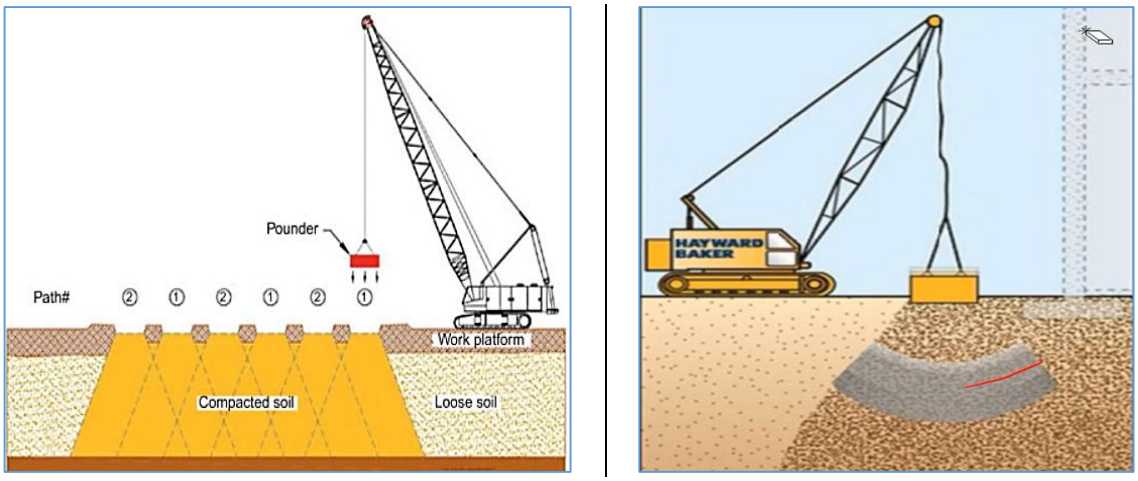

Figure 13 Photo DDC field applications.

2.1.10.3. Deep Blasting Compaction

Before an earthquake, the hazardous ground is liquefied and densified using explosives as part of the soil improvement procedure known as blasting. It works best in loose sands with less than 5% clay and 20% or less silt. In the process of blasting, which has been around for more than 80 years, explosive charges, like 60% dynamite, are installed in saturated soil at a specific depth below the surface. As the shock wave approaches, the energy released by the explosives causes compressive radial stresses in the soil mass, and as the shock wave passes, it produces tensile stress. The pore pressure is raised as a result of the cyclic stress, and the actual stresses that are exerting pressure on the soil eventually decrease. The grain particles move into a denser, more stable form when the pore water pressure decreases. Numerous soil development projects have used blasting with great success. Granular soils only need a maximum of 15% of

particles to pass through a No. 200 sieve and 3% to pass through a 0.005 mm size. The soil's moisture status is also crucial since surface tension forces in a partially saturated state reduce the effectiveness of the technique.

The technique of blasting is used to compact soil to a depth of 50 to 75 percent of its total depth. Explosive explosives are placed in drilled or jetted boreholes at this depth. Due to insufficient soil compaction after three rounds, the maximum number of blasting repetitions ranges from 2 to 3. The first explosives provide between 50 and 60 percent of the overall settlement, and the second blast adds another 20 percent. The overall depth of the compacted soil layer is about 2-10% of the surface settlement. By measuring surface settlement or utilizing procedures like the cone penetration test, standard penetration test, or weight soundings, engineers can determine the level of compaction that has been achieved.

2.1.10.4. Influence of the Deposit's Age

Numerous studies have demonstrated that soils' resistance to liquefaction gets stronger with age. For instance, Seed (1979) found that the age of reconstituted sand specimens evaluated in the lab significantly increased liquefaction resistance. Liquidation resistance grows significantly with geologic age, according to Youd and Hoose (1977) and Youd and Perkins (1978). Sediments that have been deposited recently are often far more prone to liquefaction than older deposits. Naturally sediment deposits often become older and more resistant to liquefaction as they get deeper.

2.2. Scientific Modeling

The process of creating a model to reproduce a system with specific characteristics is known as scientific modeling, and it involves choosing and identifying the relevant components of a real-world scenario. Different sorts of models can be employed for various objectives, including conceptual models for better understanding, operational models to operationalize, mathematical models to quantify, computational models to simulate, and graphical models that visualize the subject. When it is either impossible or impractical to set up experimental settings, models are often utilized. In research, modeling, and simulation are crucial. The ability to simulate the dynamics of actual systems using mathematical models or smaller-scale physical models allows researchers to explore system behavior in a detailed manner. Modeling and

simulation are used for generating data that is required for management or technical decision-making. https://en.wikipedia.org/wiki/Modeling_and_simulation

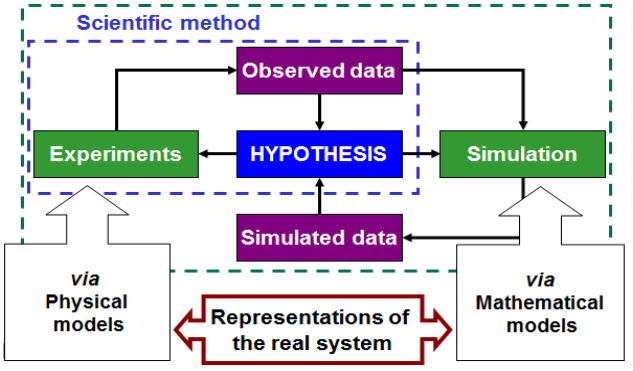

Chart 3 Flow of Modeling

The development of models is an essential step in the design and engineering process. Models enable designers and engineers to build, test, and improve their designs in a practical and meaningful way, whether they are used for prototyping, testing and analysis, visualization, or communication. Making models may be a useful tool for communicating with clients, engineers, and designers by conveying the concepts and ideas in a more tangible and comprehended way. This may be especially helpful while working on complex tasks because it might be hard to visualize the finished output. *https://www.jhmay.com/importance-model-making-design-engineering/*

2.2.1. Numerical Modeling

Numerical models are mathematical representations of actual physical processes. It varies significantly from physical laboratory modeling and full-scale field modeling in this regard. Clough and Chopra (1966) were the first to use numerical modeling techniques, such as the finite element approach, to analyze the dynamic behavior of embankment dams. Numerical techniques are now often employed in various geotechnical seismic engineering issues as tools for both investigation and design. Dam geotechnical engineering, Fell R. et al. 2005.

By Ms. Abhilasha and T. G. Antony Balan (2017), whose study highlights the use of mathematical modeling of seepage in embankment dams, one of the main causes of embankment dam failure is seepage. Numerical analysis employing computer tools is used to predict various seepage flow scenarios in embankment dams. The numerical analysis of an embankment dam is a technique that displays the problem as it occurs in the real world and then interprets it abstractly.

The two primary methods of numerical solution for the Laplace equation in complex flow conditions are finite difference and finite element. The ***Finite Difference*** method solves the Laplace equations by approximating them with a set of linear algebraic equations. The ***Finite Element*** has several advantages over the finite difference method for more complex seepage problems, such as complex geometry, varying the size of elements, and accurately modeling pockets of material in a layer. (Edris and Vanadit-Ellis 1982).

2.2.2. Finite Element Method (FEM) and Challenge with Anisotropic Materials

The Finite Element Method (FEM) is a widely used technique for seepage analysis in embankment dams. Researchers like Papagianakis and Fredlund (1984), Potts and Zdravkovic (1999), Darbandi et al. (2007), and Rushton and Redshaw (1979) have successfully used FEM for seepage analysis in embankment dams. It involves creating a mathematical model to describe the system, making assumptions for simplification, and generating a governing mathematical expression to describe the system's behavior. This method is particularly effective for dealing with physical issues controlled by differential equations. However, there are instances where analytical solutions are challenging, such as irregular regions, complex configurations, anisotropic materials, and non-linear equations.

In such cases, a numerical approach is used to get an approximation of the answer. The finite element method is one of the most important numerical solution approaches, making it easy to create general-purpose computer software for analyzing various issues. It is particularly well-suited for handling complex problem domains with predetermined requirements. A complex domain can be partitioned into smaller areas, each with an approximate solution to the differential equations. The behavior throughout the full domain is established by putting together the set of equations for each area. Discretization is the process of splitting a domain into finite regions, each called an element. The assembly method requires the solution to be continuous over the shared borders of nearby elements, as elements are joined at certain nodes.

2.2.3. Finite Element Nodes

The nodes are one of a finite element model's key components. The nodes are where finite element equations are created. The seepage equation is created for each node. All materials common to a single node contribute to the characteristics and coefficients that exist in the

equation at that node. According to the Seep/W user's manual, nodes are employed for the following tasks:

a. The geometric properties of an element, such as length, area, or volume, are calculated from the locations of the nodes in a coordinate system.
b. The key field variable is the hydraulic head or pore-water pressure, and the nodes are utilized to characterize the distribution of the main unknowns inside the element.
c. The nodes are used to link or join every component inside a domain. A common node connects all items that share it. The common nodes that connect the components make compatibility possible.

2.2.4. Numerical Analysis for Determination of Piping and Liquefaction

Integrated with Geo-Studio components like Seep/W, Slope/W, and Sigma/W, Quake/W analyzes earth structures subjected to earthquake shaking and sudden impact loads and it determines motion and excess pore-water pressures caused. In seepage analysis, the steady-state approach is used to calculate the seepage through the dam body and foundation, and in stability analysis, the Morgenstern-Price method is used to calculate the safety factor.

As stated in the U.S. Army Corps of Engineers of EM 1110-2-1901, The Laplace equation is the mathematical basis for several models or methods used in seepage analysis. SEEP/W, a GEO-STUDIO component based on finite elements, is used for seepage analysis. It is used to model the flow of water and estimate how much of it passes through the pores in soil and rock. Analysis of both straightforward and difficult seepage issues is possible because of its thorough formulation. Embankment Dam Seepage Hypothesis, according to Richards (1931), Darcy's law may be used to explain how water moves through soils both when they are saturated and when they are not (explained as follows):

$$q = k * i \quad \text{..... Equation 11}$$

q = specific discharge(discharge per unit area)
k = the hydraulic conductivity (co-efficient of permeability)
i = the gradient of the total hydraulic head

Finite element seepage analyses may be divided into two categories: steady-state seepage analyses and transient seepage analyses.

2.2.5. Seismic Analysis Method

There are two ways that an earthquake may be accounted for in a dam design. Pseudo-static is the first, while dynamic analysis methodologies are the second.

2.2.5.1. Dynamic Analysis Techniques

Dynamic analysis is essential for dam sites in seismically active zones where materials are likely to liquefy. It considers the earthquake's cyclic loading and material behavior changes with each cycle. Dynamic analysis determines the increased pressure on the dam and its foundation using an equivalent linear material model. The analysis ensures the dam's safety against deformation.

2.2.5.2. Pseudo-Static Method

If a dam and its base are not susceptible to liquefaction, seismic study of the dam can use a pseudo-static technique of analysis. (1984b, US Army Corps of Engineers).

2.2.5.3. Newmark Analysis

Newmark analysis easier to understand include: Materials have the same static and dynamic shear strengths, Critical acceleration is constant, and dynamic pore water pressure effects are disregarded.

2.2.5.4. Seep/W (SEEPage for Windows)

Seep/W is a component of Geo-Studio software (a geotechnical program) that is used to compute seepage discharge, piping potential, and Phreatic line for initial stress and dynamic analysis of dams. To resolve 2-dimensional flow scenarios including several soil layers, the Seep/W model was developed. Seep/W is a powerful finite element software product for modeling groundwater flow in porous media, capable of modeling simple saturated steady-state problems or sophisticated saturated or unsaturated transient analyses with atmospheric coupling at the ground surface.

According to Design Standard No. 13 (2014), mathematics may be used to create a numerical simulation of the SEEP/W process, which describes how water physically moves through a

particle medium. The Seep/W model is part of Geo-Studio and is based on Darcy's Law, which states that water flows in a straight line through saturated soil. The model is segmented by nodes for finite element computations, and the aquifer is assumed to be heterogeneous, isotropic, and partially confined or completely unconfined.

The steady-state seepage analysis assumes water inflow equals outflow, and the material model used is saturated or unsaturated for all materials. In a steady state, there is always a zero difference between the input flux and the output flux. In seepage analysis, as the ratio of horizontal permeability to vertical permeability (Kx/Ky) grew, the seepage amount increased as well. The findings of the slope stability study demonstrated that the safety factor reduces as the Kx/Ky ratio rises. Three finite element components—geometry, material property, and boundary condition (BC)—are essential for all seepage investigations.

2.2.5.4.1. Steady State Analysis

Steady-state flow analysis is a method where boundary conditions inside and outside the ground remain constant over time, ensuring inflow equals outflow within the analysis range. This is useful in geotechnical problems like seepage analysis, where steady states are often impossible due to nature's cyclical conditions. In steady-state analysis, the flow line is used to follow the path of a particle of water from its entrance to its exit, as the entire path is known once the flow is established. However, steady-state analysis cannot interpret data related to changes in time, only allowing instantaneous flux values. The slope of a volumetric water content function is not needed in steady-state solutions, as it is needed in the solution of the transient finite element equation. Water contents can only be viewed in steady-state solutions if a water content function is defined, which is not available in steady-state solutions. (SEEP/W, 2015)

2.2.5.4.2. Transient Analysis

Only the permeability coefficient is necessary for steady-state seepage since both the time-dependent term and the water storage term cease to exist. However, the two soil properties—namely, the co-efficient of permeability and water storage—are necessary to address the transient seepage problem associated with a saturated-unsaturated soil system (Thieu, Fredlund, et al., 2001).

In a dynamic technique known as transient analysis, the amount of time it takes for the soil to react to user boundary conditions is taken into account. It can forecast where seepage will depart

the dam face in the event of intense rainfall or the length of time it will take for a dam's core to get wet when a reservoir is quickly filled. A steady-state analysis, which simply graphs data changes with position, may be contrasted with a transient analysis. However, because there aren't only one or two flow lines in a transient process, it can't trace the flow path of a water particle throughout the full geometry.

2.2.5.4.3. Geometry

Following the establishment of the dam's dimensions per guidelines and standards, the geometry will be drawn on the SEEP/W window and discretized into small elements. Finite element numerical models are based on the ideas of subdividing (discretizing) a continuum into smaller pieces, describing the behavior or action of the individual pieces, and reconnecting all the pieces to represent the behavior of the continuum as a whole. (SEEP/W, 2008).

2.2.5.5. Material Properties:

2.2.5.5.1. Saturated / Unsaturated model

Hydraulic conductivity function, ratio, and direction, as well as volumetric water content function, are necessary when applying the saturated unsaturated type of model. Since all embankment materials are subjected to saturated and unsaturated conditions owing to reservoir water fluctuations, this sort of model is often utilized for all embankment materials. Hydraulic saturated conductivity (Ksat) and saturated volumetric water content are necessary material characteristics. The foundation materials are attached to this model because they should always be saturated independent of reservoir water fluctuations (Broaddus, 1990).

2.2.5.5.2. Hydraulic Conductivity

The hydraulic conductivity function measures a soil's capacity to transport water in saturated and unsaturated conditions. In saturated soil, solid particles fill pore spaces with water, making hydraulic conductivity the most crucial characteristic in seepage analysis.

2.2.5.5.3. Water Content Function

The water content function is crucial in understanding the relationship between pore-water pressure and water content in seepage analyses. Soil is composed of solid particles and

interstitial voids, which can be filled with water or air. In saturated soil, all voids are filled with water, and the soil's volumetric water content equals its porosity. The residual volumetric water content represents the volumetric water content of the soil where negative pore-water pressure does not cause significant changes. This value can be expressed as the degree of saturation by dividing the residual volumetric water content by the soil's porosity.

2.2.5.6. Quake/W Analysis for Liquefaction

The Yanda Embankment dam has been numerically simulated using the Geo studio (2018) program, which contains Seep/W, Slope/W, and Quake/W analysis for predicting seepage, slope stability, and dynamic response, respectively. Quake/W is a powerful piece of finite element software for simulating earthquake liquefaction and dynamic loading. Quake/W calculates the motion and extra pore-water pressures brought on by earthquake shaking, blasts, or rapid impact loads. The Yanda Dam project, located in a seismic region, has been studied using Quake/W to analyze the embankment's dynamic response. Before dynamic analysis, the ***Initial Static Stress*** is established. ***Dynamic Analysis*** uses self-weight, pore water pressure, hydrostatic pressure, and cyclic shear stress to calculate shear stresses.

2.2.5.7. Material Property and Model

When utilizing Quake/W, three distinct material models include Linear, Non-Linear, and Equivalent Linear. For this research, an Equivalent Linear Model has been selected from among these models and material parameters required for the study are Unit Weight, Poisson's Ratio, Cohesion, Internal Angle of friction, Damping Ratio, Pore-Water Pressure Function, Reduction Function (G), and Shear Module (G_{max}).

2.2.5.8. Damping Ratio

Processes that deplete the oscillation's stored energy lead to damping. In 1971, Steidel The decay of oscillations in a system following a disturbance is described by the dimensionless quantity known as the damping ratio. Based on the 2010 revision of ICOLD Bulletin 72: Guidelines for Selecting Seismic Parameters for Large Dams, for response spectra for illustrating the SEE and OBE, the degree of damping and the number of damping values provided should cover a range of values appropriate to the kind of dam and level of ground motion taken into account. Hence, according to the guideline, when analyzing embankment

dams, damping levels typically vary from 5 to 20 percent, although they can be greater than 15 percent in cases of intense shaking. There is always a certain minimum damping below the threshold shear strain, γ_c. In other words, damping rises with strain level throughout γ_c as does the size of the hysteresis loop. The damping ratio is influenced by PI, which also affects G/G_{max}. According to Vucetic & Dobry's (1991), the damping ratio declines as PI increases. Note that granular soils can also be used for the PI=0 plot.

2.2.5.9. Shear Modulus Reduction

The soil under dynamic stresses softens in response to cyclic shear strain, known as a G-reduction function. Strain softening is often approximated using empirical G/G_{max} curves, where G_{max} is the shear modulus at small stresses. Two-dimensional (2D) programs like Quake/W and other equivalent-linear response programs provide curves for G/G_{max} and strain-dependent damping coefficients for various materials. (Document of Quake/W 2014). As an alternative to the backbone curve, it is practical to plot G/G_{max} against the log.

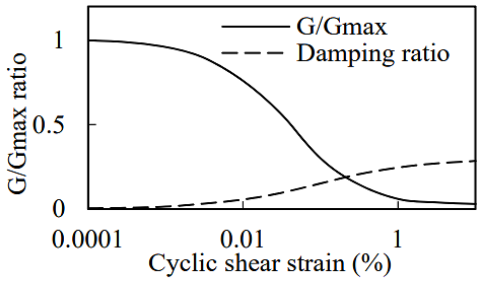

Graph 3 Modulus and damping Ratio curves (Seed and Idriss, 1970)

The curve that results is referred to as the modulus reduction curve (Graph 3). To characterize soil stiffness in ELM, it is necessary to take both G_{max} and G/G_{max} into account. Typically, as strain increases, the stiffness ratio falls while damping increases.

2.2.5.10. Poisson's Ratio

The natural tendency of a material to expand in directions counter to those of compression is known as the Poisson effect, and Poisson's ratio provides a measurement of this effect. In contrast, when a material is stretched as opposed to compressed, it often shrinks in the directions that are perpendicular to the direction of stretching. 2008; Lakes, R.; Wojciechowski, K.W. The Poisson's ratio of a stable, isotropic, linear elastic material must be between 1.0 and +0.5 since Young's modulus, shear modulus, and bulk modulus must all have positive values. Gercek, H. (January 2007).

2.2.5.11. Shear Modulus in Dynamic Analysis

Dynamic analysis is a process that captures important characteristics using various degrees of hysteresis loop representation. Three categories of dynamic analysis are linear, equivalent linear, and cyclic non-linear. The analysis is linear when the maximum shear modulus (G_{max}) is employed, which remains constant throughout the analysis and can be estimated from in-situ testing. This mode represents the cyclic stress-strain behavior of the soil with a single value for the shear modulus and damping ratio. The small-strain modulus (G_0), which is the same as the maximum modulus, is rarely employed in practice and is inappropriate for earthquake engineering applications and site reaction analyses.

The analysis is non-linear when the tangent shear modulus is used, which is the most complex but accurate analysis. This is because the analysis is conducted at any tangent point through the load line of the envelope curve. The parameter G_{tan} is entirely changeable throughout the analysis, and its values change at any point along the loaded curve line. The equivalent-linear analysis is modified to compromise both linear and non-linear analysis. The analysis becomes equivalent-leaner when using secant shear modulus (G_{sec}) in dynamic analysis. Tangent Shear Modulus is measured at each point of cyclic load and Secant Shear Modulus is when a line moves diagonally from the origin of the coordinating system to meet that intersected point.

There are three types of shear modulus (G) for cyclic loads. G_{max} stands for maximum shear modulus, G_{sec} for secant shear modulus, and G_{tan} for tangent shear modulus. Any cyclic load test performed in a lab includes a graphic showing the connection between shear stress and shear strain. Shear strain and stress are displayed in opposite directions (Y and X, respectively).

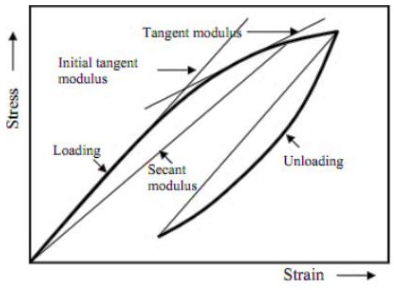

There are two types of curves in the plotting process since cyclic load is involved: the loading curve and the unloading curve. As soon as the load is discharged, the loading curve moves higher, whereas the unloading curve moves downward.

Graph 4 Cyclic Load (Vikram Anand)

2.2.5.12. Maximum Shear Modulus (G_{max})

It is a crucial consideration in the seismic design's effectiveness and the prediction of ground deformation. In practice, certain laboratory tests or seismic field tests might be used to

determine the G_{max} value. A Ibrahim *et al.*, 2019. To determine G_{max}, in-situ measurements of shear-wave velocity and sampling are essential for response analysis. G_{max} is fundamental for material properties, and seismic geophysical tests calculate it using empirical formulas based on laboratory testing. Even if laboratory tests or seismic field tests can be used to determine G_{max}, these methods are not as accurate as field V_S due to sampling disturbances (Stokoe, 2004). G_{max} and Vs are primarily functions of soil density, void ratio, and effective stress, with secondary influences including soil type, age, depositional environment, cementation, and stress history (Hardin and Drnevich 1972). G_{max} is a function of effective confining stress or overburden stress, and Quake/W requires it as a function of effective overburden stress. Soil stiffness increases with a vertical increase in effective stress, especially in granular material.

Empirical correlations have also been suggested for predicting G_{max} from SPT (Seed et al., 1986). According to PEER Report 2012/08 and Bernard R. et al., characterization of soil stress-strain behavior is essential in seismic analyses. The shear modulus of geomaterials is highly dependent on strain level, and G_{max} can be measured in the laboratory using resonant column devices or bender elements. However, high-quality samples are expensive and often not possible for cohesionless soils. Additionally, laboratory tests only measure G_{max} at discrete sample locations, which may not represent the entire soil profile. Therefore, calculating the small-strain shear modulus [G_{max} or G_o] involves the following:

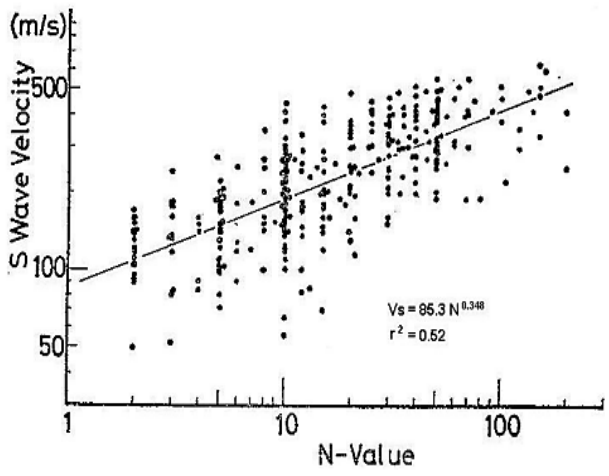

According to PEER Report 2012/08 and Bernard R. et al., Ohta and Goto [1978] developed empirical Vs correlation equations based on 289 data pairs obtained mostly from alluvial plains in Japan. Shear wave velocity (Vs) is a valuable indicator of the dynamic properties of soil and rock because of its relationship with G_{max}.

Graph 5 Vs versus SPT N-value (Ohta and Goto 1978).

$$G_{max} = \rho V_S^2 \quad \text{.....Equation 12}$$

$$V_s = 85.3 * N^{0.348} \quad \text{.....Equation 13}$$

Where:
Vs is the shear-wave velocity and **ρ** is the mass density in consistent units (**Vs** is derived from the following Graph 5).

Given that Vs is independent of the level of stress, G_{max} can be calculated most accurately from observed shear-wave velocities using in-situ seismic experiments. As a result, the most trustworthy technique for this is $G_{max}=\rho V_s^{\ 2}$ and the use of recorded shear-wave velocity.

There must be caution when selecting one of the two modulus which are maximum shear and Young/elastic modulus. Even if there is data on the young modulus, the shear modulus should not be simply calculated by using the elasticity equation (Equation *18*) that is directly related to the young modulus. Therefore, for QUAK/W analysis, the shear modulus should be determined independently from the young modulus.

$$\boldsymbol{G = \frac{E}{2(1+v)}} \qquad \text{..... } \textit{Equation 18}$$

2.2.6. Relation of Stress and Strain

The relationship between stress and strain is directly within the elastic limit. According to Hooke's law, both shearing (including torsional shearing) and direct (tensile or compressive) stress and strain have the same effects. The ratio of tensile stress to tensile strain, or Young's modulus (E), is used to quantify tensile elasticity, or the capacity of an object to deform along an axis when opposing pressures are applied along that axis. The elastic modulus is a common name for it. Whereas, the term "Shear Modulus **(G),"** also known as the "modulus of rigidity," refers to an object's ability to shear (the deformation of shape at constant volume) when subjected to opposing pressures; it is defined as the ratio of shear stress to shear strain. Both moduli are referred to as elastic constants.

2.2.6.1. Stress-Strain Behavior of Cyclically Loaded Soils

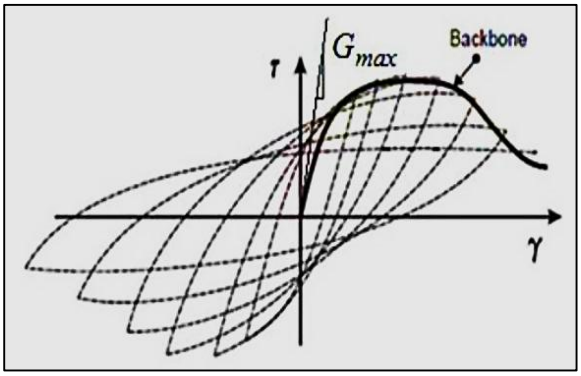

.a

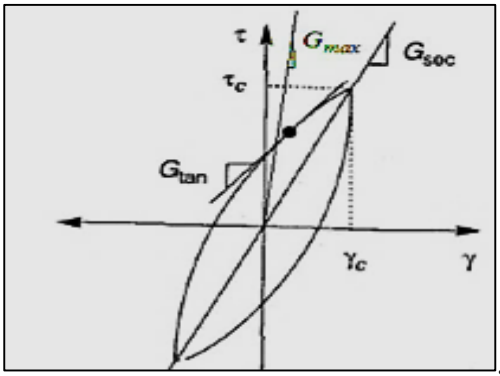

.b

Graph 6 Graphs of Stress-Strain Relationships

Undoubtedly, under dynamic/cyclic loads, their behavior is far more complicated. According to Towhata (1989), the most significant characteristic in dynamics is the cyclic stress-strain behavior of soils.

As seen in *Graph* **a** above, an idealized sequence of stress-strain (hysteresis) loops would occur in soil subjected to cyclic loading. The "skeleton curve" or "backbone" is the line connecting the tips. For the most part, the backbone curve is considered monotonic. The zero-strain modulus is also known as G_0 or G_{max}, and it is the slope of the tangent at the origin.

As shown in *Graph* ***b***, a typical hysteresis loop may be described by two characteristics: first, the slope of its tangent at various places along the loop (tangent modulus), with G_{tan} denoting its stiffness; and second. The loop's width or area is directly related to how well it can dissipate energy. Due to the unlimited number of points on a loop and the numerous distinct loops that must be taken into account, this would be mathematically challenging to include in analytical models.

The stress-strain curve's slope at a given amount of stress is considered to be the tangent modulus, whereas the slope of a secant drawn from the origin to a particular point on the stress-strain curve is represented by the secant modulus. As the strain amplitude rises, G_{max}, or simply G, drops from its maximum value. The backbone curve's greatest slope (small-strain shear modulus), G_{max}, is located near the origin. The in-situ soil properties (void ratio, mean principal effective stress, plasticity (PI), soil stress history (OCR), and loading parameters (strain amplitude, number of cycles of loading)) affect the soil's stiffness.

3. METHODOLOGY

3.1. General Description

Methodology is defined as "a set of principles and ideas that inform the design of a research study." On the other hand, the term "methods" refers to "practical procedures that are used to generate and analyze data" *(Birks and Mills, 2011).* Gathering information is not only the basic goal of the study. It goes more than that, though. Goddard and Melville (2001, p.1) claim that the real purpose of research is to find solutions to unresolved problems to advance knowledge in a particular field. Research methodology is a technique that unites all research procedures and directs the researcher in achieving the study's goals and objectives (Tibebu Solomon, 2015).

Research methodology is a framework that guides the conduct of research and ensures that the research is conducted rigorously and systematically. It encompasses the overall approach to the research, including the research design, data collection methods, data analysis methods, and the dissemination of findings. Research methods, on the other hand, are the specific techniques and procedures used to collect and analyze data. The choice of research methodology and methods is critical to the success of any research project. It is important to select an appropriate methodology and methods that are aligned with the research question, the type of data being collected, and the resources available. A pilot study may be conducted to test the feasibility of the research methodology and methods before proceeding with the full-scale study. Ethical considerations must also be taken into account throughout the research process.

3.1.1. Methodology's Work Flow

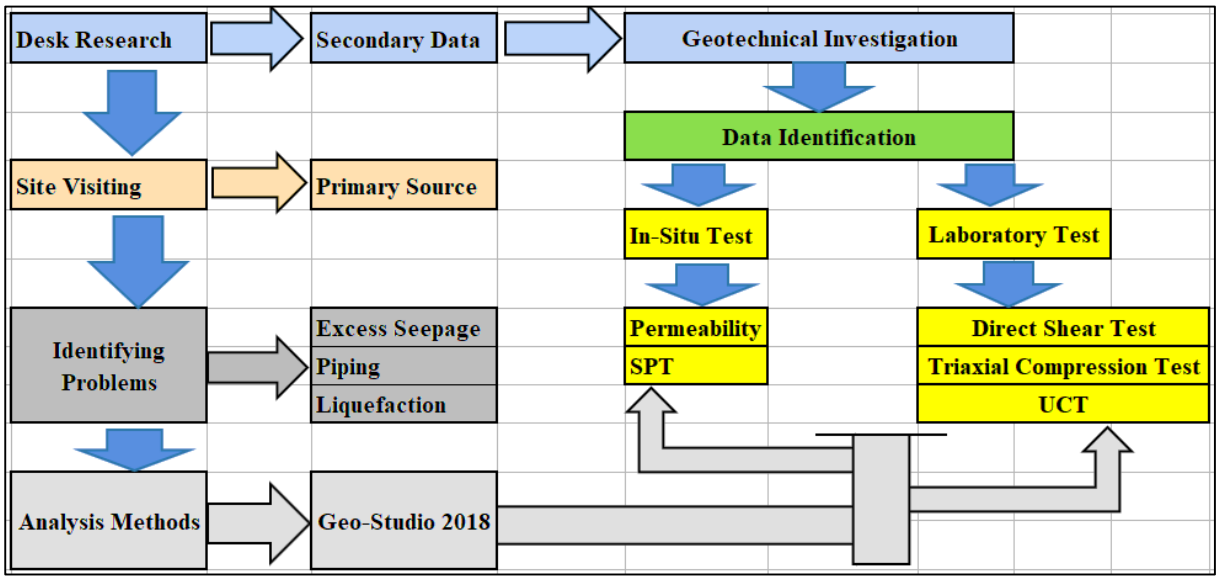

chart 4 This research Methodology's work Flow

The outcomes of any given research are mostly dependent on the availability and dependability of data relevant to the issue under consideration, as well as enough quantity and quality. Any research either relies only on primary data collection, or secondary data collection or combines both levels of data collection to get the appropriate data. Research becomes relevant and successful when data is collected systematically.

This research methodology's Activities				
No.	**Stages**	**Used data/tools**	**Descriptions about the purpose of used data/tools**	
1	**Desk Study**	**Secondary Data**	Geological Investigations	For analysis of identified problem
			Geotechnical Investigations	
			Hydrological Investigations	
2	**Site Visit**	**Primary Source**	Site visit and observation	For visualization of the project area
			Information from the site residents	
			Taking Photograph	
3	**Problem Identification**	**Piping**	The susceptible problems of the dam's foundation	
		Liquefaction		
4	**Data Identification**	**In-situ test**	Data compilation and integration for analyzing the problem such as SPT test, Permeability, Specific Gravity, Unit Weight, borehole log, Shear Strength(c' and Ø), and other standards.	
		Laboratory test		
`5	**Selection of methodology or software**	**GeoStudio/ 2018**	An all-inclusive tool for modeling` soil structures and performing geological engineering tasks is GEOSLOPE Geo-Studio 2018. A series of CAD-integrated software tools are provided, combining many analyses performed with various products into a single package. It makes use of Finite Element Analysis and includes 8 models, including Seep/W and Quake/W. SEEP/W to analyze seepage and piping. QUAK/W to analyze Liquefaction. **The limitations discussed as follows;** Geo-Studio represents soil and rock behavior using simplified material models. These models may not fully convey the complexity of real-world materials, even though they can offer accurate approximations. Certain hardware combinations or operating systems may not be compatible with Geo-Studio. Users may experience issues with the software's installation or operation on their particular PCs. It is also sensitive to antivirus software.	
		LiqiT(2004)	LiqiT is a software for assessing soil liquefaction potential using field data like SPT, CPT, and Vs.	
		Auto CAD 2007	To generate actual topo with the combination of Eagle Point using surveying data and to prepare the geometry for importing in Geo-Studio	
		Eagle Point 2007		
		Google-Earth Pro	A detailed comprehension of the physiography of the Yanda River and the meandering band that is created at the dam site every year by alluvial deposits.	
		MS Excel,2013	It is going to be used to analyze some output data like safety factors.	
6	**Data analysis**	**Using software**	To find out the actual problem and provide results for interpretation	
7	**Interpretation**	**Standards**	To set remedial measures and recommendation	

Table 5 This research methodology's Activities

3.2. Data Collection, Preparation and Analysis

A comprehensive and systematic methodology was employed to gather, analyze, and synthesize data for this study. Data was meticulously collected from both secondary and primary sources, ensuring the breadth and depth of information required to address the study's objectives. Secondary data, encompassing geological, geotechnical, and hydrological elements of the Yanda Dam Project, was meticulously reviewed and incorporated into the analysis. Primary data, in the form of photographs and field observations, further enriched the understanding of the project site and its surrounding environment. This rigorous and structured approach to data collection, preparation, and analysis formed the bedrock of the study and ensured the validity and reliability of the findings.

Therefore, The methodology specifically has involved the following activities:

- Data on dam foundation assessment have been gathered and examined from relevant secondary sources, including published papers, books, published Thesis, and technical reports such as geotechnical and engineering geological data from relevant institutions (ECDSWC, where I have been working), and projects.
- The last step involves integrating and synthesizing the data from the aforementioned sources to interpret and meet the study's objectives.

3.2.1. Primary Data Collection

Primary data collection involved physical observations and measurements, photographic documentation, and reconnaissance surveys. Site visits were conducted to visually inspect the dam and reservoir rim, assess the surrounding environment, and gather photographic evidence. These photographs provide valuable insights into the project's physical conditions and serve as visual references for further analysis. During the site visits, it was observed that a substantial volume of alluvial sediment had accumulated near and along the dam axis, a consequence of annual flood events.

The purposes of visiting the Yanda project site were to understand the project’s physical problem and become familiar with the project’s environment as well. The photos below and attached in the appendix were taken from the site during the author’s visit and rough reconnaissance. It was observed that a significant volume of alluvial deposits has been deposited near and along the dam axis throughout each year's flood season.

Photo 1 Upstream side view of the dam (Panorama photo from left to right Abutment)

Screenshot 1 accessed the road to the project site

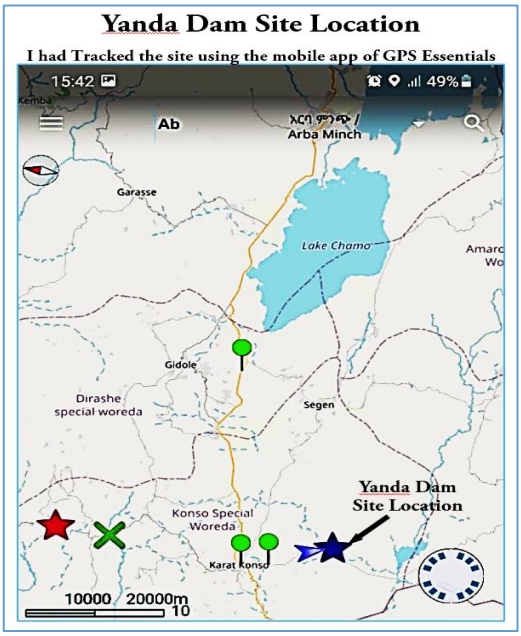

Screenshot 2 tacking road using GPS Essentials

Photo 2 Deposited material by meandering the Yanda River

Through the process of a long time meandering the river, there has been leaving 2.5m height of deposited material.

Photo 3 Small village in the area of the dam alignment

Left abutment of the dam and there is a small village

Photo 4 Right abutment of the dam

Photo 5 Top layer transported and deposited sediment material

3.2.2. Secondary Data Collection

Secondary data collection involved gathering and analyzing relevant information from existing sources, including geophysical surveys, geotechnical investigations, and engineering geological reports. These sources provided valuable insights into the subsurface geological conditions along the planned Yanda Dam foundation. Laboratory test results, conducted on soil and rock samples collected during fieldwork, were also utilized to supplement the secondary data. The specific gravity, grain size analysis, Atterberg limits, direct shear, unconfined compressive strength, bulk unit weight, moisture content, point load, and pinhole tests were performed on soil samples. Rock samples underwent specific gravity, unit weight, water absorption, and uniaxial compressive strength testing.

The laboratory test findings were used to create the dam's final design report together with the foundation boreholes (ECDSWC, 2021). For this study, secondary data from geophysical surveys, and geotechnical and engineering geological investigation methods have been employed to gather the relevant data for the evaluation of the subsurface geological condition along the planned Yanda Dam foundation.

Required index and engineering laboratory tests had been conducted in the ECDSWC's laboratory service on samples collected from the fieldwork. The types of laboratory tests conducted on soil samples include Specific gravity, Grain Size Analysis, Atterberg Limit, Direct Shear, UCS, Bulk Unit Weight, NMC, Free Swell, Water Absorption, Point Load, Pinhole, Organic Content, Sulfate, and Chloride. Similarly, rock samples are tested for specific gravity, unit weight, water absorption, and uniaxial compressive strength.

3.2.2.1. Integration of Engineering Secondary Data

The respective studies, analyses, and results concerning engineering geological, geotechnical, and hydrological conditions have been integrated to meet the objective of the present study. Through site investigation and data procurement from secondary sources with adequate analysis and experience, an appropriate model for dam foundation may be worked out.

The integration of engineering secondary data is a crucial process that involves collecting, organizing, and incorporating existing engineering data into a new or existing project. This can include data from previous studies, research papers, industry reports, and other sources. The first step in integrating engineering secondary data is to identify relevant sources of information, such as literature reviews, and then collect and organize the data in an accessible and usable manner.

The data collected and organized can be used to inform the design process, validate assumptions, provide context for findings, and benchmark against existing standards or best practices in the field. It can also improve the quality and reliability of the work by leveraging existing knowledge and expertise, ensuring that projects are based on sound evidence and aligned with industry standards and best practices.

Incorporating engineering secondary data is important for several reasons. First, it allows engineers to leverage existing knowledge and expertise, which can improve the quality and reliability of their work. By incorporating data from previous studies, research papers, and industry reports, engineers can build on the work of others and avoid reinventing the wheel.

Secondly, integrating engineering secondary data ensures that projects are based on sound evidence and aligned with industry standards and best practices, leading to more robust and effective solutions and increased confidence in project outcomes. Additionally, the integration of engineering secondary data saves time and resources by avoiding the need to conduct redundant studies or collect new data. By utilizing existing information, engineers can streamline their work and focus on adding value in other areas of the project.

3.2.2.2. Geological Engineering Investigation

For the current study, systematic field investigations have been used to collect geological engineering inquiry data. A sort of geological map gives a generalized picture of all the geological site conditions. The map can also be used to spot possible issues or advantageous aspects of the project location (Daniel Gebremichael, 2017). The engineering geological mapping of the Yanda dam foundation and its vicinity has been carried out based on the engineering characterization of the rock mass and the soils that exist at the site. The soils of the dam site area were mapped based on geotechnical properties defined during a detailed design study, ECDSWC (2021).

The detailed geological mapping showed that the project area is outcropped by Tertiary volcanics, Tertiary-Quaternary Clastic Sediments, and Quaternary Alluvium Deposits. The Tertiary volcanic rocks are outcropped around the surrounding mountains/slopes and are majorly basaltic, rhyolitic, and trachytic volcanic flow units. The feet of mountain ranges are covered by thick clastic sediment sequences. The remaining areas following the meandering Yanda River channel and its flood plains are covered with alluvium sediment deposits.

To acquire basic geotechnical data only eight boreholes were drilled on the dam foundation and used to assess the subsurface structure and materials on the foundation sites. For the present study, the mentioned data, in the previous chapter, on borehole logs and cross section was obtained from the geotechnical design report of the dam from the consulting company of ECDSWC, 2021.

Geological cross-section, in essence, shows vertical and horizontal geological variation as well as groundwater level along the concerned axis of a dam structure. To understand the foundation geological profile and lithological units, the geological cross-section during the present study has been generated along the dam axis based on the drilled hole of logs data as obtained from the design investigation report (ECDSWC, 2021).

3.2.2.3. Hydrological Estimation of Sediment Yield

One of the tributaries of the Segen River (Rift Valley Basin) is the Yanda River. The elevation of the Yanda Dam Project Catchment, which has coordinates of 37^{o}33.8'E and 5^{o}22'N, varies

from 945 to 2665 m.a.s.l. It suggests that the site's primary hydrology is one of the highly intense flash floods with a very short lifetime (Yanda).

According to the Yanda Dam and Irrigation Project Feasibility Study and Detail Design, 2022, by the ECDSWC, the Yanda River had sediment assessments based on the Weito River sediment data. The annual sediment transport was calculated by converting the daily stream flow into a series of sediment discharges using the rating equation. According to the findings, depending on the flow, 450.4 tons per day, or 117,438.4 m3/year, of suspended silt are created. Bed load makes up 10% of the suspended sediment carried at the Yanda Dam's reservoir.

3.2.2.4. Geologic Mapping

Engineering geological mapping is the systematic recording of geologic information from field exposures. This mapping is used as a source for geological, geotechnical, and engineering data as well as an organized summary of geological facts for engineering usage. Major areas are covered with volcanic sequences composed of basalt, rhyolite, trachyte, clastic sediments, and alluviums. In general, the following lithological units are outlined at the dam site during investigations:

3.2.2.4.1. Yanda Lithological Units

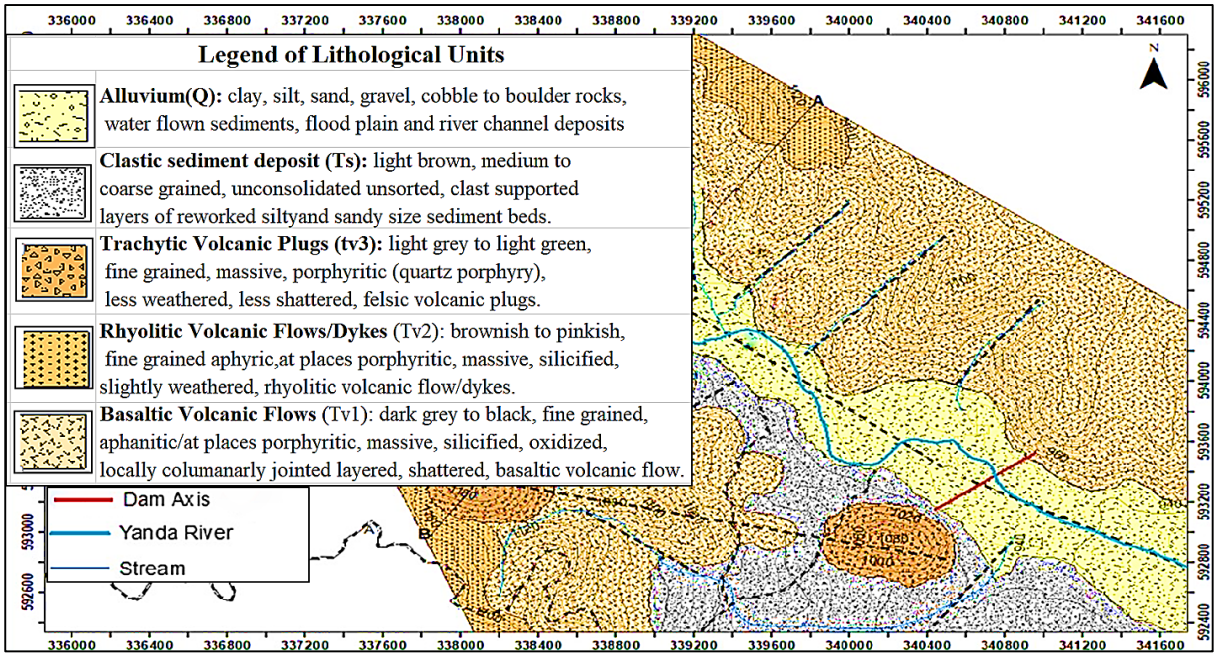

Figure 14 Geological map of Yanda dam site, reservoir area, and surroundings

The dam axis/reservoir area has competent lithological units, but there is thick, soft sediment and alluvial soil covering the bedrock. This makes the site susceptible to liquefaction and piping, making it challenging to design and construct the dam on deep alluvial-deposited soil. The maximum thickness of the alluvial deposit is around 50 meters, resulting from weathered bedrock transported and deposited by gravity and river flow.

3.2.2.4.2. Basaltic Volcanic Rock Units

The Yanda geological map study states that *basaltic* volcanic rock units have a broad range of weathering degrees, ranging from freshly weathered to extensively weathered and degraded into the soil of the silty clay kind. Generally, these rock units are fragmented, shattered, and oxidized, making them more susceptible to erosion.

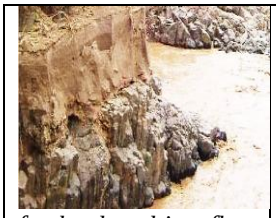

fresh basaltic flow unit, u/s left side of the dam 339754/594793 UTM location

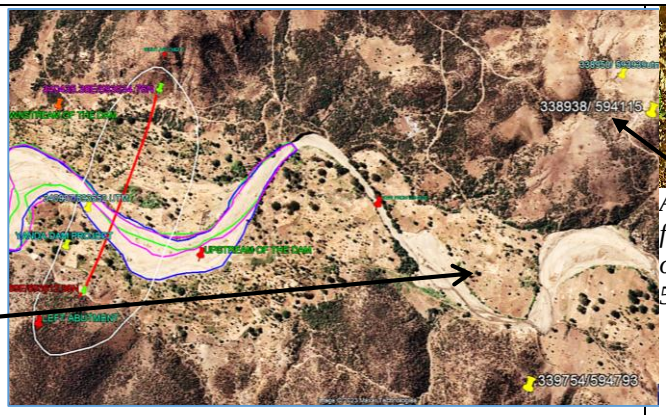

Photo 6 Satellite photograph to locate the Basalt

Aphanatic basalt rocks flow units, u/s right side of the dam 338938/ 594115 UTM location.

3.2.2.4.3. Rhyolite Volcanic Flow units

The Yanda geological map report states that **rhyolitic volcanic flow** units are massively fine-grained except for the porphyritic texture.

3.2.2.4.4. Clastic Sediment

Major portions of the Yanda reservoir area are covered with a substantial sediment deposit. This **clastic sediment** covers lowlands that are aligned with mountain chains' feet and, in certain locations, has eroded minor hills (alluvial fields of sand-dominated fluvial deposits) that are orientated away from the feet of hills.

3.2.2.4.5. River Channel Deposits

The Yanda River's bowed channel deposits sediments like sand, gravel, pebble, cobble, and boulders, varying in composition and thickness depending on the channel's location. Yanda River tributaries also have similar channel deposits.

3.2.2.4.6. Flood Plain Deposits

The Yanda River's meandering channel created a broader flood plain with fine-grained Silty-sand fraction deposits. The sediment's thickness and composition vary across the valley, with finer and thicker alluvium deposits in the periphery flood plains and coarse-grained alluvium along the river bank.

3.2.2.5. Geophysical Investigation

It is the sub-discipline of geological engineering that applies geophysics principles to the design of engineering projects such as tunnels, dams, and mines or for the detection of subsurface geo-hazards, groundwater, and pollution. Geophysical investigations are undertaken from the ground surface, in boreholes, or from space to analyze ground conditions, composition, and structure at all scales. Geophysical techniques apply a variety of physics principles such as seismicity, magnetism, gravity, and resistivity.

Resistivity imaging and vertical electrical sounding survey data on soil and rock were analyzed using ground computer tomography and with resist software. Resistivity sections (2D for imaging and 1D for a vertical electrical-sounding survey) were produced for each survey line/point. Geophysical Surveying was employed at the Yanda Dam site, using Vertical Electrical Sounding (VES) and Electrical Resistivity Imaging (ERI). A surveying map was planned to apply both investigation approaches.

Geophysical data can be integrated with other data sources like geological, hydrological, and geotechnical data to evaluate the alluvial foundation of a dam. This approach provides a comprehensive understanding of subsurface conditions and potential risks associated with dam construction and operation. Geophysical data can be correlated with existing maps and borehole data to identify the lithology and stratigraphy of alluvial deposits. Hydrological data can be integrated with geophysical data to assess groundwater levels, flow patterns, and potential

seepage pathways, assessing the hydrogeological properties of the foundation. Geotechnical data can be used to identify weak or unconsolidated materials within the foundation, assessing its stability and settlement potential.

3.2.2.5.1. Vertical Electrical Sounding(VES)

Geophysicists use electrical techniques like vertical electrical sounding (VES) to assess subsurface depth for in-situ soil salinity assessments. VES estimates the hydraulic conductivity and texture of stratified soils and sediments. Barker (1990) used VES to outline a landfill at 40 meters depth. The Yanda dam sites were investigated, with 10 VES points distributed in the sites.

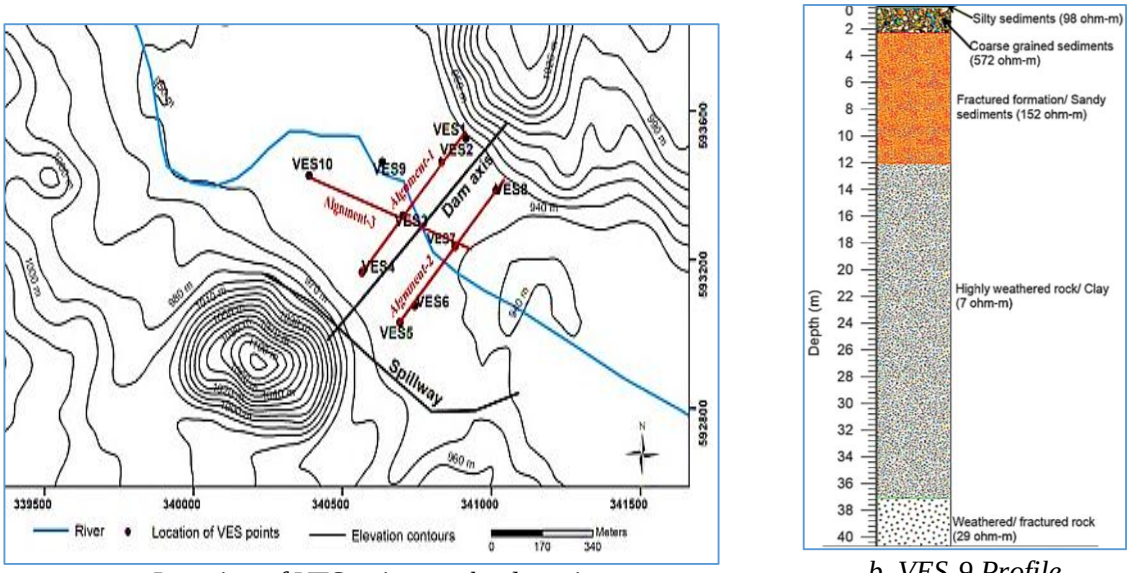

a. Location of VES points at the dam site *b. VES-9 Profile*

Figure 15 Location of VES points and Geo Electric Section

3.2.2.5.2. Geo-Electric Sections around the Dam axis

Geo-electric sections along Alignment-1, Alignment-2, and Alignment-3 reveal four types of layers. These are silty types of soil, coarse-grained clastic sediment, weathered volcanic rock/ sandy sediments, weathered/fractured rocks, and possibly saturated with groundwater.

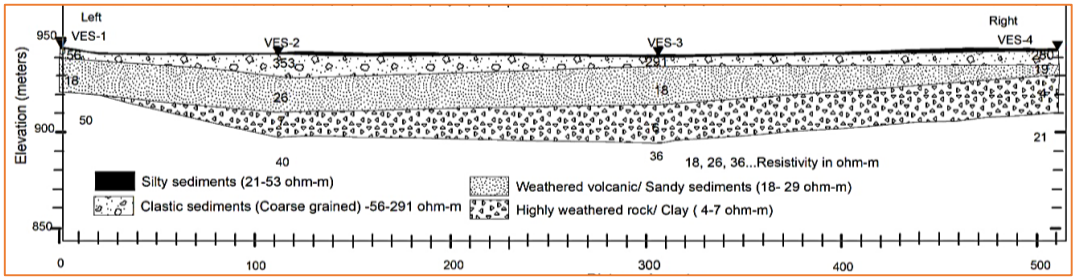

a. alignment -1

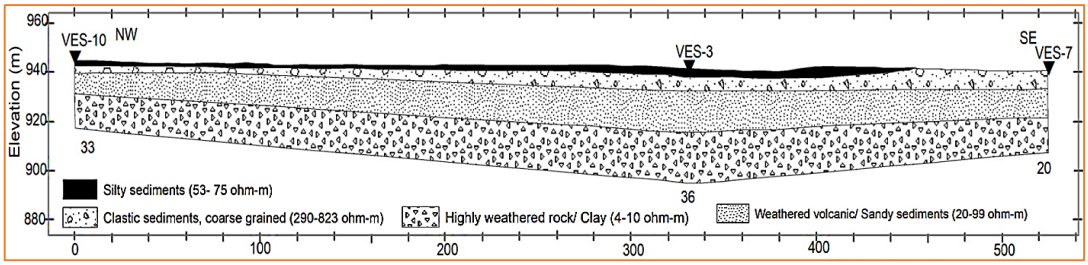

b. alignment -3

Figure 16 Geo-electric Section obtained along

3.2.2.6. Geophysical Data Interpretation

The geophysical survey at the dam site revealed weak zones and lineaments near the planned dam site. A thin top layer, possibly attributed to Silty formation, was identified in a geoelectric section. High resistivity strata, such as coarse-grained clastic sediments, were found under the thin top layer. Medium resistivity strata were found beneath clastic sediments, possibly weathered volcanic rock or sand sediments. Very low resistivity formations were found under medium resistivity, indicating worn, fractured rocks soaked with groundwater. Low resistivity rocks typically extend to over 40 meters around the dam site, indicating loose sediments or extensively weathered and decomposed rocks. Resistivity imaging survey results indicate that basalt and/or ignimbrite make up the bedrock along the dam's axis, with moderately to mildly fragmented basalt and solid ignimbrite in the left and right end slopes. Alluvium sediments and groundwater are found in flat areas around the dam axis.

3.2.2.7. Limitation of Geophysical Methodology

Geophysical methods face several limitations, including depth limitations, resolution limitations, interpretation challenges, environmental factors, cost and time limitations, and inherent limitations. Depth limitations are particularly pronounced for seismic methods, which struggle to accurately image structures at depths greater than a few kilometers. Resolution limitations are common, limiting the ability to provide detailed information about small-scale features or subtle changes in subsurface properties. Interpretation challenges are also common, especially in areas with complex geology or multiple subsurface features. Environmental factors like weather, vegetation, and surface infrastructure can affect the effectiveness of geophysical methods, leading to inaccurate results. Cost and time limitations are also significant, especially in large or remote areas. Each method has its inherent limitations, such as electromagnetic methods' difficulty in penetrating conductive materials or seismic methods' difficulty in imaging through fractured or faulted rock.

3.2.3. Tests in Geotechnical Investigation

There were two types of test executed in the Yanda Dam geotechnical investigation and summarized as follow:

	Test category	Test Type	Description
i.	**Laboratory Tests**	Direct Shear Test	Suitable only for measuring the strength parameters.
		Triaxial Compression Test	Suitable for measuring both strength parameters and stress-strain properties.
		Unconfined Compression Test	For measurement of compressive strength of rocks and fine-grained soils(sufficient cohesion).
ii.	**In-Situ Tests**	SPT, CPT, Falling Head and Packer Permeability Test	For measurement of resistance of a soil to penetration as an indication of the shearing strength.

Table 6 Tests executed in Geotechnical investigation

Summary results of in-situ and laboratory tests that had been performed for each borehole have been attached in Appendix 5.

3.2.3.1. Geotechnical Core Drilling

During the preliminary and detailed design studies, many boreholes were executed after the topographic survey to collect the essential geological and geotechnical data and evaluate the foundation's permeability and shear strength (ECDSWC, 2021). Boreholes were drilled for geotechnical assessment to identify foundation materials, gather soil and rock samples, and conduct permeability and strength tests. Eight boreholes were planned and bore along the dam axis, based on surface conditions and prior geophysical reconnaissance. Geotechnical core drilling and extraction were performed according to ASTM D2113-99. In-situ permeability measurements were also conducted in the boreholes. Core samples were stored in hardwood Core Boxes, and geological and engineering data was collected from drill cores.

No.	Activities in Borehole	Borehole ID. Only with in Dam Axis					
		Unit	YDBH-2	YDBH-3	YDBH-3B	YDBH-4	Quantity
1	GWL recording	No.	7	14		18	39
2	Falling Head Tests	No.	10	13	8	12	43
3	Packer Test	No.		1			1
4	Piezometers Installations	m		66			66
5	Rock core Sample	No.	1	3	1	4	9
6	Undisturbed Shelby Sample	No.	2				2
7	Core Soil Sample	No.	8	8		3	19
8	SPT Test	No.	11	12	12	9	44
9	Drilled Depth	m	39	66	45	60	210
10	Core box photograh	No.	8	14	8	12	42
11	Logging	m	39	66	45	60	210

Table 7 Geotechnical core drilling investigation activities and quantities.

3.2.3.1.1. Standard Penetration Test (SPT)

According to Shariatmadari et al. (2008), the standard penetration test is an in-situ procedure used to assess material resistance, density, and subsurface soil profile. The conventional penetration test is considered the most trustworthy and friendly in-situ test, but has limitations in interpretation and repeatability, according to Derbala and Bouafia (2016). In the Yanda project, standard penetration tests (SPT) were conducted when materials were suitable for meeting test assumptions. A standard SPT hammer with a trip hammer release mechanism and 60% hammer efficiency was used.

3.2.3.1.2. Permeability Test

Seepage flow is significantly impacted by joints, weathering, fractures, and other geological features. To address unfavorable seepage situations, realistic seepage management techniques must be developed (Chen et al., 2010). In borehole testing of Yanda's geotechnical investigation, Packer and Falling Head permeability had been conducted on soil and rock masses, following the U.S. Bureau of Reclamation Procedures and the British Code of Practice. For the current investigation, in the Yanda Project, eight falling head tests were performed. An open standpipe piezometer was installed at the right river bank in YDBH-4 to measure and monitor groundwater conditions in foundation layers. The piezometer was inserted for 66.0m depth below the original ground level and designed to encounter the whole depth of groundwater.

3.2.4. Yanda Dam Site Geotechnical Layer Characterization

Since the foundation is well concerned, this study has been focused on geotechnical activities of geophysical surveys and core drilling with referring to nearby associated structures to produce data by characterizing the layers in depth for the dam design. 2D engineering geological sections were created using geotechnical investigations of borehole logs and core photographs for understanding the alluvial disposition distribution within the project site foundation. The Following **Geotechnical Units or layers** are identified, characterized, and evaluated for their engineering performances.

3.2.4.1. Cohesion Soil (Alluvial Deposit)

The cohesion Soils' information, which is characterized as the Alluvial Deposit, has been summarized in the following tabulated form according to the report of ECDSWC's Geotechnical Section Work.

GTL-1: Top-Soil - Silty Clay with Trace of Sand (CL)

Test Parameters	Unit	Range	Remark
Depth/Thickness	m	0.5 to 4	At YDBH-4 to YDBH-3 from OGL
SPT Ncorr		5 to 9	Medium to stiff consistency
Dry Unit Weight, ɣd	KN/m3	14.2 and 19.4	
NMC	%	10.54 and 30.94	
LL	%	30.85 to 52.90	
PI	%	14.73 to 26.68	Low to medium plastic soil
Fine-Grained Content	%	30.85 to 52.90	
Unconfined Shear Strength	KPa	40.5 to 52	
Elastic Modulus	KPa	23,400 to 85,050	
Permeability	cm/sec	10e-04 to 10e-06	

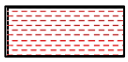

GTL-2: Flood Plain Deposit Silty Clay (CL)

Gravel (10.08% by weight) and Trace of Sand (6.65% by weight) are added to the mixture.

Test Parameters	Unit	Range	Remark
Depth/Thickness	m	6 to 25	
SPT Ncorr		14-28	Stiff to very stiff soil consistency
LL	%	31.90 to 88.20	
PI	%	11.73 to 56.57	Fine grained low plastic
Fine-grained content	%	83.27%	
UCS	KPa	172.52	Unconfined Shear Strength
Elastic Modulus	MPa	75.6 to 198	Modulus of deformation (Es)
Permeability	cm/sec	10-5 to 10-7	
C	KPa	35.63	Triaxle shear strength
Phi ø	degree	20.45	

GTL-3: Clayey Silt with the trace of Gravel (MH)

It is Palaeo channel alluvial Deposit. Low plasticity and reddish in color.

Test Parameters	Unit	Range	Remark
SPT Ncorr		13 to 20.	stiff to very stiff
Permeability	cm/sec	10-5 to 10-7	

3.2.4.2. Cohesion-less Soil (*Alluvial Deposit)*

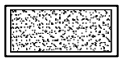

GTL-4: Fine-Grained Silty Sand (SM)

It's made up of alluvial deposits.

Test Parameters	Unit	Range	Remark
SPT Ncorr		7 to 19	Stiff to very stiff
Permeability	cm/sec	10e-5 to 10e-7	
Relative density	%	20 to 40	

GTL-5: Coarse Gravel (GM)

It's made up of alluvial deposits.

Test Parameters	Unit	Range	Remark
SPT Ncorr		21	Stiff to very stiff soil consistency
Fine-Grained Content	%	7	
Elastic Modulus	MPa	9.49 to 23.93	Modulus of deformation (Es)
Permeability	cm/sec	6e-03 to 3.39e-06	
Phi ø	degree	31.49 to 33.49	Shear strength parameters
Spesific Gravity		2.50 to 2.76	
Unit Weights	g/cc	1.42 to 1.87	
NMC	%	0.91 to 14.2	
Relative density	%	40 to 65	Compact to dense state

3.2.4.3. Cohesion-less Soil (Colluvium Deposit)

The **Cohesion-less** Soils' information, which is characterized as **Colluvium Deposit**, has been summarized in the following tabulated form according to the report of ECDSWC's Geotechnical Section Work.

GTL-6: Clastic Sediments Deposit

It is Colluvium material and Silty Gravel mixed with angular rock fragments.

Test Parameters	Unit	Range	Remark
SPT Ncorr		28 to 41	Very stiff to hard consistency
Permeability	cm/sec	2.28E-05 to 7.58E-06	

3.2.4.4. Bedrock foundation

The data of **Bedrock Foundation** have been summarized in the following tabulated form according to the report of ECDSWC's Geotechnical Section Work.

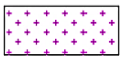

GTL-7: Moderately Weathered (Rhyolite /Trachytic Rock Mass)

Light grey, fine-grained, moderately to slightly weathered.

Test Parameters	Unit	Range	Remark
Elastic Modulus	MPa	423.68	Modulus of deformation (Es)
C	KPa	221	Shear parameters
phi ø	degree	27	Shear strength parameters
Spesific Gravity		2.33 to 2.58	
Unit Weights	g/cc	2.44 to 2.52	
RQD	%	42	
RMR		45	Rock Class-III & it implies Fair class.
Water Absorption	%	2.77 to 7.17	
Permeability	Lu	0.07	It reveals that impervious
UCS	Kpa	191	

GTL-8: Highly Weathered Grade-Iv Material

Highly weathered and intensively fractured Lower Basalt Rock Mass:

Test Parameters	Unit	Range	Remark
Elastic Modulus	MPa	416.78	Modulus of deformation (Es)
C	KPa	174	Shear parameters
Phi ø	degree	22	Shear strength parameters
Spesific Gravity		2.67 to 2.69	
RQD	%	39	
RMR		35	Rock Class-IV-poor class.
Permeability	cm/sec	1.70e-03 to 1.94e-04	Voids rock mass discontinuities
UCS	Mpa	1.38 to 39.02	Very weak to Medium Strong

GTL-9: Slightly Weathered Grade-II Material

Slightly to moderately weathered and closely fractured Lower Basalt Rock Mass:

Test Parameters	Unit	Range	Remark
Spesific Gravity		2.82	
RQD	%	35	
Permeability	cm/sec	9.25E-06 to 6.12E-07	Very low permeability
UCS	Mpa	44.99	Very weak to Medium Strong

3.2.5. Geological Profile

The following geological profile has been produced from the investigated geotechnical output report of borehole drilling. This profile configuration has helped for well understand the alluvial deposited layers and analyze the expected problem of piping and liquefaction.

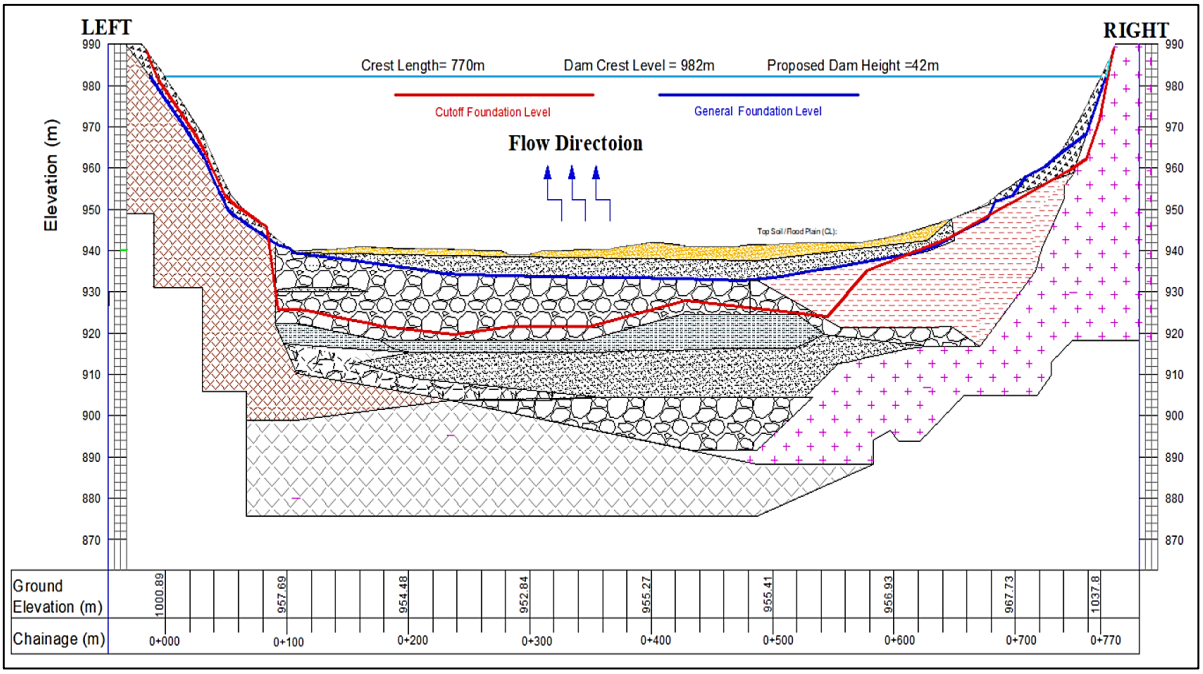

Gological Profile Legend	
GTL-1: Top-Soil - Silty Clay with Trace of Sand (CL):	GTL-5: Coarse Gravel (GM)
GTL-2: Flood Plain Deposit Silty Clay (CL)	GTL-6: Clastic Sediments Deposit
GTL-3: Clayey Silt with trace of Gravel (MH)	GTL-7: Moderately Weathered (Rhyolite /Trachytic Rock Mass)
GTL-4: Fine Grained Silty Sand (SM)	GTL-8: Highly Weathered Grade-Iv Material
	GTL-9: Slightly Weathered Grade-II Material

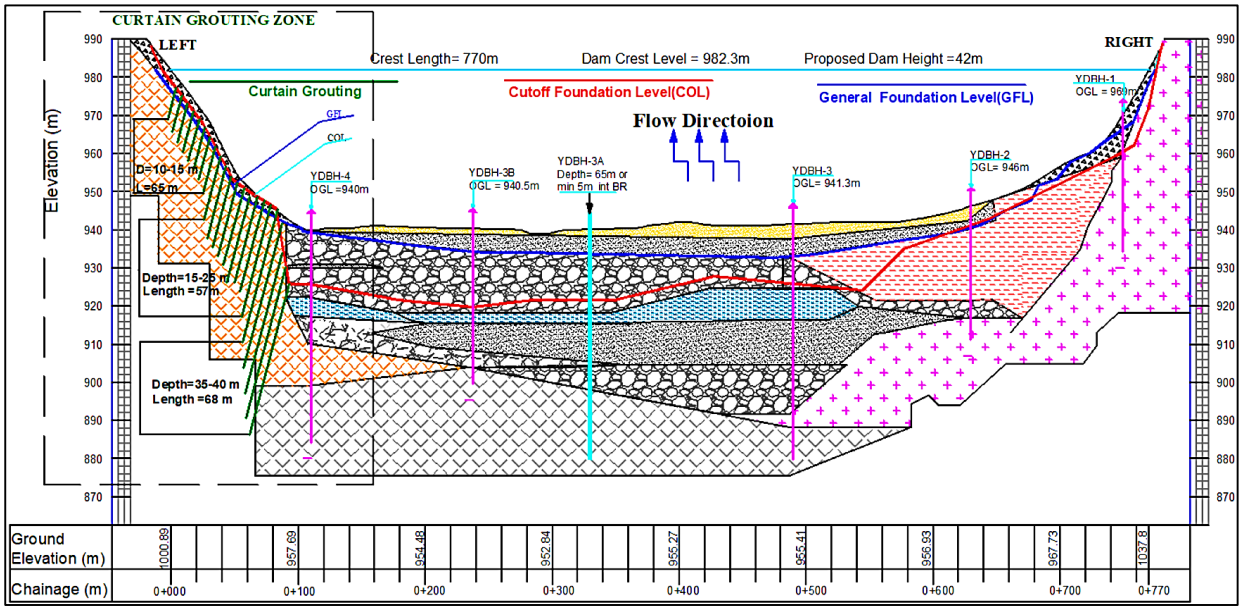

Figure 17 Geological profile and Profile with borehole Pattern

4. DATA ANALYSIS, RESULTS AND DISCUSSION

4.1. Previous Yanda Dam Design Geometry

The following drawing, which was the typical cross-sectional drawing at the chainage of 0+327.5, was done by the engineering design team of ECDSWC as the final detail design typical drawing for the project of Yanda Dam and irrigation construction. However, for this thesis work in the next chapter, there are going to be some modifications to some extent, and some adjustments with explanations will be attached in the appendix.

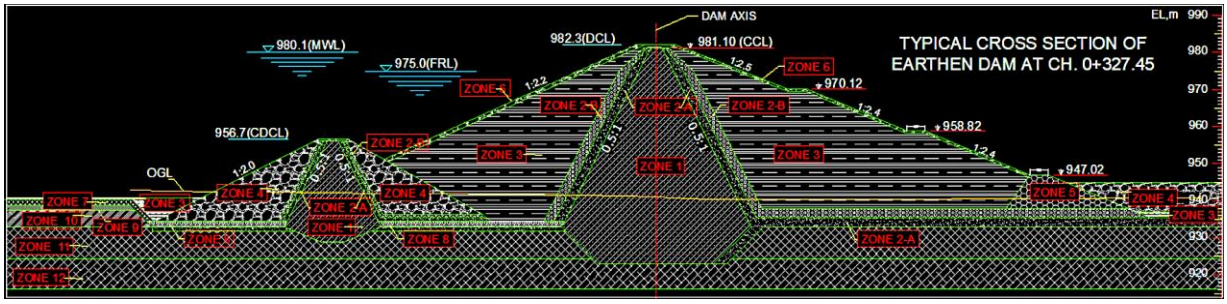

Figure 18 Previous Typical cross-section of Yanda dam at 0+327.5

The sections of the dam body that make up the zoned cross section are;

EARTHEN FILLED ZONING:	FOUNDATION ZONING:
Zone 1 - Clay Core	Zone 9 - Silty Clay Foundation
Zone 2-A - Fine Filter	Zone 10- Silty Sand Foundation
Zone 2-B - Coarse Filter	Zone 11- Coarse Gravel Foundation
Zone 3 - Shell Fill	Zone 12- Clayey Silt Foundation
Zone 4 - Rock fill	Zone 13- Silty Clay With Traces Of Gravel Foundation
Zone 5 - Toe Drain	Zone 14- Silty Gravel
Zone 6 - Rip Rap	Zone 15- Slightly Weathered Lower Basalt
Zone 7 - Clay Blanket	Zone 16- Moderately Weathered Trachyte
Zone 8 - Gravelly Clay(GC)	Zone 17- Highly Weathered Lower Basalt
Zone 2-Ai- Fine Filter For Dispersive Foundation	Zone 18- Concrete
Zone 2-Bi - Coarse Filter For Dispersive Foundation	

Table 8 Zoned Dam bodies cross-section description

4.2. The River Course's Physiography

The Yanda River has 500-800 meters of meandering belt at the dam site. Each year the meandering belt has varied in shape and dimension. The following pictures show how the riverside width is varied each year. The photos have been taken from the Google Earth Pro application and used for this research purpose.

Legend of Yanda River Course Boundary History

	2022/2021/2020 River Course Boundary
	2019/2016 River Course Boundary
	2013 River Course Boundary

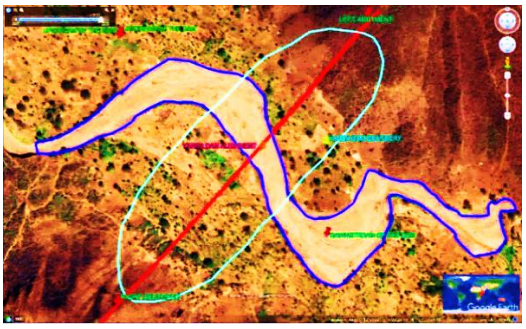

a. satellite image of the dam site in January 2022(red line is the dam seat)

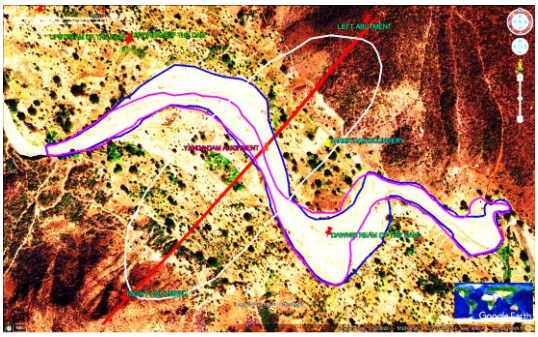

b. Satellite image in January 2022

c. Satellite image in January 2021

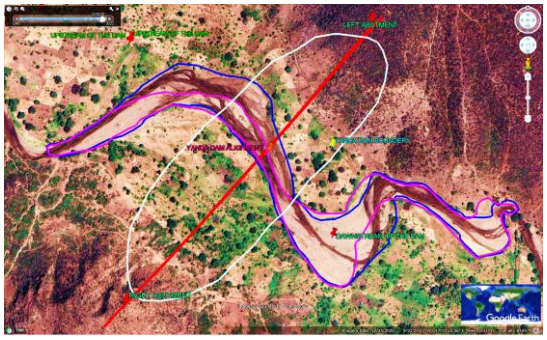

d. Satellite image in December 2020

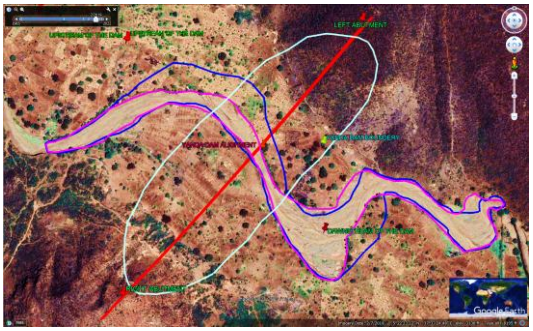

e. Satellite image in February 2019

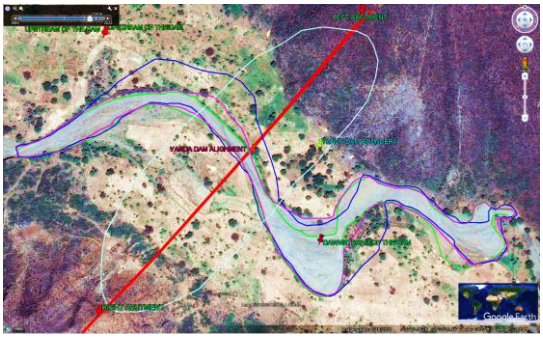

f. Satellite image in February 2016

g. Satellite image in December 2013

Figure 19 Satellite images to show the river meandering in Years(2013-2022)

4.3. The Dam Site Topography

The Yanda River is transported in the perpendicular direction of the dam alignment along the cross-sectional broad U-shaped valley that has the Yanda Dam alignment. The elevation of the river bed is 940.0 meters above sea level. The series of figures below show the morphology of the river at the dam location, both upstream and downstream.

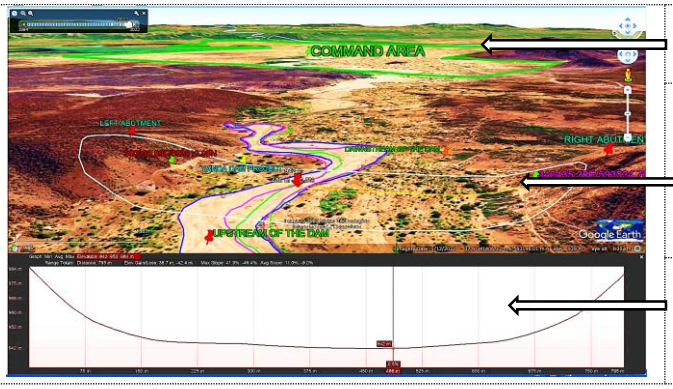

DawnStream Yanda proposed the Irrigation Command Area

Yanda Dam wide U-shape location and alignment, The Yellow line is the center line of the dam, and the white line is the boundary of the dam site

Yanda dam site longitudinal profile section of 1D modeling

a. View from upstream

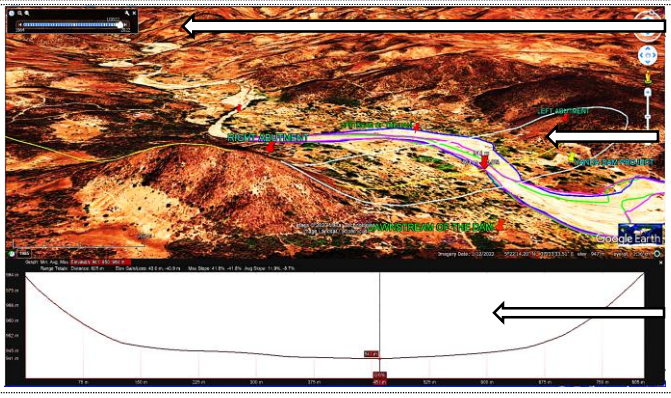

UpStream Yanda River overview

Location and alignment of the wide U-shaped Yanda Dam. The dam's center line is indicated by a yellow line, while the dam's boundary is defined by a white line. The placement of the coffer dam is shown by the yellow line next to the right abutment and on the left side of the reader.

Yanda dam site longitudinal profile section of 1D modeling

b. View from Downstream

Figure 20 Current Google Earth satellite imaging of the dam site in 2022

4.3.1. Eagle Point and Auto CAD Softwar

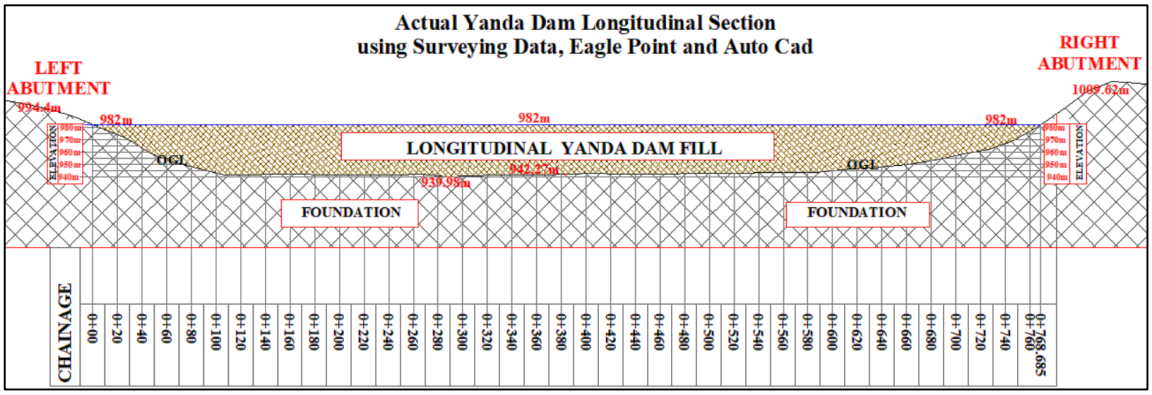

Figure 21 Actual Yanda Dam longitudinal section using surveying data

Here, Eagle Point and Auto-Cad software have been used in conjunction with the primary surveying reading data to provide a comprehensive understanding of the dam's location and section pertaining to practical application.

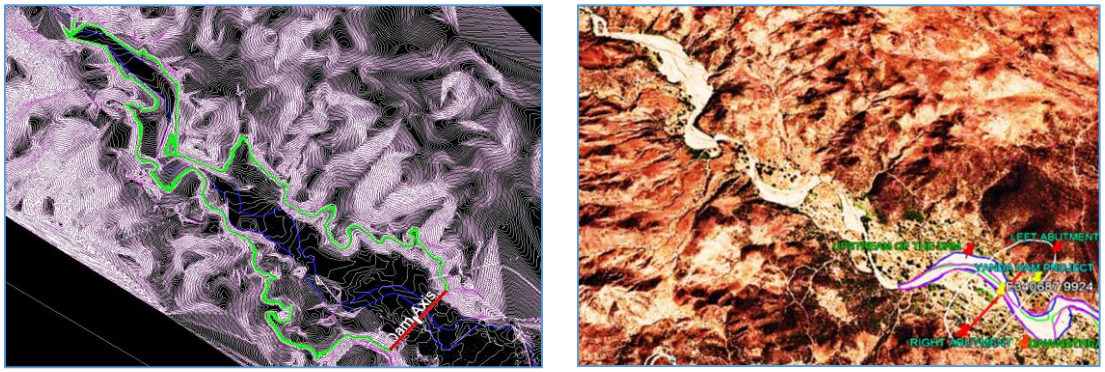

Figure 22 Comparison of the topo created using surveying data and satellite photographs

4.4. Adjusted Yanda Dam's cross-section profile

To conduct this research, the researcher has chosen to take three representative cross-sections based on the geological profile at the changes of 0+110.3, 0+327.5, and 0+630. To analyze the problems of each layer, based on the geotechnical investigation report, the foundation's soil layers should be characterized and identified in detail. Therefore, the following drawings have been adjusted and prepared for the next seepage and liquefaction analysis.

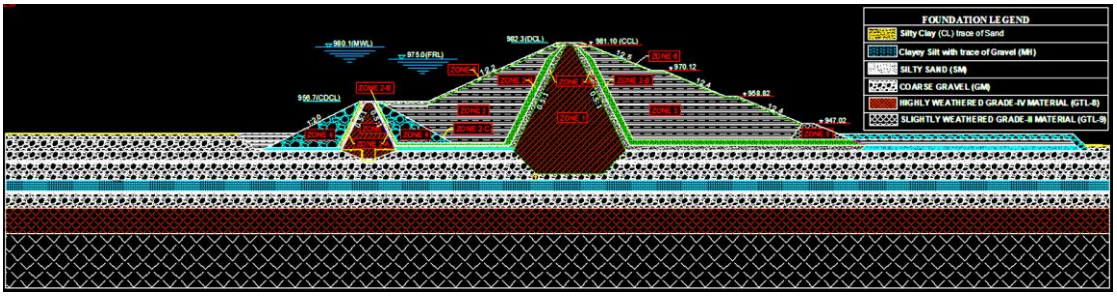

a. Adjusted cross-section of Yanda Dam at chainage 0+110.3

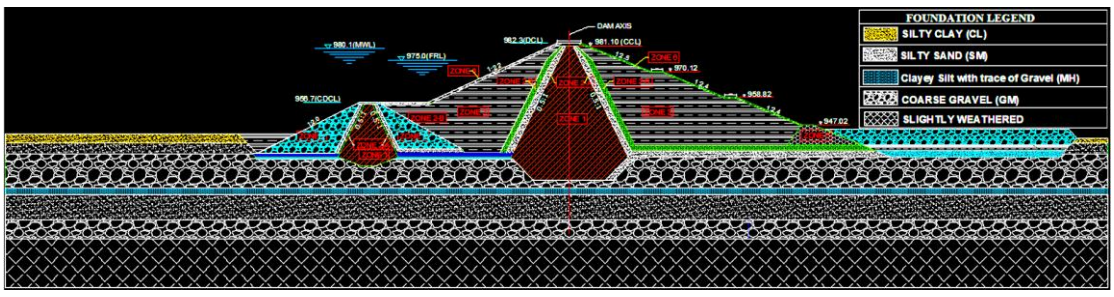

b. Adjusted cross-section of Yanda Dam at chainage 0+327.5

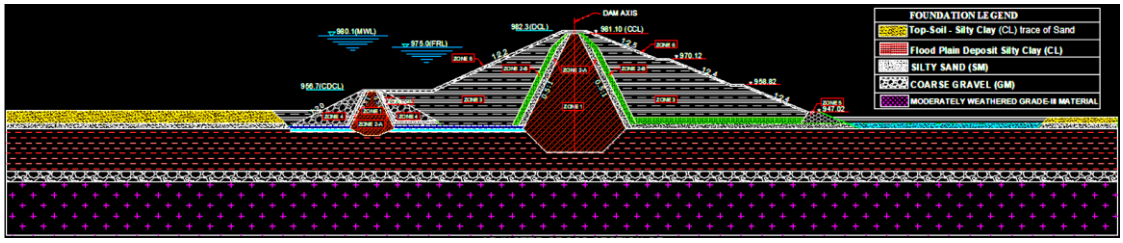

c. Adjusted cross-section of Yanda Dam at chainage 0+630

Figure 23 Adjusted Cross sections of Yanda dam for next modeling work

4.5. Numerical Modeling and Analysis

The procedure or methods used for the analysis of Yanda dam have been presented using the software of Geo-Studio 2018 as follows:

4.5.1. SEEP/W Analysis

1st. Geometry Importing

On the Seep/W window, the dam cross section has been sketched. The cross-sections utilized in the analysis have been shown in Figure 24. Drawing the dam's dimensions or geometry would be done using two different approaches. The first involves selecting the x and y coordinate points from each curved point or required point, then manually entering those points to define the dialogue box list. Alternately, it could be imported data from an AutoCAD design that has already been created directly and automatically into the GeoStudio File dialogue box by adjusting the coordinate points and using the Import Region button. Nonetheless, the second choice has been made for this study.

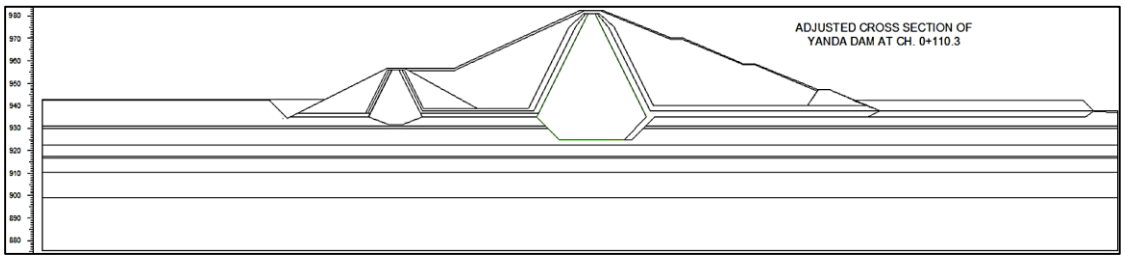

a. Adjusted Gometry Cross-Section of at chainage 0+110.3

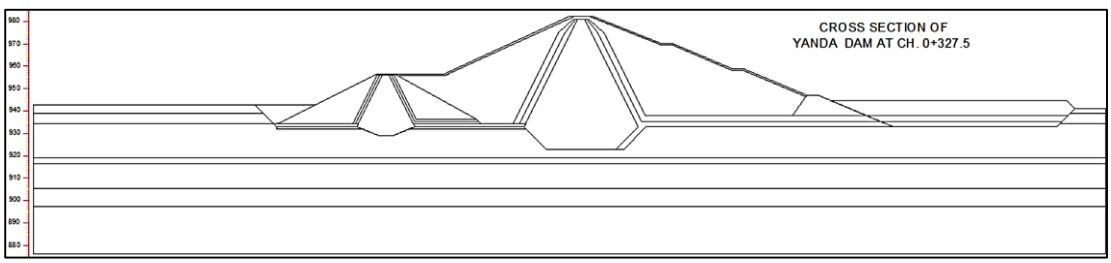

b. Adjusted Gometry Cross-Section of at chainage 0+327.5

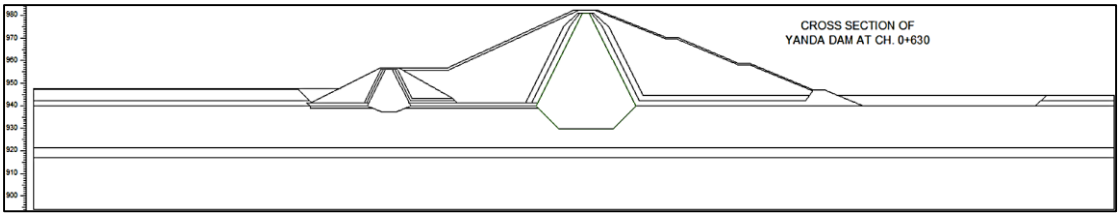

c. Adjusted Gometry Cross-Section of at chainage 0+630

Figure 24 Adjusted design Drawings for importing into Geo-Studio work

2nd. Defining Material...

Each material has been allocated to its corresponding area. Those filled dam materials and the layered foundation materials would be given distinct engineering characteristics in this stage, and each material would be distinguished by color, as seen in the dialog box that follows. Each area would be allocated a material attribute and material model. The study would employ the unit weight, angle of friction, and cohesiveness of the material as input factors.

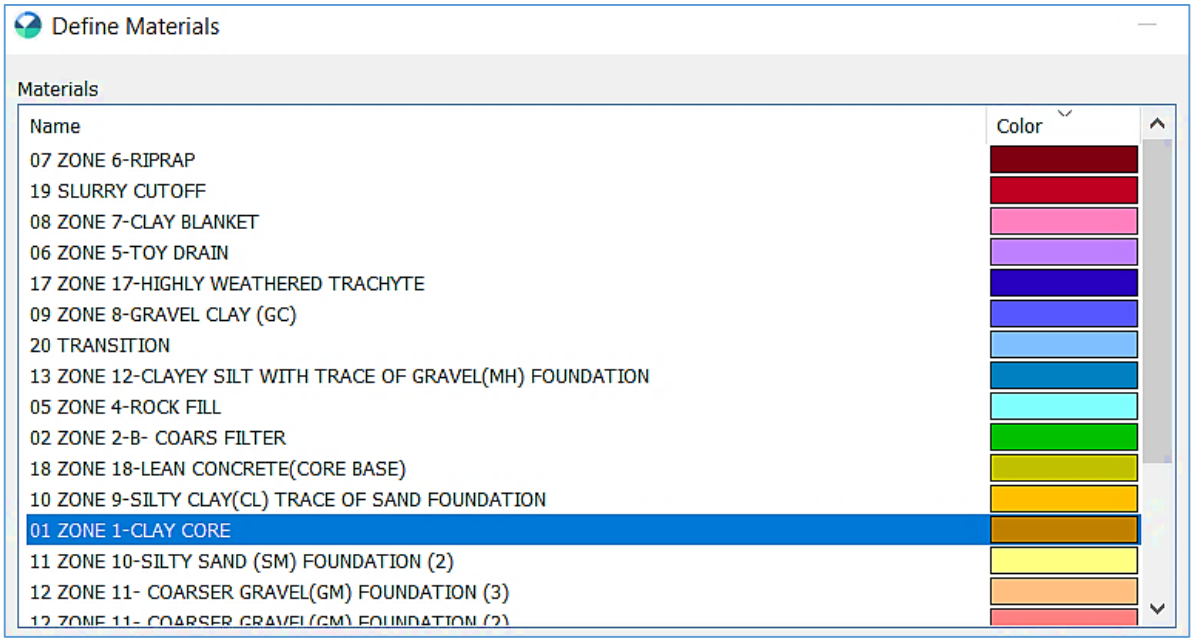

4.5.2. Parameters used for seepage analysis

The coefficient of permeability for the foundation and embankment materials was taken from the Yanda Dam final design report and prepared according to ECDSWC, 2022, as well as a few other standards. In this investigation, pore water has been extracted from the Seep/w result. After the issue was resolved, the findings were examined and spoken about.

Method of analysis	**Seepage Analysis**			
Material Model:	**Saturated/Unsaturated**			
Filled material and Alluvial layers	**Compressibility**	**SWC**	**RWC**	**Saturated Kx**
	1/KPa	**Porosity**	**SWC/10**	**m/sec**
ZONE 1-CLAY CORE	1e-07	0.5	0.05	6.5e-09
ZONE 2-B- COARS FILTER	1e-08	0.31	0.031	4e-06
ZONE 2-A -FINE FILTER	1e-08	0.29	0.029	1e-06
ZONE 3-SHELL FILL	1e-09	0.37	0.037	2.07e-05
ZONE 4-ROCK FILL	1e-10	0.24	0.024	0.00012
ZONE 5-TOY DRAIN	1e-10	0.24	0.024	0.00012
ZONE 6-RIPRAP	1e-10	0.24	0.024	0.00012
ZONE 7-CLAY BLANKET	1e-07	0.5	0.05	6.5e-09
ZONE 8-GRAVEL CLAY (GC)	1e-09	0.34	0.034	5e-09
ZONE 9-SILTY CLAY(CL)	1e-08	0.34	0.034	5.05e-07
ZONE 10-SILTY SAND (SM) FOUNDATION	1e-07	0.53	0.053	5.04e-08
ZONE 11- COARSER GRAVEL(GM)	1e-08	0.31	0.031	4e-06
ZONE 12-CLAYEY SILT(MH))	1e-07	0.34	0.034	5e-07
ZONE 15-SLIGHTLY WEATHERED	1e-10	0.52	0.052	4.93e-08
ZONE 17-HIGHLY WEATHERED TRACHYTE	1e-10	0.52	0.052	9.47e-06
SLURRY CUTOFF	1e-07	0.5	0.05	6.55e-09
TRANSITION	1e-08	0.31	0.031	4.5e-06

Table 9 Parameters used for seepage analysis

4.5.2.1. Porosity (e)

The typical values of Porosity (e) are described by Domenico and Schwartz (1997). Values of **Porosity** for Gravel (0.24-0.38), Coarse Sand (0.31-0.46), and Fine Sand (0.26-0.53). However, the grain size in itself does not affect the value of porosity, as well-rounded, similarly packed sediments, notwithstanding their particle size, will maintain similar porosities.

4.5.2.2. Anisotropy (K_H/K_V)

According to the Design Standards, Embankment Dams /DS-13(8)-4.1(2014), the following permeability of various embankment materials have been listed.

Material	**K_H/K_V Range**	**Reference**
Embankment core	4 to 9	Cedergent, H.R. 1977., U.S. Army Corps of Engineers,1986. EM 1110-2-1901., Casagrande, A. 1940., Esmiol, E.E., 1977., Hirschfeld, R.C.1973.
Nonstandard placement	9 to 36	
Hydraulic fill	64 to 225	
Embankment shell	4 to 9	
Embankment shell	1 to 4	
Anisotropy (K_H/K_V) of embankment materials, K_H/K_V increases with placement water content		

Table 10 Permeability of various embankment materials

4.5.2.3. Pore-Water Pressure Ratio (Ru)

A pore-water pressure ratio (Ru) value has been utilized to connect the overburden stress to pore water pressure during the computation of slope stability for stage construction and end of

construction. The Ru value for non-free drained material is displayed in Table 11 and was taken from the project's design report (ECDSWC, 2022).

Material Zone	PWP Ratio Ru (during of construction)	PWP Ratio Ru (end of construction)
Impervious Core (Zone 1)	0.45	0.4
U/S Clay Blanket/GC	0.45	0.4
Silty Sand Foundation	0.35	0.3
(Zone 2),(Zone 3),(Zone 4) and (Zone 5)	-	-

Table 11 Pore-Pressure Ratio (ECDSWC's Yanda Dam design Report(2022)

4.5.2.4. Boundary Condition (BC)

Boundary conditions are essential for any analysis, including susceptible seepage problems on Seep/W. These conditions provide information about the behavior of the system at its boundaries, which is crucial for determining the solutions. In the case of seepage problems, the boundary conditions specify the hydraulic total head difference between two points or the specified flow rate into or out of the system. These conditions serve as the driving force behind the seepage flow, determining the direction and magnitude of the flow. Without these boundary conditions, it would be impossible to obtain a solution for the seepage problem. The behavior of the system would remain unknown, and there would be no way to predict or analyze the seepage flow. Therefore, specifying boundary conditions is crucial in the analysis of susceptible seepage problems on Seep/W. These conditions are the key factors that provide the necessary information for determining the solutions to these problems.

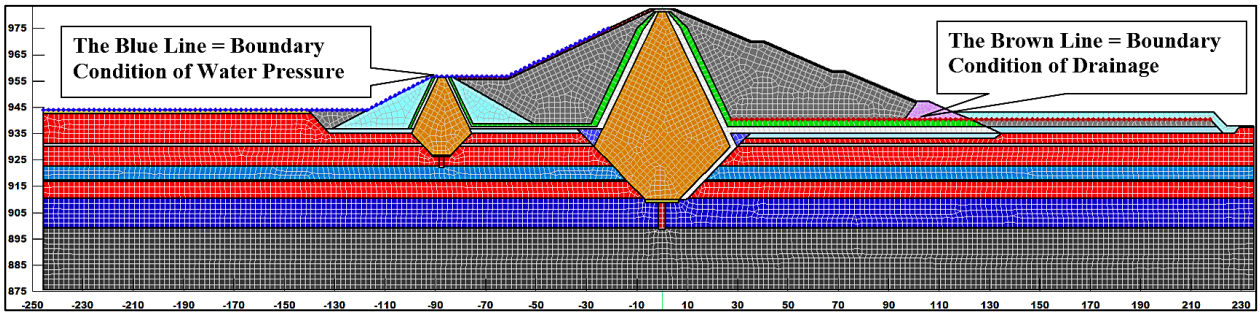

Figure 25 Boundary condition of Seep/W Yanda dam

4.6. Determine the Seepage Protection Options

According to EM 1110-2-1901, even though choosing a cutoff can be challenging and expensive, using a flow nets system can help compare various under-seepage control techniques for a dam and its foundation. This allows engineers to assess the relative advantages and

efficacy of each technique, aiding in the selection of the most suitable one. The flow nets system helps in understanding the flow patterns and potential areas of under-seepage, enabling a more informed decision-making process regarding the choice of under-seepage control measures.

Therefore, it is important to analyze the steady seepage to understand the amount of water flowing through the embankment's foundation. This will help in calculating the pore water pressure within the foundation, which is crucial for the piping analysis. The steady seepage analysis will be conducted at three specific chainages - 0+110.3, 0+327.5, and 0+630. These chainages were selected based on the geological profile of the foundation, which indicates the presence of multiple alluvial deposited layers with varying thicknesses. The presence of these layers increases the likelihood of abnormal seepage, which can lead to concentrated leakage and ultimately result in piping issues. Therefore, it is crucial to analyze the steady seepage to assess the potential seepage flow and pore water pressure within the foundation. By conducting these analyses, we can better understand the potential issues related to seepage and piping in the embankment's foundation. This information will be valuable for designing appropriate measures to address these problems and ensure the stability and integrity of the Yanda Dam.

According to the geological profile (figure 17), the dam's foundation is highly exposed to abnormal seepage, with materials deposited from 940m a.s.l to 890m a.s.l capable of passing large amounts of water. The study focuses on materials found in the foundation of a 50m deep down. The seepage examination will determine the flux through the dam body and foundation, and the distribution of pore water pressure is crucial for steady-state seepage study. The author provides twenty options for regulating seepage without piping, allowing for comparison, analysis, and selection of the minimum risk remedial measure.

The essential considerations while choosing a treatment method are the quantity of seepage, hydraulic gradient, safety factor, and cost. It appears that using a cutoff wall rather than a clay blanket is the better method of waterproofing the dam because of the substantial thickness of the sediments, the extended reservoir of the dam, and the associated expenses. The finite element technique and the Seep/W software were used to accomplish this aim. Using the numerical analysis approach, the Seep/W software is a finite element program that can theoretically simulate seepage (Krahn, 2009).

4.6.1. Seepage Control Options at chainage 0+110.3

4.6.1.1. Option 1:-Base Case

This option would be regarded as a base case that only has a key trench and no corrective measures implemented.

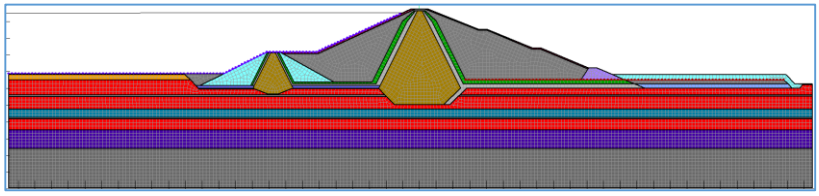

a. Drawing for option-1 evaluation

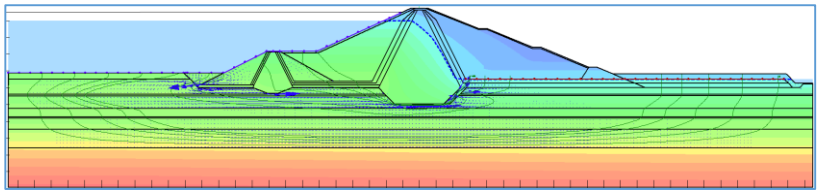

b. Seep/W analysis for option 1

Flow No.	Flow Travel Distance (m)	Water Flux (m³/sec/m²)
2	524.39	1.33E-22
3	472.53	2.82E-08
4	447.74	2.94E-08
5	432.40	3.01E-08
6	428.09	2.99E-08
7	265.48	3.46E-22
8	227.43	2.22E-19
9	167.43	3.45E-20
10	137.95	1.81E-20
11	125.74	1.21E-20
AVG	**322.92**	**1.18E-08**

c. Summary of analyzed water path and flux

4.6.1.2. Option 2

This method has involved reducing the surplus cutoff that stretched below the alluvial foundation while maintaining the upstream blanket and all cutoff as originally designed. This study has been important since it evaluated the water flux and flow route length to see if restorative methods would work better overall.

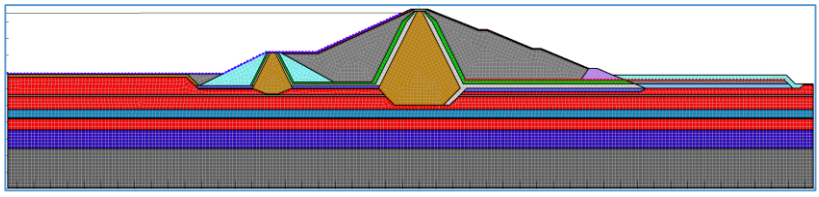

a. Drawing for option 2 evaluation

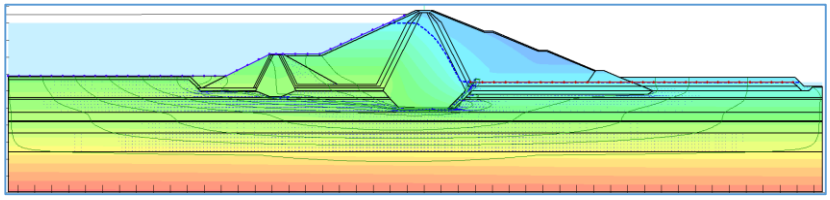

b. Seep/W analysis for option 2

Flow No.	Flow Travel Distance (m)	Water Flux (m³/sec/m²)
2	555.55	7.12E-10
3	478.50	2.93E-08
4	421.38	3.23E-08
5	380.98	3.71E-08
6	377.32	1.73E-27
7	304.39	2.96E-19
8	255.17	2.48E-19
9	225.98	2.20E-19
10	191.43	1.90E-19
11	146.38	1.49E-19
AVG	**333.71**	**9.94E-09**

c. Summary of analyzed water path and flux

4.6.1.3. Option 3

In this option, the coffer dam's clay-filled cutoff has been extended to a height of 927 meters, and a soil-bentonite slurry has been applied at a depth of 4 meters. Gravel clay (GC) has also been used beneath the main dam shoulder in place of the u/s blanket protection mechanism. The main dam's trench cutoff has not been extended and has been simply taken from the previous original design.

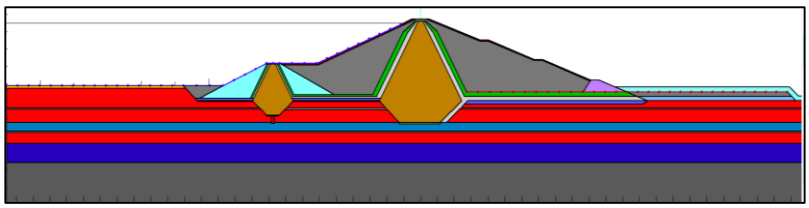

a. Drawing for option 3 evaluation

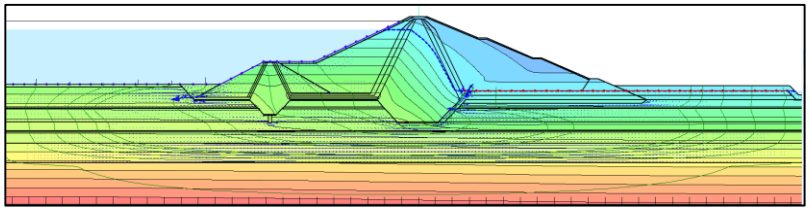

b. *Seep/W analysis for option 3*

Flow No.	Flow Travel Distance (m)	Water Flux (m³/sec/m²)
2	516.43	2.22E-21
3	479.58	3.13E-08
4	456.21	3.29E-08
5	442.47	3.48E-08
6	442.65	3.63E-08
7	338.89	6.11E-21
8	325.66	3.04E-19
9	191.14	1.86E-19
10	147.81	1.49E-19
11	132.74	1.32E-19
AVG	**347.36**	**1.35E-08**

c. *Summary of analyzed water path and flux*

4.6.1.4. Option 4

In this option, soil-bentonite slurry with a depth of 10 meters for the main dam and 4 meters for the coffer dam has been conducted without applying the protection mechanism of u/s blanket and gravel clay. This has been done by extending the main dam's (15.39 meters) and coffer dam's (4.85 meters) clay-filled cutoff up to the elevation of 910 meters and 927 meters, respectively.

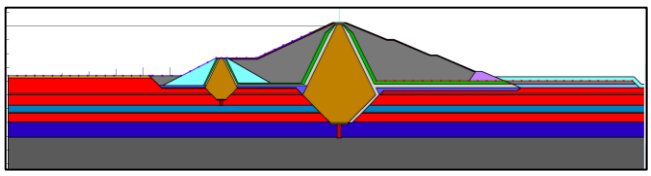

a. Drawing for option 4 evaluation

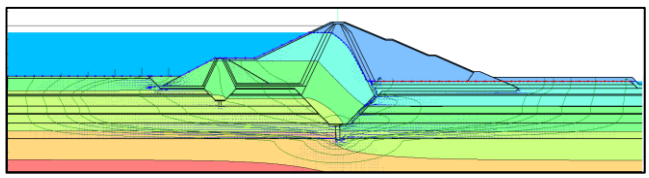

b. Seep/W analysis for option 4

Flow No.	Flow Travel Distance (m)	Water Flux (m³/sec/m²)
2	533.20	5.67E-23
3	476.10	1.18E-08
4	445.86	1.40E-08
5	427.79	1.56E-08
6	426.49	1.65E-08
7	307.78	2.21E-19
8	284.73	2.06E-19
9	190.18	1.41E-19
10	158.91	1.16E-19
11	143.28	1.06E-19
AVG	**339.43**	**5.79E-09**

c. *Summary of analyzed water path and flux*

4.6.1.5. Option 5

This working option is similar to option 1, but the difference is that here the upstream clay-filled blanket has been applied.

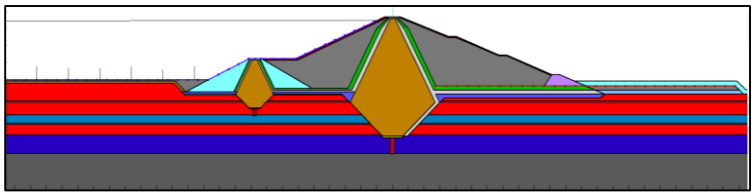

a. Drawing for option 5 evaluation

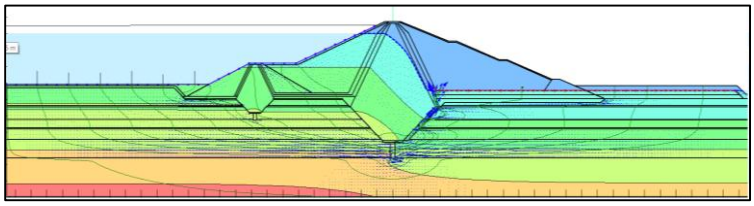

b. Seep/W analysis for option 5

Flow No.	Flow Travel Distance (m)	Water Flux (m³/sec/m²)
2	481.20	1.12E-08
3	410.20	1.47E-08
4	368.32	1.65E-08
5	336.54	1.34E-24
6	272.79	1.96E-19
7	252.16	1.84E-19
8	227.40	1.57E-19
9	202.72	1.46E-19
10	159.50	1.16E-19
11	143.92	1.02E-19
AVG	**285.48**	**4.25E-09**

c. *Summary of analyzed water path and flux*

In order to provide a restricted layer above the coarse gravel (GM) foundation material with the property of high permeability material, a 1 m thick GC material at the D/S main dam has been proposed at chainage 0+110.3 and option 3. The properties of GC material include very low compressibility, good to fair shear strength, and impermeable permeability. In order to lessen the risk of piping, the plan also favored to strengthen the foundation by extending the water flow beneath the dam foundation. The heading water's flow path from u/s to d/s while altering the GC foundation's layer has been simulated using the Seep/w program.

4.6.1.6. Option 6

Similar to option 3, this working option would also employ a protective remedial strategy, with the exception of placing GC material beneath the dam's downstream shoulder.

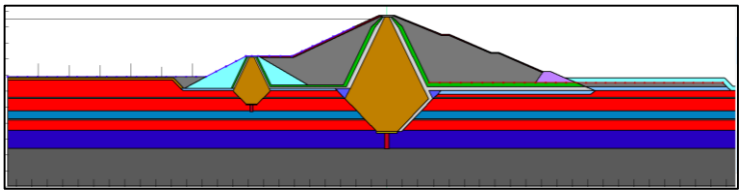

a. Drawing for option 6 evaluation

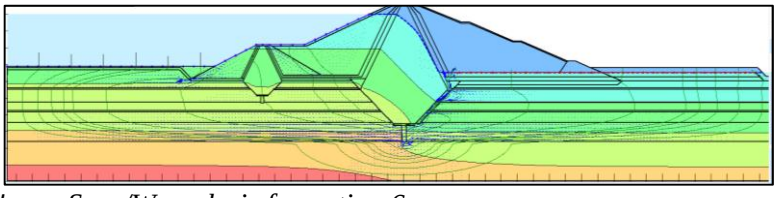

b. Seep/W analysis for option 6

Flow No.	Flow Travel Distance (m)	Water Flux (m³/sec/m²)
2	544.84	9.63E-21
3	515.73	9.38E-09
4	500.69	1.13E-08
5	491.47	1.22E-08
6	490.00	1.26E-08
7	437.72	1.42E-08
8	298.41	2.88E-23
9	227.35	1.63E-19
10	165.24	1.19E-19
11	147.25	1.04E-19
AVG	**381.87**	**5.97E-09**

c. Summary of analyzed water path and flux

4.6.1.7. Option-7

In this case, the GC material foundation treatment and the u/s blanket foundation treatment have both been rejected. However, all other remedial treatments utilized in option 1 have been modified, including applying soil-bentonite slurry to the lower portion of the extended trench cutoffs of the coffer dam and the main dam.

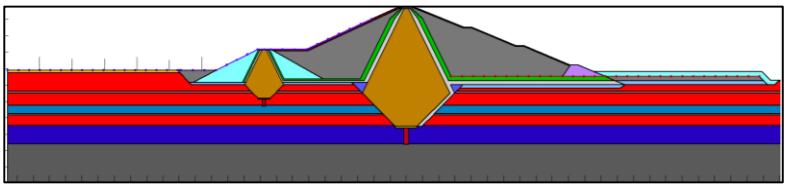

a. Drawing for option 7 evaluation

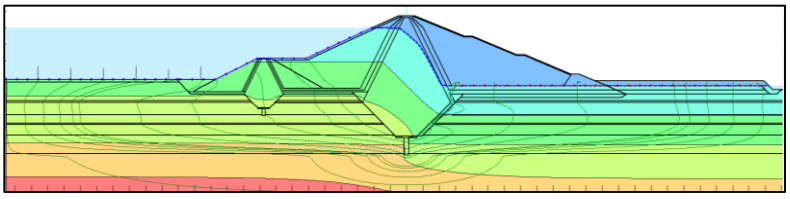

b. Seep/W analysis for option 7

Flow No.	Flow Travel Distance (m)	Water Flux (m³/sec/m²)
2	538.12	3.81E-22
3	500.07	1.05E-08
4	480.50	1.20E-08
5	470.94	1.28E-08
6	475.77	1.31E-08
7	376.86	9.56E-28
8	275.56	2.97E-21
9	225.78	1.62E-19
10	165.09	1.17E-19
11	147.08	1.06E-19
AVG	**365.58**	**4.84E-09**

c. Summary of analyzed water path and flux

4.6.1.8. Summarized the Remedial Options of 0+110.3

The two most important factors to consider while choosing among the aforementioned possibilities are water flux and distance (flow route). Priority has been given to the option with the longer flow channel and somewhat lower water flux discharge as an appropriate corrective measure. Therefore, based on the analysis above, alternatives 5 and 7 could have been chosen by comparing them relative to one another.

Options	Average Flow Path Distance (m)	Average Water Flux (m³/sec/m²)	Descriptions
Option-1	322.92	1.18E-08	*Option of Base Case (without any Remedial Measure but only Key Trench)*
Option-2	333.71	9.94E-09	*Original taken design with U/S Blanket without complete and slurry cutoff.*
Option-3	347.36	1.35E-08	*Option without U/S Blanket and not applying slurry cutoff, but only compacted backfill trench(complete cutoff)*
Option-4	339.43	5.79E-09	*Option with Main Dam(MD) & Coffer Dam(CD) Complete cutoff combined with 10m & 4m Soil-bentonite Slurry Cutoff, respectively. But without the u/s blanket.*
Option-5	285.48	4.25E-09	*Option with Main Dam(MD) & Coffer Dam(CD) Complete Cutoff combined with 10m & 4m Soil-bentonite Slurry Cutoff, respectively. And with U/S Blanket and GC material.*
Option-6	381.87	5.97E-09	*MD & CD Complete cutoff combined with 10m & 4m Soil-bentonite Slurry Cutoff, respectively. And without U/S Blanket without GC.*
Option-7	365.58	4.84E-09	***Selected Remedy** with MD & CD Complete cutoff combined with 10m & 4m Soil-bentonite Slurry Cutoff, respectively. And without U/S Blanket*
*"*Original Design" means actual design data taken from the institute of ECDSWC*			
0+110.3			

Table 12 Summarized the remedial options of 0+110.3

Options 5 and 7 have different water flux values, however option 5's flow path distance is shorter. Option 5 is not as cost-effective as option 7 since it requires more GC material and U/S blanket, which comes with a higher expense. This is because the hydraulic gradient is inversely proportional to the flow path, thus it is best to use the longer way to reduce the danger of pipe. For the purposes of this study project, option 7 has been chosen as the corrective action.

Consequently, the evaluated and chosen remedy of Option-7 in chainage 0+110.3 is 58.98 percent more effective (lower/reduced water flow) than Option-1 (The Base Case) and 51.3 percent better (lower/reduced water flux) than that of Option-2's original design.

4.6.2. Seepage Control Options at Chainage 0+327.5

4.6.2.1. Option 1: Base Case

In this option, only the key trench has been adapted, but any remedial options have not been utilized.

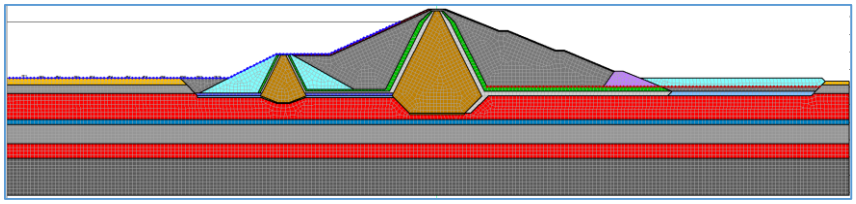

a) Drawing for 0+327/option-1 evaluation

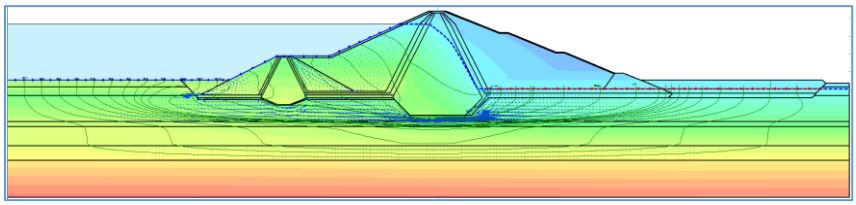

b) Seep/W analysis for 0+327/option-1

Flow No.	Flow Travel Distance (m)	Water Flux (m³/sec/m²)
1	502.48	3.57E-21
2	455.53	3.10E-26
3	420.38	9.67E-20
4	389.56	6.55E-09
5	367.98	2.05E-08
6	351.32	2.63E-08
7	340.50	1.01E-19
8	333.42	4.59E-20
9	330.53	7.59E-28
10	345.64	9.91E-28
11	318.56	3.89E-26
12	285.90	3.16E-25
13	235.21	1.64E-20
14	196.87	2.48E-20
15	202.11	1.31E-20
16	167.94	2.11E-20
17	142.35	5.85E-20
18	126.51	7.06E-20
19	123.51	7.78E-20
AVG	**296.65**	**2.80E-09**

C) Summary of analyzed water path and flux

4.6.2.2. Option-2

In this option, adapting all originally designed cutoff and upstream blanket without extending extra cutoff downward the alluvial foundation.

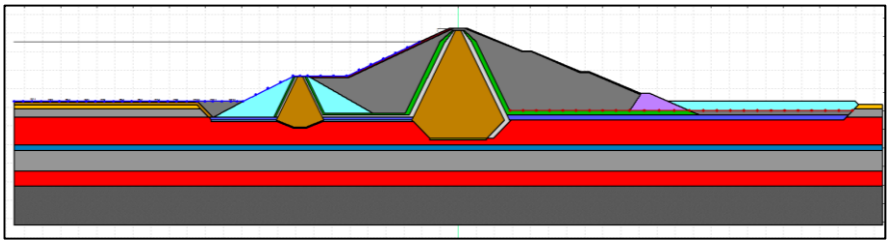

a. Drawing for 0+327/option 2 evaluation

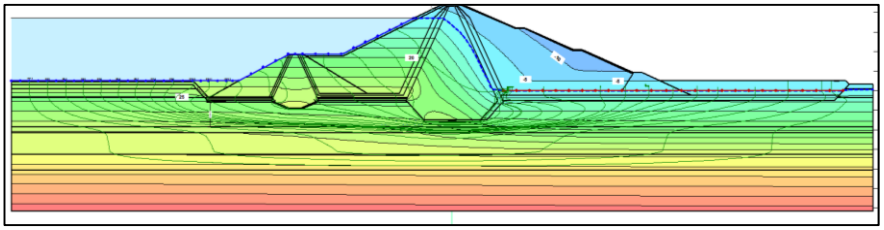

b. Seep/W analysis for 0+327/option 2

Flow No.	Flow Travel Distance (m)	Water Flux (m³/sec/m²)
1	491.02	4.14E-23
2	448.83	3.30E-27
3	410.77	7.54E-09
4	380.34	1.35E-08
5	360.14	2.43E-08
6	344.40	3.52E-20
7	332.24	4.60E-21
8	322.54	5.35E-25
9	307.17	4.17E-27
10	323.52	6.86E-27
11	294.45	6.75E-26
12	276.09	3.61E-25
13	230.92	1.00E-19
14	203.19	1.42E-20
15	208.43	2.14E-20
16	174.72	1.45E-20
17	144.80	5.09E-19
18	126.87	7.23E-20
19	123.32	6.81E-20
AVG	**289.67**	**2.38E-09**

c. Summary of analyzed water path and flux

4.6.2.3. Option-3

This alternative calls for a wall of soil bentonite slurry with a depth of 25 m without extending the core key trench without complete cutoff under the main dam(MD) and the coffer dam(CD).

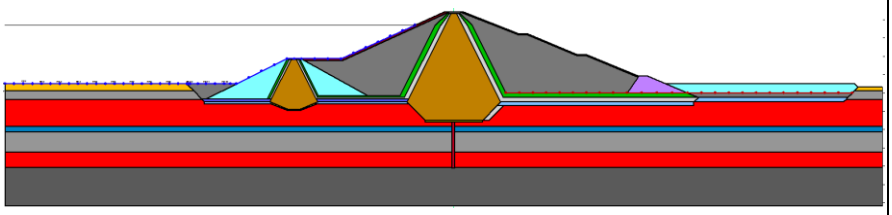

a. Drawing for 0+327/option 3 evaluation

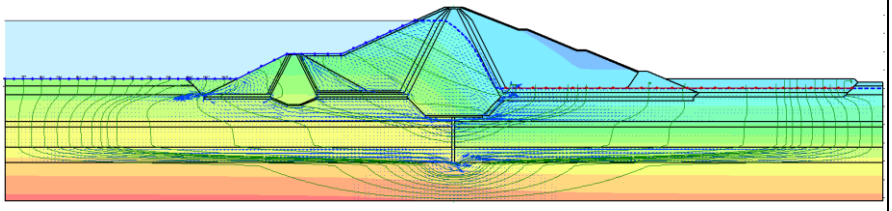

c. Seep/W analysis for 0+327/option 3

Flow No.	Flow Travel Distance (m)	Water Flux (m³/sec/m²)
1	577.54	6.76E-21
2	542.79	1.04E-21
3	533.25	4.37E-22
4	511.83	1.88E-23
5	499.64	1.47E-24
6	493.72	4.21E-21
7	476.87	8.99E-27
8	470.90	1.23E-27
9	468.78	3.97E-28
10	462.53	2.26E-20
11	417.96	6.56E-09
12	339.33	2.36E-24
13	307.58	1.92E-26
14	221.09	3.09E-21
15	219.76	2.50E-21
16	189.16	2.32E-21
17	151.57	6.81E-21
18	120.24	6.81E-20
19	102.14	5.32E-20
AVG	**374.04**	**3.45E-10**

b. *Summary of analyzed* water path and flux

4.6.2.4. Option-4

With extending extra depth cutoff up to 916.5m.a.s.l and 924.5m.a.s.l dawn ward the foundation for the main dam and cor dam respectively, 5m of soil bentonite slurry would be installed below the extended complete cutoff of the coffer dam.

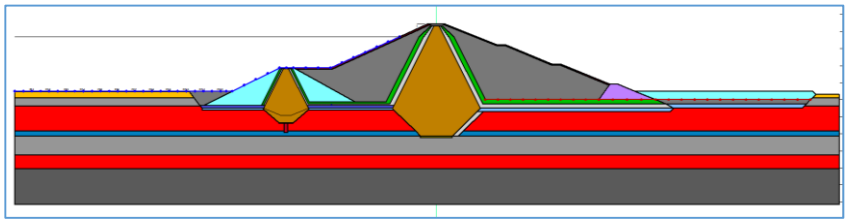

a. Drawing for 0+327/option 4 evaluation

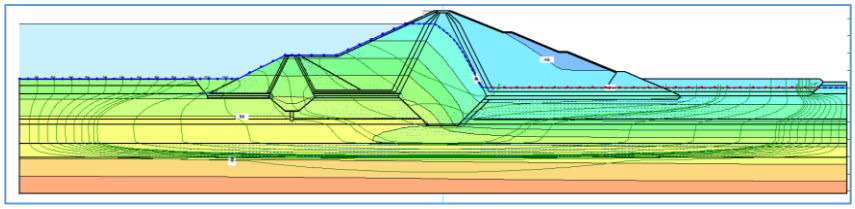

b. Seep/W analysis for 0+327/option 4

Flow No.	Flow Travel Distance (m)	Water Flux (m³/sec/m²)
1	572.03	1.08E-19
2	546.40	6.38E-21
3	535.17	9.48E-22
4	532.25	1.30E-21
5	518.71	4.08E-23
6	511.55	6.47E-24
7	505.16	1.17E-24
8	502.91	2.26E-25
9	502.94	6.75E-26
10	506.09	2.69E-26
11	450.00	2.64E-20
12	379.86	8.37E-09
13	335.17	3.02E-27
14	245.86	3.06E-20
15	234.28	2.25E-24
16	219.98	1.81E-21
17	162.27	3.54E-21
18	124.26	5.71E-20
19	104.21	5.14E-20
AVG	374.45	4.40E-10

c.Summary of analyzed water path and flux

4.6.2.5. Option-5

Only 5 meters of soil bentonite slurry would be put below the extended full cutoff of the coffer dam in this option, which would require extending the extra depth cutoff up to 924.5 m.a.s.l. and adding an extra depth of cutoff up to 916.5 m.a.s.l. to the foundations for the main dam. Also, GC would be blanketed under the downstream main dam shoulder.

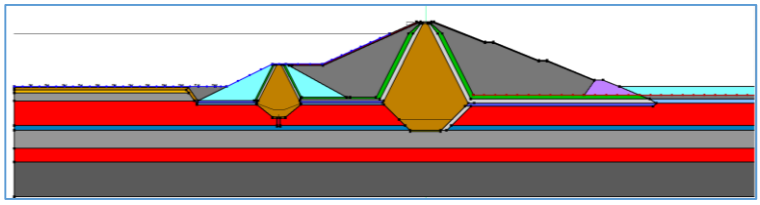

a. Drawing for 0+327/option 5 evaluation

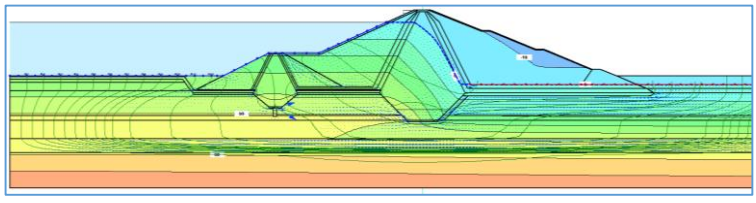

b. Seep/W analysis for 0+327/option 5

Flow No.	Flow Travel Distance (m)	Water Flux (m³/sec/m²)
1	567.37	1.08E-18
2	555.41	3.29E-20
3	529.32	1.86E-20
4	517.36	6.83E-21
5	507.36	1.69E-21
6	497.74	7.67E-22
7	496.32	2.12E-21
8	489.47	3.89E-21
9	481.83	7.09E-23
10	476.45	3.31E-23
11	460.41	6.46E-24
12	413.17	1.03E-25
13	363.66	5.71E-28
14	310.12	9.51E-09
15	307.44	4.12E-09
16	294.66	8.20E-09
17	249.07	1.60E-08
18	220.33	5.51E-20
19	99.54	7.24E-20
AVG	412.48	1.99E-09

c. *Summary of analyzed water path and flux*

4.6.2.6. Option-6

The current scenario calls for a wall of soil bentonite slurry to follow the extended full cutoffs of the main dam and the coffer dam, with a depth of 10 m and 5 m, respectively. The beginning of the foundations of the coffer dam (922 m a.s.l.) and the main dam (912.4.5 m a.s.l.) would likewise be elevated by that extra depth cutoff. The GC material and the U/S clay layer blanket would not be changed, though.

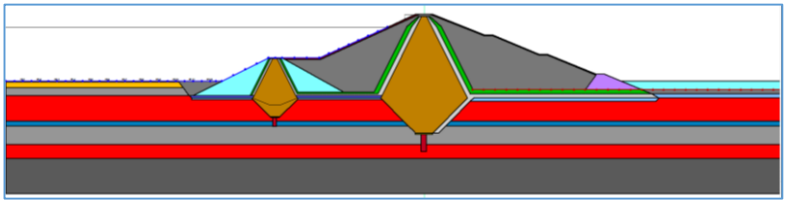

a. Drawing for 0+327/option 6 evaluation

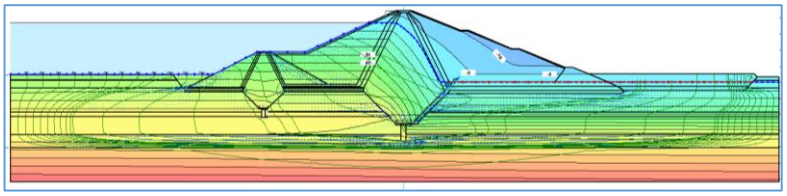

b. Seep/W analysis for 0+327/option 6

Flow No.	Flow Travel Distance (m)	Water Flux (m³/sec/m²)
1	574.46	1.38E-19
2	549.47	7.15E-21
3	540.56	1.04E-21
4	538.59	2.05E-21
5	525.15	5.13E-23
6	519.45	1.02E-23
7	515.14	1.95E-24
8	514.83	4.35E-25
9	520.33	2.64E-22
10	519.49	6.02E-26
11	469.11	2.63E-20
12	407.78	8.50E-09
13	324.30	2.63E-27
14	263.23	5.66E-25
15	247.95	1.69E-24
16	240.24	4.18E-24
17	164.08	4.04E-21
18	123.94	5.15E-20
19	104.90	5.18E-20
AVG	403.32	4.47E-10

c. *Summary of analyzed water path and flux*

4.6.2.7. Option-7

Under this option, a layer of soil bentonite slurry would be placed 10 meters below the extended full cutoff of the main dam and 5 meters below the coffer dam. Further, the additional depth cutoff would be extended to the dawn of the foundation for the main dam (916.5 m a.s.l., 7.38 m extra depth) and the coffer dam (924.5 m a.s.l., 4.47 m extra depth), respectively. Without GC, material would need to be modified.

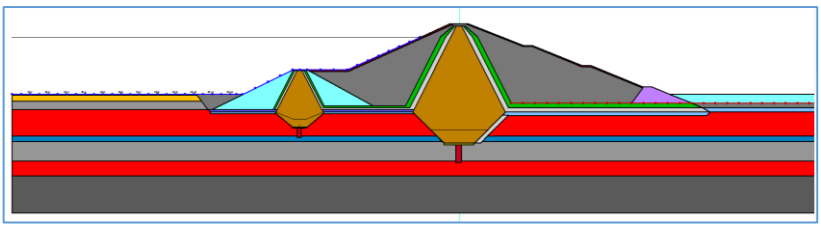

a. *Drawing for 0+327/option 7 evaluation*

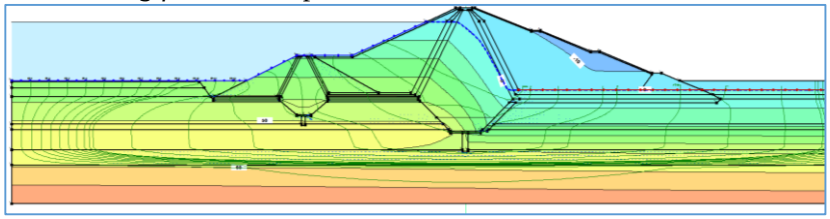

b. *Seep/W analysis for 0+327/option 7*

Flow No.	Flow Travel Distance (m)	Water Flux (m³/sec/m²)
1	572.84	1.21E-19
2	547.04	7.34E-21
3	536.24	9.84E-22
4	533.72	2.67E-21
5	523.41	4.19E-23
6	512.32	6.57E-24
7	507.58	1.33E-24
8	511.36	2.48E-25
9	505.03	7.44E-26
10	509.10	2.96E-26
11	462.90	3.26E-22
12	371.43	4.42E-09
13	325.00	9.24E-27
14	246.79	2.52E-24
15	244.37	2.04E-24
16	225.52	2.28E-21
17	161.11	3.40E-21
18	123.00	5.26E-20
19	102.95	5.18E-20
AVG	395.88	2.33E-10

c. *Summary of analyzed water path and flux*

4.6.2.8. Summarized the Remedial Options of 0+327.5.

Option 7 has been determined to be superior to the other alternatives based on the options' summary. The reason for this is because the chosen option has a minimum water flux of 2.33e-10m3/sec/m2 and a rather lengthy flow route of 395.88m.

Options	Average Flow Path Distance (m)	Average Water Flux ($m^3/sec/m^2$)	Descriptions
Option -1	**296.65**	**2.80E-09**	*Option of Base Case Value (without any Remedial Measure but only Key Trench)*
Option -2	**289.67**	**2.38E-09**	***Original taken** design with U/S Blanket without complete and slurry cutoff.*
Option -3	**374.04**	**3.45E-10**	*Option with soil bentonite slurry with a depth of 25 m and the core key trench, without complete cutoff under the main dam(MD).*
Option -4	**394.16**	**4.40E-10**	*Option with some extra depth of complete cutoff for both Main Dam(MD) and Coffer Dam(CD). But 5m Slurry Cutoff only for Coffer Dan(CD) without the U/S Blanket.*
Option -5	**412.48**	**1.99E-09**	*Option with some extra depth of complete cutoff for both Main Dam(MD) and Coffer Dam(CD). But 5m Slurry Cutoff only for Coffer Dan(CD) with the combination of the U/S Blanket.*
Option -6	**403.32**	**4.47E-10**	*Option with some extra depth of complete cutoff for both Main Dam(MD) and Coffer Dam(CD). In addition, 10m & 5m Slurry Cutoff for both MD & CD without the U/S Blanket.*
Option -7	**395.88**	**2.33E-10**	***Selected Remedy** with MD & CD Complete cutoff combined with 10m & 5m Soil-bentonite Slurry Cutoff, respectively. And without U/S Blanket*
*"*Original Design" means actual design data taken from the institute of ECDSWC*			
0+327.5			

Table 13 Summarized the remedial options of 0+327.5

In chainage 0+327.5, therefore, the solution that Option-7 has chosen and studied is 91.7 percent more effective (lower/reduced water flux) than Option-1 (the base case) and 90.2 percent better (lower/reduced water flux) than Option-2's original design.

4.6.3. Seepage Control Options at Chainage 0+630

4.6.3.1. Option 1-Base Case

Without employing an upstream blanket and any other extra complete cutoff, but only the key trench, analysis has been done as follows;

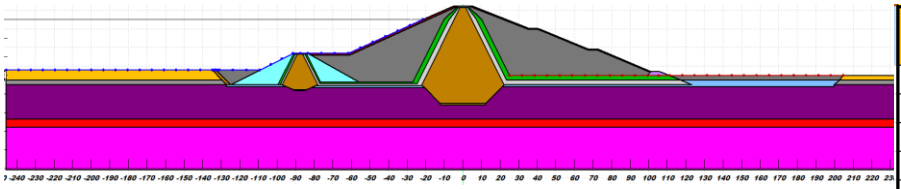

a) Drawing for 0+630/Option 1 evaluation

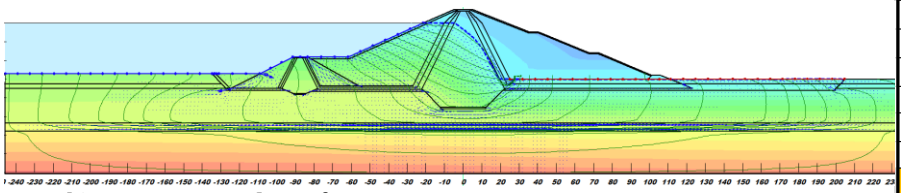

b) Seep/W analysis for 0+630/Option 1

Flow No.	Flow Travel Distance (m)	Water Flux (m³/sec/m²)
8	515.18	2.3E-09
9	477.85	8.3E-09
10	445.97	1.0E-08
11	423.94	1.0E-08
12	411.04	9.8E-09
13	393.26	1.2E-08
14	297.92	1.2E-08
15	245.55	5.5E-20
16	183.93	4.4E-24
17	144.99	3.0E-22
18	123.45	1.2E-19
19	112.03	3.0E-20
AVG	**314.59**	**5.35E-09**

c. Summary of analyzed water path and flux

4.6.3.2. Option 2:

Here all originally proposed cutoff and the upstream blanket has been adapted.

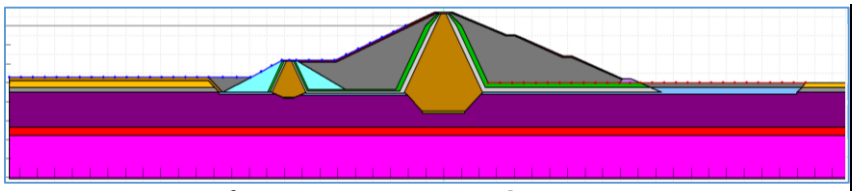

a. Drawing for 0+630/option 2 evaluation

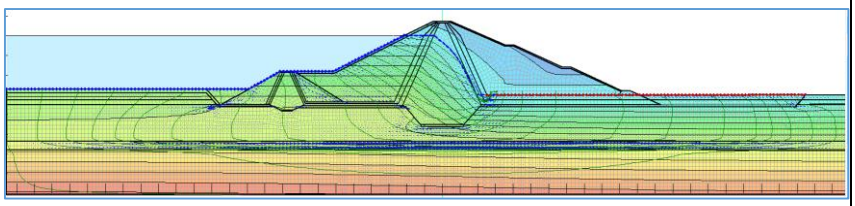

b. Seep/W analysis for 0+630/Option 2

Flow No.	Flow Travel Distance (m)	Water Flux (m³/sec/m²)
8	556.95	9.0E-10
9	516.03	2.3E-09
10	481.41	6.9E-09
11	450.21	9.9E-09
12	429.57	1.0E-08
13	417.97	9.8E-09
14	380.83	1.2E-08
15	299.55	1.2E-08
16	249.41	5.6E-20
17	177.67	9.6E-24
18	139.92	6.1E-22
19	120.27	1.8E-19
AVG	**351.65**	**5.3E-09**

c. *Summary of analyzed water path and flux*

4.6.3.3. Option-3

Here all original proposed cutoff and upstream blanket treatment have been adapted but GC material would be utilized under the main dam shoulder.

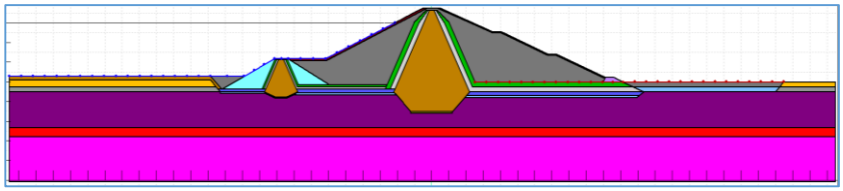

a. Drawing for 0+630/Option 3 evaluation

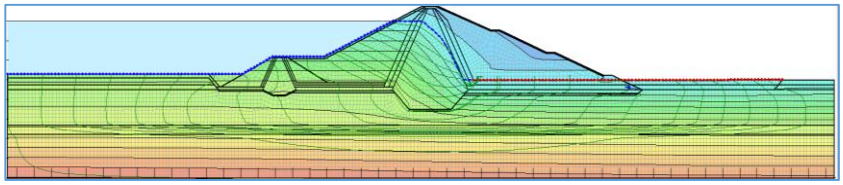

b. Seep/W analysis for 0+630/Option 3

Flow No.	Flow Travel Distance (m)	Water Flux (m³/sec/m²)
8	551.43	8.9E-10
9	506.82	2.5E-09
10	461.20	9.4E-09
11	424.77	1.0E-08
12	391.99	1.0E-08
13	364.04	9.7E-09
14	340.33	9.6E-09
15	280.33	9.9E-09
16	272.95	4.8E-20
17	195.55	5.2E-25
18	156.46	1.7E-23
19	127.62	1.6E-20
AVG	**339.46**	**5.2E-09**

c. Summary of analyzed water path and flux

4.6.3.4. Option-4

Here, the whole cutoff trench that was originally suggested has been modified, and GC material would be used beneath the main dam shoulder. However, no upstream clay blanket would be used.

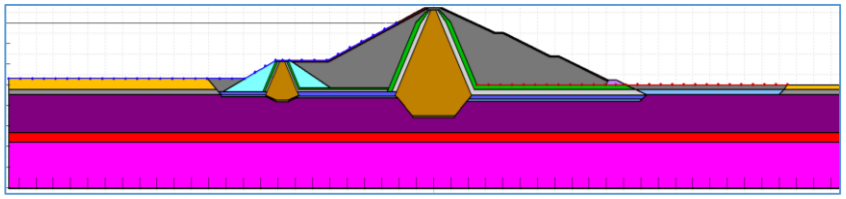

a. Drawing for 0+630/Option 4 evaluation

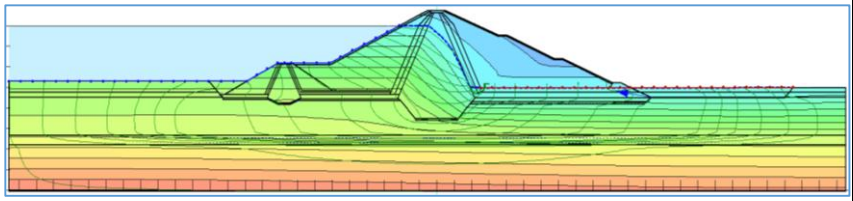

b. Seep/W analysis for 0+630/Option 4

Flow No.	Flow Travel Distance (m)	Water Flux (m³/sec/m²)
8	548.22	7.3E-10
9	507.14	2.6E-09
10	462.33	9.5E-09
11	426.56	1.0E-08
12	397.62	1.0E-08
13	381.65	9.7E-09
14	367.04	1.0E-08
15	274.41	1.0E-08
16	267.58	4.5E-20
17	197.14	4.8E-25
18	160.94	9.6E-24
19	136.77	1.9E-21
AVG	**343.95**	**5.2E-09**

c. *Summary of analyzed water path and flux*

4.6.3.5. Option-5-

In the absence of an upstream blanket and GC material beneath the downstream main dam shoulder, the additional complete cutoff would be extended to a depth of 922.39 meters above sea level, and a 5-meter soil-bentonite slurry wall would be installed beneath the main dam's complete cutoff.

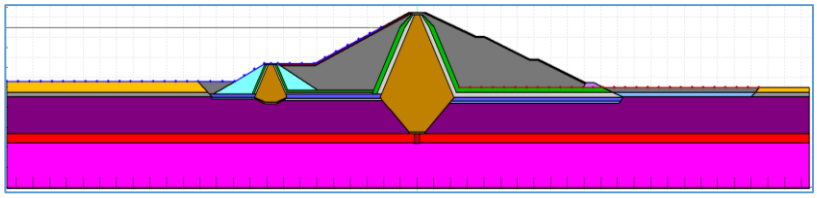

a. *Drawing for 0+630/Option 5 evaluation*

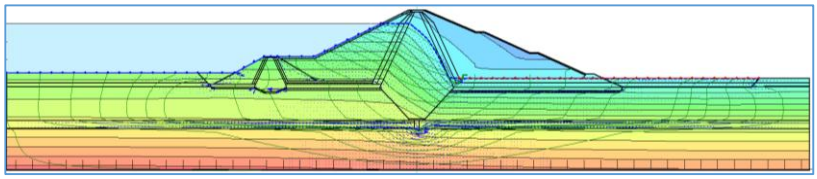

b. *Seep/W analysis for 0+630/Option 5*

Flow No.	Flow Travel Distance (m)	Water Flux (m³/sec/m²)
8	550.15	1.0E-09
9	509.84	2.7E-09
10	464.46	5.3E-09
11	431.36	6.8E-09
12	403.00	7.6E-09
13	386.46	7.7E-09
14	374.05	8.4E-09
15	275.48	8.8E-09
16	259.26	1.2E-09
17	201.90	4.2E-25
18	159.98	2.5E-23
19	133.94	5.0E-22
AVG	**345.82**	**4.14E-09**

c. *Summary of analyzed water path and flux*

4.6.3.6. Option-6

In the absence of an upstream blanket and GC material beneath the downstream main dam shoulder, a 10 m soil-bentonite slurry wall would need to be installed immediately below the main dam's complete cutoff, extending the additional complete cutoff to a depth of 927.64 m.a. s.l. (2.11 m extra depth).

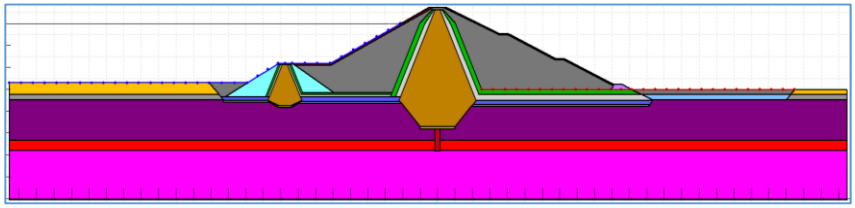

a. Drawing for 0+630/Option 6 evaluation

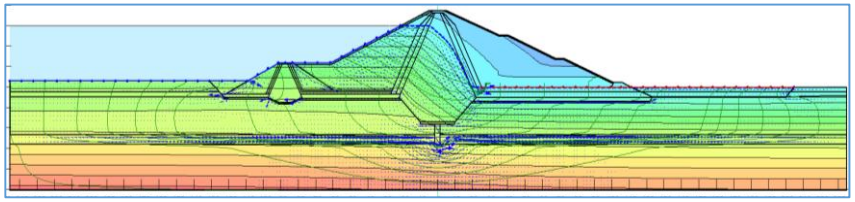

b. Seep/W analysis for 0+630/Option 6

Flow No.	Flow Travel Distance (m)	Water Flux (m³/sec/m²)
8	548.83	8.4E-10
9	509.38	2.8E-09
10	463.90	5.5E-09
11	430.16	7.0E-09
12	401.80	7.8E-09
13	385.45	7.9E-09
14	372.79	8.6E-09
15	275.39	8.8E-09
16	259.59	1.2E-09
17	201.01	2.9E-25
18	157.61	1.4E-23
19	117.58	1.1E-19
AVG	**343.62**	**4.21E-09**

c. *Summary of analyzed water path and flux*

GC material, which is impermeable, low compressible, and has good to fair shear strength, has been suggested for use in this study's main dam, which would be 2 meters thick. A restricted layer with moderate dispersivity would be created by the dam above the silt clay foundation material. Using Seep/w software to estimate the heading water flow channel, the dam's strength would be increased by extending the water flow beneath the foundation.

4.6.3.7. Summarized the Remedial Options of 0+630

Options 6 and 7 have been summarized, with option 6 being the best choice out of the group. Given that the foundation is below the groundwater table, it is preferable to utilize a deeper slurry cutoff approach in order to limit additional dewatering costs, even if option 6 is good during construction and option 5 is somewhat better than the chosen option. 343.62 meters is a rather lengthy flow route for the chosen choice, and 4.21e-09m3/sec/m2 is the minimum water flux.

Options	Average Flow Path Distance (m)	Average Water Flux ($m^3/sec/m^2$)	Descriptions
Option-1	314.593	5.35E-09	*Option of Base Case Value (without any Remedial Measure but only Key Trench)*
Option-2	351.65	5.30E-09	*Original taken design with U/S Blanket, But without Complete & Slurry Cutoff*
Option-3	339.46	5.17E-09	*Option with U/S Blanket & GC, But without Complete & Slurry Cutoff*
Option-4	343.95	5.22E-09	*Option with only GC, But without U/S Blanket, Complete & Slurry Cutoff*
Option-5	345.82	4.14E-09	*Option with Main Dam's(MD) Complete and 5m Slurry Cutoff & Without U/S Blanket*
Option-6	343.62	4.21E-09	*Selected Remedy with MD's Complete and 10m Slurry Cutoff & GC, But without U/S Blanket.*
*"*Original Design" means actual design data taken from the institute of ECDSWC*			
0+630			

Table 14 Summarized the remedial options of 0+630

Therefore, in chainage 0+630 the analyzed and selected remedy of *Option-6* is 20.57 percent better(Lower/Reduced water flux) than that of the original design of *Option-2* and 21.24 percent better(Lower/Reduced water flux) than that of *Option-1(the base case).*

4.6.3.8. Summary of Added Dimensions of Remedial Cross-Section

The following table and AutoCAD drawings are prepared and summarized as the final drawing with recommended Remedial measures. Then the drawings would be used for the next liquefaction assessment with numerical methods.

Analyzed Chainages	Bottom Width(m)		Extra Compacted Back Fill Cutoff(m)		Soil- Bentonite Cutoff Wall Depth(m)	
	MD*	CD*	MD*	CD*	MD*	CD*
0+110.3	13.30	7.13	15.39	4.85	10	4
0+327.5	16.40	9.30	7.38	4.47	10	5
0+630	19.88	-	2.11	-	10	-
MD = Main Dam, CD* = Coffer Dam*						

Table 15 Summary of Added Dimensions of Remedial Cross-Section

In general, the following summarized added remedial dimensions and a final prepared drawing based on the selected remedial options. This summarization will be used in the next liquefaction analysis.

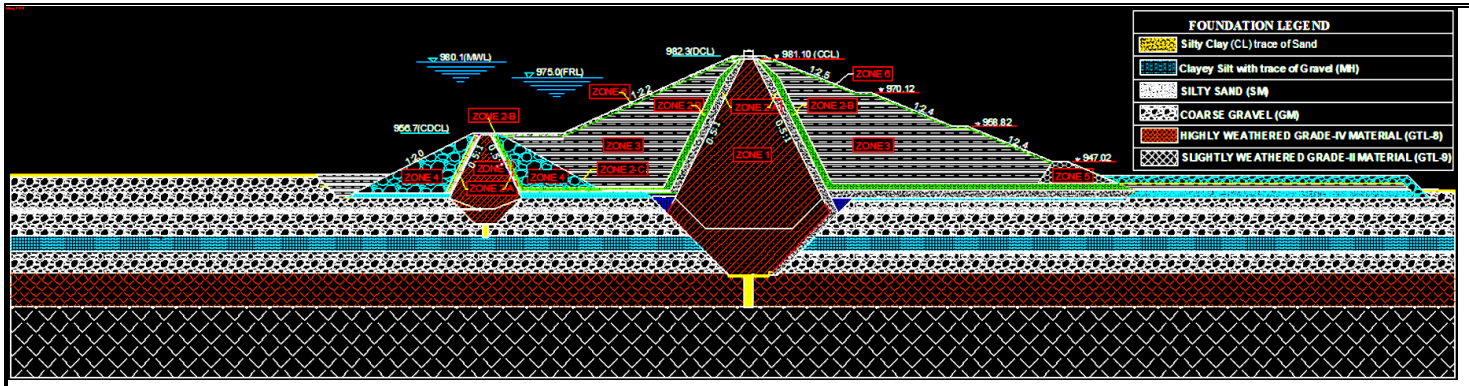	*Final Drawing with Selected Remedy of Cross Section at 0+110.3*
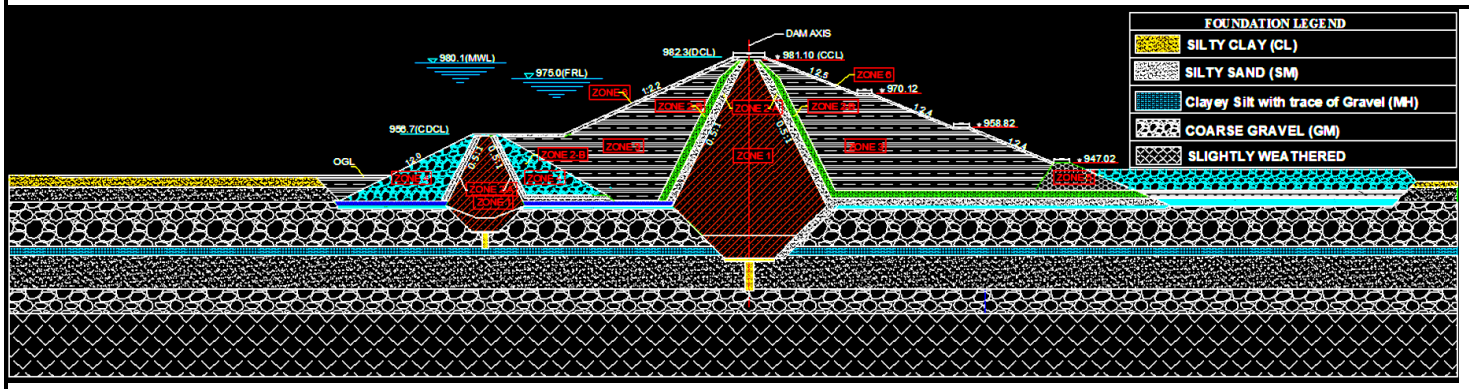	*Final Drawing with Selected Remedy of Cross Section at 0+327.5*
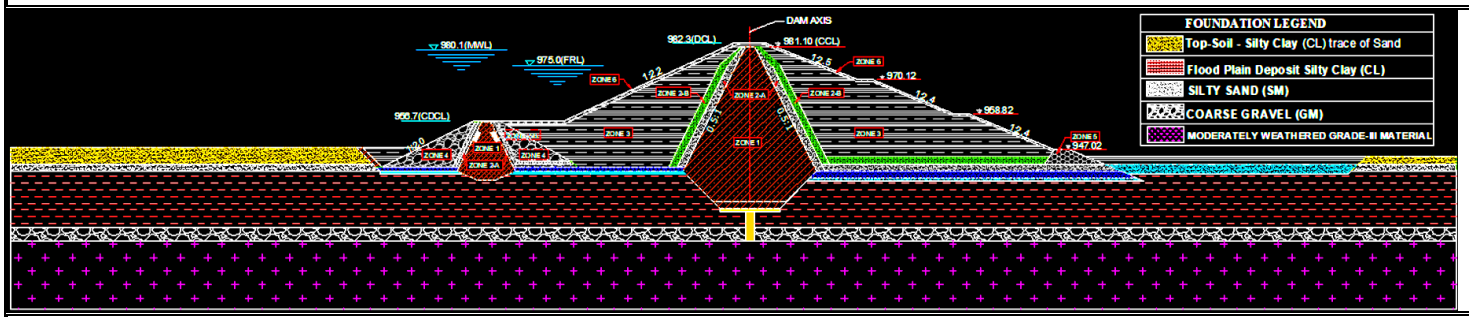	*Final Drawing with Selected Remedy of Cross Section at 0+630*

Figure 26 Final Drawing with Selected Remedial Measure and Cross Sections

4.7. The Recommended Cross-Section Profile for the Excessive Seepage Controlled Mechanism

The following schematic drawing has been done based on the above final prepared recommended Compacted Back Fill Cutoff and Soil-Bentonite Slurry by summarizing the analyzed results of the three chainages 0+110.3, 0+327.5, and 0+630 and demonstrating the overall longitudinal cross-section with the selected remedial water-proofed mechanisms.

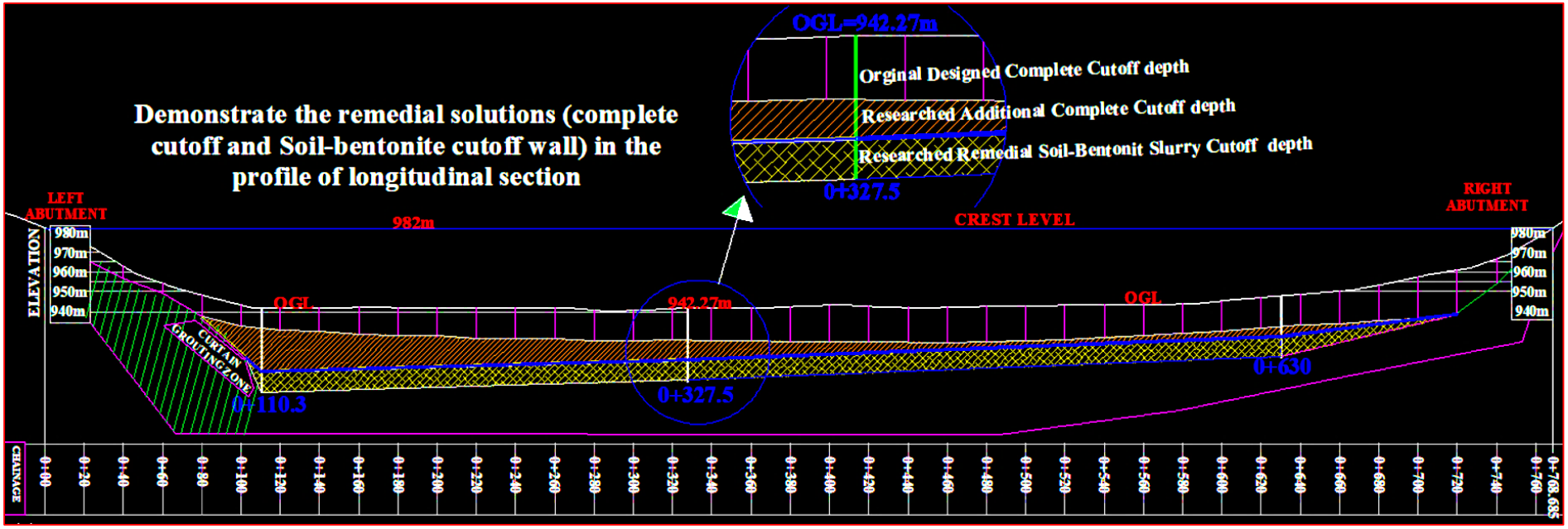

Figure 27 Longitudinal Section of researched remedial cutoff and slurry drawing

4.7.1. Comparing the Cost

Rather than choosing to use upstream clay blanketed, the suggested ultimate corrective methods in this research have been chosen for the soil-bentonite slurry and complete cutoff. This clearly summarizes the suggested remedial solution's viability costs as being less expensive than the upstream clay blanket. The proposed cutoff and soil-bentonite slurry are 32,672,066.1 birr more cost-effective than the clay blanket filling work at the upstream dam section, as indicated and computed in the accompanying Tables 16 and 17. According to the analysis of this study, the research and remedial techniques found above for the protection of abnormal seepage or pipe difficulties are thus far preferred options over any others.

Source	Type Of Work	Width	Depth	Length	Total Volume	Total Area	Current * Rate	Total Price
		m	m	m	(m3)	(m2)	(birr)	(birr)
Design Report of ECDSWC(2022)	U/S blanket	600	2.25	200	270,000		534.65	144,355,500
	Clearance/Strip	600	0.2	200		120,000	25.71	3,085,200
	Foundation grading and Compaction	600	0.3	200	36,000		421.87	15,187,320
Total Cost								**162,628,020**

Table 16 U/S blanket's cost for comparison with complete and slurry cutoff

Comparing the cost of the estimated original design and this researched remedial solution to approve the feasibility and financial effectiveness of the dam with new finding methods.

Place of Work	Type of Work	Item	Longitudinal WorkingArea	0+327.5 Average Width of Top & Bottom	0+110.3 Average Width of Top & Bottom	0+630 Average Width of Top & Bottom	Average Width of Three Chainage	Total Volume (Addtion)	Total Work (Addtion)	Total Volume (Ommition)	Current * Rate	Total Price
			(m2)	m	m	m	m	(m3)	(hr)	(m3)	(birr)	(birr)
MAIN DAM	Fill Work	Complete Cutoff	4,877.7	23.9	28.4	16.7	23.0	112,170.1			534.65	**59,971,754.1**
		Slurry Cutoff	5,646.3	1.5	1.5	1.5	1.5	8,469.5			1,467.0	**12,424,490.9**
		Filter f1	6,506.7	2.8	2.8	2.8	2.8	18,153.8			534.65	**9,705,929.4**
	Excavation	Complete Cutoff	4,877.7	27.3	31.2	19.5	26.0	126,868.2			134.6	**17,073,917.0**
		Slurry Cutoff	5,646.3	1.5	1.5	1.5	1.5	8,469.5	338.8		10,000.0	**3,387,796.9**
	Mass concrete (C-20)	Design Report	577.5	31.2	31.2	24.1	28.8	16,645.0		**(7,816.8)**	3,485.0	**(27,241,585.4)**
		This Research	556.8	16.4	13.3	17.9	15.9	8,828.2				
	Dynamic Compacton	This Research	480.0				600.0	**288,000.0**			108.0	**31,104,000.0**
Total Cost												**106,426,303**

MAIN DAM Cutoff

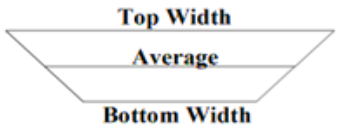

COFFER DAM Cutoff

Current * Rate

The rate has been adapted from the current working Bill of Quantity rated price that still used by of ECDSWC(2023)
=For slurry cutoff excavation, Long armed excavator (about10m) would be estimated as 10,000birr, hourly and hourly 25m3 may be excuted means per day(25m3*8hr) 200m3 can excavate. The total working volume is 8,469.5m3 and this volume is divided by per day performance of 200m3, 42.35 or about 43 days needed to complete the whole volume of work. Per day (10,000birr*8hr) 80,000birr should be paid. so, in totaly (80,000birr*43days)

Place of Work	Type of Work	Item	Longitudinal Working Width	0+327.5 Area	0+110.3 Area	0+630 Area	Average Area of Three Chainages	Total Volume (Addtion)	Total Work (Addtion)	Total Volume (Ommition)	Current * Rate	Total Price
			(m)	(m2)	(m2)	(m2)	(m2)	(m3)	(hr)	(m3)	(birr)	(birr)
COFFER DAM	Fill Work	Complete Cutoff	500.0	97.9	77.9	0.0	58.6	29,299.4			534.65	**15,664,897**
		Slurry Cutoff	500.0	7.5	6.0	0.0	4.5	2,250.0			1467.0	**3,300,683**
	Excavation	Complete Cutoff	500.0	101.8	82.3	0.0	61.3	30,669.4			134.6	**4,127,481**
		Slurry Cutoff	500.0	7.5	6.0	0.0	4.5	2,250.0			194.0	**436,590**
Total Cost												**23,529,651**
Total of main dam and cofferdam cutoff and slurry work												**129,955,954**

Total deducted price from U/S blanket fill work	**32,672,066.1**
Therefore, the suggested cutoff and soil bentonite slurry work is cost-effective compared to an earlier planned u/s blanket since the options stated in this research have offered a preferable anomalous seepage prevention remedial alternative!	

Table 17 Complete and slurry cutoff cost comparison with U/S blanket

4.7.1.1. Comparing Annual Water flow With and Without Remedial Measures

The Yanda dam loses 12,094.34 m3 per year in the Base Case (no corrective measures implemented), has been compared to 5,175.56 m3 in the scenario where the dam implements selected corrective measures. All things considered, the dam with the suggested corrections would be 57.21% safer than the Base Case dam in the absence of such measures. On the other hand, the saved quantity would be 6918.78 m3 (the difference between 12,094.34 m3 and 5,175.56 m3). Generally speaking, 0.02% and 0.03% of conserved water would be lost yearly with the base case and proposed remedial steps, respectively.

With Selected Remedial Options					
For Chainage	0+110.3	0+327.5	0+630	Calculated Values	Remark
Seconds (in a Year)				31,536,000	A
flow($m^3/sec/m^2$)	4.84E-09	2.33E-10	4.21E-09	3.09304E-09	B
Area(Water Contact Dam Cross sectional area) (m^2)				53,059.74	C
Yearly flow(m^3/m^2)				0.0975	A*B
Total flow (m^3)				**5,175.56**	A*B*C
Total flow (l/Year)				**5,175,562.82**	

With Base Case					
For Chainage	0+110.3	0+327.5	0+630	Calculated Values	Remark
Seconds (in a Year)				31,536,000	A
flow($m^3/sec/m^2$)	1.35E-08	2.80E-09	5.35E-09	7.22788E-09	B
Area (Water Contact Dam Cross sectional area) (m^2)				53,059.74	C
Yearly flow(m^3/m^2)				0.2279	A*B
Total flow (m^3/Year)				**12,094.35**	A*B*C
Total flow (l/Year)				**12,094,345.51**	

Table 18 Comparing Annual Water Flow Under the Foundation

4.7.2. Estimation of Hydraulic Gradient and Factor of Safety

The empirical calculation procedures developed by Bligh (1910) and Lane (1935) are in theory designed for pipe inspection.

$$C=L/h \quad \text{.....Equation 14}$$

Where: - L is the length of the seepage path, and h represents the overall head loss.

$$h = h_1-h_2 \quad \text{.....Equation 15}$$

The following formulas have been derived from the previous section of equations 1, 2,3,4, and 5

$$i_{cr} = (G_s - 1)(1 - n) \qquad n = \frac{e}{1 + e}$$

$$i_{cr} = \frac{G_s - 1}{1 + e} \qquad e = \frac{n}{1 - n}$$

$$i_e = (h_1 - h_2)/L$$

$$FS = \frac{i_{cr}}{i_e}$$

Where;

Gs = Specific Gravity
e = Void Ratio
n = Porosity
i_{cr} = Critical Gradient
i_e = Exit Gradient

h_1 = U/S hydraulic head
h_2 = D/S hydraulic head
L = Length flow path
FS = Factor of Safety

Specific Gravity from Report at different depths of YDBH-3B

Specific Gravity(Gs)	
G1	2.59
G2	2.59
G3	2.59
G4	2.68
G5	2.50
G6	2.50
Average	**2.575**

Table 19 Specific Gravity from ECDSWC's Report

Porosity from reference for Gravel (0.24-0.38), Coarse Sand (0.31-0.46), and Fine Sand (0.26-0.53).

Porosity – n (%)	
Porosity 1	0.31
Porosity 2	0.39
Porosity 3	0.40
Average	**0.36**

Table 20 Porosity from Standard reference

- Using the above tabulated referenced data, a critical gradient has been calculated.

  i_{cr} = (Gs-1)(1-n) =(2.575-1)*(1-0.36) = 1.003

- Exit gradient has also been calculated for each flow path and then, to check the safety of the foundation, the weighted creep ratio(C) has been computed based on the aforementioned formula and as computed in the following tables 21, 22, and 23.

4.7.2.1. Calculation of Factor of Safety at chainage of 0+327.5

Flow No.	Flow Travel Distance (m)	Water Flux ($m^3/sec/m^2$)	H	iex	icr	FS	C
1	572.84	1.21E-19	37.0	0.06	1.003	15.5	15.5
2	547.04	7.34E-21	37.0	0.07	1.003	14.8	14.8
3	536.24	9.84E-22	37.0	0.07	1.003	14.5	14.5
4	533.72	2.67E-21	37.0	0.07	1.003	14.5	14.4
5	523.41	4.19E-23	37.0	0.07	1.003	14.2	14.1
6	512.32	6.57E-24	37.0	0.07	1.003	13.9	13.8
7	507.58	1.33E-24	37.0	0.07	1.003	13.8	13.7
8	511.36	2.48E-25	37.0	0.07	1.003	13.9	13.8
9	505.03	7.44E-26	37.0	0.07	1.003	13.7	13.6
10	509.10	2.96E-26	37.0	0.07	1.003	13.8	13.8
11	462.90	3.26E-22	37.0	0.08	1.003	12.5	12.5
12	371.43	4.42E-09	37.0	0.10	1.003	10.1	10.0
13	325.00	9.24E-27	37.0	0.11	1.003	8.8	8.8
14	246.79	2.52E-24	37.0	0.15	1.003	6.7	6.7
15	244.37	2.04E-24	37.0	0.15	1.003	6.6	6.6
16	225.52	2.28E-21	37.0	0.16	1.003	6.1	6.1
17	161.11	3.40E-21	37.0	0.23	1.003	4.4	4.4
18	123.00	5.26E-20	37.0	0.30	1.003	3.3	3.3
19	102.95	5.18E-20	37.0	0.36	1.003	2.8	2.8
AVG	395.88	2.33E-10	37.0	0.09	1.003	10.73	10.70

Table 21 Calculation of Factor of Safety at chainage of 0+327.5

The critical exit hydraulic gradient, the factor of safety, and the weighted creep ratio have been assessed and computed based on the results of the Seep/W flow route distance and water flux discharge. After comparing it to the safety factor value of 10.73, it was discovered that the average weighted creep ratio at chainage 0+327.5 is 10.7. Consequently, in terms of critical gradient and outflow, seepage beneath the chainage is invulnerable to pipes.

4.7.2.2. Calculation of Factor of Safety at chainage of 0+110.3

Flow No.	Flow Travel Distance (m)	Water Flux ($m^3/sec/m^2$)	H	iex	icr	FS	C
2	538.12	3.81E-22	34.9	0.06	1.003	**15.5**	**15.4**
3	500.07	1.05E-08	34.9	0.07	1.003	**14.4**	**14.3**
4	480.50	1.20E-08	34.9	0.07	1.003	**13.8**	**13.8**
5	470.94	1.28E-08	34.9	0.07	1.003	**13.5**	**13.5**
6	475.77	1.31E-08	34.9	0.07	1.003	**13.7**	**13.6**
7	376.86	9.56E-28	34.9	0.09	1.003	**10.8**	**10.8**
8	275.56	2.97E-21	34.9	0.13	1.003	**7.9**	**7.9**
9	225.78	1.62E-19	34.9	0.15	1.003	**6.5**	**6.5**
10	165.09	1.17E-19	34.9	0.21	1.003	**4.7**	**4.7**
11	147.08	1.06E-19	34.9	0.24	1.003	**4.2**	**4.2**
AVG	**365.58**	**4.84E-09**	34.923	0.10	1.003	**10.50**	**10.47**

Table 22 Calculation of Factor of Safety at chainage of 0+110.3

The process has been carried out in accordance with the chainage 0+327.5 computation. The average weighted creep ratio at chainage 0+110.3 is 10.47, which is comparable to the factor of safety. Because of this, seepage beneath the chainage is impervious to pipes in terms of critical gradient and exit.

4.7.2.3. Calculation of Factor of Safety at Chainage of 0+630

Flow No.	Flow Travel Distance (m)	Water Flux ($m^3/sec/m^2$)	H	iex	icr	FS	C
8	548.83	8.4E-10	30.14	0.05	1.003	**18.3**	**18.2**
9	509.38	2.8E-09	30.14	0.06	1.003	**17.0**	**16.9**
10	463.90	5.5E-09	30.14	0.06	1.003	**15.4**	**15.4**
11	430.16	7.0E-09	30.14	0.07	1.003	**14.3**	**14.3**
12	401.80	7.8E-09	30.14	0.08	1.003	**13.4**	**13.3**
13	385.45	7.9E-09	30.14	0.08	1.003	**12.8**	**12.8**
14	372.79	8.6E-09	30.14	0.08	1.003	**12.4**	**12.4**
15	275.39	8.8E-09	30.14	0.11	1.003	**9.2**	**9.1**
16	259.59	1.2E-09	30.14	0.12	1.003	**8.6**	**8.6**
17	201.01	2.9E-25	30.14	0.15	1.003	**6.7**	**6.7**
18	157.61	1.4E-23	30.14	0.19	1.003	**5.2**	**5.2**
19	117.58	1.1E-19	30.14	0.26	1.003	**3.9**	**3.9**
AVG	**343.62**	**4.21E-09**	**30.14**	**0.09**	**1.003**	**11.4**	**11.4**

Table 23 Calculation of Factor of Safety at chainage of 0+630

The process has been carried out in the same manner as the calculations for the aforementioned chainages. The average weighted creep ratio at chainage 0+630 is 11.4, which is similar to the factor of safety. As a result, seepage below the chainage is resistant to pipes with respect to critical gradient and exit.

The water flow values for these three chainages, 0+110.3,327.5, and 630, could be added up to 4.88e-09 m3/m2/s, 2.33e-10 m3/m2/s, and 4.21e-09 m3/m2/s, respectively.

Lastly, the study work has assessed a number of strategies for seepage management through the substantial alluvial dam foundation—up to 50 m thick—of Yanda Dam. The assessment has made use of seepage quantity and hydraulic gradient, which are the two parameters that show how well seepage management strategies are working. The results of the study generated by the Seep/W tool have been used to calculate the seepage and hydraulic gradient for each option.

Installing a cutoff wall with a depth of 10 meters below the main dam and 4 meters below the coffer dam has been the chosen method (based on better performance) to limit seepage, decrease hydraulic gradient, and increase safety factors. This decision has been made based on the two performance indicators, seepage and hydraulic gradient. Based on the aforementioned safety evaluation using the data of Seep/W output findings, all estimated safety factors have been therefore within the intended range.

4.7.3. Why Upstream Clay Blanket is not recommended for this study?

According to works of literature, when a clay blanket is used in a dam reservoir, it may be subjected to failure in case of a fast drawdown of the reservoir water level. Due to the result of the Seep/W analysis of Yand Dam, the output value of water flux with the upstream blanket has been higher than the selected option.

Based on the intrinsic properties of the topsoil, the Yanda Dam geotechnical assessment by the ECDSWC categorized the upper river course layer as silt clay (CL). For general engineering reasons, soils were classed as soil type CL, which was categorized as an impermeable blanket and judged suitable for the construction of earth dams, according to the following Table 24 from IS 8826 (1978).

Therefore, near the upstream side of Yanda dam, the naturally alluvial deposited topsoil of CL has improved enough to be regarded as an impervious blanket.

Relative Suitability	Homogeneous Dykes	Zoned Earth Dam		Impervious Blanket
		Impervious	Pervious Casing	
Very Suitable	GC	GC	SW, GW	GC
Suitable	CL, CI	CL, CI	GM	CL, CI
Fairly Suitable	SP, SM, CH	GM, GC, SM, SC, CH	SP, GP	CH, SM, SC, GC
Poor	-	ML, MI, MH	--	--
Not Suitable	-	OL, OI, OH, Pt	--	--
Note—Refer IS : 1498-1970(Classification and identification of soils for general engineering purpose)				

Table 24 Suitability of Soils for Construction of Earth Dams(IS 8826-1978.)

4.8. Yanda Dam's Liquefaction Analysis

4.8.1. Evaluation of Liquefaction

In the evaluation of liquefaction, there should be considered three critical aspects: Liquefaction Susceptibility, Liquefaction Initiation, and Liquefaction Effects

4.8.1.1. Liquefaction Susceptibility

The following information should be taken into account when liquefaction susceptibility is assessed. The Yanda Dam foundation would be assessed according to criteria since not all soils are prone to liquefy.

Historical Criteria: Due to the Yand Dam's location in an active seismic area and the frequency of earthquakes in the surrounding area, the foundation could be vulnerable to liquefaction.

Geologic Criteria: The dam base could be liquefiable and have a high liquefaction potential because the project foundation is piled deep up to 50 meters with alluvial and colluvium deposition material, which the geotechnical investigation determined to be young deposits and saturated. The site is also composed of loose granular soils with few fines. Thus the location is regarded as most sensitive from a geological perspective.

Compositional Criteria: According to Idriss and Boulanger (2006) and Bray and Sancio (2006), the base deposited material could be susceptible to liquefaction because the Yanda Dam location site is made up of various irregular layers with poorly graded soils, cohesionless, gravel to coarse silty, and there are low plasticity fines with less than 37 percent Liquid Limit (especially in YDBH 3B and YDBH 4).

4.8.1.2. Liquefaction Initiation

As previously mentioned, the stratified soils that form the foundation of the Yanda dam are liable to liquefaction, however, this does not imply that the soils would liquefy. However, to potentially liquefy the soils, there must be initiation of liquefaction. The initiation depends on the ***stress state of the soil***, the ***duration of the loading,*** and the ***amplitude of the loading***. As

the duration and amplitude of the load are higher, the pore pressure becomes highly developed to initiate the liquefaction occurrence.

4.8.1.3. Liquefaction Effects

After evaluating the susceptibility and initiation of the soils, there is the effect of liquefaction. When the liquefaction effects could experience some unacceptable phenomena at the Yanda Dam site, there should be found out a typical solution known as **Ground Improvement**.

4.8.2. Methods of Evaluation

On the other hand, based on the Yoshida, N. (Ed.). (1998), any evaluation of a soil's susceptibility to liquefaction must consider the soil's physical characteristics (unit weight, mean grain size, and fines content), geomorphological and geological conditions (water table, type of soil, geological age), susceptibility to liquefaction, and dynamic deformation traits. The book outlines three methods for evaluating soil liquefaction: **Preliminary, Simplified**, and **Detailed.**

4.8.2.1. Preliminary Method

Preliminary Method requires only the geomorphological condition of the site. The Yanda project geographic area, being a part of the Ethiopian Rift system and active seismic area, is the result of Geomorphological activities. Some of those activities are erosion, sedimentation, piling up alluvial deposits, and other geologic processes that result in the current geomorphologic features of the site. Hence as a preliminary judgment due to the existence of a wide extent of the process of sedimentation and alluvial soiled layer foundation, the project area is prone to the actuality of liquefaction. It has long been recognized that saturated sands, silty sands, and gravelly sands are susceptible to liquefaction.

4.8.2.2. Simplified Method

The simplified Method is used in various design codes and requires factors like soil classification, unit weight, water table, SPT N-value, maximum horizontal ground surface acceleration, and earthquake magnitude. The first step to evaluate the potential of liquefaction is the identification of the grain size distribution of the soil. The first step in engineering assessment is determining whether soils of a "potentially liquefiable nature" are present at a

site. This raises the question of which types of soils are potentially vulnerable to liquefaction. It is widely recognized that relatively clean sandy soils with few fines are potentially vulnerable to seismically induced liquefaction. However, there is significant controversy regarding the liquefaction potential of silty soils and coarser, gravelly soils.

In this Yanda dam research and simplified method, "Simplified Procedure" empirical calculation has been included. Using the above necessary parameters, Such empirical equations are Cyclic Stress Ratio (CSR), Cyclic Resistance Ratio (CRR), Magnitude Scaling Factor(MSF), and Factor of Safety(FS). The SPT produces soil samples from which index values of fine content are calculated (The 1996 workshop, sponsored by NCEER). In the original development, Seed et al. (1985) found that for a given SPT N-values, CRR increases with increased fine content. The CRR increase is because of greater liquefaction resistance and an increase in compressibility.

The graph curve of Tsuchida's demonstrates the determination of whether it is liquefiable based on the gradation and leads to further analysis of the liquefaction of susceptible soil in the situation of dynamic using numerically and empirically. If the dams feature embankments or foundation soils that might lose a considerable portion of their strength as a result of earthquake shaking, dynamic analysis for liquefaction potential, or strength loss potential, (using Quake/W), should be used.

4.8.2.3. Detailed Method

Detailed Method requires dynamic soil properties, such as shear wave velocity profile and strain-dependent properties of Shear Modulus Ratio and Damping Factor, as well as input earthquake motion. In this Yanda Dam Study, liquefaction analysis will be executed by using the combination method of ***"Simplified Procedure"*** and ***Detailed Method*** while applying the Numerical Modeling of Geo-studio families such as Quake/W (2018). In addition to that, liquefaction can be evaluated using the stress distributions in terms of ***Effective Stress*** and the analyzed calculation of such stresses would be derived from the Quake/W output result. The simplified procedure, used in engineering practice for the assessment of liquefaction potential "Simplified Procedure" originally by Seed and Indriss (1971), was subsequently updated and refined (See Youd and Indriss, 1997, Youd et al. 2001 and Seed et al. 2003).

4.8.3. Susceptibility of liquefaction for Yanda Based on Grain Size

To design, ECDSWC's design team used Tsuchida's boundaries(Grain size distribution curve) for the assessment of the liquefaction susceptibility of the Yanda Dam alluvium foundation.

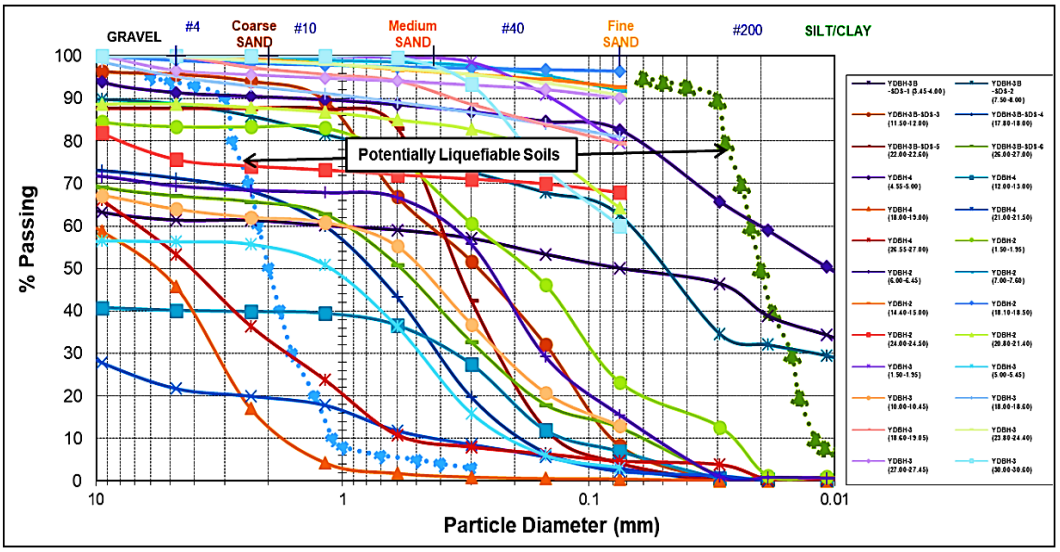

Graph 7 Grain size distribution curve

Based on Graph 7 and the Engineering design report of ECDSWC(2021), the particle size distribution of the material under liquefaction evaluation had to be displayed on the graph to evaluate the percentage of soils having a liquefaction tendency. it revealed that more than 30% of the alluvium foundation soils had crossed the limit for potentially liquefiable soils. Also, fewer than 10% of the clay material could have been found in the most liquefiable soil. The rest of the foundation materials have been revealed as well graded.

4.8.4. Proving liquefiable Fine-Grained and Clayey for Yanda

When liquefaction does occur in claylike soils, it is often at greater stresses and is more likely to take the form of cyclic mobility than flow liquefaction (Bray and Sancio, 2006). They, as stated in the literature review, provided the criteria for the susceptibility of claylike soils' liquefaction and were used to prove the susceptibility of the Yanda Dam alluvial foundation based on laboratory tests.

The normal moisture content (NMC) in the majority strata of 0+110.3, 0+327.5, and 0+630 has less than 80% of the liquid limit, and PI values are larger than 12, according to the tabulated

in-situ and laboratory data from Yanda Dam. Thus, the base of the Yanda dam has been vulnerable to liquefaction.

0+110.3/YDBH -4										
GWT = 1.43m depth from OGL(Top Soil)										
LAYER	Thickness	Initial depth	End depth	Elevation	NMC	LL	PI	Clay	Fines	SPT
	m	m	m	m	%	%	%	%	%	Ncorr
GTL-1	0.5	0.0	0.5	934.3	-	-	-	-	-	27
GTL-5	8.5	0.5	9.0	925.8	2.5	22.2	-	0.02	0.2	16
GTL-4	1.0	9.0	10.0	915.8	-	-	-	-	-	20
GTL-5	7.6	10.0	17.6	917.2	-	-	22.4	0.03	1.2	20
GTL-3	5.1	17.6	22.6	912.2	-	49.3	-	0.1	3.7	18
GTL-4	0.6	22.6	23.2	911.5	-	-	-	-	-	19
GTL-5	6.6	23.2	29.8	905.0	14.2	24.7	-	0.6	15.6	16

a. 0+110.3 each layer tested data

Where;	
Layer	Material Description
GTL-1	Silty Clay(CL) :Trace of Sand
GTL-2	Silty Clay (CL): (Intermediate Dispersive)
GTL-3	Clayey Silt(MH): Trace of Gravel
GTL-4	Silty Sand (SM): Fine Grained
GTL-5	Coarse Gravel (GM)

0+327.5 /YDBH -3/3B											
GWT = (4+1.77)/2 = 2.885m depth from OGL(Top Soil)											
LAYER	Thickness	Initial depth	End depth	Elevation	NMC	LL	PI	Clay	Fines	SPT	Relative Density
	m	m	m	m	%	%	%	%	%	Ncorr	%
GTL-1	2.7	0.0	2.7	938.3	30.9	30.9	14.7	-	79.7	29	50
GTL-4	4.6	2.7	7.4	933.6	9.6	22.4	-	0.11	5.7	15.8	62.5
GTL-5	12.1	7.4	19.5	921.5	11.9	59.0	26.6	0.29	28.9	19.2	56.9
GTL-3	5.6	19.5	25.1	915.9	23.6	58.8	-	36.3	86.8	16.5	50.0
GTL-4	9.4	25.1	34.5	906.5	16.3	31.9	14.4	0.4	52.7	23.5	75.0

b. *0++327.5 each layer tested data*

0+630 /YDBH -2										
GWT = 5.32m depth from OGL(Top Soil)										
LAYER	Thickness	Initial depth	End depth	Elevation	NMC	LL	PI	Clay	Fines	SPT
	m	m	m	m	%	%	%	%	%	Ncorr
GTL-1	5.4	0.0	5.4	942.4	5.8	38.9	26.9	-	49.2	27
GTL-4	2.5	5.4	7.9	939.9	25.8	70.6	39.4	-	92.9	21.0
GTL-2	18.5	7.9	26.4	921.4	19.2	56.6	36.8	-	77.5	20.8
GTL-5	4.5	26.4	30.9	916.9	-	-	20.7	-		33.0

c. *0+630 each layer tested data*

Table 25 Each Layer's data for Liquefaction evaluation(ECDSWC's Report)

Furthermore, from the above summary tabular data, according to Robert E. Kimmerling (1994) (using Seed's criterion) in other research, all layers' SPT N values have been less than 30, with the exception of the last layer of GTL-5 at the chainage of 0+630 (soil stiffness gets less). Therefore, each layer's foundation at the specified chainages of 0+110.3, 0+327.5, and 0+630 has been susceptible to liquefaction.

4.8.5. Earthquake in the Project Area and its Susceptibility

There are three significant seismic weak points in East Africa. The Red Sea, the Gulf of Aden, and the East African Rift System are the susceptible points. These flaws are what make up the Afar Triangle. 90% of the earthquakes in Ethiopia are caused by the East African Rift System. Historical records of earthquakes date back hundreds of years. Yanda dam project site is classified as being in seismic zone 3 (USBR, 2012). The Richter scale is approached to the magnitudes that have been recorded around the Yanda site and the hypo-central depth is lower than 20km as listed below;

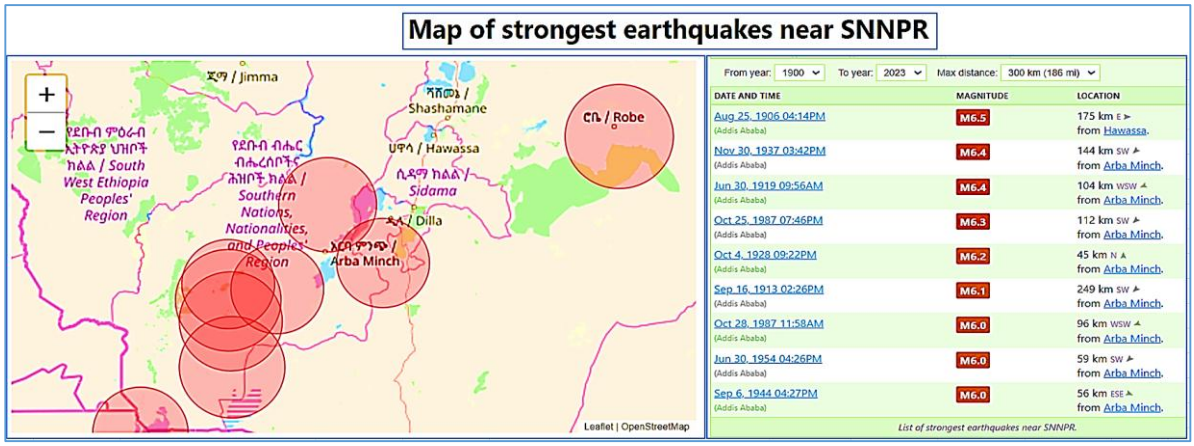

No.	Date/ Year	Location of Epicenter	Depth(H) (Epicenter to focus/Hypocenter)	Magnitude	From	Distance(R)	Region/ Country	Status
1	1906	7°1'52"N/40°3'36"E	15km	**6.5**	Goba,	9km	Oromia/Eth	Strongest Earthquakes
2	1937	5°0'18"N/ 36°45'43"E	10KM	**6.4**	Jinka	73km	SNNPR/ Ethiopia	
3	1919	5°35'20"N/36°43'26"E	15km	**6.4**	Jinka	11km		
4	1987	5°24'32"N/36°45'4"E	12km	**6.3**	Jinka	29km		
5	1928	6°26'17"N/37°34'26"E	15km	**6.2**	Arba Minch	45km		
6	1913	4 °25'23"N/35°58'52"E	10km	**6.1**	Lodwar	151km	Kenya	
7	1987	5°44'24"N/36°43'48"E	10km	**6.0**	Jinka	13km	SNNPR/ Ethiopia	
8	1954	5°41'28"N/37°8'42"E	15km	**6.0**	Jinka	55km		
9	1944	5°55'23"N/38°2'35"E	10km	**6.0**	Hagere Maryam	39km		
10	2017	7°40'16"N/38°40'6"E	10km	**5.3**	Ziway	30km	Oromia/Eth	Latest Earthquakes
11	2023	5°22'17"N/36°51'46"E	10km	**4.4**	Jinka	39km	SNNPR/ Ethiopia	
12	2016	7°5'19"N/38°28'46"E	10km	**4.4**	Hawassa	3km		
13	2014	7°24'40"N/38°48'36"E	10.7km	**4.4**	Shashemene	33km	Oromia/Eth	
14	2014	4°52'9"N/34°45'52"E	10km	**4.4**	Lodwar	215km	Kenya	
15	2023	5°29'43"N/36°6'22"E	10km	**4.3**	Bako,	60km	Oromia/Eth	
16	2022	5°42'29"N/36°51'39"E	10km	**4.3**	Jinka,	24km	SNNPR/ Ethiopia	
17	2015	7°53'37"N/38°6'53"E	10km	**4.2**	Butajira	37km		

Table 26 Summary of the earthquake near SNNPR from the above figure

The biggest challenge was that the engineering design team used PGA data and the value of PGA obtained from a geotechnical section was completely different. The Justification for both sections for adopting the various PGA values has been; that the engineering team claimed that the PGA value obtained from the geotechnical section was significantly higher. As a result, the amount of dam's price would not be feasible or economical. The geotechnical section, however, asserted that the PGA value should be utilized exactly as it was for design purposes because the PGA had been conducted by AAU and by the specialist of Prof.Ataly Ayele. Finally, with detail contrasting and comparing, the choice has been made to analyze the required objectives by modeling the dam utilizing both PGA values of 0.197g and 0.497g from the engineering designer part and the geotechnical provided value, respectively, to make apparent and comprehend what both sections sought to justify.

4.8.5.1. Yanda Dam's PGA value Based on the Geotechnical Section

The AAU Institute of Geophysics, Space Science, and Astronomy on behalf of ECDSWC's Geotechnical Section had created and reported the Site Specific Seismic Hazard Assessment (SSEHA), for the Yanda project. Since the area lacks any active faults that were thoroughly examined, other nearby seismic sources could be taken for evaluation. The Main Ethiopian Rift (MER), which includes the Yanda Dam Site, is a tectonically active area where an earthquake of magnitude **6.3** happened on July 14, 1987.

Yanda dam site has relatively higher hazard values. According to a German standard, Safety Evaluation Earthquake (SEE) is the earthquake ground motion a dam must be able to resist without uncontrolled release of the reservoir (sliding stability safety factors of slopes greater than 1.0 are required with a return period of 2,500 years). For the 2,500-year return period and 0.2 seconds spectral period, 0.4747g for rock and 0.4970g for soil had been estimated for the Yanda dam site. The results of the hazard assessment for the Yanda Dam site will be presented in Table 27.

4.8.5.2. Yanda Dam's PGA value Based on the Design Section of ECDSWC

The Yanda Dam is strategically located in a tectonically susceptible region, with damage risk being less sensitive than life loss. Therefore, taking into account the recommendations from ICOLD Bulletin 72 and site-specific facts, the SEE (PGA = 0.197g) return periods are adopted.

Ground motion amplitude in of g for Boore-Joyner-Fumal(1993,1997)		
Return period in years	Period = 0.2 sec	
	Rock	Soil
100	0.1207	0.1282
500	0.2623	0.2789
1,000	0.3573	0.3799
2,500	0.4747	**0.4970**
10,000	0.6816	0.7246

Table 27 PGA values evaluated and reported by Prof.Ataly Ayele/AAU(2020).

PGA Value(*g)		
Return period in years	Period = 0.2 sec	
	Rock	Soil
475	0.120	0.150
975	0.153	**0.197**
2475	0.211	0.264
5000	0.259	0.339
10,000	0.310	0.390

Table 28 PGA value listed (ECDSWC's Yanda Dam design report, 2022.)

4.8.5.3. The Intention of Selecting El Centro Earthquake Record

Based on the range of variation in frequency and duration of the three recording earthquakes, a comparison has been made and then one of them would be chosen. As explained in the literature section, among those well-known researchable earthquake records, the El Centro record has been selected for the reason of the following:

El Centro's record for earthquakes is Multiple peaks with intense high-frequency motion in a short amount of period. According to Arvind JS. 2023. An important development in earthquake engineering was the El Centro earthquake of 1940 which is still a well-researched occurrence. The El Centro earthquake is a perfect reference earthquake for evaluating the precision and dependability of seismic analysis software and other instruments used in earthquake engineering because of its well-defined and repeatable ground motion record. To make sure that structures are made safe and able to withstand seismic occurrences, this ground motion record is frequently used to assess the effectiveness of seismic analysis techniques and software. The tectonics in Ethiopia is of the extensional type and the depth of occurrence of earthquakes that control strong ground motion is shallow (rarely exceeds 20 km) and similar to that in California, according to the Report of site-specific hazards assessment for Yanda Dam by Prof.Ataly Ayele, 2020. (IGSSA/AAU).

4.8.6. Proving Susceptibility of Liquefaction using LiqiT Software

The Yanda Dam Project's foundation has been known to be vulnerable to the risk of liquefaction. So, in this study, LiqiT software (2004) has been used to demonstrate the liquefaction susceptibility. This program analyzes the possibility of liquefaction without taking into account the weight or load of the entire dam. However, it is useful for a project working foundation feasibility analysis before the complete design of the dam and for taking important standard consideration throughout the design of the entire dam body components.

4.8.7. Proving Prone to Liquefaction using LiqiT at 0+110.3 PGA 0.197g

Input parameters and analysis data			
In-Situ Data Type	SPT	Depth to water table	1.43m
Analysis Method	NCEEP 1998	Earthquake magnitude	6.30
Fines Correction Method	Indriss & Seed	PGA	0.19g
Chainage	0+110.3	User defined F.S.	1.00

Point ID	Depth (m)	Field N_{SPT} (blows/30 cm)	Unit weight (kN/m³)	Fines content (%)
1	0.50	27.00	14.90	0.00
2	9.00	16.00	15.00	0.20
3	10.00	20.00	17.90	0.00
4	17.60	20.00	15.70	1.20
5	22.60	18.00	13.60	3.70
6	23.20	19.00	14.70	0.00
7	29.80	16.00	13.90	15.60

Depth : Depth from free surface, at which SPT was performed (m)
Field SPT : SPT blows measured at field (blows/30 cm)
Unit weight : Bulk unit weight of soil at test depth (kN/m³)
Fines content : Percentage of fines in soil (%)

a. Field input Parameters and analysis data

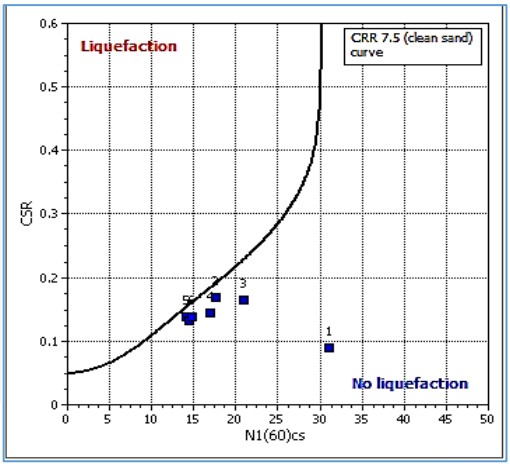

b. Result of Liquefaction Status in Graph

No	Depth	Gamma	% FC	u	Sigma	Eff. sigma	Nspt	N1(60)	N1(60)cs	CSR	CRR	F.S.
1	0.50	14.90	0.00	0.00	7.45	7.45	27.00	30.98	30.98	0.09	2.00	5.00
2	9.00	15.00	0.20	74.26	134.95	60.69	16.00	17.53	17.53	0.17	0.19	1.13
3	10.00	17.90	0.00	84.07	152.85	68.78	20.00	20.98	20.98	0.16	0.23	1.40
4	17.60	15.70	1.20	158.63	272.17	113.54	20.00	16.96	16.96	0.14	0.18	1.28
5	22.60	13.60	3.70	207.68	340.17	132.49	18.00	14.12	14.12	0.14	0.15	1.11
6	23.20	14.70	0.00	213.56	348.99	135.43	19.00	14.73	14.73	0.14	0.16	1.17
7	29.80	13.90	15.60	278.31	440.73	162.42	16.00	11.22	14.46	0.13	0.16	1.19

Table 29 Input data & Result of FoS for proving prone to liquefaction at 0+110.3 & PGA 0.197g

The analysis of the CSR against N1(60) graph revealed that all of the data for each depth was categorized in the non-liquefaction condition, and the result has proven that the safety factor is above 1 at the chainage of 0+110.3 and the PGA value of 0.197g. Because of this, the foundation surrounding this location has not liquefied.

4.8.8. Proving Prone to Liquefaction using LiqiT at 0+110.3 PGA 0.497g

Input parameters and analysis data			
In-Situ Data Type	SPT	Depth to water table	1.43m
Analysis Method	NCEEP 1998	Earthquake magnitude	6.30
Fines Correction Method	Indriss & Seed	PGA	0.49g
Chainage	0+110.3	User defined F.S.	1.00

Point ID	Depth (m)	Field N_{SPT} (blows/30 cm)	Unit weight (kN/m³)	Fines content (%)
1	0.50	27.00	14.90	0.00
2	9.00	16.00	15.00	0.20
3	10.00	20.00	17.90	0.00
4	17.60	20.00	15.70	1.20
5	22.60	18.00	13.60	3.70
6	23.20	19.00	14.70	0.00
7	29.80	16.00	13.90	15.60

Depth : Depth from free surface, at which SPT was performed (m)
Field SPT : SPT blows measured at field (blows/30 cm)
Unit weight : Bulk unit weight of soil at test depth (kN/m³)
Fines content : Percentage of fines in soil (%)

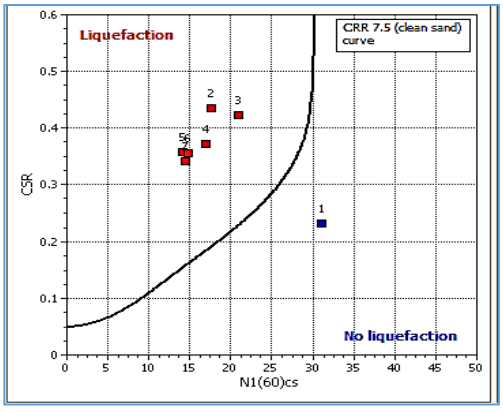

No	Depth	Gamma	% FC	u	Sigma	Eff. sigma	Nspt	N1(60)	N1(60)cs	CSR	CRR	F.S.
1	0.50	14.90	0.00	0.00	7.45	7.45	27.00	30.98	30.98	0.23	2.00	5.00
2	9.00	15.00	0.20	74.26	134.95	60.69	16.00	17.53	17.53	0.43	0.19	0.44
3	10.00	17.90	0.00	84.07	152.85	68.78	20.00	20.98	20.98	0.42	0.23	0.54
4	17.60	15.70	1.20	158.63	272.17	113.54	20.00	16.96	16.96	0.37	0.18	0.49
5	22.60	13.60	3.70	207.68	340.17	132.49	18.00	14.12	14.12	0.36	0.15	0.43
6	23.20	14.70	0.00	213.56	348.99	135.43	19.00	14.73	14.73	0.35	0.16	0.45
7	29.80	13.90	15.60	278.31	440.73	162.42	16.00	11.22	14.46	0.34	0.16	0.46

Table 30 Input data & Result of FoS for proving prone to liquefaction at 0+110.3 & PGA 0.497g

The investigated depths were classified as being in the liquefaction state at the chainage of 0+110.3 and at the PGA value of 0.497g, according to the study of the CSR against the N1(60) graph. This finding demonstrated that, with the exception of the top layer, the safety factor is less than 1 across the whole depth. This means that the spot's foundation has been susceptible to liquefaction.

4.8.9. Proving Prone to Liquefaction using LiqiT at 0+327.5 PGA 0.197g

Input parameters and analysis data			
In-Situ Data Type	SPT	Depth to water table	2.88m
Analysis Method	NCEEP 1998	Earthquake magnitude	6.30
Fines Correction Method	Indriss & Seed	PGA	0.19g
Chainage	0+327.5	User defined F.S.	1.00

Point ID	Depth (m)	Field N_{SPT} (blows/30 cm)	Unit weight (kN/m³)	Fines content (%)
1	2.70	29.00	14.90	79.70
2	7.40	15.80	17.80	5.70
3	19.50	19.20	15.80	28.90
4	25.10	16.50	14.30	86.80
5	34.50	23.50	13.60	52.70

Depth : Depth from free surface, at which SPT was performed (m)
Field SPT : SPT blows measured at field (blows/30 cm)
Unit weight : Bulk unit weight of soil at test depth (kN/m³)
Fines content : Percentage of fines in soil (%)

a. Field input Parameters and analysis data

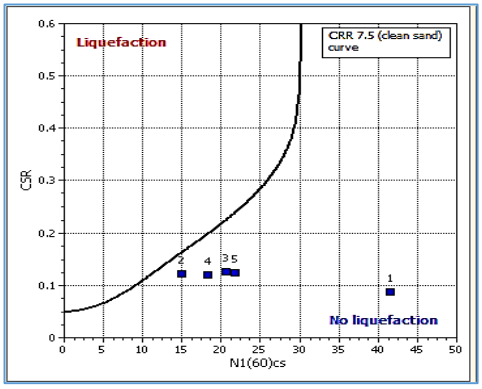

b. Result of Liquefaction Status in Graph

No	Depth	Gamma	% FC	u	Sigma	Eff. sigma	Nspt	N1(60)	N1(60)cs	CSR	CRR	F.S.
1	2.70	14.90	79.70	0.00	40.23	40.23	29.00	30.46	41.55	0.09	2.00	5.00
2	7.40	17.80	5.70	44.34	123.89	79.55	15.80	14.89	14.96	0.12	0.16	1.33
3	19.50	15.80	28.90	163.04	315.07	152.03	19.20	13.98	20.64	0.13	0.23	1.80
4	25.10	14.30	86.80	217.98	395.15	177.17	16.50	10.99	18.19	0.12	0.20	1.64
5	34.50	13.60	52.70	310.19	522.99	212.80	23.50	13.98	21.78	0.12	0.24	1.93

Table 31 Input data & Result of FoS for proving prone to liquefaction at 0+327.5 & PGA 0.197g

The findings for every depth at chainage 0+327.5 and PGA value 0.197g indicated that the safety factor has been more than 1, and the CSR compared to N1(60) examined graph demonstrated that every depth at that level has been identified as being in the non-liquefaction condition.

4.8.10. Proving Prone to Liquefaction using LiqiT at 0+327.5 PGA 0.497g

Input parameters and analysis data			
In-Situ Data Type	SPT	Depth to Water Table	2.88m
Analysis Method	NCEEP 1998	Earthquake Magnitude	6.30
Fines Correction Method	Indriss & Seed	PGA	0.49g
Chainage	0+327.5	User defined F.S.	1.00

Point ID	Depth (m)	Field N_{SPT} (blows/30 cm)	Unit weight (kN/m³)	Fines content (%)
1	2.70	29.00	14.90	79.70
2	7.40	15.80	17.80	5.70
3	19.50	19.20	15.80	28.90
4	25.10	16.50	14.30	86.80
5	34.50	23.50	13.60	52.70

Depth : Depth from free surface, at which SPT was performed (m)
Field SPT : SPT blows measured at field (blows/30 cm)
Unit weight : Bulk unit weight of soil at test depth (kN/m³)
Fines content : Percentage of fines in soil (%)

a. Field input Parameters and analysis data

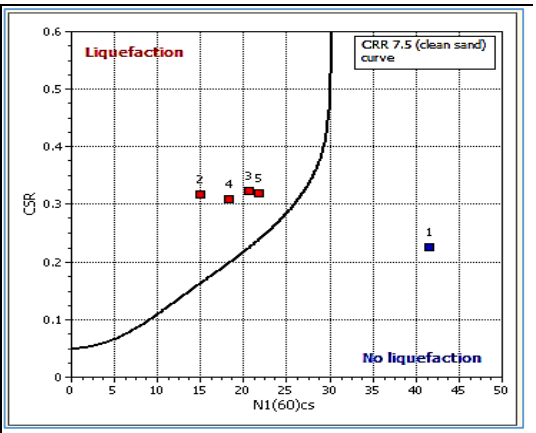

b. Result of Liquefaction Status in Graph

No	Depth	Gamma	% FC	u	Sigma	Eff. sigma	Nspt	N1(60)	N1(60)cs	CSR	CRR	F.S.
1	2.70	14.90	79.70	0.00	40.23	40.23	29.00	30.46	41.55	0.23	2.00	5.00
2	7.40	17.80	5.70	44.34	123.89	79.55	15.80	14.89	14.96	0.32	0.16	0.51
3	19.50	15.80	28.90	163.04	315.07	152.03	19.20	13.98	20.64	0.32	0.23	0.70
4	25.10	14.30	86.80	217.98	395.15	177.17	16.50	10.99	18.19	0.31	0.20	0.64
5	34.50	13.60	52.70	310.19	522.99	212.80	23.50	13.98	21.78	0.32	0.24	0.75

Table 32 Input data & Result of FoS for proving prone to liquefaction at 0+327.5 & PGA 0.497g

Upon analyzing the CSR against the N1(60)cs graph, it was determined that the depths under investigation have been at the liquefaction stage, with a chainage of 0+327.5 and a PGA value of 0.497g. This finding demonstrated that, with the exception of the top layer, the safety factor has become less than one throughout the depth. As a result, the base of this specific region has been susceptible to melting.

4.8.11. Proving Prone to Liquefaction using LiqiT at 0+630 PGA 0.197g

Input parameters and analysis data			
In-Situ Data Type	SPT	Depth to water table	5.32m
Analysis Method	NCEEP 1998	Earthquake magnitude	6.30
Fines Correction Method	Indriss & Seed	PGA	0.19g
Chainage	0+630	User defined F.S.	1.00

Point ID	Depth (m)	Field N_{SPT} (blows/30 cm)	Unit weight (kN/m³)	Fines content (%)
1	5.40	27.00	18.00	49.20
2	7.90	21.00	16.30	92.90
3	26.40	20.80	16.90	77.50
4	30.90	33.00	13.90	0.00

Depth : Depth from free surface, at which SPT was performed (m)
Field SPT : SPT blows measured at field (blows/30 cm)
Unit weight : Bulk unit weight of soil at test depth (kN/m³)
Fines content : Percentage of fines in soil (%)

a. Field input Parameters and analysis data

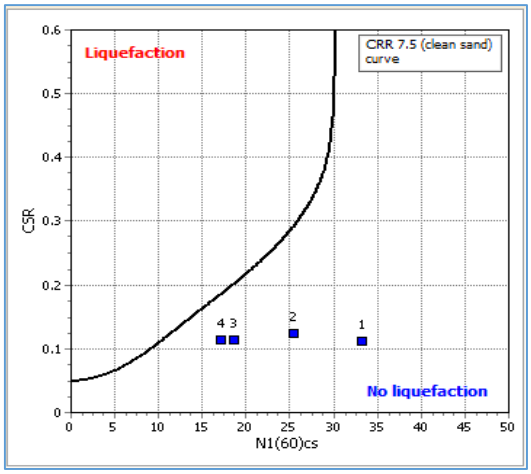

b. Result of Liquefaction Status in Graph

No	Depth	Gamma	% FC	u	Sigma	Eff. sigma	Nspt	N1(60)	N1(60)cs	CSR	CRR	F.S.
1	5.40	18.00	49.20	0.78	97.20	96.42	27.00	23.47	33.16	0.11	2.00	5.00
2	7.90	16.30	92.90	25.31	137.95	112.64	21.00	16.98	25.38	0.12	0.29	2.35
3	26.40	16.90	77.50	206.79	450.60	243.81	20.80	11.32	18.58	0.11	0.20	1.76
4	30.90	13.90	0.00	250.94	513.15	262.21	33.00	17.10	17.10	0.11	0.19	1.63

Table 33 Input data & Result of FoS for proving prone to liquefaction at 0+630 & PGA 0.197g

The CSR versus N1(60) investigated graph showed that the whole depth of each data has been classified in the non-liquefaction condition. At chainage 0+630 and PGA value 0.197g, the result suggested that the safety factor exceeded 1. This specific site's foundation would be hence resistant to liquefaction.

4.8.12. Proving Prone to Liquefaction using LiqiT at 0+630 PGA 0.497g

Input parameters and analysis data			
In-Situ Data Type	SPT	Depth to water table	5.32m
Analysis Method	NCEEP 1998	Earthquake magnitude	6.30
Fines Correction Method	Indriss & Seed	PGA	0.49g
Chainage	0+630	User defined F.S.	1.00

Point ID	Depth (m)	Field N_{SPT} (blows/30 cm)	Unit weight (kN/m³)	Fines content (%)
1	5.40	27.00	18.00	49.20
2	7.90	21.00	16.30	92.90
3	26.40	20.80	16.90	77.50
4	30.90	33.00	13.90	0.00

Depth : Depth from free surface, at which SPT was performed (m)
Field SPT : SPT blows measured at field (blows/30 cm)
Unit weight : Bulk unit weight of soil at test depth (kN/m³)
Fines content : Percentage of fines in soil (%)

a. Field input Parameters and analysis data

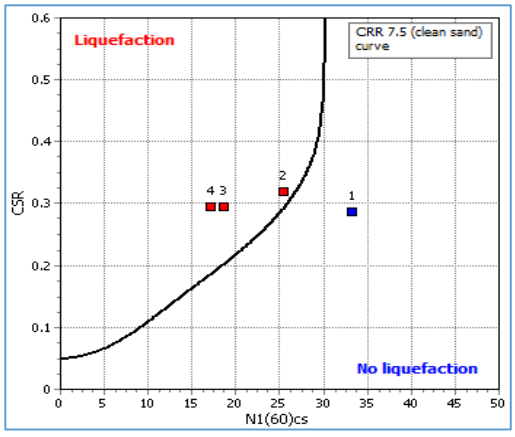

b. Result of Liquefaction Status in Graph

No	Depth	Gamma	% FC	u	Sigma	Eff. sigma	Nspt	N1(60)	N1(60)cs	CSR	CRR	F.S.
1	5.40	18.00	49.20	0.78	97.20	96.42	27.00	23.47	33.16	0.29	2.00	5.00
2	7.90	16.30	92.90	25.31	137.95	112.64	21.00	16.98	25.38	0.32	0.29	0.91
3	26.40	16.90	77.50	206.79	450.60	243.81	20.80	11.32	18.58	0.30	0.20	0.68
4	30.90	13.90	0.00	250.94	513.15	262.21	33.00	17.10	17.10	0.29	0.19	0.63

Table 34 Input data & Result of FoS for proving prone to liquefaction at 0+630 & PGA 0.497g

A study of the CSR vs N1(60)cs graph has led to the classification of the examined depths as being in the liquefaction stage at the chainage of 0+630 and at the PGA value of 0.497g. This result showed that the safety factor has been less than one at all depths, with the possible exception of the top layer. The foundation of this particular location would be hence vulnerable to liquefaction.

4.8.13. Summary of the above LiqIT Analysis

For each considered chainage of 0+110.3, 0+327.5, and 0+630, using the two challenged PGA values of 0.194 and 0.497, proving the existence of liquefaction in the specific project site has been analyzed using the LiqIT program. As the demonstration showed at the PGA of 0.497, the liquefaction hazardous exists and it indicates that the ground motion is strong and at this level, it can be decided that the site is a seismically active area. Whereas at the PGA level of 0.197, the susceptibility of liquefaction is out of risky level.

4.9. Evaluating the Liquefaction Using Quake/W

The foundation of The Yanda Dam Project has a history of being susceptible to the risk of liquefaction, as was previously mentioned. To assess the foundation's potential for liquefaction under the constrained overloaded stress of the entire super dam body, GeoStudio software will be employed in this study. The weight or load of the entire dam is taken into consideration while analyzing the likelihood of liquefaction in this software. To take key standard considerations into account while designing the full dam body components, it will be beneficial for project design working of foundation feasibility study of the complete design of the dam.

4.9.1. Final Prepared Drawing for this Research of Dynamic Analysis

These drawings had been utilized for importing geometry from AutoCAD to the GeoStudio package of the Quake/W program for the analysis of the targeted value of CSR and to compute the safety factor to determine if the foundation will liquefy or not.

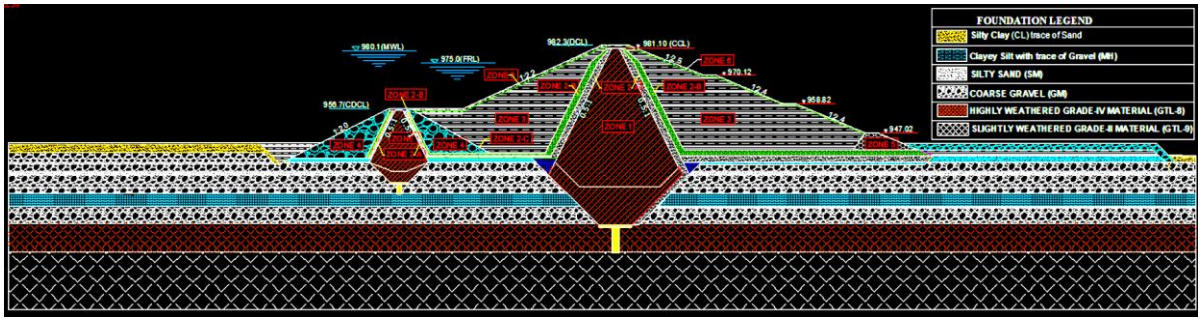

i. Selected Remedy of Cross Section at 0+110.3

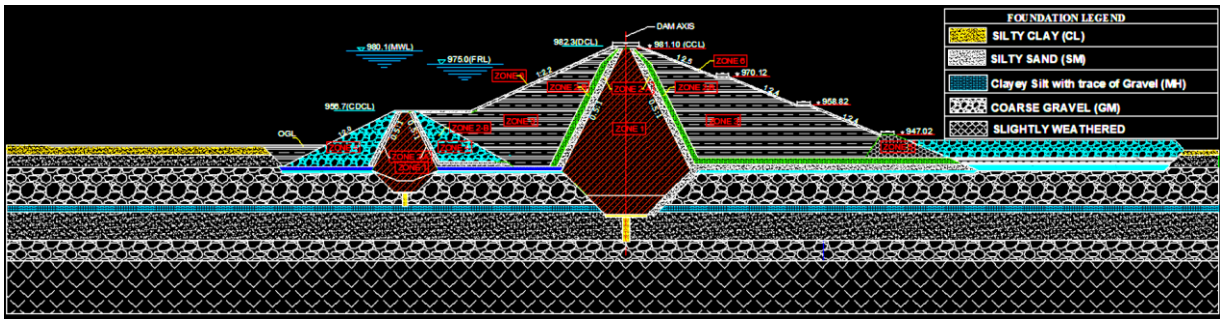

ii. Selected Remedy of Cross Section at 0+327.5

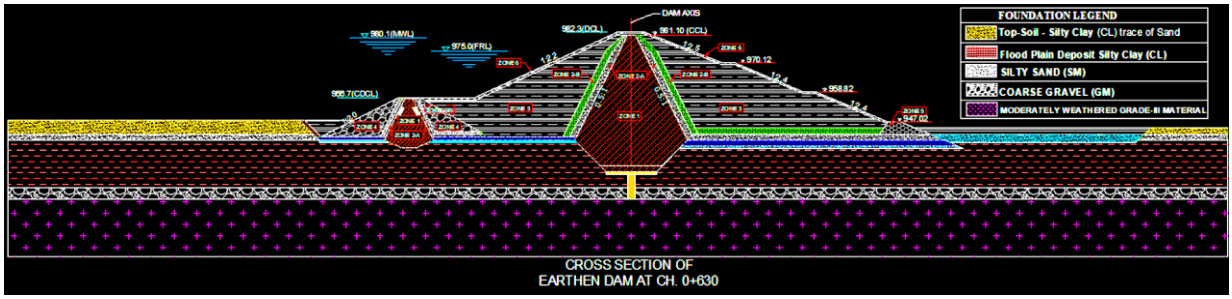

iii. Selected Remedy of Cross Section at 0+630

Figure 28 Cross Section of Yanda Dam

4.9.2. The Procedure of Quake/W Analysis

It is crucial to properly build an earthquake-resistant dam. To assure the level of safety, it is also crucial to analyze the earthen dam's seismic load. With the use of commercially available finite element-based software called Geo studio/Quake/W (2018), the current study aims to investigate the seepage behavior(as stated previously), stress fluctuation, and seismic response of the Yanda dam.

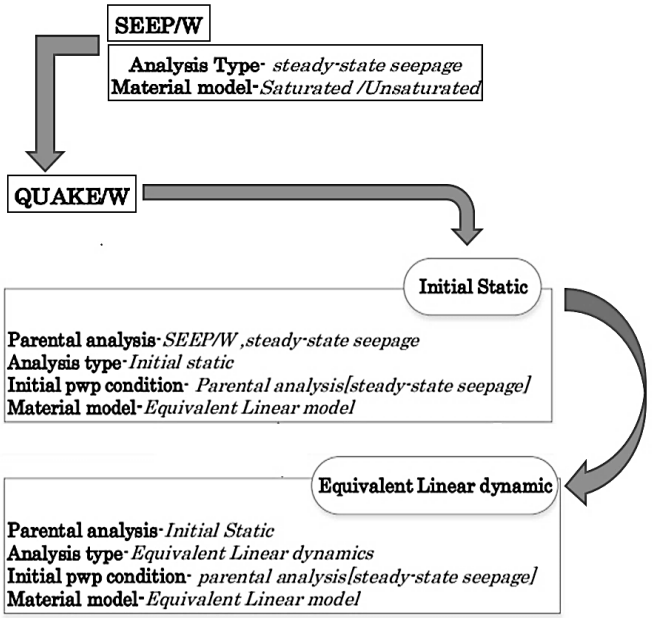

Chart 4 Procedures of analysis in this research of Seep/W and Quake/W

4.9.2.1. Initial Static Analysis

The in-situ stress of the ground condition has to be calculated as the first step in dynamic analysis, and Quake/W, 2018, can be used to compute the initial stress. The geometry of the issue domain has been sketched on Quake/W and concatenated to Seep/W in order to account for initial in-situ stresses and pore water pressure.

The initial phase of this Quake/W investigation was determining the pre-quake in situ stress state circumstances. In other words, the first static stresses have to be determined before exposing the dam to dynamic action. The in-situ static stress could possibly be determined using the Quake/W initial static analysis type. For the Initial Static analysis, the two most important soil parameters are the Poisson's ratio (v) and the total unit weight of the components. Poisson's ratio is important because it has an impact on the coefficient of earth pressure at rest.

In order to calculate the accurate total and effective stresses, the reservoir water's weight must be used as a boundary condition. The water pressure has been visually represented by the arrows (in Figure 29b) that have been perpendicular to the ground and have been thought of as boundary conditions. A boundary of the Fluid Pressure type could be used to specify the water weight or pressure. The fluid's unit weight (in the case of water) and the FSL elevation would need to be specified for this kind of boundary condition. A given water table would be used to define and calculate the initial pore-water pressures.

It is crucial to ensure that the finite element mesh is appropriate for the research once the problem has been adequately defined in terms of the geometry, boundary conditions, and material properties. Users can examine and modify the mesh using the Draw Mesh Properties command. However, using a mesh size of 1 m would require a significant amount of processing time, potentially up to half a day, due to the dam's large and deep cross-section. It should be noted that in this case, the global element size should be around 2 m. The following Figure 29 a, b, and c show the finite element mesh judged suitable for this specific study based on this user-specified criterion.

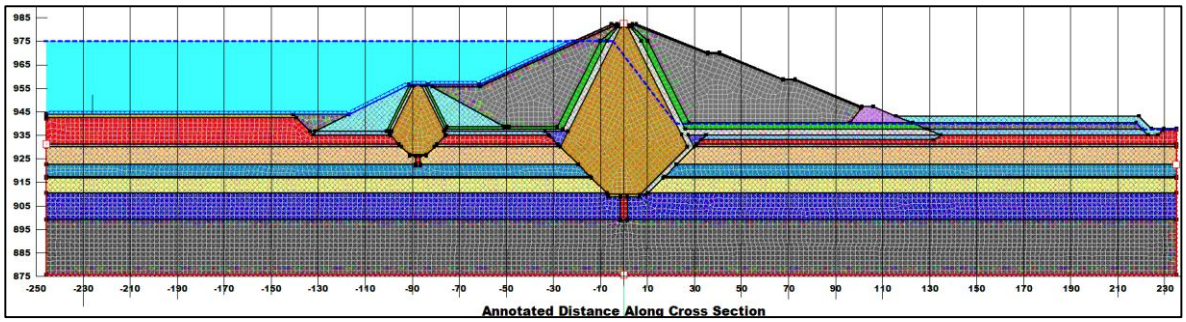

a. Initial Static Analysis for 0+110.3

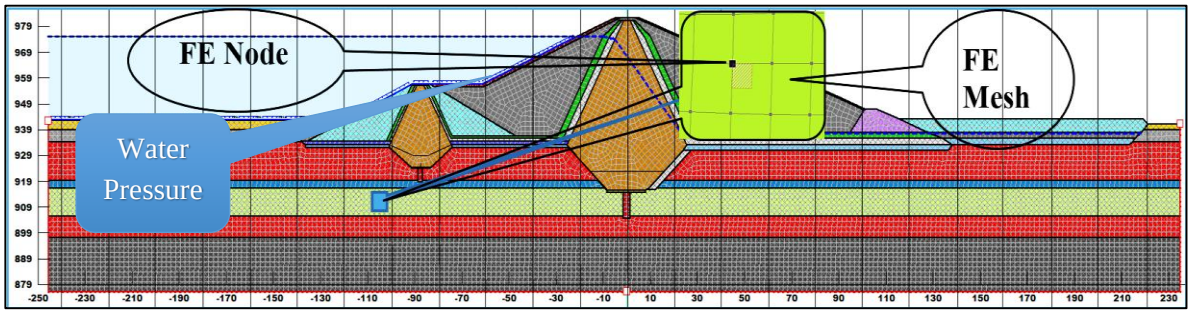

b. Initial Static Analysis for 0+327.5

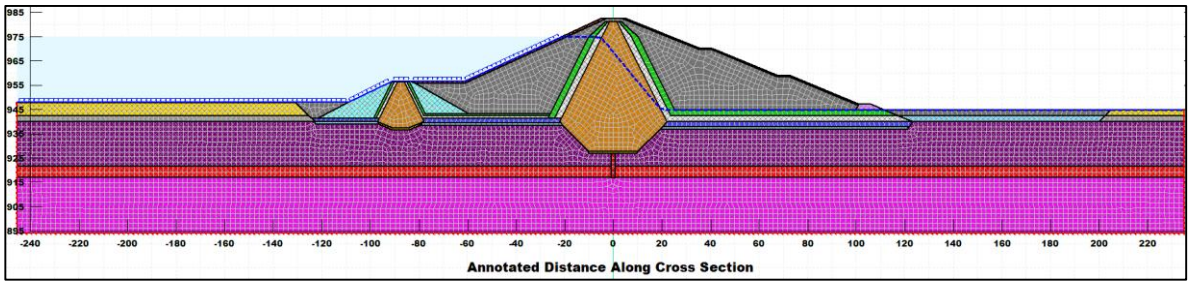

c. Initial Static Analysis for 0+630

Figure 29 Providing FE mesh, water pressure boundary, water table, and history points

4.9.2.2. Why Dynamic Analysis Techniques is the better for this study?

The pseudo-static analysis highlights risky circumstances while the dynamic analysis assures the dam's safety against deformation. This suggests that the earthquake analysis shown by the

dynamic response analysis is one that the pseudo-static analysis is unable to detect. The pseudo-static approach accounts for the influence of vibrations as an equivalent static horizontal force rather than taking into consideration the cyclical nature of earthquake stresses. As a result, the effects of an earthquake's vertical acceleration are disregarded [Terzaghi, K. (1951)]. Hence, Dynamic numerical analysis is more accurate than pseudo-static or Newmark approaches.

4.9.2.3. Equivalent Linear Dynamic

After the in situ static stresses have been determined, the dynamic analysis would be the following step. The preceding Initial Static analysis would be the "Parent" of a new Quake/W analysis created using the Define Analyses command. Both the initial stress conditions and the pore-water pressure conditions have been provided by the Parent (previous) analysis. Researchers referred to this kind of study as Equivalent Linear Dynamic. By employing the linear-elastic constitutive relationship, the equivalent linear analysis (E.L.) technique guarantees uniform soil stiffness across earthquake recordings. Nevertheless, dynamic shear strain causes a change in soil stiffness, with a distinct Gmax or stiffness value being assigned to each element.

In this research, according to the stated reason in the subtitle of time history data, the El Centro earthquake record has been selected to be used in this thesis for further analysis of the targeted objectives. The recorded earthquake's peak ground acceleration (PGA) was 0.34998g, and its duration was 64.1 seconds. El Centro recorded data was then entered as the project's horizontal earthquake recording data after the PGA and duration were modified. The following information has been presented for the chosen El Centro recorded data:

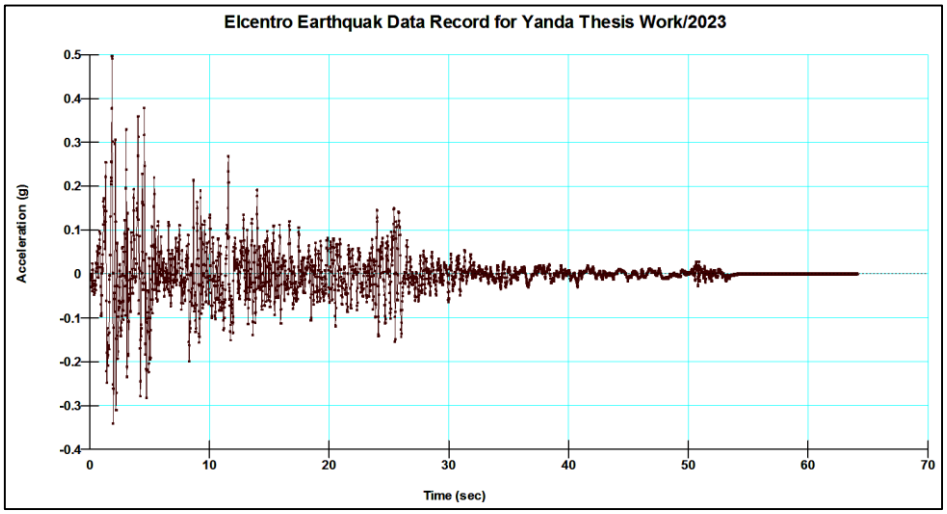

Graph 8 Chosen El Centro Earthquake data recorded

4.9.2.4. Commentary about used Acceleration Time History(ATH)

According to literature, the peak values typically happen early in an earthquake's ground shaking and shouldn't be used to continue recording values after the peak values because doing so would be computationally costly, time-consuming, and result in an excessive amount of data. Such values would neither provide any new relevant information for the study nor would they contribute any in an analogous linear analysis. Thus, based on the raw data from the engineering design report and geotechnical report of ECDSWC, respectively, the peak ground acceleration (PGA) has been adjusted for the purposes of this study analysis to be 0.497g and 0.197g. A length of 25.02 seconds, ranging from 0.98 to 26 seconds, has been identified by just taking into account the necessary peak acceleration. The rest of the duration has been trimmed.

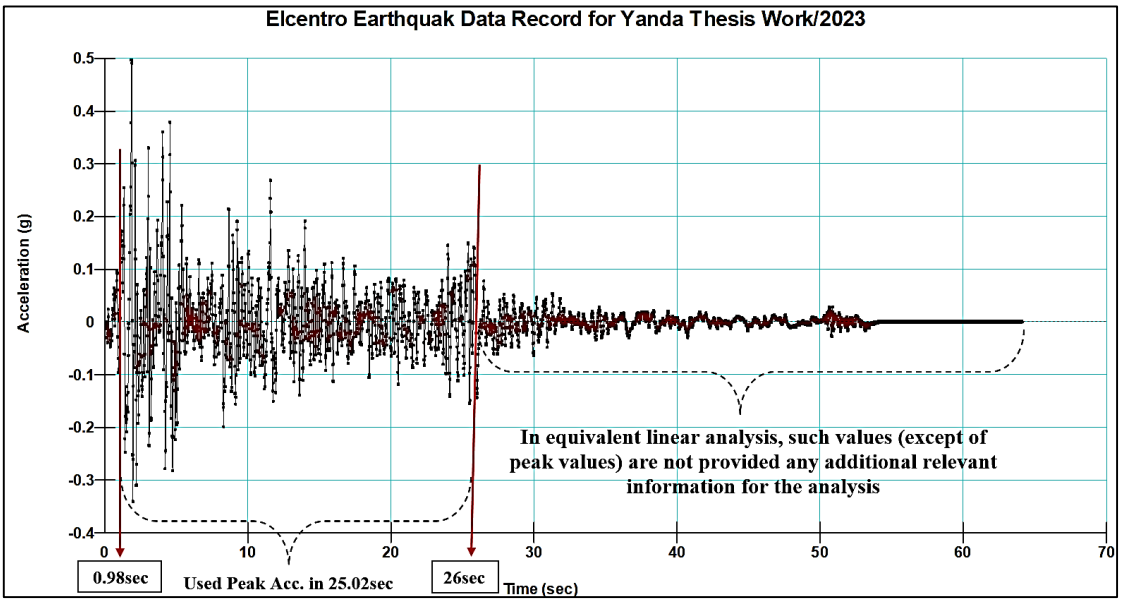

Graph 9 Showing Modified Elcentro Record for this study's dynamic analysis

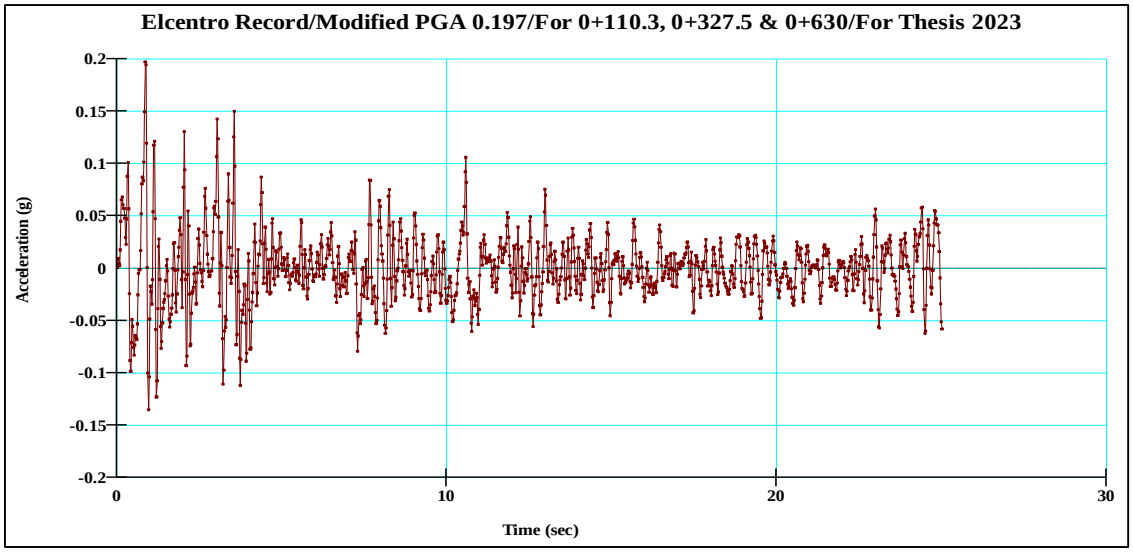

a. *Modified Elcentro Record for 0.197g*

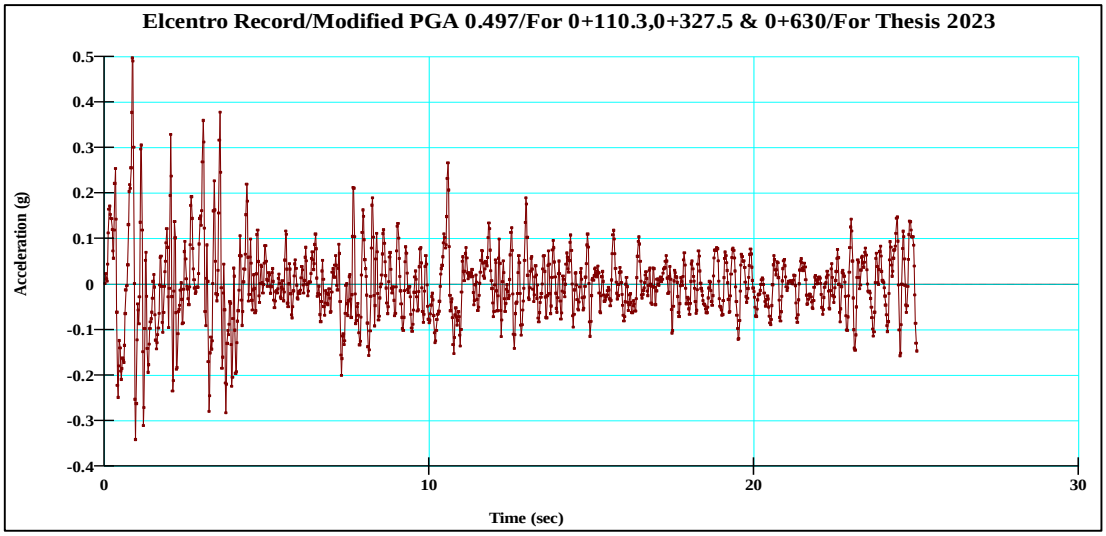

b. *Modified Elcentro Record for 0.497g*

Graph 10 Modified Elcentro Record for dynamic analysis 25.02sec duration.

4.9.2.5. Iteration

Entering the iteration value would be the next crucial step that has to be completed. Until no further adjustments to the soil's qualities are required, the analysis would be conducted again. It would be sufficient to require five iterations, per some research and Dr. Kevin Franke, the instructor for CEEN 545. The five iterations have become computationally quite demanding, based on experience. A 25.02-second shaking record with one data point every 0.02 seconds has been generated for the Yanda dam specifically for this study project. This indicated that a total of 1251 data points would be used to make the total. The total number of finite element analyses would thus be 5*1251 = 6255 after five iterations (five times such a change in time of 0.02 seconds).

4.9.2.6. Boundary Conditions

All boundary conditions in QUAKE/W must be explicitly applied to geometry elements like region faces, region lines, free lines, or free points. (QUAKE/W, 2008). The boundary condition has been added at the bottom and on the sides of the foundation in this analysis. The boundary conditions at the vertical ends of the problem have to be changed for the dynamic analysis. Now the vertical movement would be fixed, but the ground would be allowed to move laterally. These conditions allow the ground to sway from side to side when horizontal earthquake accelerations are applied.

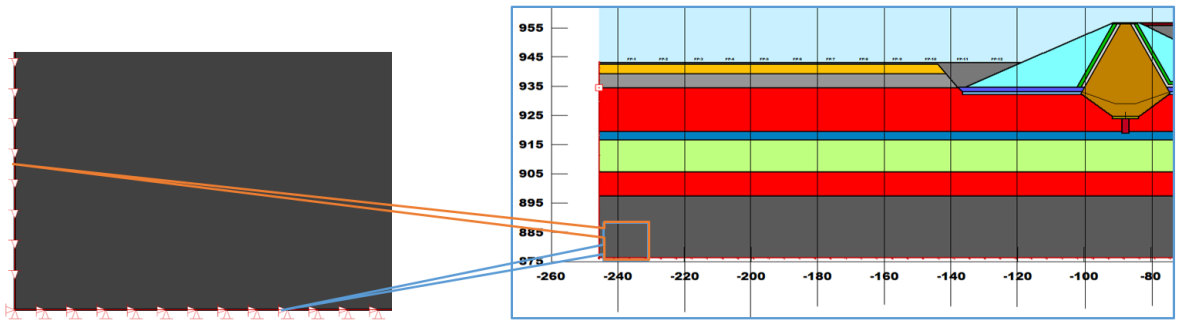

Figure 30 Vertical and Horizontal Boundary conditions for the dynamic analysis.

When integrating through the earthquake record, chosen places in QUAKE/W may be highlighted so that the results would be stored for each time step. History Points are what they are called. Here, two historical points have been described. They are shown by the two tiny red squares in the figure below.

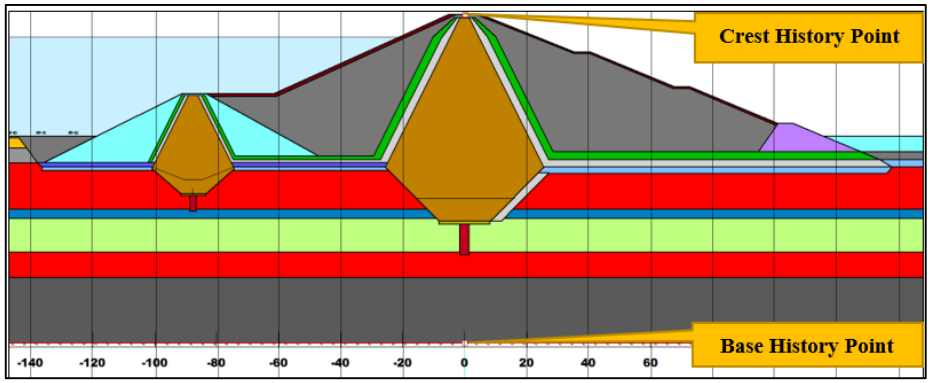

Figure 31 Crest and Base History Point for the dynamic analysis

The soil would be considered to have linear elastic behavior in its constitutive state. Yanda Dam foundation soil has a shear modulus (G_{max})that would be calculated with the product of density and wave shear velocity and 0.2 (20%) would be the constant damping ratio.

4.9.2.7. Parameters Used for Dynamic Analysis

For dynamic analysis, data accessibility has been a hindrance, especially for inputs associated with geometry, material characteristics, and earthquakes. Nonetheless, information has been acquired via the Office of ECDSWC and engineering publications. Cross-sections of three chainages have been compared and analyzed, and the feasibility study's final report's dynamic analysis assessed. When choosing the most vulnerable section for dynamic analysis, the thickness of the alluvium deposit and section size have to be taken into consideration.

Geotechnical parameters required for modeling of dynamic analysis have been presented below.

Cohesion (C')	Unit weight
Internal friction angle (ø)	Poisson's ratio
Pore-water pressure function (PWP)	Effective cohesion
Cyclic number function (Cyc)	Damping ratio
Correction coefficient for overburden (Ka)	Maximum shear modulus (Gmax)
Correction function for shear stress (Ks)	Reduction Shear modulus function (G)

4.9.2.8. Poisson's Ratio

The values of Poisson's ratio have been obtained from the geotechnical report of ECDSWC, 2022. K.R. The following table of 35 shows typical ranges of values for poison's ratio of soil materials, according to Bowles, 1996.

S.No.	Type of soil	Poisson's Ratio (v)
1	Saturated Clay	0.4-0.5
2	Unsaturated Clay	0.1-0.3
3	Silt	0.3-0.35
4	Loose Sand	0.30-0.50
5	Dense Sand	0.20-0.30

Table 35 Summarized the Poisson's ratio of different materials (K.R. Arora, 2004)

4.9.2.9. Summarized Needed Parameters as Input Data

Type of analysis	**Dynamic Analysis**					
Material Model	**Equivalent Linear**					
Filled dam material and Material Alluvial Deposited layers	**Unit Weight**	**Poisson's Ratio(v)**	**C'**	**ø**	**G_{max}**	**Damping Ratio**
	KN/m3		**Kpa**	**°**	**Kpa**	
ZONE 1-CLAY CORE	15.6	0.334	46.08	15.46	*Function*	0.2
ZONE 2-B- COARS FILTER	28	0.2	0	21	*Function*	0.2
ZONE 2-A -FINE FILTER	28	0.2	0	18	*Function*	0.2
ZONE 3-SHELL FILL	21.8	0.2	0	36.69	*Function*	0.2
ZONE 4-ROCK FILL	26	0.05	0	40	*Function*	0.2
ZONE 5-TOY DRAIN	26	0.05		40	*Function*	0.2
ZONE 6-RIPRAP	26	0.05		40	*Function*	0.2
ZONE 7-CLAY BLANKET	16.6	0.350	46.08	15.46	*Function*	0.2
ZONE 8-GRAVEL CLAY (GC)	28	0.5	46.08	21	*Function*	0.2
ZONE 9-SILTY CLAY(CL) TRACE OF SAND	14.9	0.30	27	20.5	42,521	0.2
ZONE 10-SILTY SAND (SM) FOUNDATION	13.6	0.3	0	34	36,086	0.2
ZONE 11- COARSER GRAVEL(GM)	15.8	0.02	0	33.5	39,134	0.2
ZONE 12-CLAYEY SILT	14.3	0.3	16	16.17	33,560	0.2
ZONE 15-SLIGHTLY WEATHERED	21	0.02	305	32	*Function*	0.2
ZONE 17-HIGHLY WEATHERED TRACHYTE	24.32	0.02	221	27	*Function*	0.2
SLURRY CUTOFF	14.42	0.35	60.71	21.79	*Function*	0.2
TRANSITION	28	0.2	0	21	*Function*	0.2

Table 36 Yanda Dam Summarized needed parameters as input data

- Pore-water pressure has been computed from SEEP/W and applied to this analysis
- A shaking type of analysis has been made with QUAKE/W by providing the site-specific seismic data with an equivalent linear type of model.
- Liquefaction-triggering analysis using SPT-N would follow the following flow;

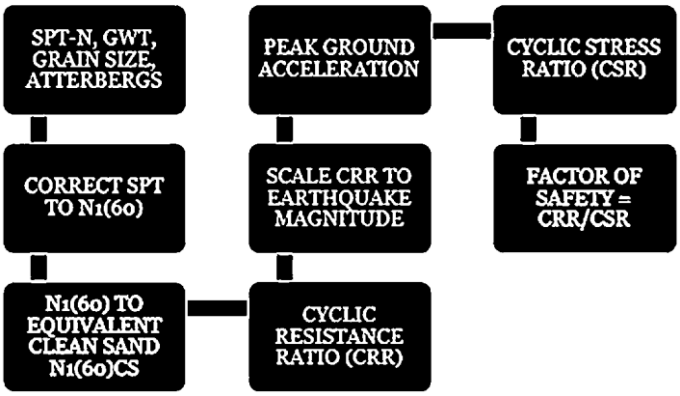

Chart 5 Flow of activities in Calculation of FoS

- Finally, all the results computed have been analyzed and discussed

4.9.2.10. Utilized Empirical Equations and Standards

The following data have been utilized by referring to the ECDSWC Geotechnical report and other standards: thickness, beginning depth, end depth, elevation, cohesion, angle of internal friction, plasticity index, relative density, fines, unit weight, and Ncorr. All of the data that were cited have been listed in the previous section. However, empirical formulae have been used to determine the rest of the parameters, including density, shear velocity, shear modulus, cycle resistance ratio, cycle stress ratio, and magnitude scaling factor. However, the Quake/W numerical modeling would be used to determine the value of the cyclic stress ratio.

4.9.2.11. Empirical Equations used in this Study

Calculation or estimation of two variables is required for the evaluation of liquefaction resistance of soils. These variables are the seismic demand placed on a soil layer, expressed in terms of cyclic stress ratio (CSR), and the capacity of the soil to resist liquefaction, expressed in terms of cyclic resistance ratio (CRR). Participants in the workshop (1996, sponsored by NCEER) provided a **Recommended** range of MSF **for engineering practice** instead of proposing a specific set of factors, and the engineer is then free to select factors from within that range that meet the application's requirements for conservatism. The new set of magnitude

scaling factors put out by Idriss (Column 3, Table 3) serves as the bottom bound for the suggested range for magnitudes less than 7.5.

4.9.2.11.1. Maximum Shear Modulus(G_{max})

$$G_{max} = Vs * \rho \quad \text{.....Equation 16}$$

Where;

$\rho = \frac{\gamma}{g}$

$Vs = 85.3 * N^{0.348}$

ρ = the mass density
γ = Unit Weight of foundation material
g = gravity(9.81)
Vs = Shear Velocity; **N** = SPT N value

4.9.2.11.2. Cyclic Resistance Ratio;

$$CRR_{7.5} = \frac{a + cx + ex^2 + gx^3}{1 + bx + dx^2 + fx^3 + hx^4} \quad \text{..... Equation 17}$$

Each constant value was listed in the previous chapter and would be listed in the next Excel sheet CSR calculation table of 37, 38, 39, 40, 41, and 42.

4.9.2.11.3. Cyclic Stress Ratio;

Cyclic Stress Ratio (**CSR**) is required to induce liquefaction for a cohesionless soil stratum of given properties at a given depth. It, seismic demand on a soil layer, is based on a peak ground surface acceleration and an associated moment magnitude.

$$CSR = \frac{\tau_{av}}{\sigma'_{vo}} = 0.65\left(\frac{a_{max}}{g}\right)\left(\frac{\sigma_{vo}}{\sigma'_{vo}}\right) r_d \quad \text{..... Equation 18}$$

Each variable was listed and explained in the previous literature. However, In this study, CSR will be estimated using the numerical modeling of Quake/W as tabulated in the next liquefaction analysis.

4.9.2.11.4. Magnitude Sealing Factors;

$$MSF = 6.9\exp\left(\frac{-M}{4}\right) - 0.058 \leq 1.8 \quad \text{..... Equation 19}$$

Based on the stated motion in the earlier chapter, **M** has been determined to be 6.3 for this research analysis. Since the value that getting the same as using the Graph 11, for this research, both MSF graphs would be used for comparing and ascertaining.

4.9.2.11.5. Factor of Safety(FS);

This result would be used for the evaluation of the factor of safety to check the potential of liquefaction. When the factor of safety becomes greater than one, the liquefaction potential is going to be safe. Allows a factor of safety against liquefaction, FS, to be calculated for a soil stratum at a given depth.

$$FS = \frac{CRR_{6.3}}{CSR} \qquad \text{..... Equation 20}$$

Where; $CRR_{6.3} = MSF_{6.3} * CRR_{7.5}$

4.9.2.11.6. Graph-Based Magnitude Scaling Factor Computation

To evaluate the liquefaction of necessary CRR_m under the site-specific earthquake magnitude, Cyclic Resistance Ratio ($CRR_{7.5}$), which has been regarded as the standard reference for 7.5 earthquakes, has been used by multiplying with the Magnitude Scaling Factor of that specific Site. Since the approaches have been updated, it would be employed in this study to calculate the earthquake magnitude at the Yanda dam site using Graph 11, or Equation 23.

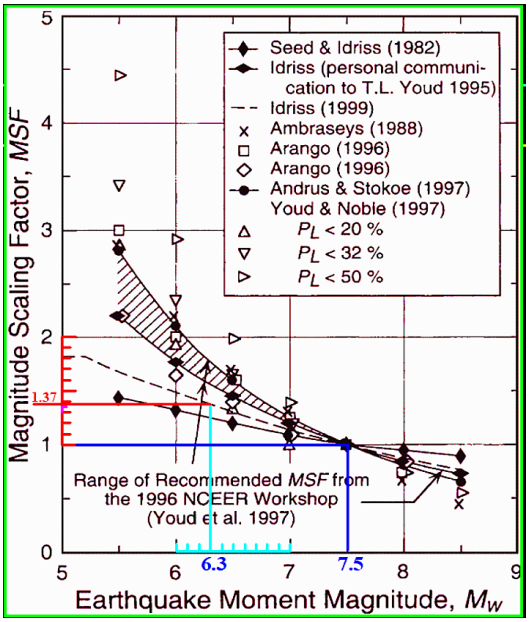

a.

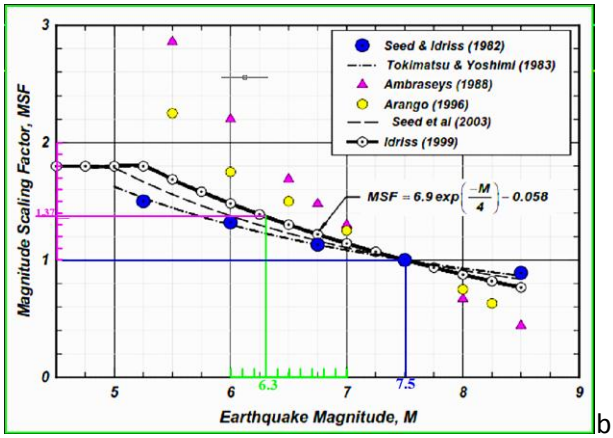

b.

Graph 11 Calculated MSF using a graph for converting $CRR_{7.5}$ to $CRR_{6.3}$

It should be noted that, after being evaluated with various earthquake magnitude values, the results for both graphs (a and b) have been quite comparable. Consequently, since equation 23 and one of the two previously mentioned graphs represent updated references, only one of them and the equation would be employed for this research analysis task.

4.9.2.12. Cyclic Stress Ratio (CSR)

It should be noted that, after evaluating various earthquake magnitude values, the results for both graphs (a and b) have been quite comparable. Consequently, since equation 23 and one of the two previously mentioned graphs represent updated references, only one of them and the equation would be employed for this research analysis task. One important metric that can be determined in an Equivalent Linear analysis is the Cyclic Stress Ratio (CSR). In short, the greater the CSR, the more likely liquefaction will occur. The following result from the dynamic part of the study has been used to determine CSR values. There would only be one CSR value since there would only be one peak value from the shaking. Consequently, CSR contour plots and graphs produced by all-time steps are similar. Just to maintain consistency for other variables, the values have been maintained for all time steps even though they would only be available for the most recent time step. Even with its irregular shading, it nonetheless identifies areas that might liquefy (Figures 32, 33, and 34).

4.9.2.12.1. Showcase of Liquefaction-Prone Strata at 0+110.3

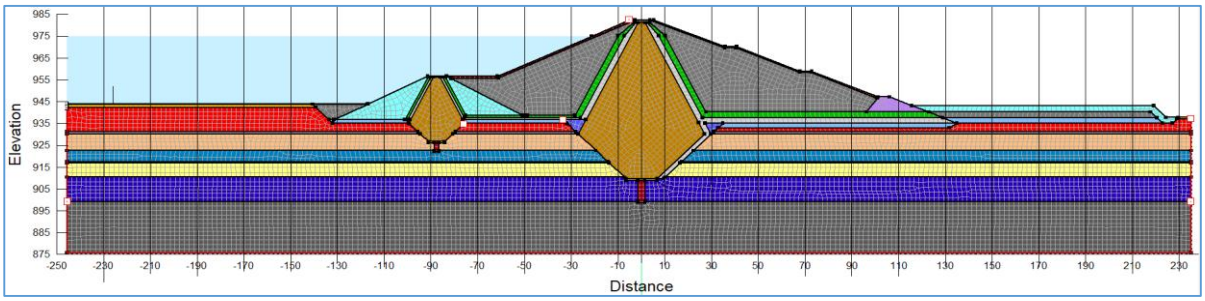

Prepared foundation layer for 0+110.3

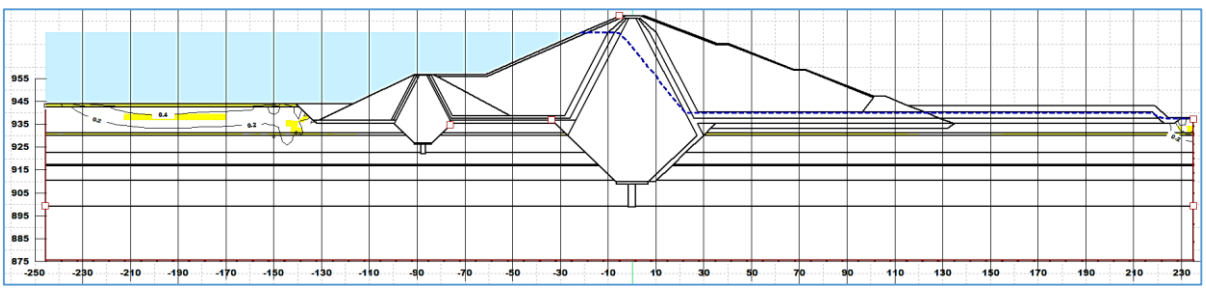

PGA = 0.197

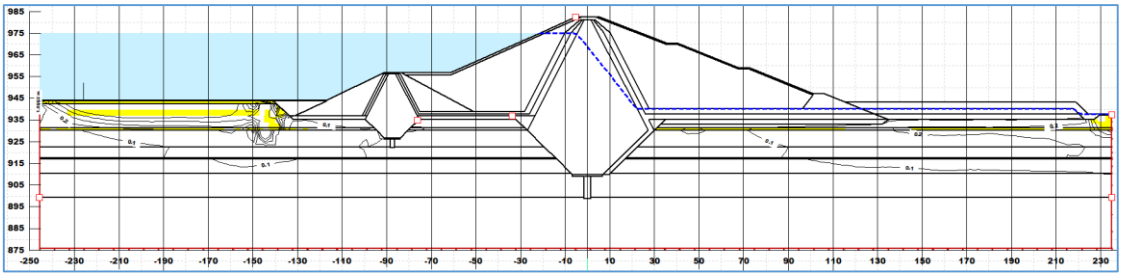

PGA = 0.497

Figure 32 CSR Contours that Prone to Liquefaction at 0+110.3

4.9.2.12.2. Showcase of Liquefaction-Prone Strata at 0+630

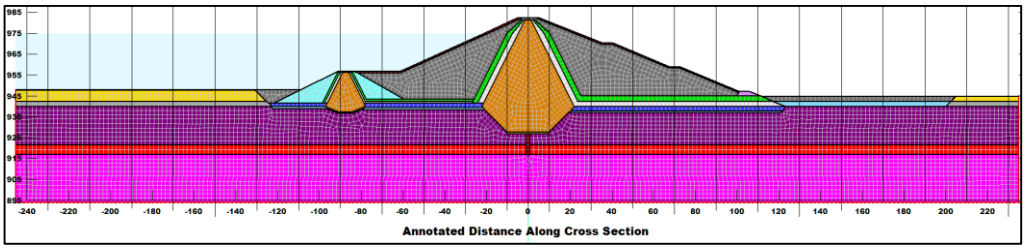

Prepared foundation layer for 0+630

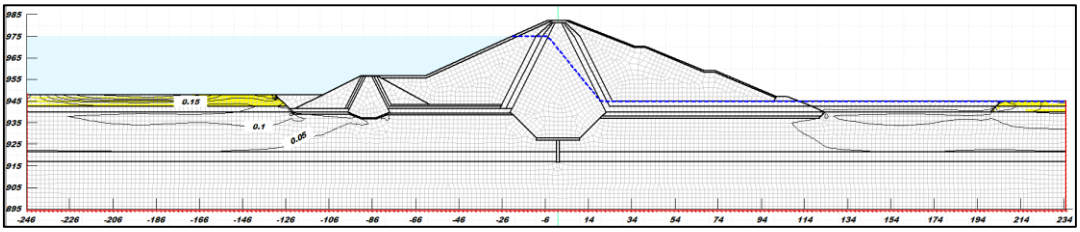

PGA = 0.197

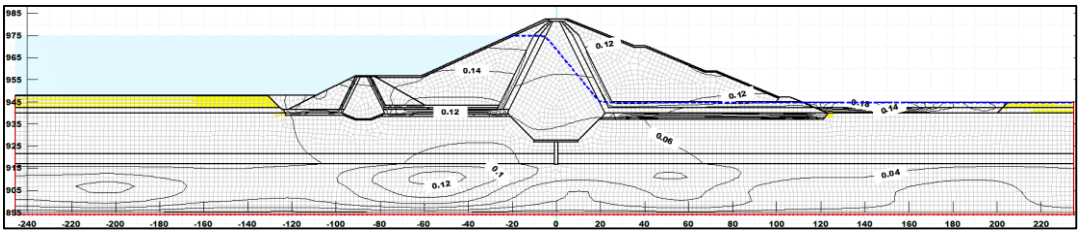

PGA = 0.497

Figure 33 CSR Contours that Prone to Liquefaction at 0+630

4.9.2.12.3. Showcase of Liquefaction-Prone Strata at 0+327.5

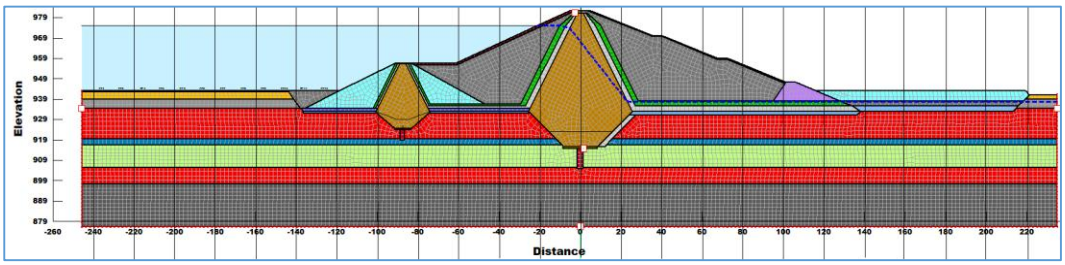

Prepared foundation layer for 0+327.5

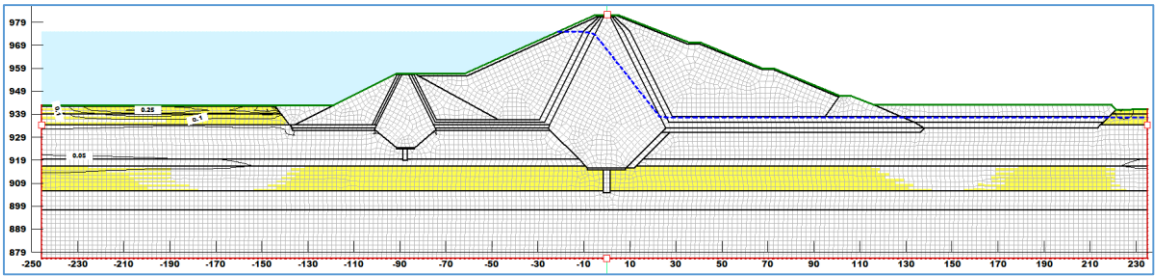

PGA = 0.197

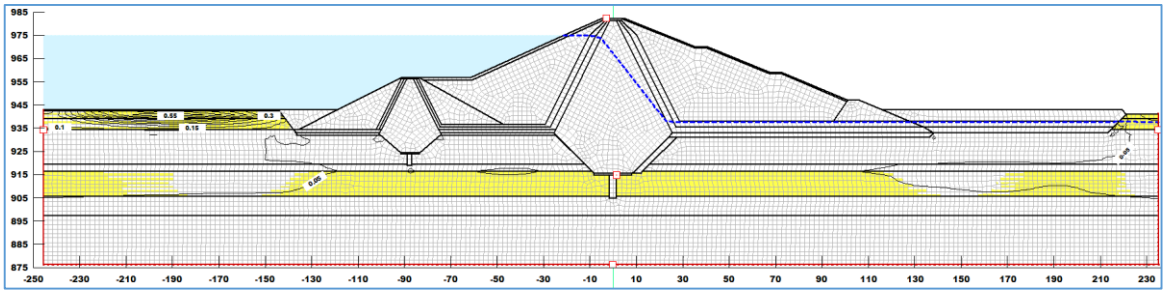

PGA = 0.497

Figure 34 CSR Contours that Prone to Liquefaction at 0+327.5

4.9.3. This Research's Quake/W Output and Visualized Results

One of the attractive things about QUAKE/W is how easily its results can be analyzed, evaluated, and shown. It is essential for any finite element analysis since so many data points are involved. The only visual aids that can efficiently examine a significant amount of the data are graphs and outlines. Nevertheless, it is often necessary to examine the digital data at a particular node or a Gauss integration point inside an element in order to examine details. In Geo-Studio, users may access any output data for nodes and Gauss points placed anywhere in the model using the View Results Information command. Any one node can be clicked to view the output at that node when the command is selected.

The CSR calculated value has been obtained from each modeled dam section (0+110.3, 0+327.5, and 0.630) and from each defined foundation layer to determine the factor of safety for the possibility of liquidation. Around 24 annotated lines have been established from the top of the dam crest to the necessary foundation depth along the dam cross section and each layer of the u/s and d/s section. The CSR values have been then manually extracted from each layer of the alluvial foundation along the annotated line and inputted into the prepared tabular Excel sheet.

4.9.3.1. Dynamic Analyzed CSR Results for PGA value of 0.197g

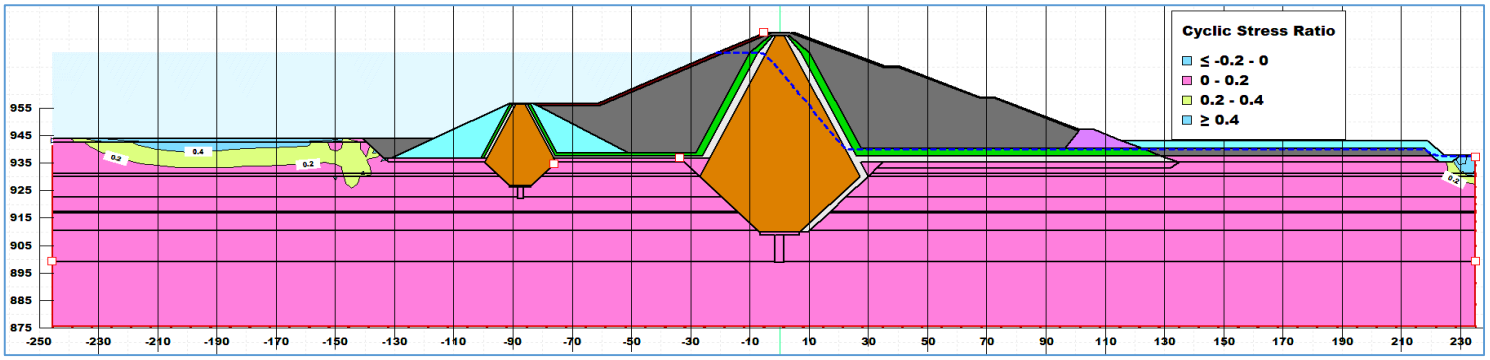

a. CSR Output Result with contour at 0+110.3

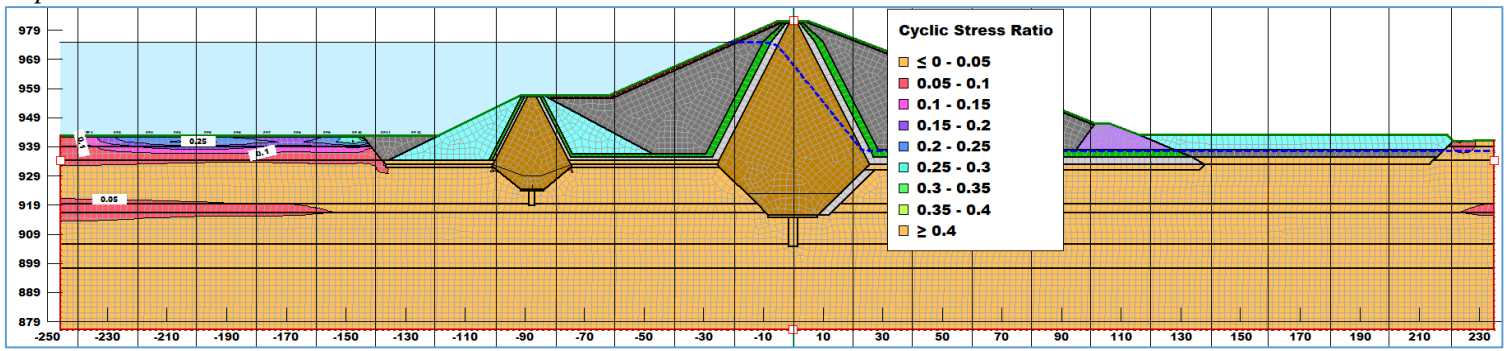

b. CSR Output Result with contour at 0+327.5

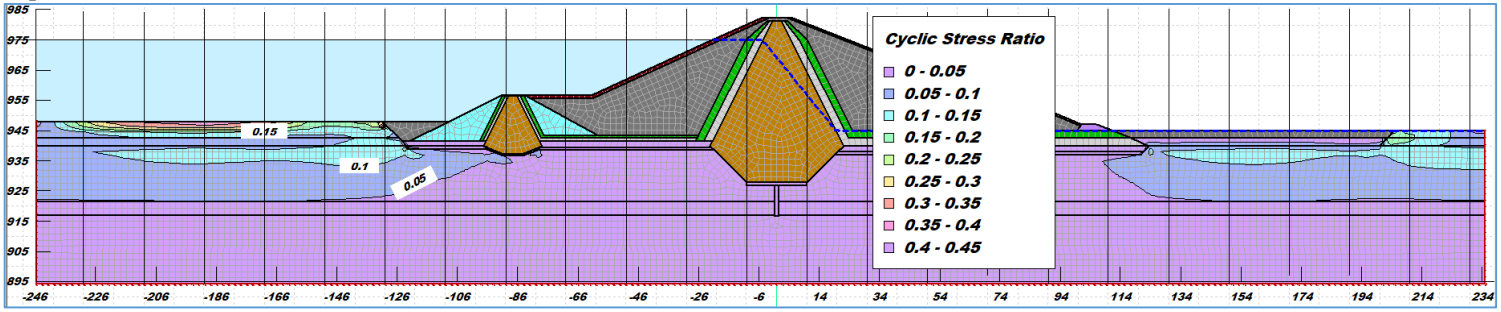

c. CSR Output Result with contour at 0+630

Figure 35 Dynamic analyzed model of CSR Output display with contour using PGA 0.197g

4.9.3.2. Dynamic Analyzed CSR Results for PGA value of 0.497g

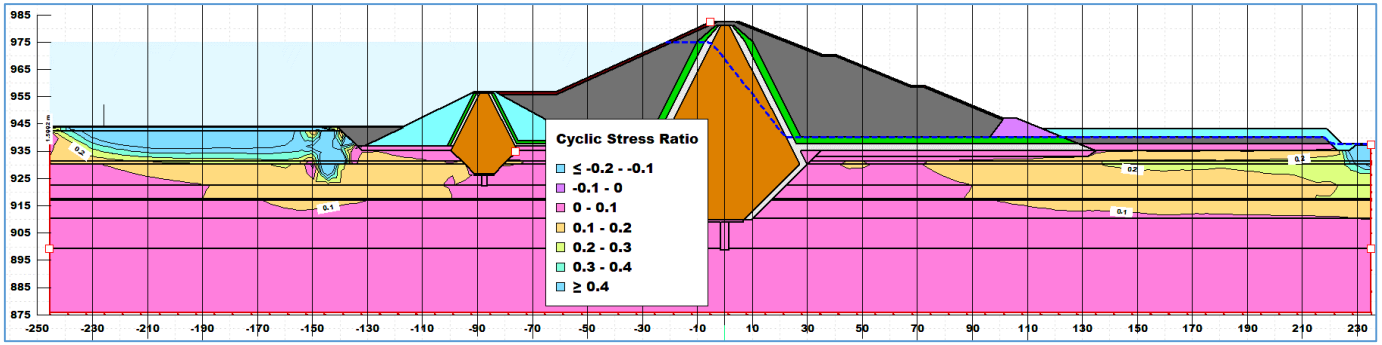

a. CSR Output Result with contour at 0+110.3

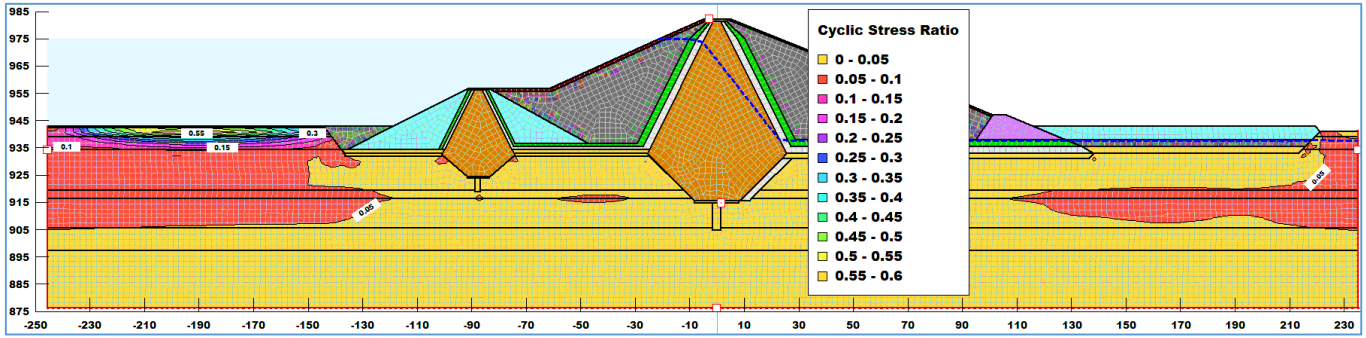

b. CSR Output Result with contour at 0+327.5

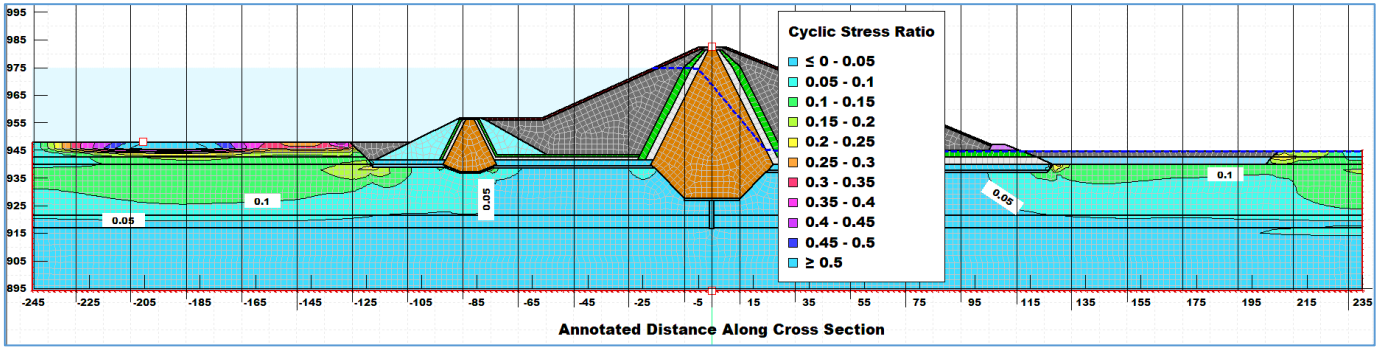

c. CSR Output Result with contour at 0+630

Figure 36 Dynamic analyzed model of CSR Output display with contour using PGA 0.497g

4.9.3.3. Excel Sheet Output Result at 0+110.3 for PGA value of 0.197g

Dyanamic Analysis has been done at Chainage 0+110.3 and Bore Hole - YDBH-4																												
LAYER	MATERIAL DISCRIPTION	PGA=0.197g																										
		Thickness	Initial depth	End depth	Elevation	C	ϕ	PI	Relative Density	Fines	Unit Weight (γ)	Density = γ/g	Ncorr	Vs	Gmax	$CRR_{7.5} = \frac{a + cx + ex^2 + gx^3}{1 + bx + dx^2 + fx^3 + hx^4}$									CRR (7.5)	MSF (6.3)	CRR (6.3)
		m	m	m	m	Kpa	o	%	%	%	KN/m3	(kg/m3)		m/s	(Kpa)	a	b	c	d	e	f	g	h			CRR(7.5)*MSF
GTL-1	Topsoil: Silty Clay With Trace of Sand (CL)	0.5	0.0	0.5	943.3	27.0	20.5	-	-	0.2	14.9	154.4	27	268.6	41,477	4.84E-02	-1.25E-01	-4.72E-03	9.58E-03	6.14E-04	-3.29E-04	-1.67E-05	3.71E-06	0.32	1.37	0.44
GTL-5	Coarse Gravel (GM)	8.5	0.5	9.0	934.8	-	33.5	-	40-65	1.2	15.0	156.0	16	223.9	34,914									0.17	1.37	0.24
GTL-4	Fine Grained Silty Sand (SM)	1.0	9.0	10.0	933.8	-	34.0	-	20-40	1.2	17.9	185.5	20	241.9	44,886									0.22	1.37	0.30
GTL-5	Coarse Gravel (GM)	7.6	10.0	17.6	926.2	-	33.5	22.4	40-65	3.7	15.7	163.1	20	243.0	39,631									0.22	1.37	0.30
GTL-3	Clayey Silt with trace of Gravel (MH):	5.1	17.6	22.6	921.2	53.3	31.5	-	-	12.4	13.6	141.0	18	233.2	32,888									0.20	1.37	0.27
GTL-4	Fine Grained Silty Sand (SM)	0.6	22.6	23.2	920.5	-	34.0	-	20-40	15.6	14.7	152.9	19	237.7	36,339									0.21	1.37	0.28
GTL-5	Coarse Gravel (GM)	6.6	23.2	29.8	914.0	-	33.5	-	40-65		13.9	144.8	16	223.9	32,404									0.17	1.37	0.24

$CRR_{7.5}$ is the Cyclic Resistance Ratio for magnitude 7.5 earthquakes; which is approximated by Thomas F. Blake with the following equation:

x= $(N_1)_{60}$;	a = 4.844E-02,	d= 9.578E-03,
e =6.136E-04,	b = -1.248E-01,	g= -1.673E-05;
f= -3.285E-04,	c = - 4.721E-03,	h= 3.714E-06.

This equation is valid for $(N_1)_{60}$ less than 30 and may be used in spreadsheets and other analytical techniques to approximate the simplified base curve for engineering calculations.

a. Important data and calculated values for Dynamic Analysis of CSR

CSR from each annotated Cross Sectional Points in Quake/W Dynamic Analysis using PGA = 0.197g																																		
UPSTREAM																DAWNSTREAM																		COMULATIVE AVERAge	
-250	-230	-210	-190	-170	-150			-130	-110	-90	-70	-50	-30	-10		10	30	50	70	90	110	130		150	170	190	210	230						
						CSR (avg)	FS= CRR/ CSR								CSR (avg)	FS= CRR/ CSR							CSR (avg)	FS= CRR/ CSR						CSR (avg)	FS= CRR/ CSR	CSR (avg)	FS= CRR/ CSR
0.11	0.52	0.99	1.03	0.89	0.77	0.72	0.62																				1.81	1.81	0.24	0.62	0.72
0.02	0.03	0.06	0.06	0.06	0.04	0.05	5.09	0.07	0.05	0.06	0.05	0.03	0.03		0.05	4.92		0.04	0.04	0.06	0.06	0.07	0.10	0.06	3.86	0.10	0.12	0.11	0.13	0.27	0.20	1.17	0.06	3.73
0.04	0.07	0.12	0.13	0.13	0.16	0.11	2.78	0.10	0.08	0.07	0.07	0.05	0.05		0.07	4.33		0.10	0.07	0.06	0.09	0.10	0.14	0.09	3.27	0.14	0.16	0.15	0.18	0.33	0.25	1.18	0.10	2.93
0.03	0.03	0.05	0.06	0.06	0.06	0.05	6.27	0.06	0.06	0.06	0.04	0.04	0.04		0.05	5.92		0.03	0.04	0.04	0.06	0.08	0.10	0.06	5.10	0.11	0.11	0.10	0.12	0.13	0.13	2.41	0.06	4.78
0.02	0.03	0.05	0.06	0.07	0.07	0.05	5.39	0.06	0.06	0.05	0.04	0.05	0.05	0.05	0.05	5.33	0.04	0.04	0.05	0.05	0.06	0.07	0.09	0.06	4.78	0.10	0.10	0.11	0.11	0.13	0.12	2.26	0.06	4.24
0.02	0.03	0.04	0.05	0.06	0.07	0.04	6.32	0.06	0.06	0.06	0.04	0.05	0.06	0.07	0.06	5.12	0.04	0.04	0.06	0.06	0.06	0.07	0.09	0.06	4.73	0.10	0.11	0.11	0.11	0.13	0.12	2.38	0.07	4.33
0.01	0.02	0.03	0.03	0.04	0.05	0.03	7.36	0.04	0.05	0.04	0.03	0.04	0.06	0.06	0.05	5.27	0.04	0.03	0.03	0.04	0.04	0.06	0.07	0.04	5.49	0.08	0.09	0.09	0.09	0.11	0.10	2.40	0.05	4.69

b. Liquefaction Factor of Safety Output Excel Results

Table 37 Calculation of factor of safety from output result of CSR at 0+110.3 & PGA 0.197g

4.9.3.4. Excel Sheet Output Result at 0+110.3 for PGA value of 0.497g

Dyanamic Analysis has been done at Chainage 0+110.3 and Bore Hole - YDBH-4																													
LAYER	MATERIAL DISCRIPTION	PGA=0.497g																											
		Thickness	Initial depth	End depth	Elevation	C	ϕ	PI	Relative Density	Fines	Unit Weight (γ)	Density = γ/g	Ncorr	Vs	Gmax	$CRR_{7.5} = \frac{a + cx + ex^2 + gx^3}{1 + bx + dx^2 + fx^3 + hx^4}$								CRR (7.5)	MSF (6.3)	CRR (6.3)
		m	m	m	m	Kpa	o	%	%	%	KN/m3	(kg/m3)		m/s	(Kpa)	a	b	c	d	e	f	g	h			CRR(7.5)*MSF
GTL-1	Topsoil: Silty Clay With Trace of Sand (CL)	0.5	0.0	0.5	943.3	27.0	20.5	-	-	0.2	14.9	154.4	27	268.6	41,477	4.84E-02	-1.25E-01	-4.72E-03	9.58E-03	6.14E-04	-3.29E-04	-1.67E-05	3.71E-06	0.32	1.37	0.44
GTL-5	Coarse Gravel (GM)	8.5	0.5	9.0	934.8	-	33.5	-	40-65	1.2	15.0	156.0	16	223.9	34,914									0.17	1.37	0.24
GTL-4	Fine Grained Silty Sand (SM)	1.0	9.0	10.0	933.8	-	34.0	-	20-40	1.2	17.9	185.5	20	241.9	44,886									0.22	1.37	0.2982
GTL-5	Coarse Gravel (GM)	7.6	10.0	17.6	926.2	-	33.5	22.4	40-65	3.7	15.7	163.1	20	243.0	39,631									0.22	1.37	0.3022
GTL-3	Clayey Silt with trace of Gravel (MH):	5.1	17.6	22.6	921.2	53.3	31.5	-	-	12.4	13.6	141.0	18	233.2	32,888									0.20	1.37	0.27
GTL-4	Fine Grained Silty Sand (SM)	0.6	22.6	23.2	920.5	-	34.0	-	20-40	15.6	14.7	152.9	19	237.7	36,339									0.21	1.37	0.2828
GTL-5	Coarse Gravel (GM)	6.6	23.2	29.8	914.0	-	33.5	-	40-65		13.9	144.8	16	223.9	32,404									0.17	1.37	0.2385

$CRR_{7.5}$ is the Cyclic Resistance Ratio for magnitude 7.5 earthquakes; which is approximated by Thomas F. Blake with the following equation:

$x = (N_1)_{60}$;	a = 4.844E-02,	d= 9.578E-03,
e =6.136E-04,	b = -1.248E-01,	g= -1.673E-05;
f= -3.285E-04,	c = - 4.721E-03,	h= 3.714E-06.

This equation is valid for $(N_1)_{60}$ less than 30 and may be used in spreadsheets and other analytical techniques to approximate the simplified base curve for engineering calculations.

a. Important data and calculated values for Dynamic Analysis of CSR

CSR from each annotated Cross Sectional Points in Quake/W Dynamic Analysis using PGA = 0.497g																																COMULATIVE AVERAge	
UPSTREAM																DAWNSTREAM																	
-250	-230	-210	-190	-170	-150			-130	-110	-90	-70	-50	-30	-10			10	30	50	70	90	110	130			150	170	190	210	230				
						CSR (avg)	FS= CRR/ CSR								CSR (avg)	FS= CRR/ CSR								CSR (avg)	FS= CRR / CSR						CSR (avg)	FS= CRR/ CSR	CSR (avg)	FS= CRR/ CSR
0.26	1.19	1.95	1.87	1.51	1.46	1.37	0.32																									1.37	0.32
0.11	0.07	0.10	0.11	0.12	0.11	0.10	2.30	0.18	0.09	0.09	0.09	0.07	0.07		0.10	2.44		0.06	0.08	0.09	0.11	0.13	0.18	0.18	1.30	0.20	0.26	0.92	0.21	0.48	0.35	0.69	0.17	1.42
0.08	0.13	0.14	0.17	0.19	0.06	0.13	2.31	0.21	0.13	0.12	0.11	0.09	0.12		0.13	2.31		0.14	0.12	0.14	0.15	0.18	0.23	0.25	1.20	0.25	0.29	1.01	0.27	0.52	0.39	0.76	0.18	1.63
0.07	0.05	0.08	0.11	0.14	0.18	0.10	2.91	0.14	0.11	0.11	0.08	0.08	0.07		0.10	3.09		0.07	0.08	0.09	0.11	0.14	0.17	0.19	1.60	0.18	0.29	1.04	0.19	0.27	0.23	1.31	0.17	1.82
0.05	0.05	0.06	0.09	0.11	0.13	0.08	3.21	0.12	0.11	0.08	0.08	0.08	0.08	0.08	0.09	3.02	0.08	0.07	0.09	0.09	0.10	0.13	0.14	0.16	1.70	0.17	0.27	0.98	0.18	0.22	0.20	1.35	0.17	1.60
0.04	0.05	0.07	0.10	0.13	0.15	0.09	3.21	0.12	0.11	0.08	0.09	0.09	0.09	0.10	0.10	2.93	0.08	0.08	0.10	0.10	0.11	0.14	0.14	0.16	1.74	0.18	0.28	1.00	0.18	0.21	0.19	1.46	0.18	1.61
0.02	0.05	0.07	0.06	0.10	0.13	0.07	3.29	0.09	0.10	0.06	0.07	0.07	0.08	0.11	0.08	2.93	0.08	0.05	0.04	0.07	0.08	0.12	0.12	0.14	1.75	0.16	0.26	0.92	0.14	0.17	0.15	1.55	0.16	1.52

b. Liquefaction Factor of Safety Output Excel Results

Table 38 *Calculation of factor of safety from output result of CSR at 0+110.3 & PGA 0.497g* `

4.9.3.5. Excel Sheet Output Result at 0+327.5 for PGA value of 0.197g

a.

Dynamic Analysis has been done at Chainage 0+327.5 and Bore Hole - YDBH-3 & 3B																											
LAYER	MATERIAL DISCRIPTION	PGA=0.197g																									
		Thickness	Initial depth	End depth	Elevation	C	ϕ	PI	Fines	Unit Weight (γ)	Density = γ/g	Ncorr	Vs	Gmax	$CRR_{7.5} = \frac{a + cx + ex^2 + gx^3}{1 + bx + dx^2 + fx^3 + hx^4}$									CRR (7.5)	MSF (6.3)	CRR (6.3)
		m	m	m	m	Kpa	°	%	%	KN/m3	(kg/m3)		m/s	(Kpa)	a	b	c	d	e	f	g	h			CRR(7.5)*MSF
GTL-1	Topsoil: Silty Clay With Trace of Sand (CL)	2.7	0.0	2.7	938.3	27.0	20.5	14.7	79.7	14.9	154.4	29.0	275.3	42521.4	4.84E-02	-1.25E-01	-4.72E-03	9.58E-03	6.14E-04	-3.29E-04	-1.67E-05	3.71E-06	0.38	1.37	0.53
GTL-4	Fine Grained Silty Sand (SM)	4.6	2.7	7.4	933.6	-	34.0	-	3.0	17.8	185.0	15.8	222.6	41191.8									0.17	1.37	0.23
GTL-5	Coarse Gravel (GM)	12.1	7.4	19.5	921.5	-	33.5	26.6	90.9	15.8	164.1	19.2	238.4	39133.8									0.21	1.37	0.29
GTL-3	Clayey Silt with trace of Gravel (MH):	5.6	19.5	25.1	915.9	-	33.0	-	7.0	14.3	148.3	16.5	226.3	33560.4									0.18	1.37	0.25
GTL-4	Fine Grained Silty Sand (SM)	9.4	25.1	34.5	906.5	-	34.0	14.4	60.1	13.6	141.0	23.5	255.9	36086.0									0.26	1.37	0.36

x= $(N_1)_{60}$;	a = 4.844E-02,	d= 9.578E-03,
e =6.136E-04,	b = -1.248E-01,	g= -1.673E-05;
f= -3.285E-04,	c = - 4.721E-03,	h= 3.714E-06.

a. Important data and calculated values for Dynamic Analysis of CSR

CSR from each Annotated Cross Sectional Points in Quake/W Dynamic Analysis using PGA = 0.197g																																	
UPSTREAM																DAWNSTREAM																COMULATIVE AVERAge	
-240	-220	-200	-180			-160	-140	-120	-100	-80	-60	-40	-20			20	40	60	80	100	120	140	160			180	200	220				
				CSR (avg)	FS= CRR/ CSR									CSR (avg)	FS= CRR/ CSR									CSR (avg)	FS= CRR/ CSR				CSR (avg)	FS= CRR/ CSR	CSR (avg)	FS= CRR/ CSR
0.09	0.21	0.26	0.22	0.20	2.68	0.22	0.25							0.23	2.27													0.07	0.07	7.23	0.19	2.79
0.09	0.09	0.10	0.09	0.09	2.56	0.09	0.07							0.08	2.90													0.04	0.04	6.18	0.08	2.90
0.05	0.04	0.04	0.04	0.04	6.55	0.04	0.04	0.03	0.02	0.02	0.01	0.01	0.02	0.02	11.97	0.01	0.01	0.01	0.01	0.01	0.02	0.02	0.02	0.01	20.06	0.02	0.02	0.03	0.02	12.77	0.02	12.02
0.06	0.06	0.06	0.06	0.06	4.13	0.05	0.04	0.03	0.03	0.03	0.03	0.03	0.02	0.04	6.89	0.02	0.02	0.02	0.02	0.02	0.03	0.04	0.04	0.03	9.30	0.04	0.04	0.05	0.04	5.62	0.04	6.53
0.04	0.04	0.04	0.04	0.04	8.69	0.04	0.03	0.03	0.03	0.03	0.03	0.03	0.02	0.03	12.30	0.02	0.02	0.03	0.03	0.03	0.03	0.03	0.04	0.03	13.52	0.03	0.03	0.04	0.03	10.72	0.03	11.60

b. *Liquefaction Factor of Safety Output Excel Results*

Table 39 Calculation of factor of safety from output result of CSR at 0+327.5 & PGA 0.197g

4.9.3.6. Excel Sheet Output Result at 0+327.5 for PGA value of 0.497g

Dynamic Analysis has been done at Chainage 0+327.5 and Bore Hole - YDBH-3 & 3B

PGA=0.497g

$$CRR_{7.5} = \frac{a + cx + ex^2 + gx^3}{1 + bx + dx^2 + fx^3 + hx^4}$$

LAYER	MATERIAL DISCRIPTION	Thickness	Initial depth	End depth	Elevation	C	ϕ	PI	Fines	Unit Weight (γ)	Density = γ/g	Ncorr	Vs	Gmax	a	b	c	d	e	f	g	h	CRR (7.5)	MSF (6.3)	CRR (6.3)
		m	m	m	m	Kpa	°	%	%	KN/m3	(kg/m3)		m/s	(Kpa)											CRR(7.5)*MSF
GTL-1	Topsoil: Silty Clay With Trace of Sand (CL)	2.7	0.0	2.7	938.3	27.0	205.0	14.7	79.7	14.9	154.4	29.0	275.3	42,521	4.84E-02	-1.25E-01	-4.72E-03	9.58E-03	6.14E-04	-3.29E-04	-1.67E-05	3.71E-06	0.38	1.37	0.53
GTL-4	Fine Grained Silty Sand (SM)L	4.6	2.7	7.4	933.6	-	34.0	-	3.0	17.8	185.0	15.8	222.6	41,192									0.17	1.37	0.23
GTL-5	Coarse Gravel (GM)	12.1	7.4	19.5	921.5	-	32.5	26.6	90.9	15.8	164.1	19.2	238.4	39,134									0.21	1.37	0.29
GTL-3	Clayey Silt with trace of Gravel (MH):	5.6	19.5	25.1	915.9	-	33.0	-	7.0	14.3	148.3	16.5	226.3	33,560									0.18	1.37	0.25
GTL-4	Fine Grained Silty Sand (SM)	9.4	25.1	34.5	906.5	-	34.0	14.4	60.1	13.6	141.0	23.5	255.9	36,086									0.26	1.37	0.36

$x = (N_1)_{60}$;	a = 4.844E-02,	d = 9.578E-03,
e =6.136E-04,	b = -1.248E-01,	g = -1.673E-05;
f = -3.285E-04,	c = - 4.721E-03,	h = 3.714E-06.

a. Important data and calculated values for Dynamic Analysis of CSR

CSR from each Annotated Cross Sectional Points in Quake/W Dynamic Analysis using PGA = 0.497g

UPSTREAM															DAWNSTREAM														COMULATIVE AVERAGE	
-240	-220	-200	-180			-160	-140	-120	-100	-80	-60	-40	-20		20	40	60	80	100	120	140	160			180	200	220				
				CSR (avg)	FS= CRR/ CSR									CSR (avg)	FS= CRR/ CSR								CSR (avg)	FS= CRR/ CSR				CSR (avg)	FS= CRR/ CSR	CSR (avg)	FS= CRR/ CSR
0.14	0.43	0.59	0.57	0.43	1.22	0.42	0.28							0.35	1.50												0.09	0.09	5.71	0.32	1.65
0.12	0.15	0.22	0.22	0.18	1.31	0.17	0.09							0.13	1.82												0.05	0.05	4.90	0.15	1.61
0.06	0.06	0.05	0.05	0.06	4.94	0.06	0.04	0.03	0.03	0.03	0.02	0.03	0.03	0.03	8.94	0.02	0.02	0.02	0.02	0.02	0.02	0.03	0.03	0.02	13.39	0.03	0.04	0.05	0.04	7.70	0.03	8.54
0.09	0.09	0.08	0.07	0.08	3.01	0.08	0.07	0.05	0.05	0.04	0.05	0.05	0.04	0.05	4.68	0.03	0.03	0.03	0.04	0.05	0.05	0.06	0.06	0.04	5.64	0.06	0.06	0.07	0.07	3.77	0.06	4.38
0.08	0.07	0.07	0.06	0.07	5.08	0.06	0.06	0.05	0.04	0.04	0.05	0.05	0.03	0.05	7.69	0.03	0.03	0.04	0.04	0.04	0.05	0.05	0.05	0.04	8.54	0.05	0.05	0.07	0.06	6.33	0.05	7.10

b. Liquefaction Factor of Safety Output Excel Results

Table 40 Calculation of factor of safety from output result of CSR at 0+327.5 & PGA 0.497g

4.9.3.7. Excel Sheet Output Result at 0+630 for PGA value of 0.197g

Dyanamic Analysis has been done at Chainage 0+630 and Bore Hole - YDBH-2																													
		PGA=0.197g																											
LAYER	MATERIAL DISCRIPTION	Initial depth	End depth	Thickness	Elevation	C	ϕ	PI	Relative Density	Fines	Unit Weight (γ)	Density = γ/g	Ncorr	Vs	Gmax	$CRR_{7.5} = \frac{a + cx + ex^2 + gx^3}{1 + bx + dx^2 + fx^3 + hx^4}$								CRR (7.5)	MSF (6.3)	CRR (6.3)					
		m	m	m	m	Kpa	o	%	%	%	KN/m3	(kg/m3)		m/s	(Kpa)	a	b	c	d	e	f	g	h			CRR(7.5)*MSF					
GTL-1	Topsoil: Silty Clay With Trace of Sand (CL)	0.0	5.4	5.4	942.4	27.0	20.5	26.88		92.0	18.0	186.5	27.0	268.6	50,101	4.84E-02	-1.25E-01	-4.72E-03	9.58E-03	6.14E-04	-3.29E-04	-1.67E-05	3.71E-06	0.32	1.37	0.44			
GTL-4	Fine Grained Silty Sand (SM)	5.4	7.9	2.5	939.9	0.0	34.0	39.4	20-40	96.5	16.3	168.9	21.0	246.1	41,557									0.23	1.37	0.44			
GTL-2	Silty Clay (CL) intermediate dispersive	7.9	26.4	18.5	921.4	35.6	20.5	36.8		59.4	16.9	175.7	20.8	245.4	43,127									0.23	1.37	0.44			
GTL-5	Coarse Gravel (GM)	26.4	30.9	4.5	916.9	0.0	32.5	20.7	40-65		13.9	144.8	33.0	288.0	41,688									0.45	1.37	0.44			

$x = (N_1)_{60}$;	a = 4.844E-02,	d= 9.578E-03,
e =6.136E-04,	b = -1.248E-01,	g= -1.673E-05;
f= -3.285E-04,	c = - 4.721E-03,	h= 3.714E-06.

a. *Important data and calculated values for Dynamic Analysis of CSR*

CSR from each Annotated Cross Sectional Points in Quake/W Dynamic Analysis using PGA = 0.197g																																							
UPSTREAM																			DAWNSTREAM																					COMULATIVE AVERAge	
-250	-230	-210	-190	-170	-150	-130			-110	-90	-70	-50	-30	-10			10	30	50	70	90	110			130	150	170	190	210	230										
							CSR (avg)	FS= CRR/ CSR							CSR (avg)	FS= CRR/ CSR						CSR (avg)	FS= CRR/ CSR						CSR (avg)	FS= CRR/ CSR	CSR (avg)	FS= CRR/ CSR									
0.06	0.10	0.15	0.47	0.17	0.20	0.11	0.18	2.47																					0.18	0.05	0.12	3.84	0.16	2.68							
0.06	0.07	0.08	0.07	0.07	0.08	0.11	0.08	5.87																					0.09	0.03	0.06	6.89	0.07	6.07							
0.08	0.08	0.08	0.08	0.09	0.08	0.07	0.08	5.55	0.05	0.04	0.03	0.02	0.03	0.03	0.03	13.75	0.02	0.01	0.01	0.01	0.03	0.04	0.02	21.05	0.09	0.08	0.09	0.07	0.08	0.10	0.08	5.32	0.06	8.04						
0.03	0.03	0.03	0.03	0.03	0.03	0.03	0.03	15.80	0.02	0.02	0.02	0.02	0.02	0.02	0.02	21.20	0.01	0.01	0.01	0.02	0.02	0.02	0.02	27.73	0.03	0.03	0.03	0.03	0.03	0.03	0.03	16.28	0.02	19.07						

b. *Liquefaction Factor of Safety Output Excel Results*

Table 41 Calculation of factor of safety from output result of CSR at 0+630 & PGA 0.197g

4.9.3.8. Excel Sheet Output Result at 0+630 for PGA value of 0.497g

Dyanamic Analysis has been done at Chainage 0+630 and Bore Hole - YDBH-2																												
LAYER	MATERIAL DISCRIPTION	PGA=0.497g														$CRR_{7.5} = \frac{a + cx + ex^2 + gx^3}{1 + bx + dx^2 + fx^3 + hx^4}$								CRR (7.5)	MSF (6.3)	CRR (6.3)
		Initial depth	End depth	Thickness	Elevation	C	ϕ	PI	Relative Density	Fines	Unit Weight (γ)	Density = γ/g	Ncorr	Vs	Gmax												CRR(7.5)*MSF
		m	m	m	m	Kpa	o	%	%	%	KN/m3	(kg/m3)		m/s	(Kpa)	a	b	c	d	e	f	g	h			
GTL-1	Topsoil: Silty Clay With Trace of Sand (CL)	0.0	5.4	5.4	942.4	27.0	20.5	26.88		92.0	18.0	186.5	27.0	268.6	50,101	4.84E-02	-1.25E-01	-4.72E-03	9.58E-03	6.14E-04	-3.29E-04	-1.67E-05	3.71E-06	0.32	1.37	0.44
GTL-4	Fine Grained Silty Sand (SM)	5.4	7.9	2.5	939.9	0.0	34.0	39.4	20-40	96.5	16.3	168.9	21.0	246.1	41,557	$x=(N_1)_{60}$;		a = 4.844E-02,		d= 9.578E-03,				0.23	1.37	0.31
GTL-2	Silty Clay (CL) intermediate dispersive	7.9	26.4	18.5	921.4	35.6	20.5	36.8		59.4	16.9	175.7	20.8	245.4	43,127	e =6.136E-04,		b = -1.248E-01,		g= -1.673E-05;				0.23	1.37	0.31
GTL-5	Coarse Gravel (GM)	26.4	30.9	4.5	916.9	0.0	32.5	20.7	40-65		13.9	144.8	33.0	288.0	41,688	f= -3.285E-04,		c = - 4.721E-03,		h= 3.714E-06.				0.45	1.37	0.62

a. Important data and calculated values for Dynamic Analysis of CSR

CSR from each Annotated Cross Sectional Points in Quake/W Dynamic Analysis using PGA = 0.497g																													COMULATIVE AVERAge	
UPSTREAM																DAWNSTREAM														
-250	-230	-210	-190	-170	-150	-130			-110	-90	-70	-50	-30	-10		10	30	50	70	90	110			130	150	170	190	210	230			
							CSR (avg)	FS= CRR/ CSR							CSR (avg)	FS= CRR/ CSR							CSR (avg)	FS= CRR/ CSR					CSR (avg)	FS= CRR/ CSR	CSR (avg)	FS= CRR/ CSR
0.07	0.32	0.55	0.59	0.41	0.31	0.20	0.35	1.27																			0.22	0.07	0.15	3.01	0.27	1.62
0.07	0.09	0.14	0.13	0.14	0.12	0.14	0.12	2.69																			0.14	0.11	0.12	2.60	0.11	2.97
0.11	0.11	0.12	0.12	0.12	0.11	0.12	0.11	2.71	0.09	0.06	0.03	0.03	0.03	0.04	0.05	6.67	0.02	0.02	0.02	0.02	0.04	0.06	0.03	9.88	0.09	0.09	0.08	0.08	0.10	0.13	0.10	3.27	0.07	4.22
0.04	0.04	0.04	0.04	0.05	0.05	0.04	0.04	14.47	0.04	0.04	0.03	0.03	0.03	0.03	0.03	20.63	0.02	0.02	0.02	0.02	0.03	0.03	0.02	26.61	0.04	0.04	0.04	0.04	0.04	0.05	0.04	14.66	0.04	17.74

b. Liquefaction Factor of Safety Output Excel Results

Table 42 Calculation of factor of safety from output result of CSR at 0+630 & PGA 0.497g

4.9.3.9. Discussion on the CSR Output Results

4.9.3.9.1. Quake/W Result at 0+110.3

Compared to the ground acceleration of 0.497g, Yanda Dam's 0.197g (PGA) ground acceleration could be comparatively safer. However, table 37 highlights and makes clear that, based on the Quake/W analysis result of table 38, the project still appeared safe at the PGA point of 0.497g with some corrected measurements at the top layer and the following one. Ten meters has been the total depth measured in this stratum.

4.9.3.9.2. Quake/W Result at 0+327.5

Because of the result's summary of table 39, building the Yanda Dam with a ground acceleration of 0.197g (PGA) rather than 0.497g (in table 40) has been comparatively safer. It should be emphasized, therefore, that the Quake/W analysis result showed that there would not be liquefaction hazards at either PGA value along the designated annotation places from -240 up to 240 in the modeled image, or throughout the depth. Thus, in contrast to the ECDSWC engineering section, table 40 shows that the PGA value of 0.497g should be considered for further study since it could be safer for the Yanda dam project.

4.9.3.9.3. Quake/W result at 0+630

As a result of summarized table 41, building the Yanda Dam at 0.197g (PGA) as opposed to 0.497g (PGA) is safer overall. However, table 42 shows that, based on the Quake/W evaluated result, the project remained safe at the PGA value of 0.497g and did not require corrective action because the factor of safety has a greater value than one.

4.9.3.9.4. Soil Improvement to Mitigate Liquefaction Problem

Soil improvement involves altering soil characteristics by increasing density, reducing volume change variations, and controlling water action (Daryaei and Eslami, 2017). Popular deep soil treatment methods are deep vibro-compaction, deep dynamic compaction, deep soil mixing, jet grouting, and blast densification. Deep vibro techniques and grouting are expensive, while *deep dynamic compaction* is limited to shallow and middle depths. Blast densification is a fast, simple, and cost-effective method that requires less equipment and can be used in various

depths. Explosive Compaction (EC) or Blast Densification (BD) is a common deep soil improvement technique used to densify loose, saturated granular soils.

In this study, as discussed in the literature section, for such chainages of 0+110.3 with those identified hazard layers under the upstream with a depth of 0.5m, the appropriate ground improvement method is the removal and replacement method. On the other hand, for the downstream, with up to a depth of 10m from OGL, deep dynamic compaction (DDC), which is also known as heavy tamping or dynamic consolidation, has been chosen and recommended for remedial measures as soil compaction because it is less expensive and more widely used than other deep densification solutions. According to the Washington State Department of Transportation, the costs of DDC are up to 50% lower than other deep densification remedies and are around two-thirds that of stone columns.

On the other hand, as an alternative option, deep blasting compaction is also recommended, according to the discussion within the literature section. Blasting compaction is relatively more economical and uses less construction time. As stated in the Final Report by Robert E. Kimmerling (1994), the cost and construction duration had been estimated as follows;

Stone columns	Estimated time	5 to 6 months	Hence blasting was relatively better than the stone column methods
	Cost per m^3 of treated soil	\$10.15/m^3	
Blast Densification	Estimated time	3 weeks	
	Cost per m^3 of treated soil	\$3.48/m^3	

Table 43 Comparison of alternative ground improvement options with cost and duration

In soils with low relative density (RD 50–60%), EC performance is most effective. Several techniques are used to assess the effectiveness of EC. Typically, settlement, excess PWP, and CPT findings are reported following an explosion. To determine the degree of soil liquefaction, results from excess PWP are employed. The amount of strength that EC achieves is measured via CPT. The settlement also offers helpful information about the soil's density. Case histories indicate that the settlement was between 2-10% of the treated soil layer thickness. This range is large when compared to the settlement brought on by earthquakes, which is around 3-4%.
In addition, according to Shakeran et al. (2016), EC is most successful in fine-to-medium sands with a fine content of less than 5% that have been hydraulically deposited and have an initial relative density of between 30% and 60%. Additionally, it has been shown that EC is a useful technique for enhancing the density, stability, and resilience of the target soils. Based on the

justification of the above literature, the Yanda Dam has the following characteristics to determine whether the foundation along the chainage of 0+110.3 can be improved by deep blasting compaction or explosive compaction.

Parameters	Value	Tested Depth(m)	Bore hole
Fine content (%)	0.725	4.55-13	YDBH-3B
Relative density (%)	35-65	1.95-12.45	YDBH-4
Liquefiable depth(m)	10		

Table 44 Yanda Dam Soil characteristic

Therefore, for the downstream liquefaction problem of chainage 0+110.3, based on the above-tabulated data, the preferable option for ground improvement should be blasting compaction (explosive compaction) rather than the other options.

4.9.4. Effects of the Dam's Loaded Stress

The foundation has been put under stress by the embankment-filled material load, as shown by the modeling. The modeling's output showed that the maximum total stress has got equivalent results at both the PGA(0.197g) and PGA(0.497g) levels. Consequently, one of the two figures is shown here below.

One of the most significant and challenging topics in geotechnical earthquake engineering is liquefaction. Due to the location of the Yanda Project in a seismically dangerous area where embankment dams will be built, this problem will be crucial. Pore water pressure increases and gets close to total stress (load due to earthquake) during this event. As a result, the effective stress has been zero, the soil's shear strength is also zero, and the soil becomes unstable. The current study has used the Geo-Studio program to evaluate the susceptible failure of embankment dams caused by liquefiable soil layers in their foundations. The soil stiffness is generally a function of the stress state. As the confining stress increases, the soil stiffness increases.

The results of the subsequent numerical modeling, as displayed in the Excel spreadsheets and figures, indicated that the effective stress increased as the overburden stress increased and the layer depth moved downward, without taking into account the variety of different layered materials. Here the effective stress, which has been considered as mean effective stress,

is the difference between Mean Total Stress and Water Pressure. It should be noted that, since the project's foundation layers are different in soil type and thickness, the mean effective stresses have been going to be different values. For instance, at chainage of 0+110.3, the layer of GTL-5 is layered in three different depths from topsoil (OGL) which are at depths of 9m, 17.6m, and 29.8m, there mean effective stresses have been calculated as 99.4Kpa, 109.1Kpa and 117.7Kpa (average in the upstream side), 185.4Kpa, 227.3Kpa, and 248.5Kpa (in the downstream side) and 74.4KPa, 108.4KPa, and 120.3KPa (in the overall average column) respectively. Similarly, at the chainage and layers of GTL-4, which have similar material characteristics but different SPT results and different depths of 10m and 23.2m respectively, there mean effective stresses have been calculated and resulted as 133.9KPa and 202.8KPa respectively. The same is true in the chainages 0+327.5 and 0+630. The mean effective stresses in those chainages have been increased when moved to the depth downward. Since the stiffness of the GTL-5 layer is lower than the other alluvial foundation layers, its' mean effective stress has been lower than the others as shown in the following numerical calculation of tabulated Excel output results.

The Cyclic Stress Ratio (CSR) method is used to estimate the build-up of excess pore pressures during the shaking in an E.L. analysis. The principle is based on figuring out how many cycles at a specific amplitude of cyclic shear stress are necessary to trigger liquefaction. Dynamic shear stress divided by static effective overburden stress is used to calculate CSR.

4.9.4.1. Stress Distribution in Quak/W for Chainage 0+327.5

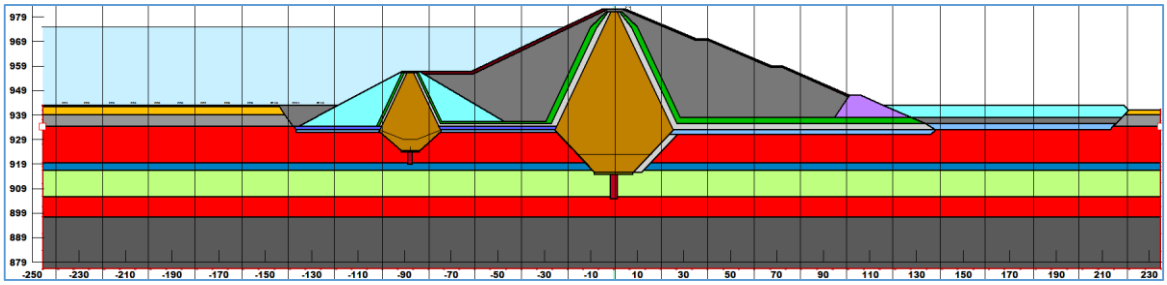

Figure 37 Yanda Dam & Foundation Cross Section at 0+327.5

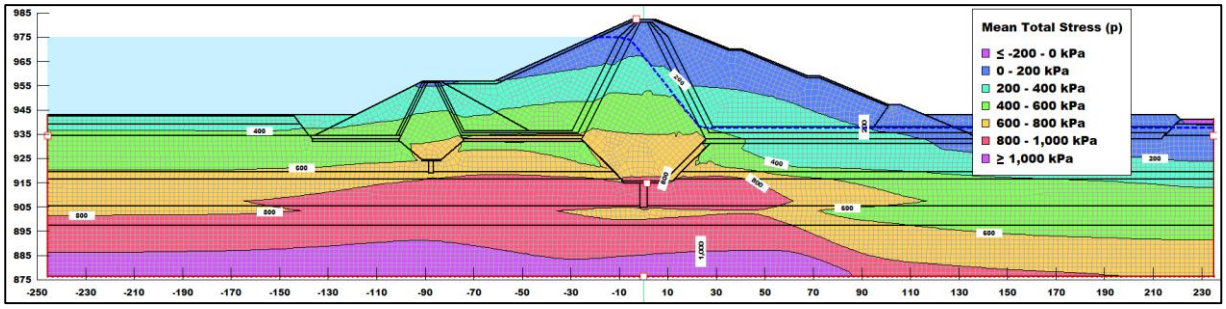

a. Mean Total Stress

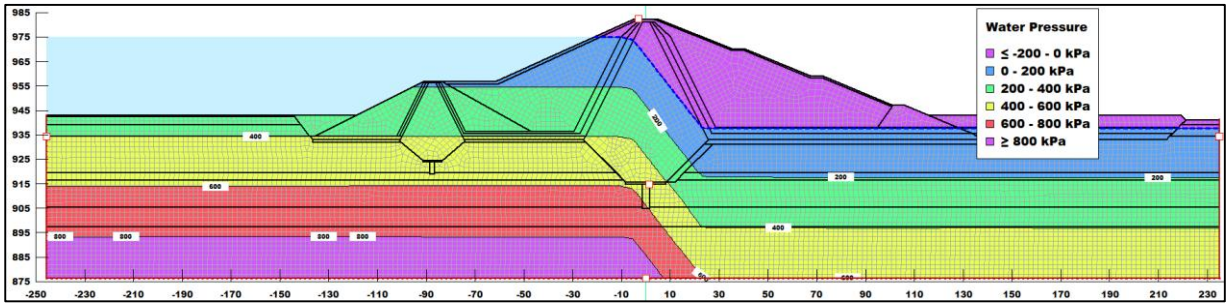

b. Water Pressure

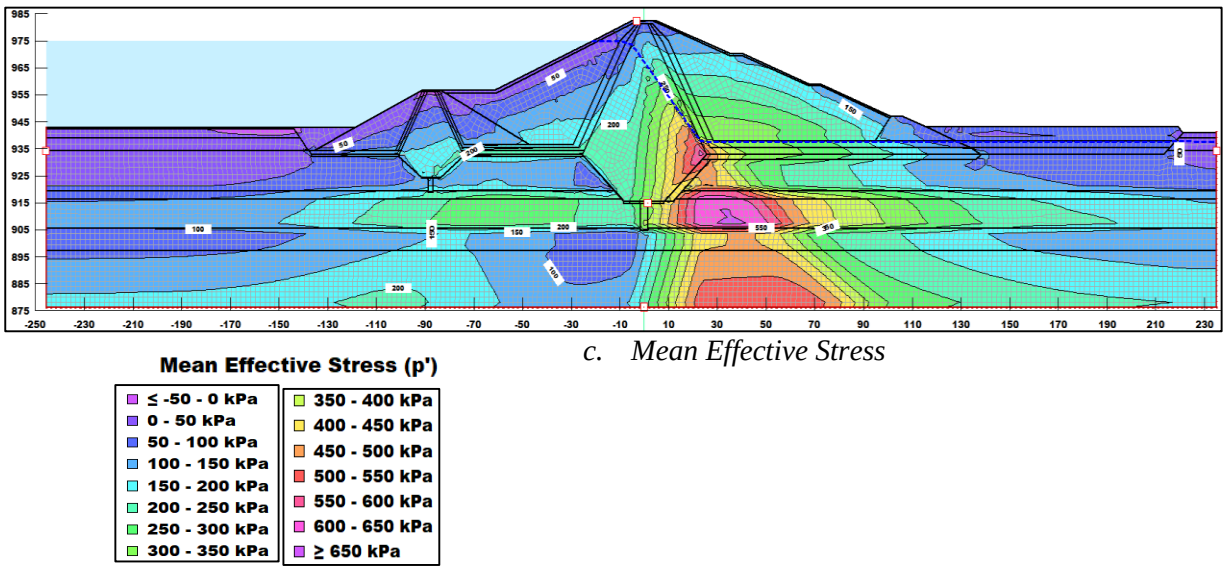

c. Mean Effective Stress

Figure 38 Total Stress, Water Pressure, and Effective Stress Distribution at 0+327.5

4.9.4.2. Computing Shear Strength using Excel Sheet at Chainage 0+327.5

In the following table, estimated values have been inputted from the final dynamic analyzed of 0+327.5 according to the above figures and the mean effective stress has been calculated from the parameters of mean total stress and water pressures

EFFECTIVE POREWATER DISTERBUTION UNDER THE DAM FOUNDATION AT 0+327.5																																			
LAYERs		ϕ	C	tan(ϕ)	Annotated chainage along Dam cross sectional		U/S FOUNDATION LAYERS															D/S FOUNDATION LAYERS													
					PARAMETERS	UNT	-240	-220	-200	-180	-160	-140	AVG	-120	-100	-80	-60	-40	-20	AVG	0	20	40	60	80	100	120	140	AVG	160	180	200	220	240	AVG
GTL-1	Topsoil: Silty Clay (CL)	20.5	27	0.3739	Mean Total Stress	KPa	345	344	342	339	344		343																					24	-25	-1
					Water Pressure		336	336	336	336	340		337																					-13	-3	-8
		$\sigma' = \sigma - u$			Mean Effective Stress		9	8	6	3	4		6																					37	-22	8
		$\tau = c + \sigma'_v \tan\emptyset$			Shear Strength		30	30	29	28	29		29																					41	19	30
GTL-4	Silty Sand (SM)	34	-	0.6745	Mean Total Stress	KPa	402	401	400	397	395	416	402																					69	36	53
					Water Pressure		376	376	376	376	376	379	376																					15	10	13
		$\sigma' = \sigma - u$			Mean Effective Stress		26	25	24	22	20	36	25																					55	25	40
		$\tau = \sigma'_v \tan\emptyset$			Shear Strength		17	17	16	15	13	24	17																					37	17	27
GTL-5	Coarse Gravel (GM)	32.49	-	0.6371	Mean Total Stress	KPa	522	521	522	524	527	538	526	563	553	625	633	610	570	592		601	479	368	354	319	255	229	372	220	213	203	209	202	209
					Water Pressure		483	483	484	485	461	484	480	483	468	496	462	483	504	483		180	124	123	141	141	123	121	136	121	121	121	139	138	128
		$\sigma' = \sigma - u$			Mean Effective Stress		39	39	38	39	66	55	46	80	84	129	172	126	66	109		421	356	245	213	178	132	108	236	98	91	83	70	64	81
		$\tau = \sigma'_v \tan\emptyset$			Shear Strength		25	25	24	25	42	35	29	51	54	82	109	80	42	70		268	227	156	136	114	84	69	150	63	58	53	44	41	52
GTL-3	Clayey Silt (MH):	33	-	0.6494	Mean Total Stress	KPa	671	672	673	677	688	715	683	754	785	827	858	842	808	812		837	833	629	587	525	460	415	612	392	380	366	343	336	363
					Water Pressure		574	574	574	545	545	574	564	545	574	574	545	574	545	559		233	191	189	189	189	188	188	195	188	187	187	187	187	187
		$\sigma' = \sigma - u$			Mean Effective Stress		98	98	99	132	143	141	119	209	211	253	313	268	263	253		604	643	440	398	336	272	227	417	204	193	179	156	149	176
		$\tau = \sigma'_v \tan\emptyset$			Shear Strength		63	64	65	86	93	92	77	136	137	164	203	174	171	164		392	417	286	258	219	176	147	271	133	125	116	101	97	114
GTL-4	Silty Sand (SM)	34.0	-	0.7	Mean Total Stress	KPa	742	743	744	749	761	787	754	823	870	910	925	906	877	885		902	913	756	661	608	547	503	699	478	456	443	424	416	444
					Water Pressure		629	629	629	629	630	630	629	630	643	644	645	643	642	641		297	278	276	275	274	259	273	276	270	261	261	252	250	259
		$\sigma' = \sigma - u$			Mean Effective Stress		113	113	115	119	131	157	125	192	228	266	280	263	235	244		605	635	481	386	334	288	230	423	208	195	182	171	166	184
		$\tau = \sigma'_v \tan\emptyset$			Shear Strength		76	76	78	81	88	106	84	130	154	179	189	178	158	165		408	429	324	260	225	194	155	285	140	131	123	115	112	124
*AVG = AVERAGE																																			

Table 45 Determination and comparison of effective stress and shear strength at 0+327.5

4.9.4.3. Stress Distribution in Quak/W for Chainage 0+110.3

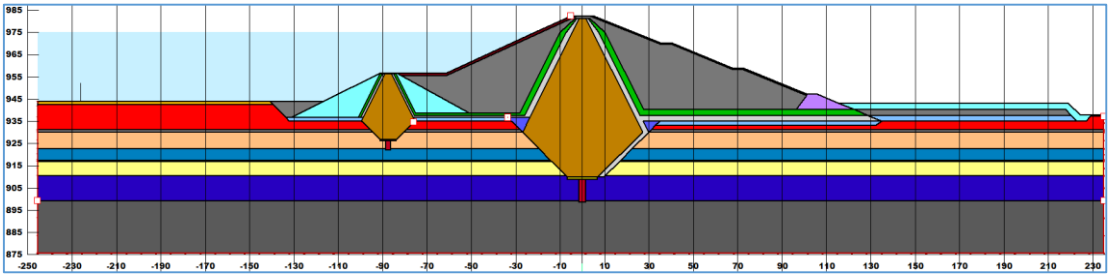

Figure 39 Yanda Dam & Foundation Cross Section at 0+110.3

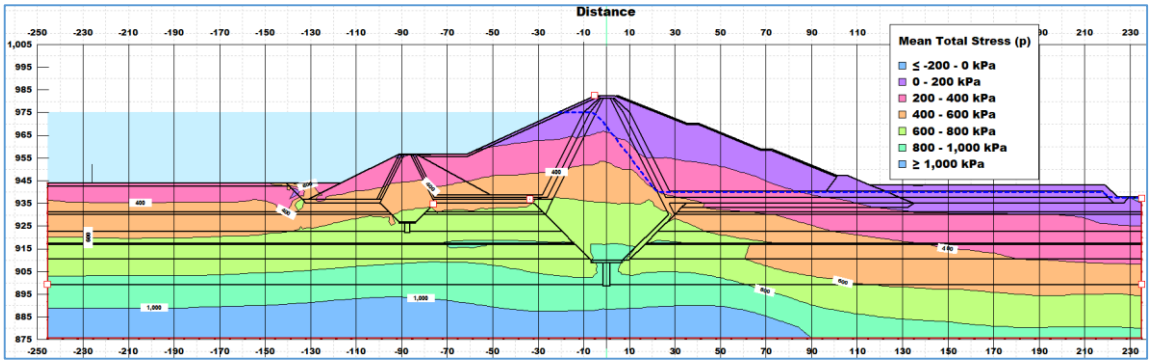

a. Mean Total Stress

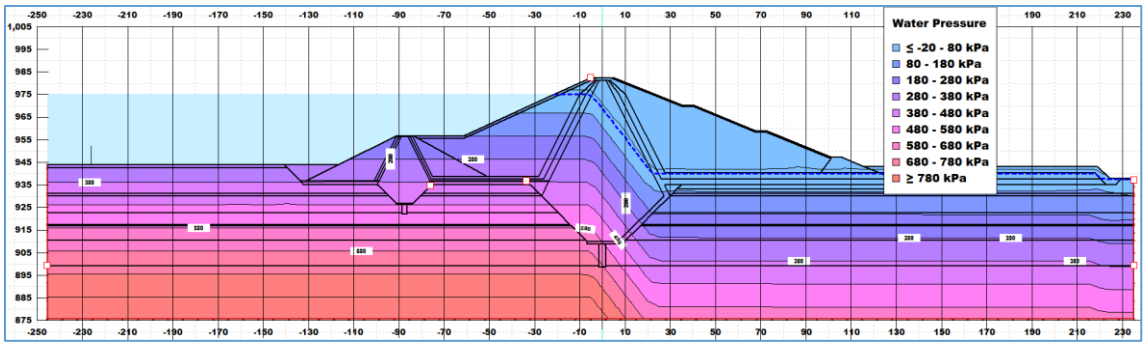

b. Water Pressure

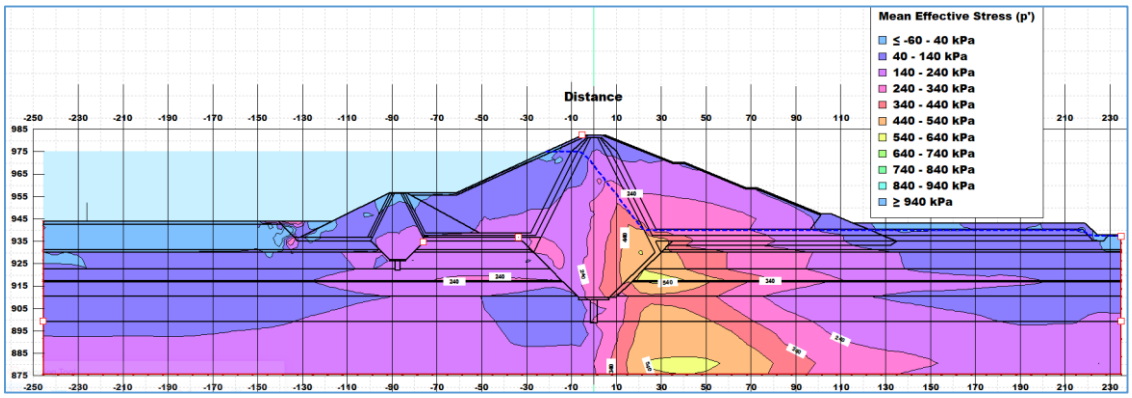

c. Mean Effective Stress

Figure 40 Total Stress, Water Pressure, and Effective Stress Distribution at 0+110.3

4.9.4.4. Computing Shear Strength using Excel Sheet at Chainage 0+110.3

In the following table, estimated values have been inputted from the final dynamic analysis of 0+110.3 according to the above figures and the mean effective stress has been calculated from the parameters of mean total stress and water pressures.

EFFECTIVE POREWATER DISTERBUTION UNDER THE DAM FOUNDATION AT 0+110.3

LAYERs		ϕ	C	tan(ϕ)	Annotated chainage along Dam cross sectional		U/S FOUNDATION LAYERS												D/S FOUNDATION LAYERS											
					PARAMETERS	UNT	-230	-210	-190	-170	-150	AVG	-130	-110	-90	-70	-50	-30	AVG	-10	10	30	50	70	90	110	130	AVG	150	170	190	210	230	AVG
GTL-1	Topsoil: Silty Clay (CL)	20.5	27	0.37	Mean Total Stress	KPa	312	310	311	307	281	304																				-55	-55
					Water Pressure		309	309	309	309	309	309																				-1	-1
		$\sigma' = \sigma - u$			Mean Effective Stress		3	1	2	-2	-28	-5																				-54	-54
		$\tau = C + \sigma'_v \tan\emptyset$			Shear Strength		28	27	28	26	17	25																				-20	-20
GTL-5	Coarse Gravel (GM)	33.5		0.66	Mean Total Stress	KPa	352	352	354	354	385	359	433	493		560	562	542	518				339	301	256	225	186	262	145	133	126	128	77	122
					Water Pressure		363	364	364	364	386	368	411	411		423	423	425	418				74	85	74	74	74	76	80	57	57	57	51	60
		$\sigma' = \sigma - u$			Mean Effective Stress		-11	-12	-11	-10	-2	-9	22	82		137	139	117	99				265	217	182	151	113	185	65	76	69	71	26	62
		$\tau = \sigma'_v \tan\emptyset$			Shear Strength		-7	-8	-7	-7	-1	-6	15	54		91	92	78	66				176	143	120	100	75	123	43	51	46	47	17	41
GTL-4	Silty Sand (SM)	34	-	0.67	Mean Total Stress	KPa	477	475	477	481	468	476	549	593		673	688	737	648				568	473	397	331	252	404	220	217	212	199	136	197
					Water Pressure		433	433	441	437	448	438	440	440		435	441	441	439				101	94	99	93	103	98	104	102	108	119	100	107
		$\sigma' = \sigma - u$			Mean Effective Stress		44	42	36	44	21	37	109	154		238	248	296	209				467	379	298	238	149	306	116	115	103	81	36	90
		$\tau = \sigma'_v \tan\emptyset$			Shear Strength		30	28	24	30	14	25	73	104		161	167	199	141				315	256	201	161	100	207	78	78	70	54	24	61
GTL-5	Coarse Gravel (GM)	33.5	-	0.66	Mean Total Stress	KPa	498	506	509	518	515	509	547	579	616	612	624	607	598			531	421	367	322	285	258	364	234	230	246	229	150	218
					Water Pressure		480	456	499	456	499	478	499	499	487	471	499	476	488			121	115	157	157	157	114	137	114	157	144	143	103	132
		$\sigma' = \sigma - u$			Mean Effective Stress		18	50	10	62	16	31	48	80	129	141	125	131	109			410	306	210	165	129	143	227	119	73	102	86	47	85
		$\tau = \sigma'_v \tan\emptyset$			Shear Strength		12	33	7	41	11	21	32	53	85	93	83	87	72			271	203	139	109	85	95	150	79	48	67	57	31	57
GTL-3	Clayey Silt (MH):	31.5	53.33	0.61	Mean Total Stress	KPa	614	612	615	626	632	620	673	718	765	787	815	806	761			802	697	603	522	449	400	579	371	362	351	321	302	341
					Water Pressure		554	554	526	526	554	543	555	526	529	555	527	555	541			187	186	214	214	213	184	200	213	213	184	184	159	190
		$\sigma' = \sigma - u$			Mean Effective Stress		60	58	89	100	77	77	119	192	236	232	288	251	219			616	511	389	308	236	216	379	158	149	167	138	143	151
		$\tau = C + \sigma'_v \tan\emptyset$			Shear Strength		90	89	108	115	101	100	126	171	198	195	230	207	188			431	367	292	242	198	186	286	150	145	156	138	141	146
GTL-4	Silty Sand (SM)	34	-	0.67	Mean Total Stress	KPa	649	649	651	662	685	659	705	752	790	835	851	831	794			799	738	641	558	485	435	610	409	402	391	362	338	381
					Water Pressure		566	566	566	570	567	567	567	571	571	572	568	571	570			232	232	231	230	229	229	230	228	228	228	228	202	223
		$\sigma' = \sigma - u$			Mean Effective Stress		83	82	85	92	118	92	139	181	219	263	283	259	224			567	507	411	328	256	206	379	181	174	163	134	136	158
		$\tau = \sigma'_v \tan\emptyset$			Shear Strength		56	55	57	62	80	62	93	122	148	178	191	175	151			383	342	277	222	173	139	256	122	117	110	91	91	106
GTL-5	Coarse Gravel (GM)	33.5	-	0.66	Mean Total Stress	KPa	655	654	655	665	680	662	704	726	747	765	745	709	733			649	630	509	463	418	386	509	379	375	368	352	323	360
					Water Pressure		584	621	584	621	621	606	615	615	615	615	615	615	615			279	243	242	279	242	279	261	279	279	242	279	254	266
		$\sigma' = \sigma - u$			Mean Effective Stress		71	33	71	44	59	55	89	111	132	150	131	94	118			369	387	268	184	175	107	249	100	97	126	73	69	93
		$\tau = \sigma'_v \tan\emptyset$			Excess PWP		47	22	47	29	39	37	59	74	87	99	86	62	78			244	256	177	122	116	71	164	66	64	83	49	46	62

*AVG = AVERAGE

Table 46 Determination and comparison of effective stress and shear strength at 0+110.3

4.9.4.5. Stress Distribution in Quak/W for Chainage 0+630

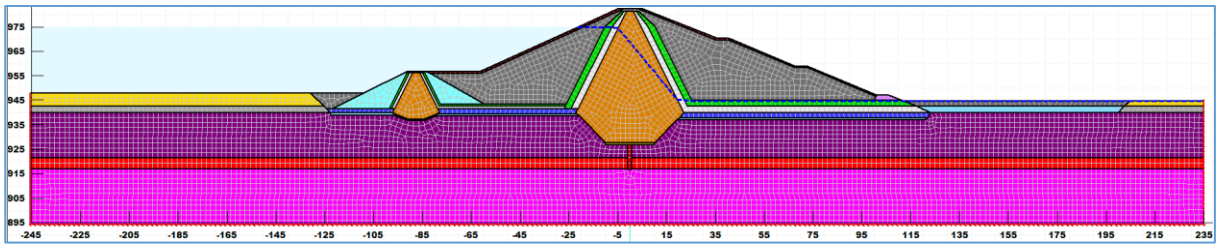

Figure 41 Yanda Dam & Foundation Cross Section at 0+630

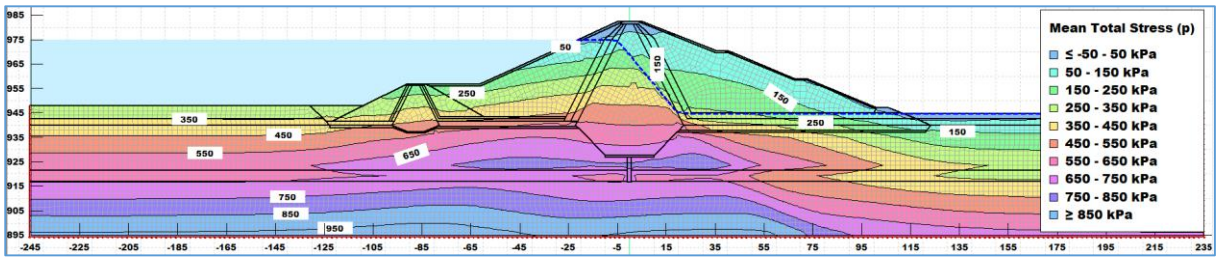

a. Mean Total Stress

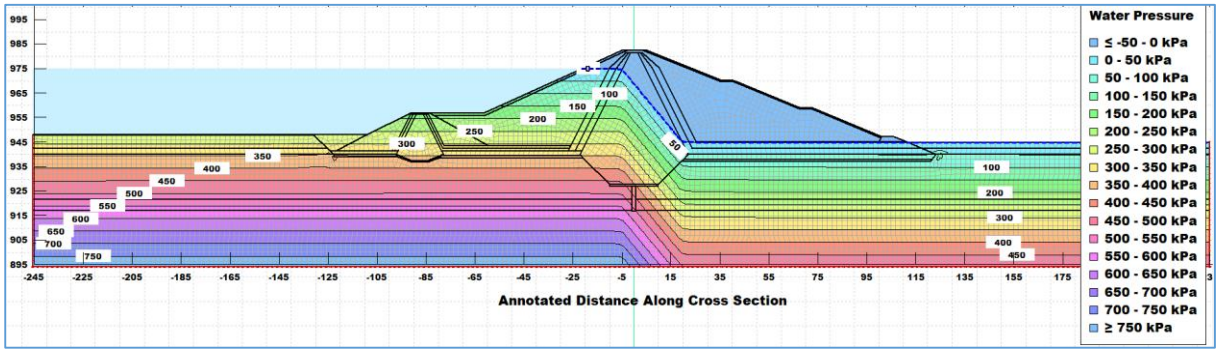

b. Water Pressure

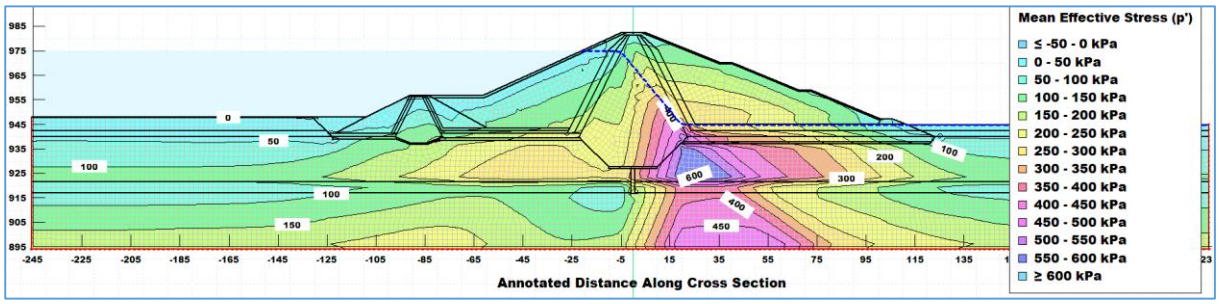

c. Mean Effective Stress

Figure 42 Total Stress, Water Pressure, and Effective Stress Distribution at 0+630

4.9.4.6. Computing Shear Strength using Excel Sheet at Chainage 0+630

In the following table, estimated values have been inputted from the final dynamic analysis of 0+630 according to the above figures and the mean effective stress has been calculated from the parameters of mean total stress and water pressure.

EFFECTIVE POREWATER DISTERBUTION UNDER THE DAM FOUNDATION AT 0+630

LAYERs		ϕ	C	tan(ϕ)	Annotated chainage along Dam cross sectional		U/S FOUNDATION LAYERS														D/S FOUNDATION LAYERS													
					PARAMETERS	UNT	-250	-230	-210	-190	-170	-150	-130	AVG	-110	-90	-70	-50	-30	-10	AVG	0	10	30	50	70	90	110	130	AVG	150	170	190	210	230	AVG
GTL-1	Topsoil: Silty Clay (CL)	20.50	27.00	0.37	Mean Total Stress	KPa	292	323	296	297	322	293	329	306																			35	35	35.11
					Water Pressure		280	303	286	286	303	286	303	291																			23	23	23.46
		$\sigma' = \sigma - u$			Mean Effective Stress		12	20	10	11	20	7	26	15																			12	12	11.65
		$\tau = c + \sigma'_v \tan \emptyset$			Shear Strength		31	35	31	31	34	30	37	33																			31	31	31.36
GTL-4	Silty Sand (SM)	34.00	-	0.67	Mean Total Stress	KPa	350	382	350	350	350	383	393	357																			73	70	71.59
					Water Pressure		319	343	319	319	319	344	353	324																			48	48	47.84
		$\sigma' = \sigma - u$			Mean Effective Stress		31	39	31	31	31	39	40	35																			26	22	23.75
		$\tau = \sigma'_v \tan \emptyset$			Shear Strength		21	26	21	21	21	26	27	23																			17	17	17.22
GTL-2	Silty Clay (CL) intermediate dispersive	20.45	35.63	0.37	Mean Total Stress	Kpa	505	504	505	505	506	510	563	505	553	628	671	679	681	735	658		779	715	544	504	395	307	276	503	223	218	213	198	194	209
					Water Pressure		425	424	425	425	425	425	446	425	415	443	441	421	422	488	438		320	158	140	156	139	138	151	172	128	128	128	128	130	128
		$\sigma' = \sigma - u$			Mean Effective Stress		80	80	80	80	81	85	116	86	138	185	230	258	259	247	220		459	557	403	348	256	168	125	331	94	90	85	70	63	81
		$\tau = c + \sigma'_v \tan \emptyset$			Shear Strength		66	66	66	65	66	67	79	68	52	69	86	97	97	92	82		171	208	151	130	96	63	47	124	71	69	67	62	59	66
GTL-5	Coarse Gravel (GM)	32.49	-	0.64	Mean Total Stress	KPa	618	619	619	618	618	622	634	618	653	671	686	684	656	624	662		624	641	529	447	408	369	346	481	336	330	324	316	315	324
					Water Pressure		546	546	546	546	547	547	547	546	546	547	546	546	546	546	546		354	252	251	251	251	251	251	266	251	251	251	251	251	251
		$\sigma' = \sigma - u$			Mean Effective Stress		71	72	72	71	71	75	87	74	107	124	140	137	109	78	116		270	389	278	196	158	118	95	215	84	79	73	65	64	73
		$\tau = \sigma'_v \tan \emptyset$			Shear Strength		45	46	46	45	45	48	55	47	68	79	89	87	70	50	74		172	248	177	125	100	75	60	137	54	50	47	41	40	46

*AVG = AVERAGE

Table 47 Determination and comparison of effective stress and shear strength at 0+630

4.9.4.7. Demonstration of Effective Stress and Shear Strength using Excel Graph

To more easily visualize the stress distribution, the above tabulated calculated data to compare and understand the relationship between effective stress, shear strength, and CSR.

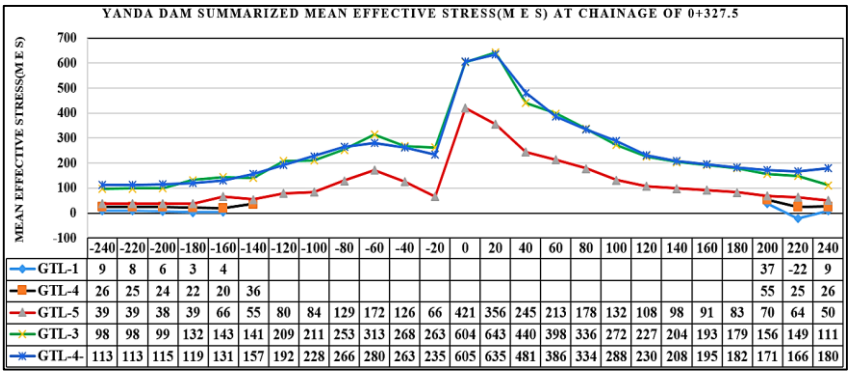

	-240	-220	-200	-180	-160	-140	-120	-100	-80	-60	-40	-20	0	20	40	60	80	100	120	140	160	180	200	220	240
GTL-1	9	8	6	3	4																		37	-22	9
GTL-4	26	25	24	22	20	36																	55	25	26
GTL-5	39	39	38	39	66	55	80	84	129	172	126	66	421	356	245	213	178	132	108	98	91	83	70	64	50
GTL-3	98	98	99	132	143	141	209	211	253	313	268	263	604	643	440	398	336	272	227	204	193	179	156	149	111
GTL-4-	113	113	115	119	131	157	192	228	266	280	263	235	605	635	481	386	334	288	230	208	195	182	171	166	180

a. Mean Effective Stress Graphed with Excel

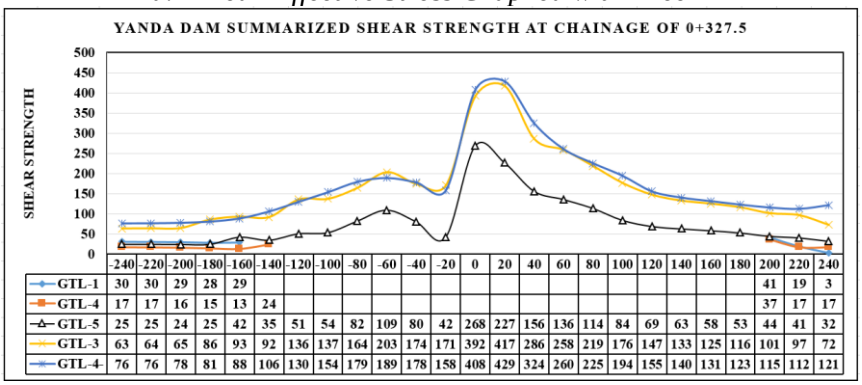

	-240	-220	-200	-180	-160	-140	-120	-100	-80	-60	-40	-20	0	20	40	60	80	100	120	140	160	180	200	220	240
GTL-1	30	30	29	28	29																		41	19	3
GTL-4	17	17	16	15	13	24																	37	17	17
GTL-5	25	25	24	25	42	35	51	54	82	109	80	42	268	227	156	136	114	84	69	63	58	53	44	41	32
GTL-3	63	64	65	86	93	92	136	137	164	203	174	171	392	417	286	258	219	176	147	133	125	116	101	97	72
GTL-4-	76	76	78	81	88	106	130	154	179	189	178	158	408	429	324	260	225	194	155	140	131	123	115	112	121

b. Shear Strength Graphed with Excel

Graph 12 Comparison of MES and Shear Strength with Excel Graph

Therefore, according to the above figures, the graphs have been compared both mean effective stress and shear strength. The graphs drawing showed that both parameters are leaner and parallel. Hence, particularly in cohesion-less soil, shear strength is directly proportional to mean effective stress. This fact has been similarly shown in the next two chainages 0+110.3 and 0+630.

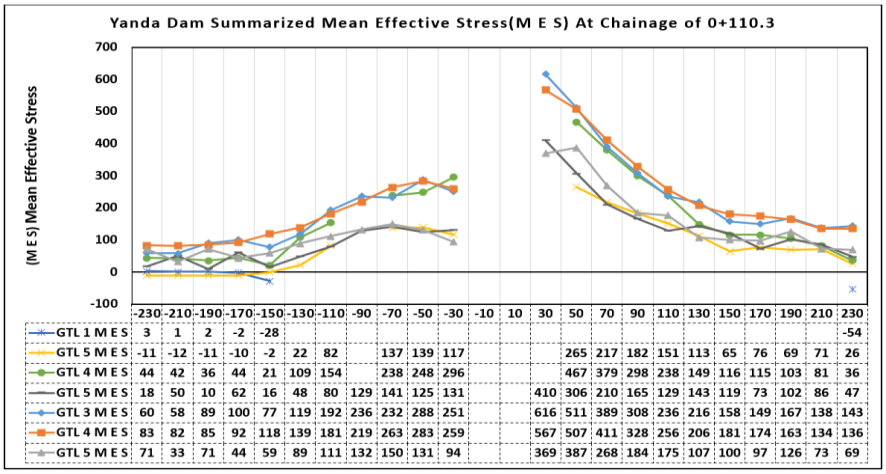

	-230	-210	-190	-170	-150	-130	-110	-90	-70	-50	-30	-10	10	30	50	70	90	110	130	150	170	190	210	230
GTL 1 M E S	3	1	2	-2	-28																			-54
GTL 5 M E S	-11	-12	-11	-10	-2	22	82		137	139	117				265	217	182	151	113	65	76	69	71	26
GTL 4 M E S	44	42	36	44	21	109	154		238	248	296				467	379	298	238	149	116	115	103	81	36
GTL 5 M E S	18	50	10	62	16	48	80	129	141	125	131			410	306	210	165	129	143	119	73	102	86	47
GTL 3 M E S	60	58	89	100	77	119	192	236	232	288	251			616	511	389	308	236	216	158	149	167	138	143
GTL 4 M E S	83	82	85	92	118	139	181	219	263	283	259			567	507	411	328	256	206	181	174	163	134	136
GTL 5 M E S	71	33	71	44	59	89	111	132	150	131	94			369	387	268	184	175	107	100	97	126	73	69

Graph 13 Summarized MES with Excel Graph for 0+110.3

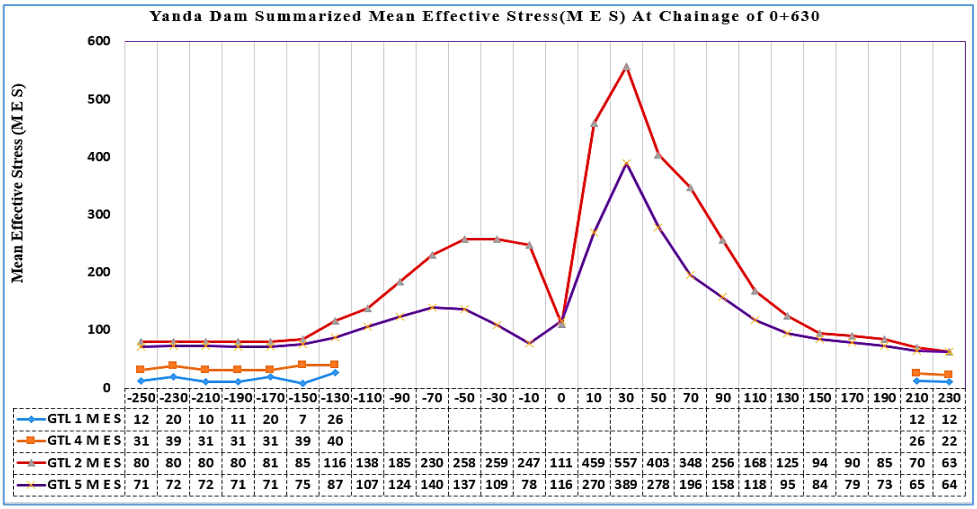

	-250	-230	-210	-190	-170	-150	-130	-110	-90	-70	-50	-30	-10	0	10	30	50	70	90	110	130	150	170	190	210	230
GTL 1 M E S	12	20	10	11	20	7	26																		12	12
GTL 4 M E S	31	39	31	31	31	39	40																		26	22
GTL 2 M E S	80	80	80	80	81	85	116	138	185	230	258	259	247	111	459	557	403	348	256	168	125	94	90	85	70	63
GTL 5 M E S	71	72	72	71	71	75	87	107	124	140	137	109	78	116	270	389	278	196	158	118	95	84	79	73	65	64

Graph 14 Summarized MES with Excel Graph for 0+630

4.9.5. Yanda Dam's Ground Response Analysis Result

To analyze the ground response as a result of the input value of the earthquake record, one of the key goals of employing Quake/W analysis is to look at the earthquake record. Comparing values at historical locations is one of the finest techniques to examine a dynamic reaction. One of those history points was at the fixed base, while the other was at the dam crest, according to this research on Yanda Dam. An exact reproduction of the input acceleration time history is represented by the acceleration at the base history point. Additionally, the base acceleration as well as the calculated relative acceleration by the FE are provided at the history point of the crest.

There are numerous ways to display and view the results, as was previously mentioned for the static analysis. This is especially true for the dynamic portion of the analysis. Here, only a small portion of what is possible and accessible will be discussed. At the top of the dam and the foundation of the problem, it would be established the History Points and generated graphs specific to the History Points using the Draw Graph command. For instance, it is easy to make graphs of x-accelerations vs time for both the crest and the base and plot them simultaneously (Graph 15)

According to the literature discussion on ground response, the dynamic analysis of the Yanda Dam considers it to be a non-linear elastic-plastic analysis due to the various filled materials and alluvial material in the dam body and foundation. Moustafa (2012) states that strong

earthquakes are more likely to change material behavior from elastic to plastic compared to weak earthquakes. Therefore, since the earthquake acceleration used in this study is strong (M = 6.3 and PGA = 0.497), a plasticity analysis will be conducted to investigate the seismic response of the Yanda earth-fill dams. Consequently, the dam's acceleration (ground response) decreases from the base to the crest.

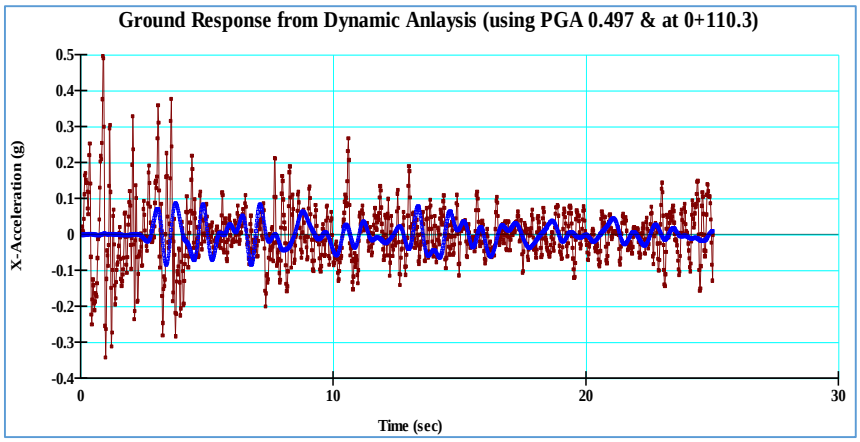	At crest peak value is 0.0876g at 3.3.72sec & At base peak value is 0.497g at 0.86sec *The Blue line is Crest Ground Response, and The Dark Brown line is Base Ground Response*
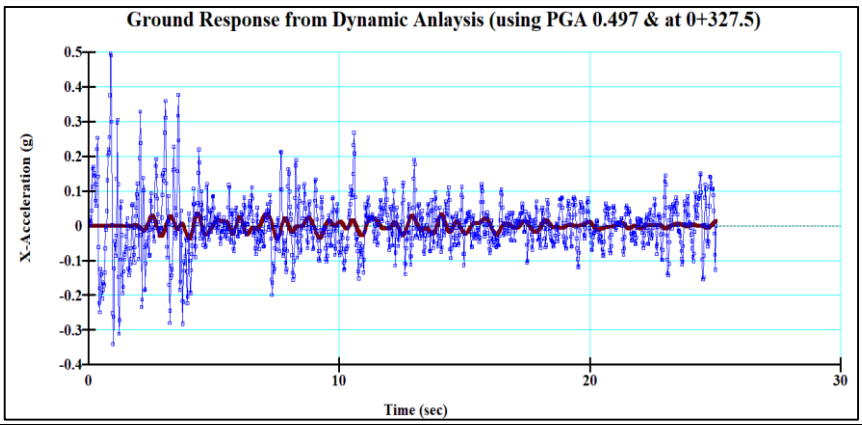	At crest peak value is 0.0346g at 4.36sec and At base peak value is 0.497g at 0.86sec. *The Blue line is Base Ground Response, and The Dark Brown line is Crest Ground Response*
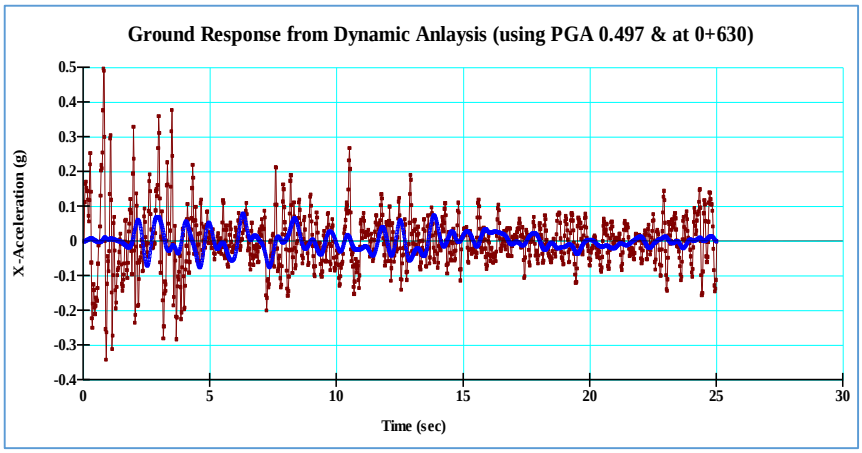	At crest peak value is 0.0796g at 6.3sec and At base peak value is 0.497g at 0.86sec. *The Blue line is Crest Ground Response, and The Dark Brown line is Base Ground Response.*

Graph 15 Comparison of Ground Response at the Crest with Base for 0+110.3, 0+327.5, and 0+630

4.9.6. Settlement Result and Allowance of Yanda Dam

The output results of the dynamic analysis of Yanda Dam showed that the settlement ranged from -0.18m to 0.08m, -0.12m to 0.01m, and -0.12m to 0.02m at chainages of 0+110.3, 0+327.5, and 0+630, respectively.

As stated in the Indian Standard (IS 8826-1978), to account for post-construction vertical deformation due to compression and settling of the embankment and foundation, a building should increase the dam's crest above the top level. The additional height is created by a longitudinal crest that ranges from zero at the abutments to a maximum in the center of the gorge. The additional height should compensate for fill material compression, which generally accounts for 0.2% to 0.4% of embankments and rock fill dams. Rock fill that has been dumped might distort more severely. For foundation settling and embankment compression in earth and rock fill dams, a provision of 1% to 2% of the embankment height above the top level can be used.

4.9.6.1. Settlement analysis at 0+110.3 using the PGA of 0.497g

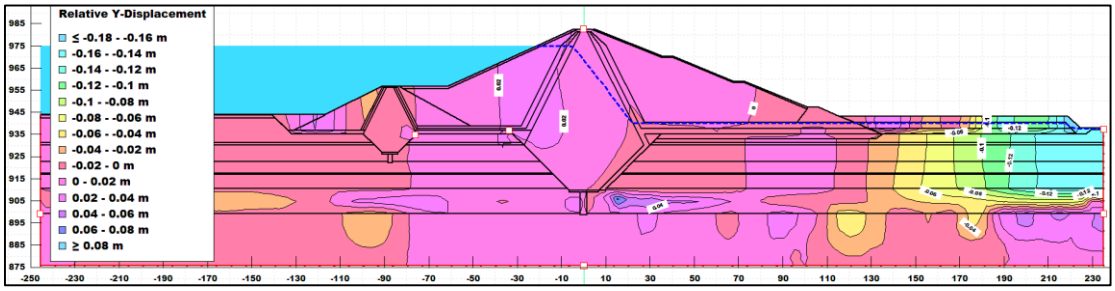

Figure 43 Quak/W output result of Vertical Settlement with Counters

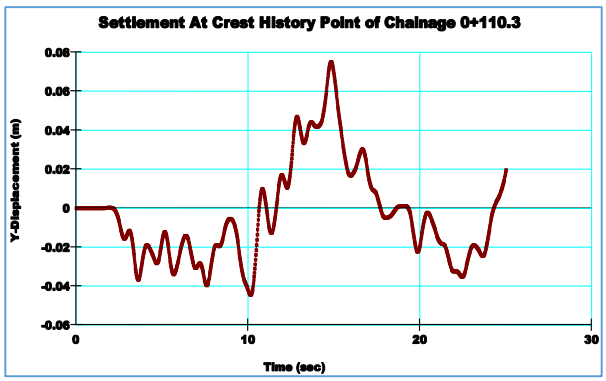

a. *Relative Vertical settlement*

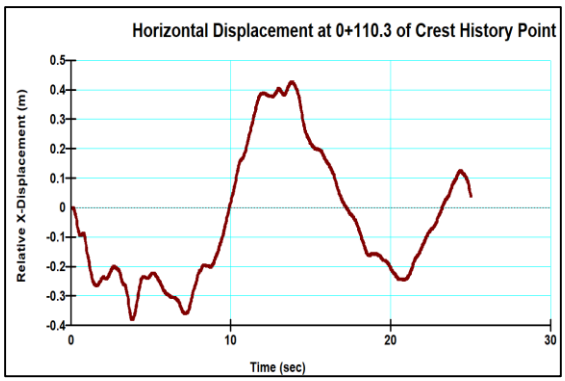

b. *Relative Horizontal settlement*

Graph 16 Relative Vertical and Horizontal Settlement at 0+110.3

4.9.6.2. Settlement analysis at 0+327.5 using PGA of 0.497g

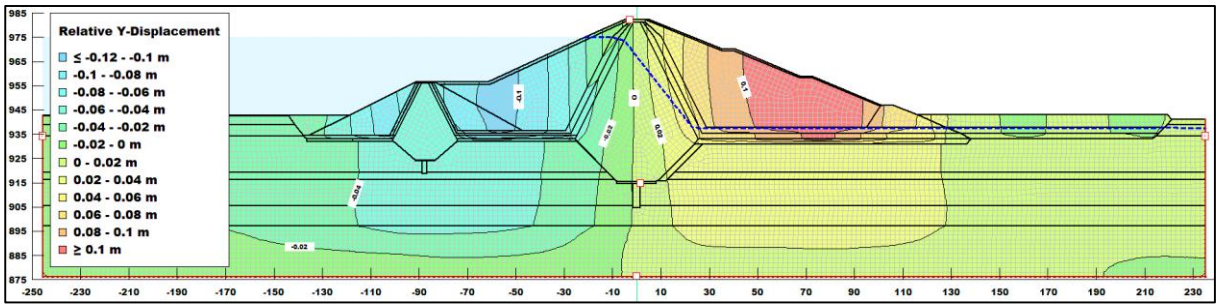

Figure 44 Quak/W output result of Settlement with Counters for 0+327.5

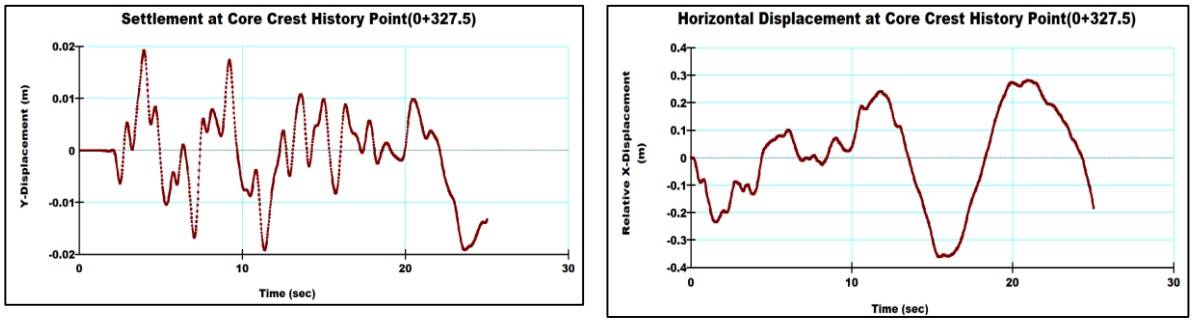

a. *Relative Vertical settlement* *b. Relative Horizontal settlement*

Graph 17 Relative Vertical and Horizontal Settlement at 0+327.5

4.9.6.3. Settlement analysis at 0+630 using PGA of 0.497g

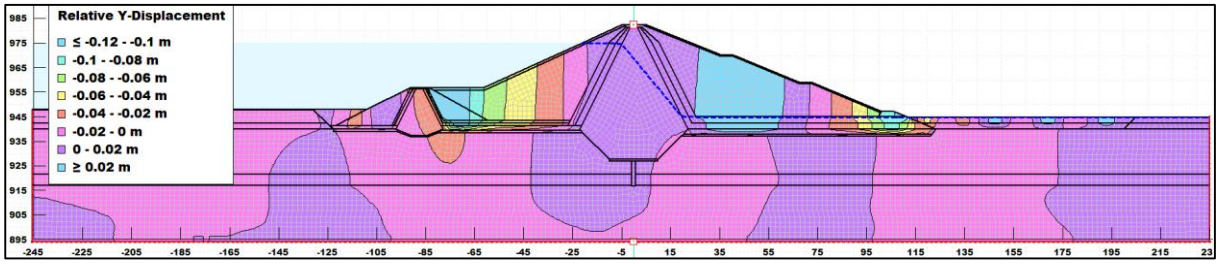

Figure 45 Quake/W output result of Settlement with Counters Display for 0+630

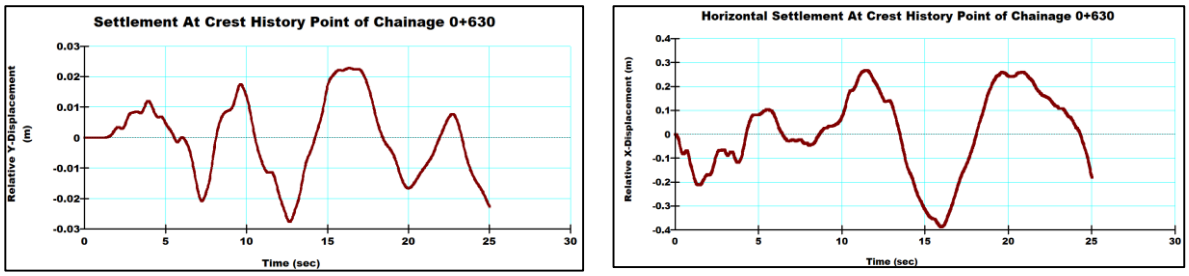

a. *Relative Vertical settlement* b. *Relative Horizontal settlement*

Graph 18 Relative Vertical and Horizontal Settlement at 0+630

4.9.7. Slope Stability

4.9.7.1. U/S and D/S Slope Stability analysis at 0+327.5 using PGA of 0.497g

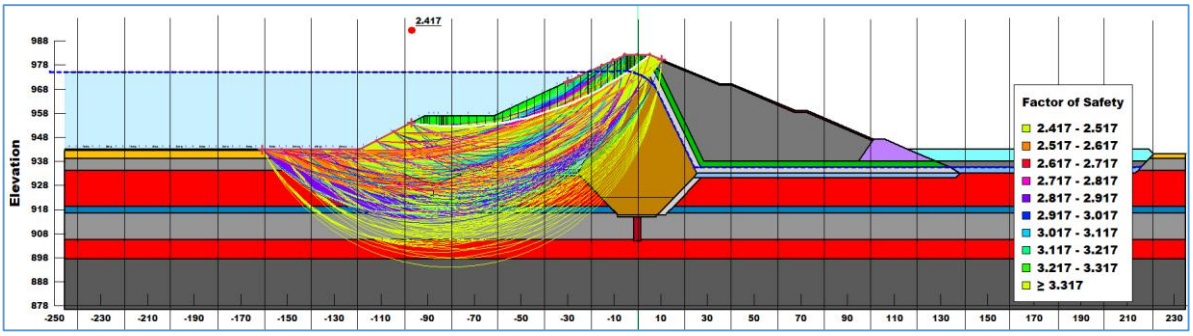

Figure 46 U/S Slope Stability -The critical Safety factor value is 2.417. So the slope stability is safe

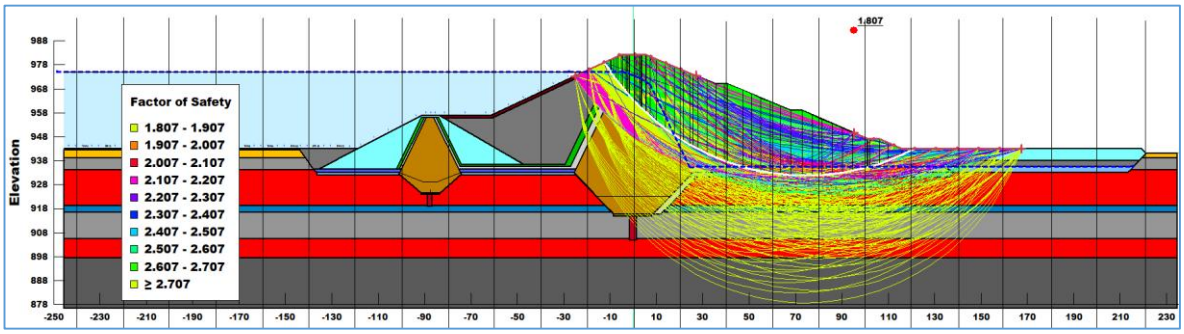

Figure 47 D/S Slope Stability - The critical Safety factor value is 1.807. So the slope stability is safe.

4.9.7.2. U/S and D/S Slope Stability analysis at 0+110.3 using PGA of 0.497g

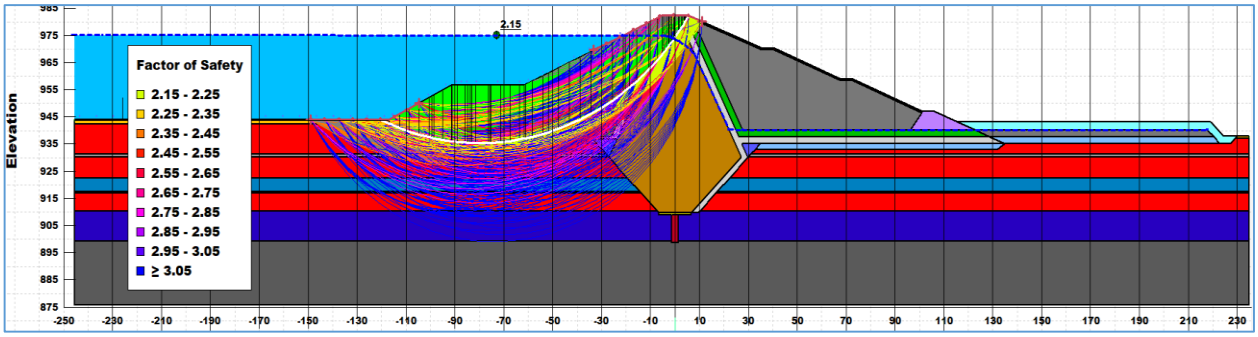

Figure 48 U/S Slope Stability - The critical FoS value is 2.15. So the slope stability is safe.

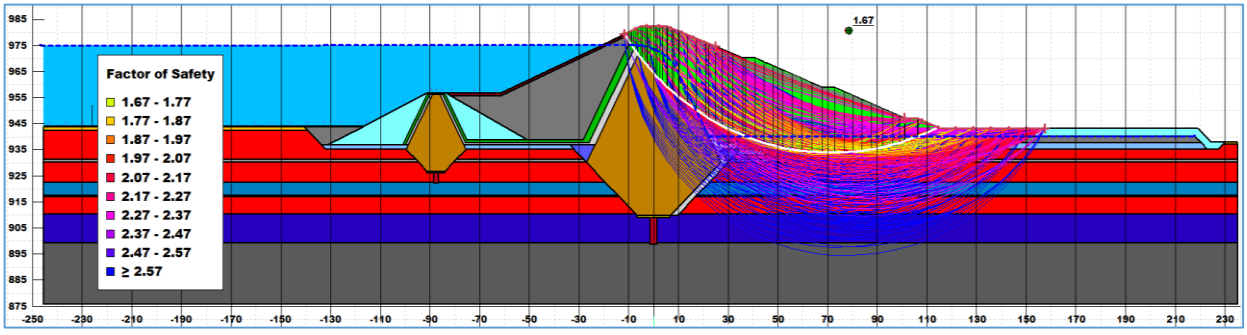

Figure 49 D/S Slope Stability - The critical Safety factor value is 1.67. So the slope stability is safe.

4.9.7.3. U/S and D/S Slope Stability analysis at 0+630 using PGA of 0.497g

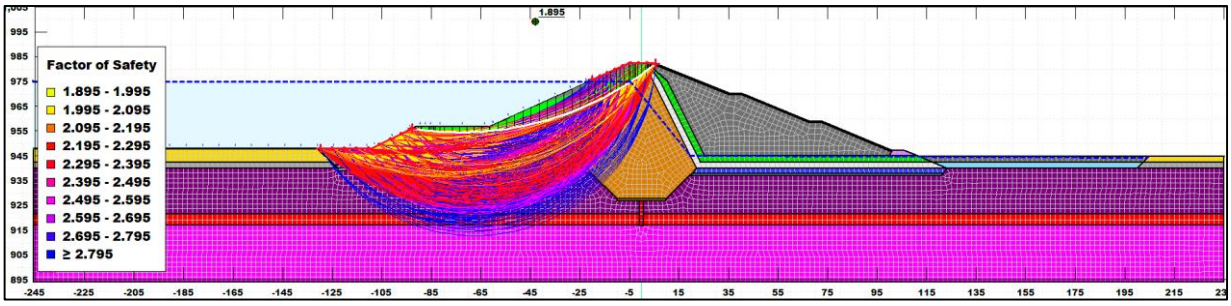

Figure 50 U/S Slope Stability - The critical FoS value is 1.895. So the slope stability is safe.

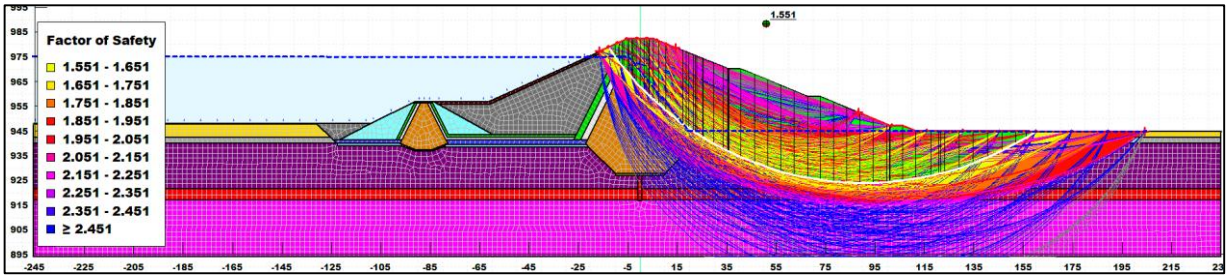

Figure 51 D/S Slope Stability - The critical FoS value is 1.551. So the slope stability is safe

4.9.7.4. Summary of the Slope Stability Analysis

The above figures showed that the critical slope stability factors of safety have been valued as 2.417, 2.15, and 1.895 for the upstream side of the dam at chainages of 0+327.5, 0+110.3, and 0+630 respectively. On the other hand, they have been valued as 1.807, 1.67, and 1.551 for the downstream side of the dam at chainages of 0+327.5, 0+110.3, and 0+630 respectively. Therefore, since those values of the safety factor have been estimated under the peak ground acceleration of 0.497g and the FoS values are more than the standard of 1.1, the dam is safe under the consideration of slope stability.

5. CONCLUSION AND RECOMMENDATION

5.1. Conclusion and

Water for irrigation over 5,500 hectares is intended to be stored at the Yanda Dam, a large embankment dam on the Yanda River. The alluvium foundation beneath the dam seat is mostly made up of loose sand and silty sand soils, according to the analysis of the geotechnical in-situ test and ensuing laboratory tests. Based on the evaluation of liquefaction susceptibility based on grain size distribution and the analysis (by means of both empirical and numerical approaches) of the data using Quake/W and LiqiT software, the foundation has been deemed vulnerable to liquefaction and piping. The research evaluated the dam's vulnerability to these risks and recommended corrective actions.

For piping mitigation, the study recommends extending the clay core key trench to the required depth and installing a soil-bentonite slurry cutoff wall. An upstream blanket is not necessary due to siltation in the upstream top-deposited layer. For liquefaction mitigation, deep blasting compaction is recommended due to its cost-effectiveness and local availability.

In addition, the dam's analysis has taken into account the linear elastic-plastic behavior of the soil under both static and dynamic circumstances. The evaluation's output could come in the form of charts or numbers. To reduce foundation piping, excessive seepage prevention measures would be implemented across the depth of the studied alluvial soil layers.

For the dam cross-section of chainage 0+110.3, Seven options have been analyzed with different means of protection techniques. From those options, the seventh option in the list (Option 7) with the flow path of 365.58m and flow flux amount of 4.84*e-09 m3/sec/m2 has been selected. The selected option has the extending main dam and coffer dam clay-filled cutoff up to the elevation of 910m and 927m respectively, soil-bentonite slurry with a depth of 10 meters for the main dam and 4 meters for the coffer dam is conducted without applying the protection mechanism of u/s blanket.

For the dam cross-section of chainage 0+327.5, Seven options have been analyzed with different means of protection techniques. From those options, the seventh option in the list (Option-7) with a flow path of 395.88 m and flow flux amount of 2.33*e-10 m3/sec/m2 has been selected. For this alternative, a 10 m and a 5 m layer of soil bentonite slurry would be laid

down below the extended complete cutoff of the main dam and the coffer dam, respectively. The extra depth cutoff would be also extended up to 916.5 m a.s.l and 924.5 m a.s.l dawn of the foundation for the main dam and coffer dam, respectively.

For the dam cross-section of chainage 0+630, Six options have been analyzed with different means of protection techniques. From those options, the sixth option in the list (Option-6) with a flow path of 343.62m and flow flux amount of 4.21e-09 m3/sec/m2 has been selected. Without applying an upstream blanket and using GC material under the downstream main dam shoulder, the extra complete cutoff would be extended up to the depth of 922.39m a.s.l. and installing a 10m soil-bentonite slurry wall below the complete cutoff of the main dam.

In sum, the performance of selected analyzed remedy options is summarized as follows in the matter of water flux.

Analyzed Chainages	Comparison of Selected Remedial Measures' Performance of Water Flux Reduction (%)		Description
	with applying only U/S Blanket	with Base Case (Not applying any Remedial Measures	
0+110.3	51.3	59	The analyzed and selected remedy of ***Option-7*** is ***51.3*** % better than that of original design of ***Option-2*** *and also* ***59.0*** % more effective than the ***Option-1*** *(without any Remedial Measures).*
0+327.5	90.2	91.7	The analyzed and selected remedy of ***Option-7*** is ***90.2*** % better than that of original design of ***Option-2*** *and* ***91.7*** % more effective than the ***Option-1.*** *(without any Remedial Measures).*
0+630	20.6	21.24	The analyzed and selected remedy of ***Option-6*** is ***20.6*** % better than that of original design of ***Option-2.*** and **21.24** % better than of ***Option-1*** *(without any Remedial Measures).*

*"*Original Design" means actual design data that taken from the institute of ECDSWC*

Table 48 Comparison of selected remedy option with Other Options

In general, remedial measures used for the prevention of piping have been adapted to extended clay core key trench up to the required depth and soil-bentonite slurry cutoff for those three cross sections (0+110.3, 0+327.5 and 0+630) rather than an upstream blanket. According to the U.S. Army Engineer Division, the Ohio River in 1945, since the Yanda upstream top deposited layer has siltation over time and has a tendency to reduce under seepage, the proposed upstream blanket has not been necessary to use as the remedial measure for prevention of piping.

Based on cost-effectiveness, speedy covering of a large area through compaction, and accessibility in the area, the four solutions that were evaluated were deep dynamic compaction,

deep blasting compaction, stone columns, and taking out and replacing, blasting, and dynamic compaction.

From each soil layer's CSR values along the annotated cross-section, the output results of liquefaction's safety factor were calculated using the Quake/W numerical analysis. These findings were then manually entered into the Excel sheet in tabular form. Likewise, the annotated cross-section of the dam has been manually filled in for each layer and pointing node, and the mean total stress, water pressure, mean effective stress, and shear strength have all been taken from the Quake/W result information.

According to the general output results of the factor of safety with the PGA value of 0.497g, the risk of liquefaction would exist at the chainage of 0+110.3 in the most downstream part of the upper three layers up to the depth of 10 meters from OGL. The liquefaction graph output result showed that the risk around the extended toe drain is about 240 meters from the center of the core. The rest of the dam's cross sections have been shown to be safe and free from liquefaction hazards. Therefore, the remedial solution for that liquefied part of the dam at 0+110.3 has been ground improvement, and the mechanism has been densification of the soil's layer. Then, from those mechanisms, deep blasting compaction has been selected as the last remedial solution.

5.2. Recommendations

- Taking into account the findings of this research, if a selected site for dam construction is prone to liquefaction, with detailed modeling and analysis, engineers can make an economic project by keeping alluvium beneath the dam instead of excavating or rejecting the site.
- Based on the information that was available from the conclusions of the geotechnical research, the recommended foundation remedial measures were completed. However, further verification during design and construction by adapting additional geotechnical and laboratory tests is necessary.
- To make the dam cost-effective, and since the foundation is made of loose alluvial deposits, the foundation condition must be closely monitored and authorized throughout excavation. The appropriateness of the material dug for dam fill must also be taken into account.

5.3. Limitations to doing Yanda Dam analysis

The following limitations should be considered when interpreting the results of this study:
Some of the data is limited and insufficient for a comprehensive advanced numerical analysis. Although some of the materials' strengths (c and Ø) were known, elastic (ρ, v, G_{max}) characteristics and compressibility data were not provided. The permeability of the materials and the hydraulic conductivities at a certain depth of the foundation layer were also unknown. This made it difficult to accurately assess the liquefaction potential of the foundation. As a result, the author has employed typical values of the materials' permeability that have been accepted by various standards.

The engineering design team used PGA data, but the geotechnical section provided different values. The engineering team claimed the geotechnical section's higher PGA value would make dam fallout unfeasible or economical. The geotechnical section argued the PGA value should be used for design purposes, as it was conducted by AAU and Prof. Ataly. To analyze the objectives, the dam was modeled using both PGA values, 0.197g, and 0.497g, to understand their justifications.

Despite these limitations, the study provides a valuable assessment of the risks of seepage, liquefaction, and piping in the Yonda Dam foundation. The recommended remedial measures are based on the best available data and should help mitigate these risks.

5.4. Validations of the Results

- **Actual** and **reliable data** (from the well-known ECDSWC in Ethiopia)
- Remedial measures have been **compared with the original, Base Case** of Yanda Dam, and other studies (***Ghordanloo Dam*** *in Iran (2015),* ***Tarbela Dam*** *in Pakistan (2003),* ***Arrow Dam (Keenleyside*** *Dam) in Canada, and* ***Reza Mahinroosta*** *in 2012 in his article).*
- **LiqiT**, **AutoCAD**, **Eagle Point**, and **Google Earth Pro have been used** for further comprehension.
- Comparison of **FoS** against Liquefaction with **Effective Stress** and **Shear Strength.**
- The recommended remedies are **practical** due to **equipment availability.**
- **Visiting** the actual location of the dam's construction site.

REFERENCES

ICOLD (1995). Embankment Dam Engineering. International Commission on Large Dams (ICOLD). ISBN: 2880210825.

Novak, P., Moffat, A., Nalluri, C., & Narayanan, R. (2007). Hydraulic structures (4th ed.). CRC Press. ISBN: 9780415393866.

Zhang, Y., & Zhang, C. (2004). Engineering of Dams: Principles and Cases. CRC Press. ISBN: 084931764X.

Sissakian, V., Al Shamali, R., Al-Ansari, N., & Knutsson, S. (2019). Dams and Reservoirs, Societies and Environment in the 21st Century. Springer. ISBN: 9783030293411.

Abdel Razek. M. et al., (2021). Analysis and Estimation of Seepage through Earth Dams with Internal Cut Off. Research article, 1-10. DOI: https://doi.org/10.21203/rs.3.rs-298691/v1

Aboelela M.M. (2016). Control of Seepage through Earth Dams Based on Previous Foundation Using Toe Drainage Systems. Journal of Water Resource and Protection, 8, 1158-1174. Retrieved from https://www.researchgate.net/publication/309884506.

Abuzeid, N. (1994). Investigation of channel seepage areas at the existing Kaffrein Dam site (Jordan) using electrical-resistivity measurements. Journal of Applied Geophysics, 32, 163-175. Retrieved from https://doi.org/10.1016/0926-9851(94)90018-3

Bieniawski, Z.T. (1978) Determining Rock Mass Deformability: Experience from Case Histories. International Journal of Rock Mechanics and Mining Sciences, 15, 237-247. https://doi.org/10.1016/0148-9062(78)90956-7

Bieniawski, Z.T. (1989) Engineering Rock Mass Classification. John Willey and Sons, New York, 251 p.

Bowles, J. E. (1984). Physical and geotechnical properties of soils(2nd ed.). New York: McGraw-Hill. Retrieved from https://www.academia.edu/36318420/

Bowles, J. E. (1997). Foundation Design and Analysis, 5th ed., McGraw-Hill, New York, 263pp. Retrieved from https://www.academia.edu/37455233/

D'Appolonia, D.J.(1980b). Soil bentonite slurry trench cutoffs. Journal Geotechnical Eng. Div., ASCE, vol. 106, no. GT4, pp. 399-417

Cedergren, H.R.(1977). Seepage, Drainage, and Flow Nets, Second Edition, John Wiley and Sons, Inc., New York.

Lin, C. P., Hung, Y. C., Yu, Z. H., & Wu, P. L. (2013). Investigation of abnormal seepages in an earth dam using resistivity tomography. Journal of Geoengineering, 8(2), 61-70. Retrieved from https://doi.org/10.6310/jog.2013.8(2).4

Casagrande, A. (1940), Seepage Through Dams, Contributions to Soil Mechanics 1925-40.

Hossain N. & Hazegh A. (2018). Comparison of pseudo-static, Newmark, and dynamic response analyses of the final pit wall of the Sungun Copper Mine. DOI:10.22059/IJMGE.2018.229315.594661

Ohsaki, Y. 1970. Effects of Sand Compaction on Liquefaction during the Tokachi-oki Earthquake, Soils and Foundations, 10(2): 112-128. Retrieved from https://doi.org/10.3208/sandf1960.10.2_112

Rampello, S., Cascone, E. & Grosso, N. (2009). Evaluation of the seismic response of a homogeneous earth dam. Soil Dynamics and Earthquake Engineering, 29, 782–798. DOI:10.1016/j.soildyn.2008.08.006

Serafim, J.L. and Pereira, J.P. (1983) Considerations on the Geotechnical Classification of Bieniawski. Proceedings of International Symposium on Engineering Geology and Underground Openings, Lisbon, Portugal, 1983, 1133-1144.

Zen, K. & H. Yamazaki 1990. Mechanism of Wave-Induced Liquefaction and Densification in Seabed, JSSMFE Proc., 30(4): 90-104. Retrieved from https://doi.org/10.3208/sandf1972.30.4_90

Bernard R. Wair Jason T. DeJong, Davis Thomas Shantz. 2012. Guidelines for Estimation of Shear Wave Velocity Profiles. PEER Report 2012/08. Retrieved from

Ishihara, K., Y. Kawase & M. Nakajima (1980). Liquefaction Characteristics of Sand Deposits at an Oil Tank Site during the 1978 Miyagiken-Oki Earthquake, JSSMFE Proc., 20(2): 97- 111. Retrieved from https://doi.org/10.3208/sandf1972.20.2_97

R. W. Jibson, (1993). Predicting Earthquake-Induced Landslide Displacements Using Newmark's Sliding Block Analysis, Transportation Research Record 1411, 17 p.

Jin, W.; Deng, Z.; Wang, G.; Zhang, D.; Wei, L. (2022). Internal Erosion Experiments on Sandy Gravel Alluvium in an Embankment Dam Foundation Emphasizing Horizontal Seepage and High Surcharge Pressure. *Water* 2022, *14*, 3285. Retrieved from https://doi.org/10.3390/w14203285

A.Ibrahim et al. (2019). Maximum shear modulus evaluation based on continuous wavelet transform of bender element test. Journal of Physics Conference Series 1349(1):012019. DOI:10.1088/1742-6596/1349/1/012019

Rezagholilou A. (2006), Seepage Design Criteria In Embankment Dams On Alluvium Foundation. Retrieved from https://www.researchgate.net/publication/293521292/

Nusier, O.K., Alawneh, A. & Malkawi, A.I. (2002). Remedial measures to control seepage problems in the Kafrein dam, Jordan. Bull Eng Geol Environ 61, 145–152. Retrieved from https://doi.org/10.1007/s100640100131

Bell F.G. (2007). Engineering Geology. Second Edition.

Fattah M., Al-Neami M. and Jajjawi N. (2014). Prediction of liquefaction potential and pore water pressure beneath machine foundations Open Engineering, vol. 4, no. 3, pp. 226-249. Retrieved from https://doi.org/10.2478/s13531-013-0165-y

Hedayati Talouki, H., Lashkaripour, G.R., Ghafoori, M. et al. (2015). Assessment and presentation of a treatment method for seepage problems of the alluvial foundation of Ghordanloo dam, NE Iran. J Geol Soc India 85, 377–384. https://doi.org/10.1007/s12594-015-0227-2

Hvorslev, M. (1951) Time Lag and Soil Permeability in Ground-Water Observations, Waterways Exper. Sta. Corps of Engrs, U.S. Army, Vicksburg.

ICOLD Bulletin 148. (2016). electing seismic parameters for large dams, guidelines Committee on Seismic Aspects of Dam Design, International Commission on Large Dams, Paris. https://www.researchgate.net/publication/320536997/

IS 8826-1978. Guidelines for Design of Large Earth and Rock-Fill Dams. Bureau of Indian Standard, New Delhi.

Richards, K.S., Reddy, K.R. (2007). Critical appraisal of piping phenomena in earth dams. Bull Eng Geol Environ 66, 381–402. https://doi.org/10.1007/s10064-007-0095-0

Mahir Uddin Crowhury. (1948). The Thesis On The Control Of Seepage Under Dams On Previous Foundations.

Molinder.G. (2016). Internal erosion in the previous foundation of an embankment dam a case study on the Lossen Da. https://www.researchgate.net/publication/305775344/

Tefera, M., Chernet, T. and Haro, W. (1996). Geological map of Ethiopia 2nd ed. and its explanatory notes (scale 1:2,000,000). Ethiopian Institute of Geological Surveys, Ministry of Mines and Energy, Addis Ababa.

Muhammad Tariq S. (2003). Control of seepages through deep alluvium foundation of Tarbela Dam Project – Pakistan.

Murthy, V.N.S. (2003). Geotechnical Engineering: Principles and Practices of Soil Mechanics and Foundation Engineering (1st ed.). CRC Press. https://doi.org/10.1201/9781482275858

Nusier, O.K., Alawneh, A. & Malkawi, A.I. (2002). Remedial measures to control seepage problems in the Kafrein dam, Jordan. Bull Eng Geol Environ 61, 145–152. https://doi.org/10.1007/s100640100131.

Peter G. Nicholson, (2015). Soil Improvement and Ground Modification Methods.

Fekadu, K., & Laike (1996). Seismic hazard assessment for Ethiopia and the neighboring countries.

Sianko, I., Ozdemir, Z., Khoshkholghi, S., Garcia, R., Hajirasouliha, I., Yazgan, U., & Pilakoutas, K. (2020). A practical probabilistic earthquake hazard analysis tool: case study Marmara region. Bulletin of earthquake engineering, 18, 2523-2555.

Army, U. S. A. C. E. (1986). EM 1110-2-1901.

Army, U. S. A. C. E. (1994). EM 1110-2-2300.

Wieland, M. (2014). Seismic Hazard and Seismic Design and Safety Aspects of Large Dam Projects. In: Ansal, A. (eds) Perspectives on European Earthquake Engineering and Seismology. Geotechnical, Geological and Earthquake Engineering, vol 34.

Institution, B. S. (1983, January 1). British Standard Specification for Aggregates from Natural Sources for Concrete.In-Text Citation: (Institution, 1983)

N. (2018, January 4). Blasting Technique for Ground Improvement. CivilDigital. https://civildigital.com/blasting-technique-for-ground-improvement/

Hamakareem, M. I. (2020, July 27). How to Use Blasting for Deep Compaction of Soil? The Constructor. https://theconstructor.org/geotechnical/blasting-deep-compaction-soil/

Mahdi Shakeran, Abolfazl Eslami, Majid Ahmadpour, (2016). "Geotechnical Aspects of Explosive Compaction", Shock and Vibration, vol. 2016, Article ID 6719271, 14 pages, 2016. https://doi.org/10.1155/2016/6719271

Appendix 1. Photographs Taken as primary data

To the side of the left abutment, there is a small village along the axis/location of the dam

Appendix 2. Yanda Dam site location view from Google Earth

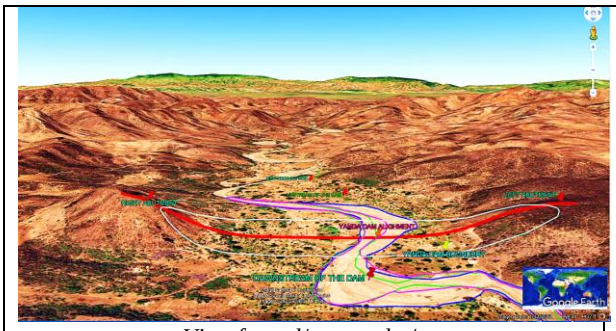

View from d/s toward u/s

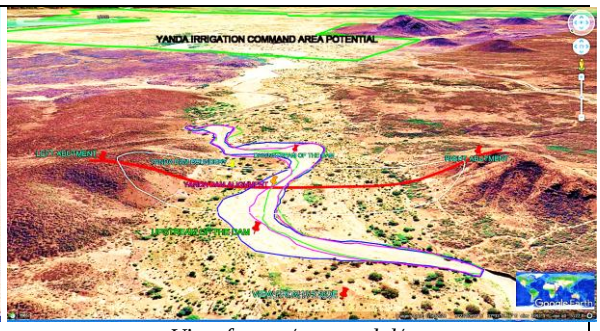

View from u/s toward d/s

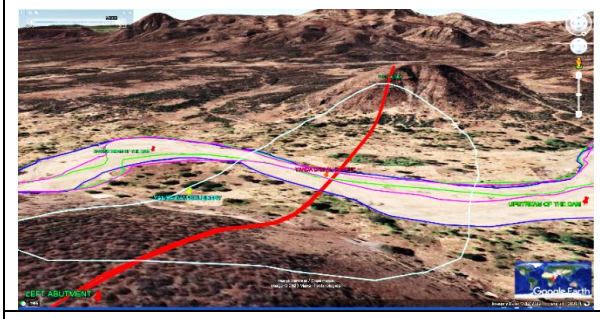

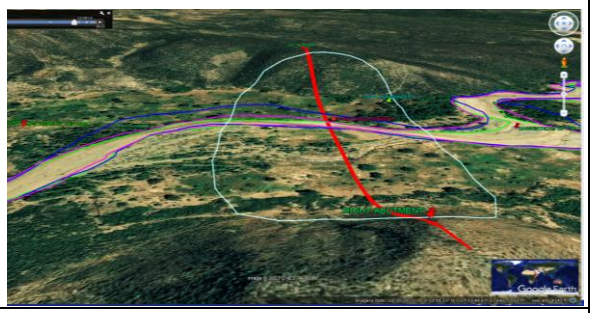

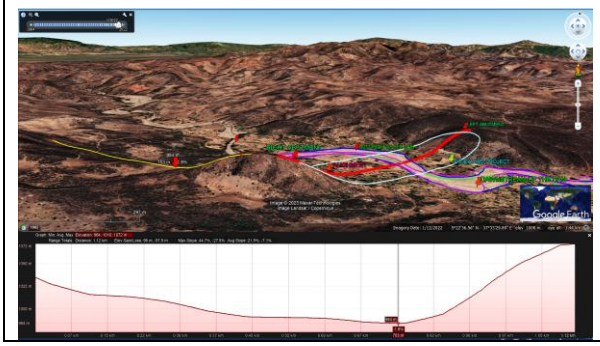

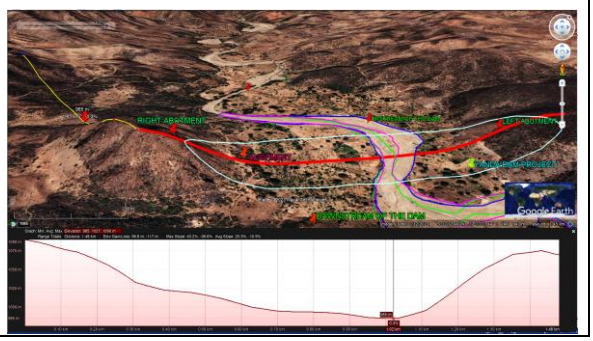

Appendix 3. U/S Dam Geometry Adjustment

The adjacent intended geometry between the coffer dam and the main dam, nevertheless, has been deemed inappropriate and should have been adjusted based on experience. The following analysis will be carried out utilizing seep/w software evaluations to ascertain that evaluation.

1st. Taken two other extra options

- **AutoCAD adjusted the proposed geometry**

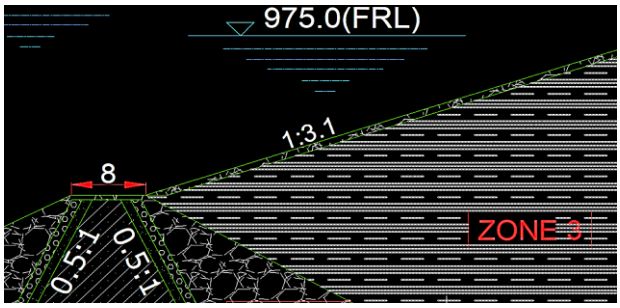

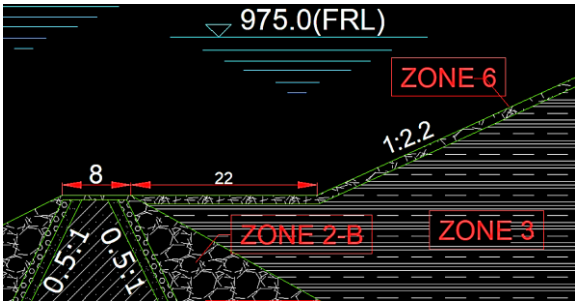

- **Imported the geometry to the GeoStudio for extra analysis;**

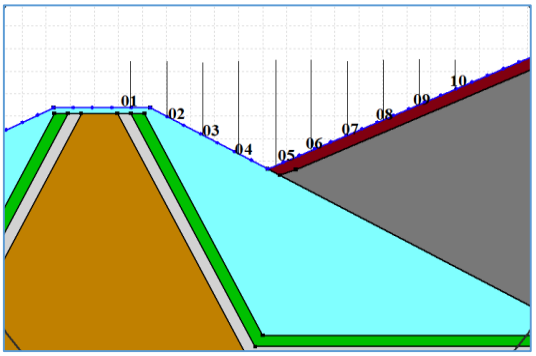

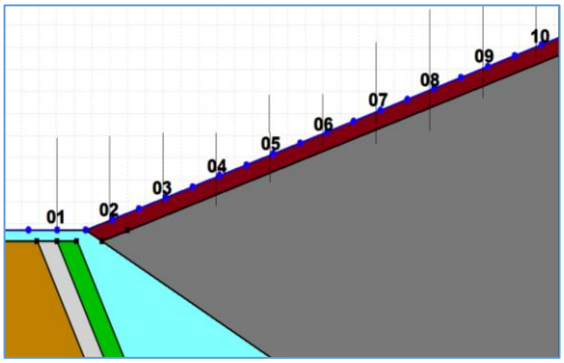

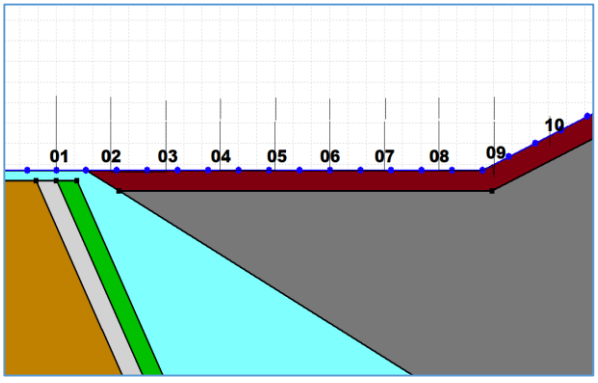

- **2nd Analysis and find out any defect**

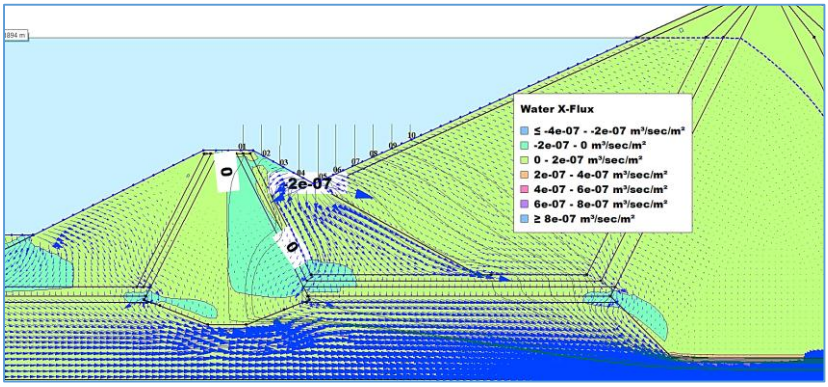

Option 1

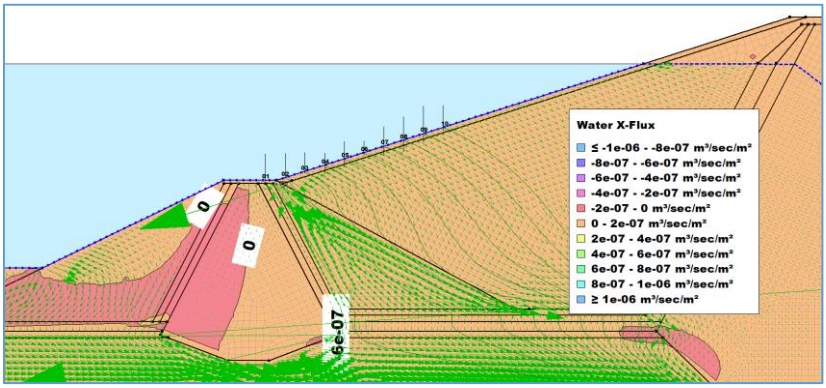

Option 2

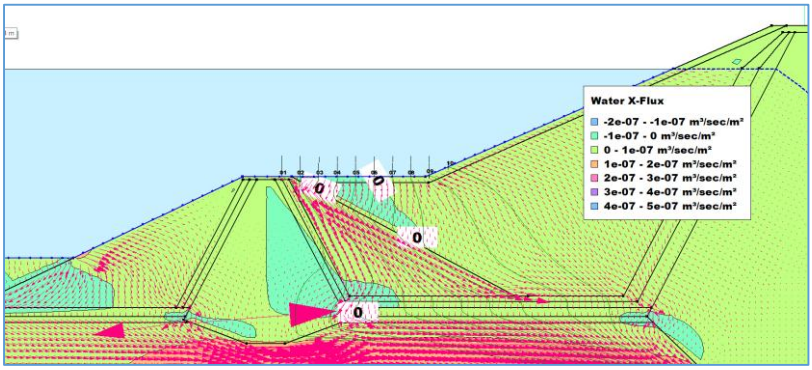

Option 3

3rd analysed result

OPTION 1			OPTION 2			OPTION 3				
Flow path	Travel Distance (m)	Average Water Flux (m³/sec/m²)	Flow path	Travel Distance (m)	Average Water Flux (m³/sec/m²)	Flow path	Travel Distance (m)	Average Water Flux (m³/sec/m²)		Minimam Water Flux
1	183.12	1.7E-21	1	165.33	3.22E-21	1	178.61	3.20E-21		1.74E-21
2	180.99	1.7E-21	2	147.34	5.24E-20	2	168.94	4.13E-21		1.71E-21
3	178.48	1.7E-21	3	143.94	6.63E-20	3	160.38	1.57E-20		1.73E-21
4	161.19	4.8E-21	4	137.13	1.77E-19	4	146.85	1.03E-20		4.75E-21
5	124.78	7.6E-19	5	132.20	6.22E-19	5	145.30	**1.27E-20**		1.27E-20
6	128.61	8.0E-19	6	129.37	7.82E-19	6	139.29	**6.57E-20**		6.57E-20
7	121.11	1.5E-18	7	128.74	1.02E-18	7	131.97	**2.01E-19**		2.01E-19
8	120.22	2.1E-17	8	124.71	1.51E-18	8	124.73	**5.84E-19**		5.84E-19
9	115.88	3.1E-17	9	124.13	1.75E-17	9	120.21	**1.23E-18**		1.23E-18
10	113.65	3.6E-17	10	120.06	2.38E-17	10	116.54	**2.27E-17**		2.27E-17
Average	**142.80**	**9.13E-18**	Average	**135.30**	**4.55E-18**	Average	**143.2835**	**2.48E-18**	Average	**2.48E-18**

4th Comparing good optional geometry economically

Fill Work	Ommition(area)		Addition (area)	Length (0+50-0+720)	Omm-Volume (m3)	Add-Volume (m3)	Rate (Birr)	Cost(birr)
	a	b	c	d	e	f	g	h
	m2	m2	m2	m2	(a-c)*d			(e*g)-(f*g)
Shell	293.02	39.30		670.00	169,992.40	-	1,144.85	194,615,799.14
RipRap			14.85	670.00	-	9,952.58	474.84	(4,725,884.04)
Total deducted cost(birr)								**189,889,915.10**

Table ……Estimation of quantity & cost of the U/S geometry options

a	The omitted shell quantity that difference between option 2 and option 3
b	The Shell quantity that was omitted from the additional fill of option 2
c	The added RipRap quantity that difference between option-2 and option-3
d	The effective filled length from left abutment to right abutment
e	Omitted volume from option 2
f	Added volume quantity to option 3
g	Cost Rate based on the ECDSWC site experience
h	The cost that going to be deducted from the total project price

In option 1, according to the analysis, the dam is affected by negative water flux around the adjacent area between the coffer dam and the main dam. This negative effect can cause the following:

Erosion and instability: Negative water flux can lead to erosion of the earthen dam structure, compromising its stability and increasing the risk of failure.

Sedimentation: Reduced water levels can cause sediment to accumulate in the reservoir behind the dam, reducing its capacity and potentially impacting downstream water quality.

The selected option 3 is better than the rest of the two options. Based on the result of the seepage analysis, the distance of the flow path is higher than the rest of the two and the water flux is lower than the rest of the two options. In addition to that according to the above computed table, the preferred option is economically better than the closest option 2. The overall estimated project cost of **189,889,915.10** birr will be deducted. This amount of money is a significant cost in construction to make it economical. Therefore, according to the numerical evaluation, there is safety from the negative water flux around the adjacent area relative to option 1 and economically minimizes the project cost relative to option 2, the Yanda dam option-3 geometry has been recommended for the next researched topics.

Appendix 4. Photos of Long Armed Excavator for Slurry Cutoff

The following photos were taken from the site of the Kuraz (Lot 1) irrigation project located in the Southern Region of Ethiopia(SNNP). The excavator was at desilting work from a deep and wide canal.

Appendix 5. Laboratory Test Result at Dam Foundation Soil Material

S.no.	Soil Sample Information			Soil Laboratory Test																	
	Sample Id	Sample Type	Sample depth (m)	NMC (%)	Specific gravity	Unit weight (gm/cc)	Double Hydrometer	Free swell (%)	Atterberg limit (%)			Grain size (%)					UCS (KPa)	Direct Shear strength		Triaxial Shear Strength Test	
									LL (%)	PL (%)	PI (%)	Clay (%)	Silt (%)	Sand (%)	Gravel (%)	% fine		C (kPa)	ϕ (degree)	C (kPa)	ϕ (degree)
1	YDBH-2	SPT-1	1.50-2.00	10.54		1.94			52.90	26.02	26.88			8.03	0.00	91.97					
2	YDBH-2	CPT-1	4.00-4.50	1.00		1.72			24.90	NP	-			81.12	12.49	6.39					
3	YDBH-2	SPT-2	6.00-6.45	21.98		1.56	66.5		58.40	25.84	32.56			7.08	0.15	92.77					
4	YDBH-2	UD-1	7.00-7.60	24.36		1.51			80.00	33.81	46.19			2.52	1.00	96.48	193.02	41.47	40.99	67.23	15.53
5	YDBH-2	SPT-3	7.60-8.05	31.19		1.90			73.30	28.89	44.41			6.84	3.84	89.32					
6	YDBH-2	SPT-5	14.40-15.00	16.39		1.74	29.98		52.30	23.93	28.37			7.74	24.33	67.92					
7	YDBH-2	UD-2	17.50-18.10	31.69		1.63	97.17		88.20	31.63	56.57			1.13	0.00	98.87	152.22	48.71	24.43	4.02	25.37
8	YDBH-2	SPT-6	18.10-18.55	24.32		1.73			68.50	25.36	43.14			2.96	0.00	97.04					
9	YDBH-2	SPT-7	20.80-21.45	8.79		1.65			31.90	20.17	11.73			24.43	11.26	64.31					
10	YDBH-2	SPT-8	24.00-24.50	14.75		1.87			42.00	21.34	20.66			27.96	12.62	59.42					
11	YDBH-3	SPT-1	1.50-2.00	30.94		1.42			30.85	16.12	14.73			20.35	0.00	**79.65**					
12	YDBH-3	CPT-1	5.00-5.45	9.56		1.76				NP						**3.17**					
13	YDBH-3	CPT-2	10.00-10.45	0.91		1.66				NP				51.00	36.00	13.00					
14	YDBH-3	CPT-3	18.00-18.60	25.25		1.7			59.00	33.85	25.15			14.19	4.78	81.03	208.73	10.58	25.36	4.70	25.74
15	YDBH-3	CPT-4	18.60-19.05	20.52		1.57								20.52	0.00	59.48					
16	YDBH-3	CPT-5	23.80-24.40	18.12		1.15								9.12	0.00	90.88					
17	YDBH-3	CPT-6	27.00-27.45	27.49		1.15								6.51	3.40	90.88					
18	YDBH-3	CPT-7	30.00-30.60	18.44		1.24			35.70	21.27	14.43			39.88	0.00	60.12					
19	YDBH-3B	SDS-1	3.45-4.00	1.92	2.59	1.61			22.40	NP	NP	0.11	8.20	87.48	4.21	8.31					
20	YDBH-3B	SDS-2	7.50-8.00	0.79	2.59	1.87			23.98	NP	NP	0.06	2.90	68.34	28.70	2.96					
21	YDBH-3B	SDS-3	11.50-12.00	1.29	2.59	1.77	85.71 (D)		28.70	NP	NP	0.12	4.06	83.58	12.23	4.18					
22	YDBH-3B	SDS-4	17.50-18.00	5.1	2.68	1.66			21.90	NP	NP	0.68	11.90	54.53	32.89	12.58					
23	YDBH-3B	SDS-5	22.00-22.60	29.09	2.5	1.30			58.82	30.74	28.08	36.30	46.38	8.74	8.58	82.68		16.00	16.17		
24	YDBH-3B	SDS-6	26.00-27.00	2.83	2.5	1.76	78.57 (D)		28.00	NP	NP	0.36	6.60	33.23	59.81	6.96					
25	YDBH-4	SPT-1	4.55-5.00	2.54	2.65	1.53	38.61 (ID)	Nil	22.20	NP		0.02	0.44	45.28	54.26	0.23					
26	YDBH-4		12.00-13.00		2.76				NP	NP	NP	0.03	1.19	20.52	78.26	1.22					
27	YDBH-4		18.00-19.00		2.74				NP	NP	NP	0.10	3.64	49.50	46.64	3.74		53.33	31.49		
28	YDBH-4	SPT-2	20.55-21.00					50.00	49.30	26.89	22.41										
29	YDBH-4		21.00-21.50		2.76				NP	NP	NP	0.09	12.27	70.68	16.60	12.36		0.00	33.49		
30	YDBH-4	SPT-3	26.55-27.00	14.21	2.68	1.42	36.69 (ID)	30.00	24.70	NP		0.60	14.97	53.90	30.54	15.57					
31	YDBH-6	SPT-1	1.50-2.00	21.68	2.51	1.45	22.56 (ND)	Nil	30.40	16.41	13.99	12.71	41.86	40.81	4.61	54.57		26.33	7.89		